Methodology Development and Synthesis of a Biologically Relevant Natural Product and Targeted Scaffold Discovery for Serine Hydrolase Inhibition

Anne F. Kornahrens

Trinity Term, October 2016

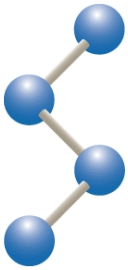

THE SCRIPPS RESEARCH INSTITUTE

A thesis submitted to

The board of the faculty of the Medical Sciences Division for the degree of Doctor of Philosophy in Biochemistry at the University of Oxford

and

The Scripps Research Institute for the degree of Doctor of Philosophy in the subject of Chemistry at The Scripps Research Institute

for the Skaggs-Oxford Fellowship program

For KUK & FWK

Abstract

The phenomenal potential of synthetic chemistry to influence small molecule therapeutic development represents my overarching theme. The goal of designing or discovering a novel clinical candidate or biological target can be achieved through a variety of avenues available to synthetic organic chemists. The potential of natural product total synthesis and inhibitor development as impactful projects were pursued with the use and development of methodology.

The natural product streptonigrin, a potent antitumor antibiotic, showed promise in clinical trials ultimately terminated in the 1970s. The underexplored mechanism of action prompted a reexamination of this potential therapeutic. The Donohoe group successfully designed a modular total synthesis accessing streptonigrin in 11 steps and 14% yield. The introduction of an asymmetric Suzuki–Miyaura reaction yielded a key intermediate in 42% ee and 65% yield, which represents the first example of purely synthetic access to enantioenriched late-stage streptonigrin analogues.

The "hydrogen-borrowing" method allows the functionalization of ketones with methanol and transition metal catalysts, but examples lacked application to further α-functionalization. The successful development of a novel "interrupted-hydrogen-borrowing" method allowed the use of iridium and methanol to trap the reactive enone intermediates by preventing the subsequent "hydrogen returning". Thus, this enabled these reactive intermediates to be subjected to a 1,4-conjugate addition with a nucleophilic ketone enolate and subsequent cyclization and oxidation to form highly substituted pyridines from simple ketones.

The exploration of serine hydrolases, an important mammalian enzyme class with a large portion still uncharacterized, requires inhibitors with new chemotypes

that can covalently and irreversibly bind. The small library of urea- and carbamate-containing scaffolds with varied aromatic backbone substitutions was subjected to activity-based protein profiling to allow expedient examination of the whole serine hydrolase family. The predicted strong electronic effect of the *p*-substituent was confirmed, modulating the reactivity of the electrophilic urea or carbamate moiety. MudPIT analysis of a subset supported the demonstrated reactivity profile and identified the uncharacterized serine hydrolase PNPLA4 as a selective target of one inhibitor. This potent and selective inhibition was verified by in vitro and in cell assays and validates this chemotype as a family of serine hydrolase inhibitors.

Acknowledgments

During the last five years, I was lucky to be a part of an exciting and unique graduate program that spanned two continents and two wonderful institutions. Therefore, my thanks go first to Prof. Ian Wilson for accepting me into this program and for his tireless support and administrative efforts. Transferring countries of residence in the middle of the PhD is a feat I only achieved with his help. Additionally, I'm grateful to the chemistry and biochemistry departments at University of Oxford and the graduate program at TSRI for their assistance. The additional members of my TSRI committee (Ryan Shenvi and Ben Cravatt) and the Oxford professors who took part in my transfer-of-status and confirmation vivas (Stuart Conway and Mark Howarth) deserve special credit for accommodating the program's unique needs and for their valuable insight along the way.

My time was spent in the wonderful research groups of Prof. Timothy J. Donohoe and Prof. Dale L. Boger. Thank you, Prof. Donohoe, for welcoming me into your lab and for the dynamic learning environment you created. The critical foundation of synthetic methods I learned in Oxford served me well as I transitioned to TSRI in 2014. Prof Boger, I appreciate your great support throughout the 5 years (as we visited each time I returned to the USA for the graduate symposium) and your inspiration over the course of my exciting project completed in your group.

The people that I spent those countless hours in the lab deserve my thanks for their support, their collaborative efforts and their friendship. My Skaggs-Oxford buddies were a key support group in England and Keary and Jerry (who crossed over to continue the fun in San Diego), as well as JL, Owen and Dan made up this special group and our dinners will remain a favorite part of my time in England. My TJD lab mates who worked on the streptonigrin project (Dr. Chris Jones) and the interrupted-

hydrogen-borrowing project (Darren Poole, Di Shen, Camilla Shotton) could not have been better peers and friends. The rest of the TJD group made F7–F9 (especially F9) a great place to work. The regularity of brew time, the fun of Uni Club nights and Christmas parties and the many cultural lessons were a key part of my Oxford experience. My special thanks to Jacqueline Habegger, who knows how to cheer me up better than anyone and whose friendship and companionship means the world to me, from that first late night walk home and chat about feminism through her early morning wake up skype calls now that we're 8 hours apart. Alice Gatland was another special labmate who made me smile, introduced me to Δ and who got me swimming again. Akshat Rathi was my spiritual guide and mentor throughout the five years and my muse in trying to think critically about my work and my career. Lukas Pfeifer (technically VG, but an honorary TJD as well) let me teach him to swim, happily participated in late night hood chats and helped me dance my way out of England.

Oxford held another special place and community – that of Lincoln College. I used to say that we didn't get to choose our college (in the Skaggs-Oxford program) but were luckily automatically placed in the best one. The MCR and the friends I made there and in Bear Lane are so special to me. Special thanks to Kirstin, Lara, Anne-Clair, Jérémie, Kate, Michelle, Sasha and Phil. Our Emily Carr dance parties, champagne or tea drinking sessions and punting lessons such rich experiences to have shared with you while I was abroad for those 2.5 years.

The second half of my PhD and the time spent in San Diego held a few more sunny days and another group of special people to thank. The DLB group welcomed me, even as I arrived as a new 4th year student, and made my time in Bay 4 and Office 5 very memorable. Justin Sears was an amazing group manger, older-student mentor and friend and I only wish we could've had more time together in the DLB group and

in fun establishements around San Diego. The Camping Crew of 2016 deserve special recognition for helping me to escape San Diego every few months and allowing the joys of glamping, desert hiking and spontaneous backpacking to be (re)discovered in all of us. Brian T. Jones was always there for perspective (on life and on chemical synthesis) and while I didn't always agree (ahem, politics) our discussions and conversations always served to keep me on the right path.

My project here at TSRI depended a lot on the support of Dan Brody and on the Cravatt group. Specifically, thanks to Armand Cognetta for teaching me basically everything proteome- and cell-related and for running the MudPIT samples for me. Your advice and support were key to finishing chapter 4!

My proofreaders, Jackie, Alice, Darren, Di, Vyom, Chris and Brian luckily realized that being an editor is more than grammar and formatting but a necessary process that kept the thesis writing on track, kept my spirits up and pushed me forward. Big thanks to Alice for the submission of my Oxford copies to Exam Schools and for seeing me through the last tumultuous days.

I was so blessed to have many (30+) visitors in both locations, which kept me from feeling too homesick or too far away from support. I'd like to give a special mention to my friends that came 2+ times and/or to both locations: Katherine, Erin, Christine, John Scola, Chris Fei and members of my family: Mom, Dad, Mary, Johnny K. My special three chicas (Sarah Kate, Sarah O and Coley) made our reunions work stateside each year and always had the long-term perspective of people who know me too well.

Kevin brought sunshine, challenges and so much joy into my time at TSRI. Thank you for always having my back (or belay), for listening and for your love. My family (Mom, Dad, Mary, Eric, John and, more recently, Macallan) was the glue that

held me together over the five long years. Their support across oceans and time zones, their visits (often more for support or moving than for fun) and their willingness to always answer the calls and provide the hugs are the steady strength as I look back over these years. Thanks for helping me to learn to fail, for pushing me to persevere and truly enabling the pursuit and accomplishment of this feat.

Table of Contents

Declaration

The work presented in this thesis was conducted at the Chemistry Research Laboratory at the University of Oxford under the supervision of Prof. Timothy Donohoe and at the Beckman Center for Chemical Sciences at the Scripps Research Institute under the supervision of Prof. Dale Boger. This thesis was submitted to the board of the faculty of the Medical Sciences Division in partial fulfilment of the requirements for the degree of Doctor of Philosophy at the University of Oxford and to The Scripps Research Institute in partial fulfilment of the requirements for the degree of Doctor of Philosophy in the subject of Chemistry for The Scripps Research Institute. This is in accordance with the requirements of the Skaggs-Oxford program administered by The Scripps Research Institute. All the work is my own, except where I have either acknowledged help from a named person or given a reference to a published source.

Anne Kornahrens

Oxford, Trinity Term, 2016
TSRI, October 2016

List of Figures

Figure 4-15. (a) IC_{50} determination of selective PNPLA4 inhibition by **4.83** using HEK cell lysates (whole cell, membrane and soluble fractions) and (b) in cell treatment of transfected HEK cells with **4.83**

List of Schemes

List of Tables

List of Abbreviations and Acronyms

Å	Ångström (10^{-10} metres)
ABPP	Activity-based protein profiling
Ac	Acetyl
Ad	Adamantyl
aq.	Aqueous
Ar	Aryl
atm	Atmosphere (pressure unit)
BINAP	(±)-2,2′-Bis(diphenylphosphino)-1,1′-binaphthalene
BINOL	1,1'-Bi-2-naphthol
Bn	Benzyl
BQ	1,4-Benzoquinone
br	Broad singlet
Bu	Butyl
^{13}C NMR	Carbon-13 nuclear magnetic resonance
C–C	Carbon–Carbon (Bond)
C–H	Carbon–Hydrogen (Bond)
C–N	Carbon–Nitrogen (Bond)
cat.	Catalyst
CataCXium A	Di-(1-adamantyl)-n-butylphosphine
CD	Circular dichroism
cm	Centimeters
cm^{-1}	Wavenumbers
cod	1,5-Cyclooctadiene
Cp	Cyclopentadienyl
Cp*	Pentamethylcyclopentadienyl
CSI	Chlorosulfonyl isocyanate
Cy	Cyclohexyl
d	Doublet
dr	Diastereomeric ratio
DBU	1,8-Diazabicyclo[5.4.0]undec-7-ene
dd	Doublet of doublets
DMAP	4-(Dimethylamino)pyridine
DMEM	Dulbecco-modified eagle medium
DMF	*N*,*N*-Dimethylformamide

DMSO	Dimethylsulfoxide
DNA	Deoxyribonucleic acid
DPBS	Dulbecco's phosphate buffered saline medium
Dppf	1,1'-Bis(diphenylphosphino)ferrocene
DTBMP	2,6-Di-*tert*-butyl-4-methylpyridine
e.g.	Exempli gratia (Latin: for example)
ee	Enantiomeric excess
eq.	Equivalent(s)
ESI-TOF	Electrospray ionization – time of flight
ESI^+	Electrospray ionisation (positive ion detection)
Et	Ethyl
et al.	Et alii (Latin: and others)
EtOAc	Ethyl acetate
EWG	Electron-withdrawing group
FAAH	Fatty acid amide hydrolase
FBS	Fetal bovine serum
FCC	Flash column chromatography
FCPC	Fast centrifugal partitioning chromatography
FP-Rh	Fluorophosphonate rhodamine
FT-IR	Fourier Transform Infrared Spectroscopy
g	Gram(s)
^1H	Proton nuclear magnetic resonance
h	Hour(s)
H-B	Hydrogen-borrowing
H–G II	Hoveyda–Grubbs second-generation catalyst
HEK	Human embryonic kidney cells
HMBC	Heteronuclear multiple-bond correlation spectroscopy
HPLC	High Performance Liquid Chromatography
HRMS	High Resolution Mass Spectrometry
i	*Iso*
I-H-B	Interrupted hydrogen borrowing
IA-Rh	Iodoacetamide rhodamine
IC_{50}	Half maximal inhibitory concentration
IR	Infrared spectroscopy
J	Coupling constant

L	Ligand
LDA	Lithium diisopropylamide
m	Multiplet
M	Moles per liter (mol/L)
m/z	Mass to charge ratio
mCPBA	meta-Chloroperbenzoic acid
Me	Methyl
mg	Milligram(s)
MHz	Megahertz
min	Minute(s)
mL	Milliliter(s)
mol	Mole(s)
mol%	Molar percent
MP	Melting point
MS	Molecular sieves
n	Primary
n/o	Not observed
N2A	Neuro2A cells
NBS	*N*-Bromosuccinimide
NHC	*N*-Heterocyclic carbene
nM	Nanomolar
NOE	Nuclear Overhauser effect
NOESY	Nuclear Overhauser effect spectroscopy
NMR	Nuclear magnetic resonance spectroscopy
o	Ortho
p	Para
PG	Protecting group
pH	Negative log of hydrogen ion concentration
Ph	Phenyl
Phth	Phthalimide
Pin	Pinacol
pKa	Logarithmic acid dissociation constant
PMP	para-Methoxyphenyl
ppm	Parts per million
Pr	Propyl

PTLC	Preparative thin layer chromatography
pyr.	Pyridine
q	Quartet
R	Generic carbogenic fragment (aryl or alkyl Group)
RBF	Round-bottom flask
RCM	Ring closing metathesis
R_f	Retention factor
RSM	Recovered starting material
s	Singlet
SDS-PAGE	Sodium dodecyl sulfate-polyacrylamide gel electrophoresis
S–M	Suzuki–Miyaura reaction
SAR	Structure–activity relationship
SEGPHOS	4,4'-Bi-1,3-benodioxole-5,5'-diylbis(diphenylphosphane)
Ser	L-Serine
SH	Serine hydrolase
S_N2	Bimolecular nucleophilic substitution
t	Triplet
t	Tertiary (*tert*)
T-H	Transfer-hydrogenation
$t_{1/2}$	Half-life
temp.	Temperature
TEMPO	(2,2,6,6-Tetramethyl-piperidin-1-yl)oxyl
Tf	Trifluoromethanesulfonyl (Triflyl)
TLC	Thin layer chromatography
TM	Transition metal
TMS	Trimethylsilyl
Tol	Tolyl
UV	Ultraviolet
δ	Chemical shift
μL	Microliter(s)
°C	Degrees Celsius
[α]	Specific rotation
μ	Micro (prefix: 10^{-6})
ν̃max	Infra-red absorption maximum
(±)	Racemic

Chapter 1
Introduction

1.1 Small molecule therapeutics

Small molecule therapeutics have impacted human health over centuries of scientific discovery. Examples of small molecule medicines even appear in an ancient Egyptian medical text, circa 1800 B.C., and they were prevalent in ancient Chinese herbal medicines.[1] These early therapies were often medicinal plants, such as the bark of the willow tree used for pain or fever and the use of sweet wormwood herb as a Chinese remedy for malaria (Figure 1-1). The advent of drug development can be traced to the isolation of the active ingredient of these and other known therapies, such as the discovery of salicylic acid and artemisinin as the potent agents of these herbal remedies. Improved synthetic methods allowed the synthesis of these molecules and analogues to probe or improve their effect. The synthesized of acetylsalicylic acid in 1897 and the discovery that this analogue showed reduced digestive complications, allowed the large scale production of this efficacious drug, Aspirin.

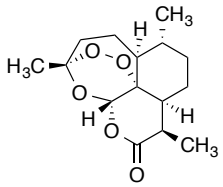

artemisinin
isolated from sweet wormwood
malaria

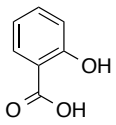

salicylic acid
isolated from willow bark
pain, fever, inflammation

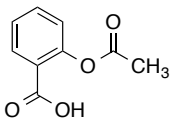

acetylsalicylic acid, aspirin
pain, fever, inflammation

Figure 1-1. Examples of small molecule therapeutics derived from herbal remedies

In addition to the isolation of active components from known treatments, serendipity has played a part in novel drug discovery. This includes the famous discovery of the antibiotic penicillin from mold in 1928 (Figure 1-2). Significantly, subsequent studies to design and synthesize new scaffolds produced inspired compounds with bacterial-killing effects, incuding Prontosil, the first sulfonamide-containing “sulfa drug”, produced and discovered through a screen at Bayer in the

1930s (Figure 1-2). Widespread use of these antibiotics in the 1940s and the pursuit of other antibacterial compounds from natural or purely synthetic sources led to the birth of modern antibiotic development.

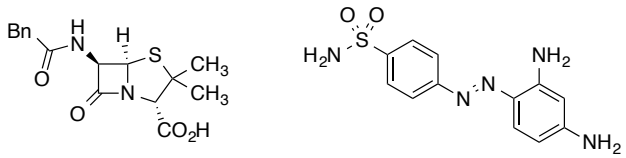

penicillin
antibiotic

Prontosil
antibiotic

Figure 1-2. Therapeutics discovered through serendipity and synthetic design

Modern small molecule pharmaceuticals (defined as less than 500 to 900 daltons in size) are not limited to antibiotic activity, but have impacted and improved human health with effects ranging from pain management, cancer treatment or antimalarial effects. An analysis of the past 40 years of drug development identified 79% of the approved new chemical entities (NCE) as small molecule therapeutics and 64% for the years 2007–2014, illustrating the continued success of small molecule therapeutic discovery.[2] The final market launch of an NCE relies on the successful navigation of a lengthy and difficult drug development process, through phase clinical trials and approval. This process can last an average of twelve years with only 10% of drugs in clinical trials successfully completing human testing. These inefficiencies result in a huge cost of each successful drug, with estimates ranging from $1.8 to 2.6 billion.[3] These endeavors all depend on the identification of a lead compound, which is a key responsibility of medicinal chemists, and this drug discovery effort is taking place in industrial, governmental and academic settings. This process to discovery and verify a clinical candidate contains a variety of opportunities for the involvement of chemists and organic chemistry along the typical pathway (Figure 1-3).[4]

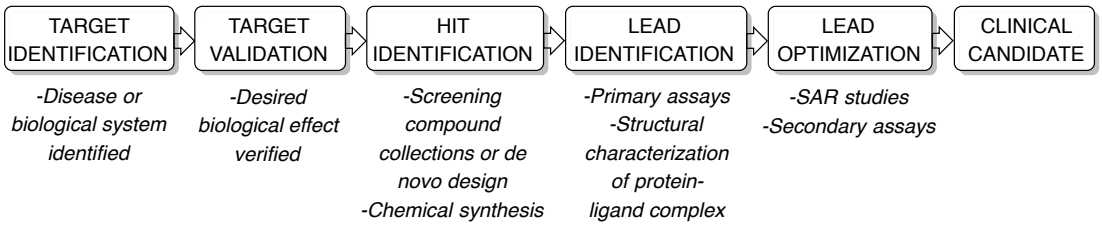

Figure 1-3. Schematic of the drug discovery process to identify potential small molecule therapeutics (Adapted from Stocks 2013[4])

Synthetic organic chemistry contributes greatly to the development of small molecule drugs through identification and synthesis of novel potential therapeutics. The choice of target structure can be derived from the vast numbers of potential scaffolds that would display the correct qualities to serve as a drug.[5] Inspiration from nature, rational design (based on the biological target or similar drugs), unbiased screening, and serendipity have all contributed to the discovery of successful molecular structures as detailed above. Some key synthetic roles that chemists play, that are utilized to discover potent compounds with biological activity in this thesis, include the construction of a natural product or designed structures and the development of novel methodologies for new scaffold synthesis.

This thesis specifically describes the work performed to develop a route to a natural product (streptonigrin) requiring the optimization of a few key steps (Chapter 2). An asymmetric variant of one key cross-coupling step was incorporated and allowed access to enantioenriched intermediates. This modular synthesis showcased methodology developed in the group to form pyridines, and my subsequent work (Chapter 3) addressed a new method to form this key moiety, prevalent in natural products and drug molecules. The successful discovery of a metal-catalyzed method to form 1,5-diketones and subsequent pyridine formation could be applied to a synthesis such as that in Chapter 2. Finally, the design and testing of potential small molecule inhibitors, another component of drug discovery through novel biology

interrogation, is covered in Chapter 4. Additional background information is provided here to describe the components of these projects that contribute to the overarching goal of small molecule therapeutic discovery.

1.2 Components of drug discovery

1.2.1 Natural products as target inspiration

Organisms such as bacteria, fungi, and plants produce small molecules (usually as secondary metabolites), which are known as "natural products" to organic chemists. Medicinal plants[6] were likely the first source of treatments that contained "small molecules", but this often occurred without the extraction or identification of the active agent. In the modern era, isolation of secondary metabolites from a variety of sources has allowed identification of potential new drugs. The richness of natural products as a source for structural inspiration for synthetic investigations is evidenced in the number of natural products, as well as derivatives and mimics of natural products, in approved small molecule drugs (accounting for 1,211 or 65% of small molecule drugs approved from 1981–2014).[2] Examples include artemisinin, penicillin and salicylic acid, introduced earlier, as well as carumonam (an antibacterial, introduced in 1988), roxithomycin (an antibacterial, introduced in 1987) and mupirocin (an antibacterial, introduced in 1985) shown in Figure 1-4.[2] The project pursued in Chapter 2 of this thesis enabled a new, modular and higher yielding total synthesis of streptonigrin that would also enable expedient access to analogues (Figure 1-4). This natural product was found to have potent antibiotic and antitumor activity and underwent unsuccessful clinical trials in the 1960s. My work builds upon the previous discoveries and proposes that streptonigrin could be revisited as a potent small molecule therapeutic (Chapter 2).

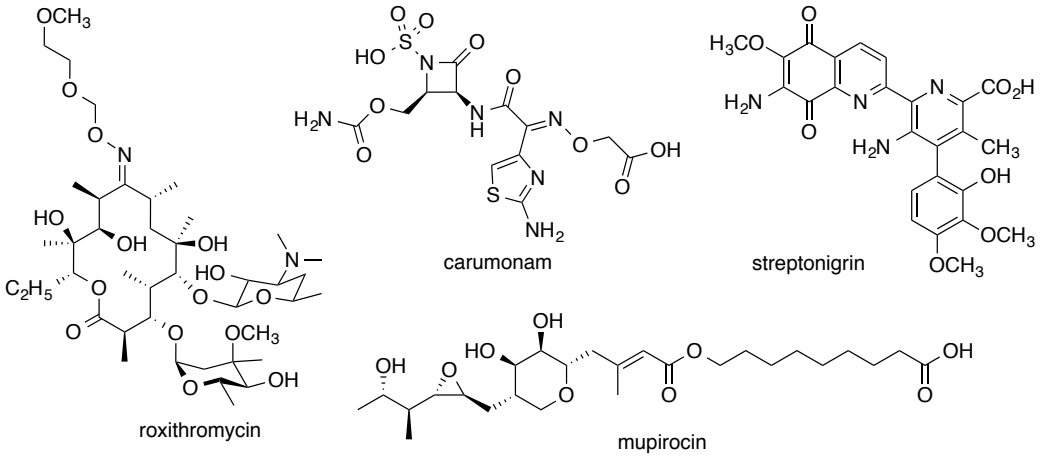

Figure 1-4. Examples of approved, natural product-based, small molecule drugs and streptonigrin (a potential drug)

1.2.2 Importance of new chemical methods to synthetic progress

Ultimately, it is chemical methods that enable natural product and lead compound synthesis. The challenge of a difficult or unique molecular structure designed by nature pushes the boundaries of the synthetic methods available and inspires the continued discovery of additional methods.[7] This challenge leads to the cycle of development, testing and modification of methods through the platform of natural product synthesis and has contributed to the tens of thousands of available methods for small molecule synthesis.[8] Thus, effective method development has a key role in the quick, easy and inexpensive creation of novel small molecule drugs.

The methods used in Chapter 2 to construct the key pyridine core of the natural product were previously developed in the Donohoe group. The ring-closing metathesis allowed access to the dihydropyridone precursor from two differently substituted substrates. This natural product synthesis showcased the potential of this pyridine-forming method and also extended the scope that could be incorporated. Pyridines are known to be a key component of many drug molecules, including the well-known Claritin and Nexium and the lung cancer drug Xalkori (Figure 1-5).[9]

The project described in Chapter 3 of this thesis was pursued to enable the branched α-alkylation of substituted ketones. The formation of 1,5-diketones and

subsequent cyclization and oxidation allowed the application of this new methodology to a expedited synthesis of tetrasubstituted pyridines. While this methodology hasn't yet been directly applied to the synthesis of streptonigrin, the new method to form pyridines will likely be applied to this or another total synthesis soon to demonstrate its utility.

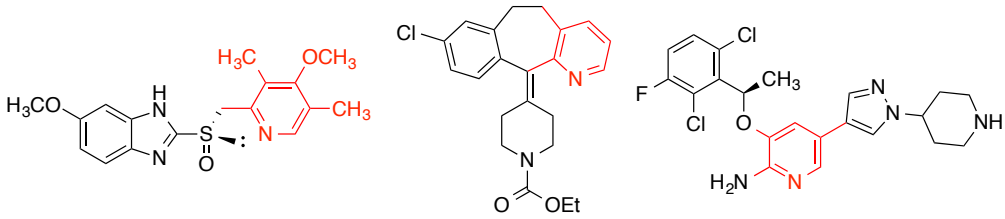

Figure 1-5. Common small molecule drugs that contain a pyridine scaffold

1.2.3 Drug discovery depends on elucidation of biological targets

These advances in chemical synthesis and scaffold construction have enabled the generation of chemical libraries which house the compilation of many molecular structures. The potential identification of new drugs is enabled through exploration of the new chemical space covered by newly synthesized and inspired scaffolds. Often, the biological target of these compounds might have a known effect or role in a certain pathophysiology (classical pharmacology). The development of assays to probe the small molecule's effect allows the subjection of newly created or libraries of compounds to primary and secondary assays (see Figure 1-3).

Additionally, known drugs can be utilized to probe disease states, including the use of aspirin for the elucidation of its mechanism of activity 50 years after its synthesis and market release. The breakthrough was made in 1971 by British pharmacologist John Robert Vane that aspirin suppresses the synthesis of prostaglandins and thromboxanes. This furthers the understanding of this drug's effects and provides additional elucidation of biological processes in the body.

Crizotinib, introduced as a pyridine-containing drug above, is a lung cancer treatment and acts as an inhibitor of anaplastic lymphoma kinase (ALK). Mutations in the ALK oncogene are the major cause of hereditary neuroblastoma which allows ALK to be a tractable therapeutic target. This inspired the targeting of ALK and the creation of cancer drugs such as crizotinib. These examples show the potential of small molecules to be used to probe biological effects, which is possible with both previously approved drugs with known therapeutic effect but unknown mechanism of action, or with potential drugs, such as streptonigrin. Other small molecules that may not have a therapeutic effect can still be used as probes to discover new targets, such as the use of small molecule inhibitors.

Binding of small molecules to uncharacterized or unannotated targets can enable the discovery of new targets related to a specific biological activity of interest and the elucidation of enzymatic roles that were previously unexplored. In Chapter 4, the creation of a new small molecule family and their subsequent testing provided a new biological target and allowed for the identification of a specific and potent small molecule inhibitor. A library of serine hydrolase inhibitors with benzothiadiazin-3-one 1,1-dioxide and benzooxathiazin-3-one 1,1-dioxide cores was created and tested for their inhibitory effect by activity-based protein profiling.[10] The resulting inhibitors show the desired modulated reactivity (dependent on backbone aromatic substitution choice) and a selective PNPLA4 inhibitor was discovered and described.

1.3 Conclusion

A researcher interested in influencing human health is greatly benefited by developing and utilizing chemical tools to identify new small molecule lead compounds. As presented herein, the targeting of natural product structures can be a useful source of new therapeutics and synthetic targets. The discovery and

development of new chemical methods allows the synthesis of these natural scaffolds as well as analogues and de novo designed compounds. The use of small molecules as drugs requires a specific therapeutic effect, but these same compounds can allow investigation of biological pathways through exploring their mechanisms of action or through the use of small molecule inhibitors. My goals in this thesis focus on exploring the biological activity of a natural product and on discovering new activities using designed small molecules, with method development and utilization forming the key tool by which synthetic success is achieved.

1.4 References

1. Nakanishi, K. *Comprehensive natural products chemistry*; Meth-Cohn, O.; Barton, S. D.; Nakanishi, K., Eds.; Elsevier, **1999**; Vol. 1-8, pp. xxi–xxxviii.

2. Newman, D. J.; Cragg, G. M. *J. Nat. Prod.* **2016**, *79*, 629–661.

3. The price of failure. *economist.com*.

4. Stocks, M. In *Introduction to Drug Research and Development*; Elsevier, **2013**; pp. 81–126.

5. Bauer, R. A.; Wurst, J. M.; Tan, D. S. *Curr. Opin. Chem. Biol.* **2010**, *14*, 308–314.

6. Atanasov, A. G.; Waltenberger, B.; Pferschy-Wenzig, E.-M.; Linder, T.; Wawrosch, C.; Uhrin, P.; Temml, V.; Wang, L.; Schwaiger, S.; Heiss, E. H.; Rollinger, J. M.; Schuster, D.; Breuss, J. M.; Bochkov, V.; Mihovilovic, M. D.; Kopp, B.; Bauer, R.; Dirsch, V. M.; Stuppner, H. *Biotechnol. Adv* **2015**, *33*, 1582–1614.

7. Churcher, I. *Nat. Chem.* **2013**, *5*, 554–555.

8. Gronowitz, S. *Award Ceremony Speech*; Frangsmyr, T., Ed.; Nobel Lectures, Chemistry 1981-1990, **1992**.

9. Pozharskii, A. F.; Soldatenkov, A.; Katritzky, A. R. *Heterocycles in Life and Society: An Introduction to Heterocyclic Chemistry, Biochemistry and Applications*; John Wiley & Sons.

10. (a) Leung, D.; Hardouin, C.; Boger, D. L.; Cravatt, B. F. *Nat. Biotechnol.* **2003**, *21*, 687–691; (b) Liu, Y. S.; Patricelli, M. P.; Cravatt, B. F. *Proc. Natl. Acad. Sci. U.S.A.* **1999**, *96*, 14694–14699.

Chapter 2

The total synthesis of biologically active natural product streptonigrin and enantioenriched analogues

2.1 Introduction

Streptonigrin (**2.1**, Figure 2-1), a potent tetracyclic natural product, was first isolated by Rao and Cullen[1] in 1959. Its highly substituted tetracyclic aminoquinone framework and potent antitumor and antibiotic effects have inspired biochemists and organic chemists for the decades since its discovery. Promising clinical trials were halted due to severe toxicity, but the potential of this scaffold has remained underexplored. This is showcased by the dearth of total syntheses enabling late-stage analogue production and the lack of elucidation of the causation and potential prevention of its prohibitive side effects.

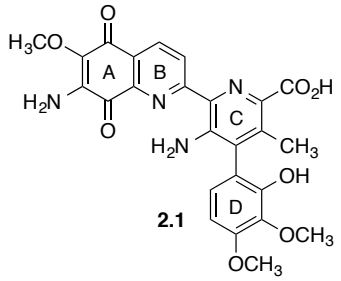

Figure 2-1. Structure of **2.1**, the natural product streptonigrin

2.1.1 Discovery and isolation of the natural product streptonigrin

The bacterial species *Streptomyces* and *Actinomyces* have produced a plethora of diverse natural products, including **2.1**, which was initially isolated from *Streptomyces flocculus* by Rao and Cullen. The name streptonigrin is derived from the dark color of the crystalline substance ("coffee-brown to almost black"). It was also discovered in *Streptomyces rufochromogenes* and *Streptomyces echinatus* and named "rufochromomycin" and in *Actinomyces albus var. bruneomycini* under the name "bruneomycin."[2] Other antibiotics isolated from similar bacterial strains with similar molecular framework include streptinigrone (**2.2**), lavendamycin (**2.3**), and 10-*O*-demethylstreptonigrin (**2.4**, Figure 2-2).[3]

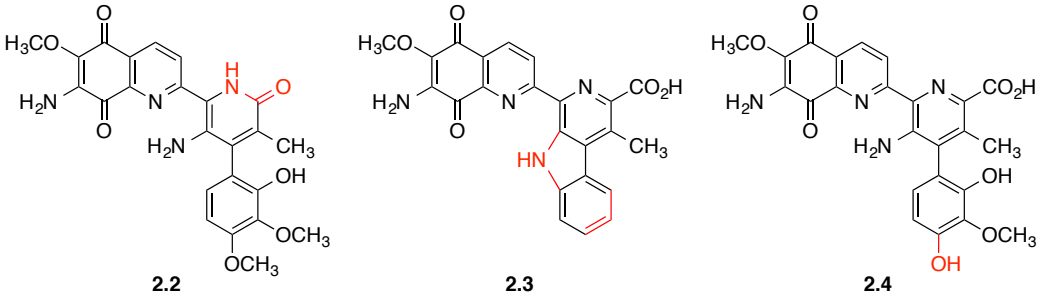

Figure 2-2. Related antibiotics also isolated from *Streptomyces* species (structural differences highlighted in red)

The initial characterization by Rao and Cullen concluded only that it was a weak acid and had "quinonoid properties." The culture from *S. flocculus* containing **2.1** was shown to have antitumor activity against adenocarcinoma 755 in mice and human tumor type #1 in rats as well as antibiotic properties against Gram-positive and Gram-negative bacteria.[1] Though **2.1** was initially isolated utilizing countercurrent distribution chromatography with no yield reported,[1] it has since been isolated through extraction from the culture filtrate with purification by Sephadex column chromatography to give a net yield of 13 mg per liter of culture filtrates.[4,5]

2.1.2 Identification and characterization

Streptonigrin has garnered interest due to specific structural features, which were first elucidated by Rao, Biemann and Woodward in 1963 using degradation and derivatization procedures.[6] Additional support for the proposed structure came from NMR studies published in 1974,[7] and though later revised by Gould,[8] they confirmed the structure through identification of all carbon, nitrogen and hydrogen resonances.

Further early confirmation of the structure and additional spatial analysis were obtained through X-ray diffraction analysis by Chiu and Lipscomb in 1974 (Figure 2-3).[9] The crystal structure showed the ABC rings oriented in a plane, held in place by hydrogen bonding between the amino group on ring C and the quinolone nitrogen in ring B. In contrast, the D ring was found to be almost perpendicular, oriented 85° to the ABC plane. The reported space group, $P2_12_12_1$, established that the unit cell was

optically active or containing only one hand of the skewed molecule. This could arise from selected crystallization of a racemic mixture, and since **2.1** does not contain any heavy atoms, no absolute configuration was established.

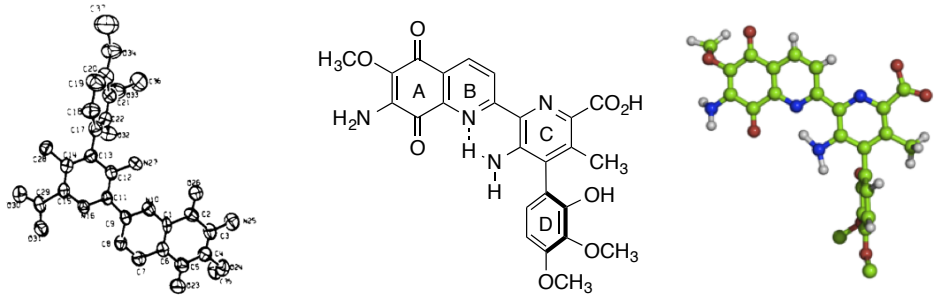

Figure 2-3. X-Ray crystal structure of **2.1** showing the planarity of the ABC rings and the D-ring rotation (adapted from Chiu and Lipscomb, 1974) and computer-generated models included for clarity[9]

Harding and coworkers used variable temperature ^{1}H-NMR experiments[10] to show that the major spatial configuration of **2.1** in solution coincides with the structure observed in the solid state and established that streptonigrin exists as a zwitterion in aqueous solution at pH 5.0–9.0 (Figure 2-4). The chirality of naturally derived **2.1**, first indicated by Chiu and coworkers' space group assignment,[9] could only arise from one of two possible centers of stereochemical information in the molecule: rotational hindrance of the biaryl bonds connecting ring B–C or ring C–D. Only the latter was expected to be configurationally stable, as the B–C axis has only one *ortho* substituent. The ABC ring system is also held in plane by hydrogen bonding between the pyridine 5'-amino group and the quinolinequinone nitrogen (Figure 2-4). Rotation about the C–D bond is restricted by steric hindrance of the amine and methyl groups on the C ring and the hydroxyl group on ring D. Thus **2.1** is axially chiral and was the first 'skewed' phenyl pyridine discovered in nature.[9,11]

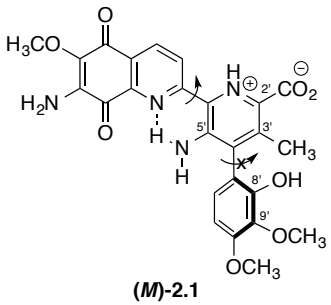

(*M*)-**2.1**

Figure 2-4. Solution conformation of (*M*)-**2.1** (in aqueous solution, pH 5.0–9.0)

The absolute configuration of **2.1** was first investigated in 1981 using circular dichroism (CD) and assigned a (*P*)-configuration.[11] This was based on the shorter wavelength Cotton effect in the CD spectrum which corresponds, according to the authors, to the biphenyl conjugated band, suggesting an "*S*" configuration. Since **2.1** lacked any reference substrates, a later replication of the optical rotation analysis was carried out using exciton coupled circular dichroic (ECCD) spectroscopy to allow direct determination of the absolute configuration through interacting chromophores.[12] The synthesized streptonigrin derivative **2.5** (with *p*-nitrobenzoyl groups appended to the 5'-amino and 8'-hydroxyl moieties of the methyl ester of **2.1**) showed a clear excitation couplet around 260 nm, corresponding to the known absorbance of *p*-nitrobenzoyl (Figure 2-5). The respective point of inflection in the new CD spectrum paralleled the expected maximum in the UV spectrum and so this negative Cotton effect indicated that the chromophores are oriented such that their transition moments form an anticlockwise twist, corresponding to an (*M*)-configuration (Figure 2-5).[12]

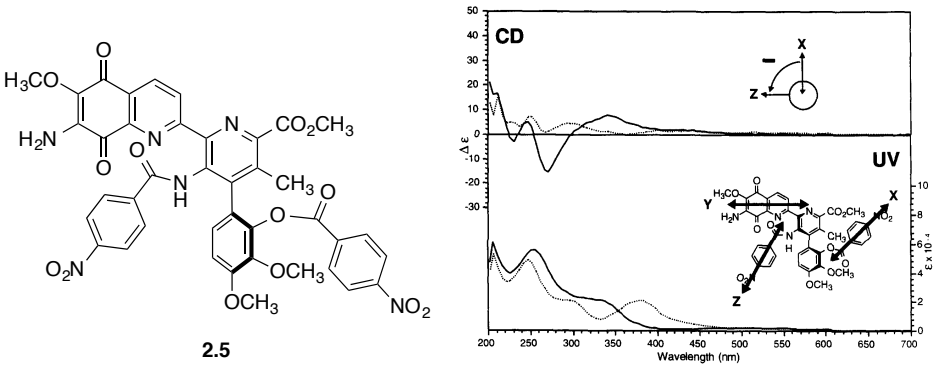

Figure 2-5. Structure of *p*-nitrobenzoyl derivative **2.5** and ECCD spectrum (adapted from Rickards 1997[12])

Bringmann and coworkers confirmed the absolute orientation of (*M*)-**2.1** using quantum mechanical CD calculations in 2008.[13] The theoretical molecular CD of (*M*)-**2.1** and (*P*)-**2.1**, generated by quantum chemical calculations, were compared to a CD curve measured experimentally, revealing acceptable agreement of the CD spectrum of (*M*)-**2.1** and experimental, while showing opposite curvature for the experimental as compared to the theoretical (*P*)-**2.1** curve (Figure 2-6).

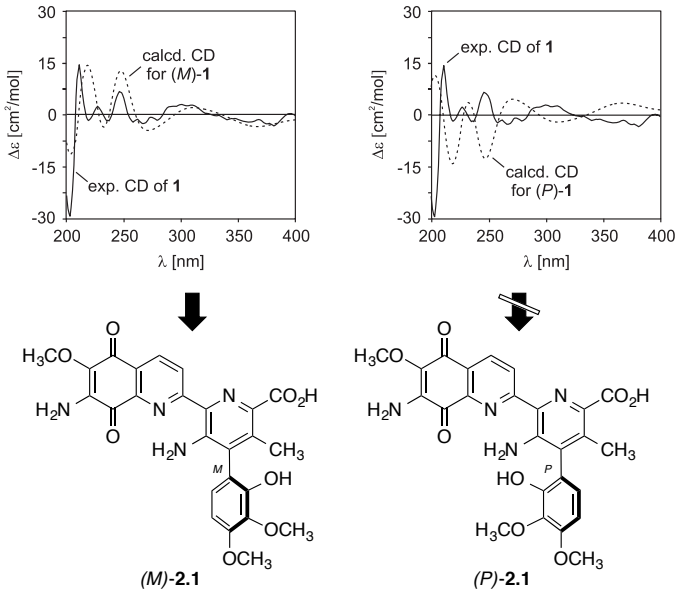

Figure 2-6. Calculated and experimental CD spectra of **2.1** [(B3LYP/6-31G*) global minimum structures] (adapted from Bringmann 2008[13])

The enantiomeric purity of naturally derived **2.1** was initially undisclosed, although samples have been measured in modern studies at >99% purity.[13] Racemization of the axial chirality in **2.1** is slow, with the persistence of optical rotation even after three hours of boiling **2.1** in a hydroxylamine/pyridine solution.[11] The buttressing effect of the bulky substituents in the adjacent positions–2'-carboxylic acid on ring C and 9'-methoxy on ring D–may contribute to the observed stability.[14] The barrier of rotation about the C–D axis has been calculated from CD measurements to be $\Delta G_{\delta} = 102.9 \pm 0.3$ kJ mol^{-1} at, 37.7 °C, meaning that at 25 °C or at physiological temperature no significant loss of optical activity occurs.[15]

2.1.3 Displayed biological activity

Preliminary studies performed on the *S. flocculus* broth filtrates showed low millimolar inhibition of a variety of Gram-positive and Gram-negative bacteria strains and were reported along with Rao and Cullen's disclosure of **2.1** as the active compound (Table 2-1).[1]

microorganism	minimum inhibitory concentration (μg/mL)
Micrococcus pyogenes var. aureus	0.39
Bacillus subtilis	<0.09
Mycobacterium tuberculosis 607	0.19
Salmonella typhosa	3.12
Klebsiella pneumoniae	1.56
Pseudomonas aeruginosa	6.25

Table 2-1. Early indications of the antibiotic activity of streptonigrin

Early studies in cell lines and animal models reported an efficacious antitumor activity against adenocarcinomas 755 in mice and human tumor type #1 in rats as well as HeLa cultures.[16-19] Clinical trials of **2.1** were initiated soon after its discovery, with patient results reported as early as 1961. Streptonigrin showed antitumor activity in patients diagnosed with breast,[17,20-22] lung,[21] head,[20] neck,[20] and cervical[17,22] cancer as well as lymphoma,[17,20-22] melanoma[22] and various sarcomas.[17,21,22] Additionally, **2.1**

gave promising results targeting Hodgkin's disease[22] and against a number of viruses[23] resulting in increased survival in mice infected with murine virus[24] and the inhibition of reverse transcriptases of avian myeloblastosis virus (AMV) and human immunodeficiency virus (HIV).[23,25,26]

The results from patient trials included some outstanding effects such as regression of massive head and neck tumors by 90%.[27] Changing the administration method from local and intravenous to continuous intravenous and intra-arterial infusions improved the therapeutic response while lowering the toxicity of this potent antitumor agent.[21,28] Unfortunately, researchers also found severe side effects including nausea, diarrhea, alopecia, mental confusion and severe bone marrow depression, with this last symptom cited as extreme and as the cause of treatment cessation or patient death in some cases.[25] Lack of request by researchers to conduct further research ultimately led to the discontinuation of clinical trials by the US National Cancer Institute in 1977, after seven types of tumors were successfully tested in phase II trials.[29]

It has only been in the years since 1977 that the mechanism of action of **2.1** has been elucidated. This intriguing structure **2.1** was also tested in combination therapies with improved results only shortly before the end of clinical trials.[30] The much more recent discovery that **2.1** can be bioactivated by DT-diaphorase has suggested that streptonigrin could be used to treat cancers with increased DT-diaphorase activity, for example human non-small cell lung cancer.[31,32] As recently as 2010, streptonigrin has been examined as part of a high-throughput screening assay and shown to be a potent, selective and irreversible protein arginine deiminase (PAD 4) inhibitor.[33] This suggests PAD 4 inhibition could be a plausible part of the

mechanism of action of **2.1** or suggests an additional target, as some cancer cell lines also overexpress this enzyme.

2.1.4 Mechanism of action of streptonigrin

The presence of the aminoquinone moiety suggests that **2.1** belongs in the class of anticancer agents containing this easily reduced, DNA-damaging structure along with anthracyclines, mitomycin C and mitoxantrone. Early studies demonstrated the damaging effect of **2.1** on DNA in cell and cell-free models and indicated that it interferes with cellular respiration and disrupts cellular replication of DNA.[31] The specific effects at the DNA level include production of single and double strand breaks (in vivo and in vitro), inhibition of topoisomerase II,[34] and induction of covalent DNA adducts, leading to the classification of **2.1** as a radiomimetic compound, causing DNA damage in cell-free and in cellular system via a targeted free-radical mechanism.[31] Although the flat structure of the ABC rings suggests that streptonigrin might insert between base pairs of DNA, studies have shown that **2.1** does not in fact intercalate or crosslink[35] but instead interacts with DNA electrostatically through binding the phosphine backbone.[25]

The elements found to be essential for biological activity (in cellular and cell-free models) were (i) reductive activation (ii) presence of oxygen and (iii) presence of metal ions.[25] It is presumed that **2.1** produces its genotoxic effects through the generation of free radicals in the presence of metal ions.[31] Reduction by NADH initiates the redox cycle of **2.1**, with proposed semiquinone **2.6** and hydroquinone **2.7** as important intermediates (Scheme 2-1). Radical species generated (in red) produce intracellular free radical oxygen species that can cleave DNA.[36] The agent presumed responsible for cleavage is the hydroxide radical ($OH^{\bullet-}$) and its short lifetime means that this cycle must occur close to DNA.

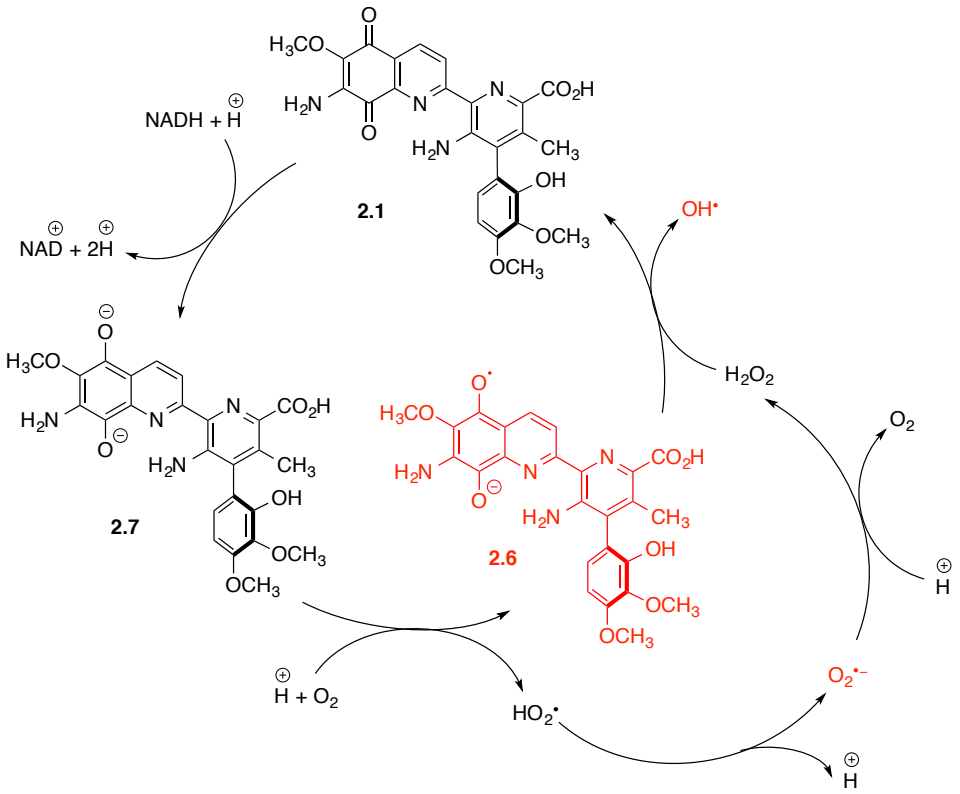

Scheme 2-1. Redox cycle of **2.1** (with potential DNA damaging elements indicated in red)

The importance of metal ions is a unique feature of the mechanism of action of **2.1** and they have been shown to be key to the redox cycle shown in Scheme 2-1. Metal complexes have been demonstrated with Zn^{2+}, Cu^{2+}, Cd^{2+}, Co^{2+}, Mn^{2+}, Pd^{2+}, and Au^{3+} and **2.1** through ion coordination with the two pyridyl nitrogens (Figure 2-7).[25] Studies of these complexes by NMR, UV-Vis spectroscopy, electrospray mass spectrometry, and X-ray diffraction analysis in solution determined that model ligands form 1:1 complexes, though excess equivalents of metal ions were required to fully complex **2.1**. This would indicate that at 37 °C, as in vivo, scavenging of metal ions most likely occurred, but the low stability of these complexes means that most of **2.1** would be present as the free drug.[25] The proposed roles of metal ions and the metal complexes have included as catalysts in the redox cycle, as delivery agents of the drug to DNA via complexation with **2.1** or semiquinone **2.6**, and, independently of the redox cycle, activation of oxygen at the metal center of the **2.1**–M^{n+} complex.[25]

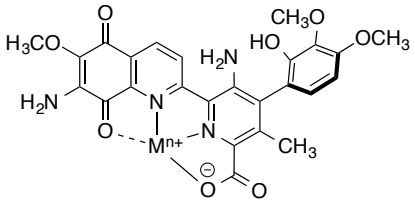

Figure 2-7. Proposed form of **2.1**–metal complex

Much of the understanding of the mechanism of **2.1** was derived from structure-activity relationship (SAR) studies of partial analogues. These data provided additional understanding of the mechanism of action through identification of the role of different structural elements. The synthesis of analogues and complete ABCD structures, as well as total and formal syntheses of **2.1** will be explored further in section 2.1.5.

2.1.5 Synthetic precedence

The synthetic studies towards partial and complete syntheses of **2.1** has spanned the fifty years since the discovery of this potent antitumor drug.[2,26,37-39] The analogues accessed, the resulting structure-activity relationship studies and the efforts towards total syntheses indicate the exquisite potential of this scaffold while allowing identification of areas for further research.

2.1.5.1 Generation of analogues and structure-activity relationship studies

Most of the analogues generated were AB- or ABC-ring substructures[2,40] which were tested to ascertain the key functional groups and ring configurations essential for biological activity as well as to help determine the mode of action[41] of **2.1** (Figure 2-8).

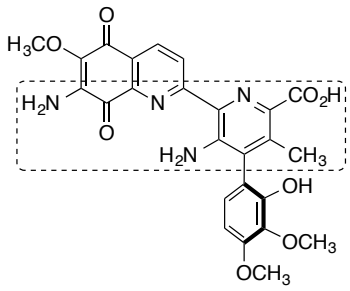

Figure 2-8. Key pharmacophore of **2.1** as proposed by Rao (box)

Key findings from the SAR studies included the importance of the quinone moiety of **2.1**, which is presumed to be critical for radical formation (see section 2.1.4). Removal of the *p*-quinone ring gave analogues with decreased activity, such as **2.8b** (Figure 2-9) blocked by an isopropylidene, which was 100 times less active than **2.1** against animal tumor model systems, and showed displayed no antibacterial or in vitro cytotoxic activity (Figure 2-9).[42] The loss of the AB system, such as CD-ring-only structure **2.8a** also showed no anticancer activity.[40] The role of the A-ring amino group was investigated through analogues with hydroxyl and methoxyl replacements which led to the loss of antimicrobial activity (see **2.9a** and **2.9b**, Figure 2-9).[41] Interestingly, carboxamide formation such as in **2.9c** was tolerated,[43] as well as C-ring amino group substitution (as in lavendamycin (see Figure 2-2) indicating select modifications are possible without loss of activity. The C-ring carboxy group was identified as part of the core pharmacophore since methyl ester **2.9d** shows only 1% of streptonigrin activity in tissue cultures[36] and no antimicrobial activity, potentially due to the prevention of zwitterion formation.[40] Structures lacking the C-ring carboxy and amino groups also proved to be inactive (**2.10a–b**).[44]

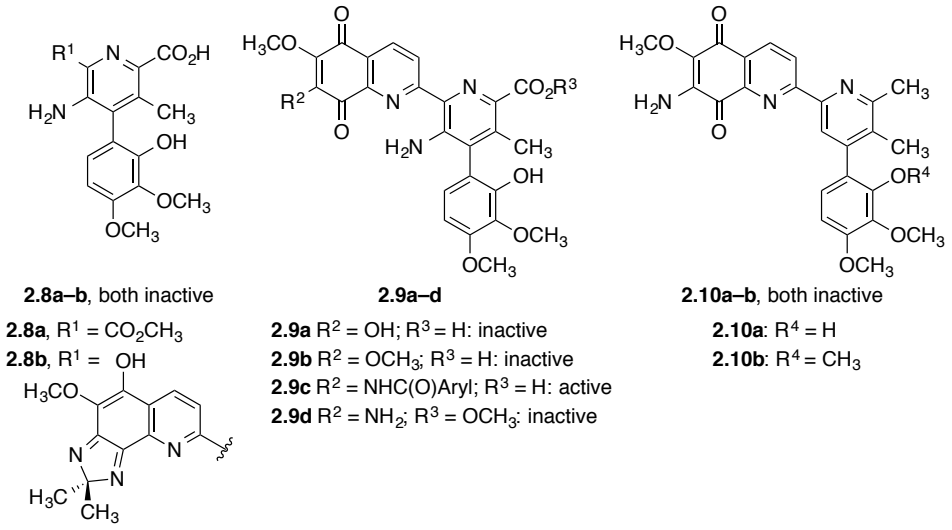

2.8a–b, both inactive

2.8a, $R^1 = CO_2CH_3$

2.8b, $R^1 =$

2.9a–d

2.9a $R^2 = OH$; $R^3 = H$: inactive

2.9b $R^2 = OCH_3$; $R^3 = H$: inactive

2.9c $R^2 = NHC(O)Aryl$; $R^3 = H$: active

2.9d $R^2 = NH_2$; $R^3 = OCH_3$: inactive

2.10a–b, both inactive

2.10a: $R^4 = H$

2.10b: $R^4 = CH_3$

Figure 2-9. Analogues of **2.1** and SAR results (in antimicrobial and antitumor assays)

The DNA cleaving ability of analogues containing just AB or ABC rings with various substituents was also explored. The quinolinequinone portion proved critical for this mechanism as AB-ring-only substructures were still able to cleave DNA in vitro (**2.11a–e**, Figure 2-10).[45-47] The role of the B-ring pyridyl nitrogen was also essential, as the removal of the ring nitrogen (such as **2.12a–c**)[47] and positional isomers (such as **2.13a–b**)[48] were shown to be incapable of cleaving DNA.

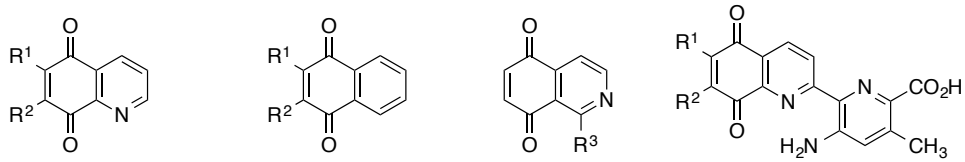

2.11a–e, all active

2.11a, $R^1 = OCH_3$; $R^2 = NH_2$

2.11b, $R^1 = NH_2$; $R^2 = OCH_3$

2.11c, $R^1 = OCH_3$; $R^2 = H$

2.11d, $R^1 = R^2 = Cl$

2.11e, $R^1 = Cl$; $R^2 = OH$

2.12a–c, all inactive

2.12a, $R^1 = Cl$; $R^2 = OH$

2.12b, $R^1 = R^2 = Cl$

2.12c, $R^1 = R^2 = H$;

2.13a–b, all inactive

2.13a, $R^3 = H$

2.13b, $R^3 =$ 2-pyridyl

2.14a–b, all active

2.14a, $R^1 = NH_2$; $R^2 = OCH_3$

2.14b, $R^1 = OCH_3$; $R^2 = NH_2$

Figure 2-10. Partial analogues of **2.1** and SAR results (in DNA cleaving assays)

The D ring confers axial chirality and is an important structural element of **2.1**, but the effect of chirality on the biological activity is underexplored. This is driven by early results showing analogues lacking the D ring gave persistent activity in

antitumor models (e.g. **2.14a–b**, Figure 2-10),[37,40] and Rao's conclusion that the D ring was not part of the key pharmacophore (see Figure 2-8).[41] However, additional studies using ABC analogues **2.14a–b** showed that the D-ring is required for one mechanism of action: induction of topoisomerase II-mediated DNA cleavage.[49] This alternative mode of action may have different structural requirements to the direct DNA cleaving mechanism and has not been explored further.

Additionally, the unnatural enantiomer of **2.1** has not been synthesized or independently tested. The only study to address the influence of the stereochemistry on the biological activity was performed on a derivative of racemic **2.1**. This was obtained through attachment of a chiral amino acid to the carboxy group of ring C, forming (*M*)- and (*P*)-**2.15** (Table 2-2).[50] The resulting diastereomers were separated and tested individually for inhibition of AMV reverse transcriptase and for antitumor activity against L5178Y cells. The diastereomeric pairs showed closely matched biological activity (compare entry 1 to 2 and entry 3 to 4) for both assays and the activity of mixtures compared to that of separated mixtures and to the activity of racemic **2.1** for the RT (AMV) assay (entries 5–7).

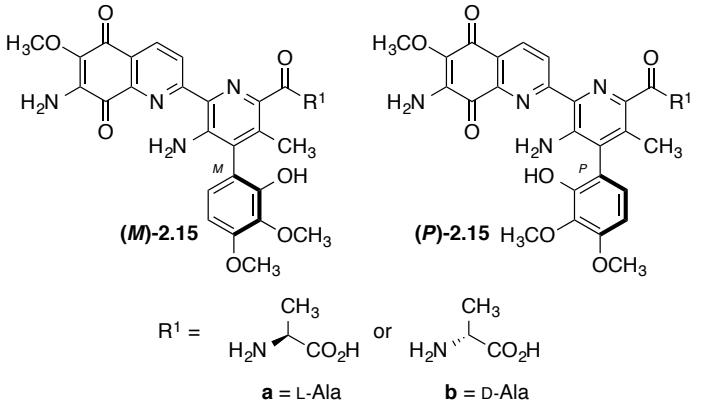

entry	compound	ID_{50} (μg/mL) RT (AMV)	L5178Y/S
1	**(*M*)-2.15a**, R^1 = L-Ala	2	>8.0
2	**(*P*)-2.15a**, R^1 = L-Ala	3	>8.0
3	**(*M*)-2.15b**, R^1 = D-Ala	2	0.13
4	**(*P*)-2.15b**, R^1 = D-Ala	2	0.04
5	**(±)-2.1**, R^1 = OH	3	0.004
6	**(±)-2.15a**, R^1 = L-Ala	3	>4.0
7	**(±)-2.15b**, R^1 = D-Ala	2	0.1

Table 2-2. Biological activity of resolved diastereomers of derivatized racemic **2.1**

Few full tetracyclic analogues have been generated and most complete ABCD structures discussed thus far were produced through derivatization of isolated **2.1**. This limits the production of analogues to basic transformations since direct isolation from fermentation is low yielding.[4] A few late-stage analogues have been accessed through fully synthetic methods, but none showed full elaboration of the substituents about the C–D bond and thus no enantioenrichment was possible or pursued (examples shown in Figure 2-11).[38,51-56]

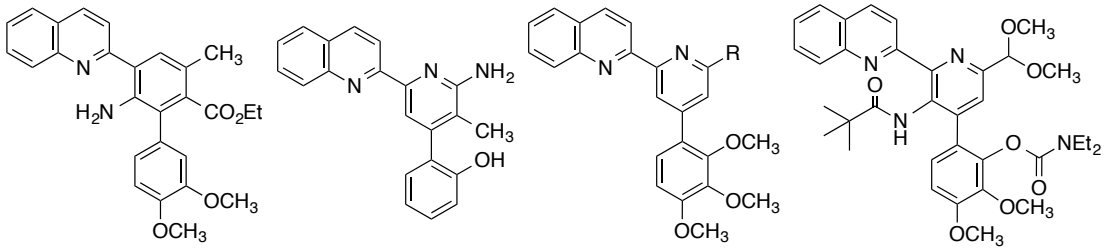

Figure 2-11. Full ABCD analogues of **2.1** generated through synthetic methods

2.1.5.2 Total and formal syntheses of streptonigrin

Pioneering synthetic work in the 1970s and 80s produced one total and two formal syntheses of **2.1** which also helped to advance organic synthetic methodology.[2] The first reported total synthesis of **2.1** was published by Weinreb and coworkers.[57] After twenty years of extensive preliminary studies, their 34-step route to **2.1** was published in 1980 with a final yield of 0.013%. The key steps included an imino Diels–Alder reaction to construct the CD rings (with ten steps needed to subsequently introduce the amino substituent on the pyridine ring) and a modified Friedlander reaction to form the quinolone quinone (Figure 2-12).

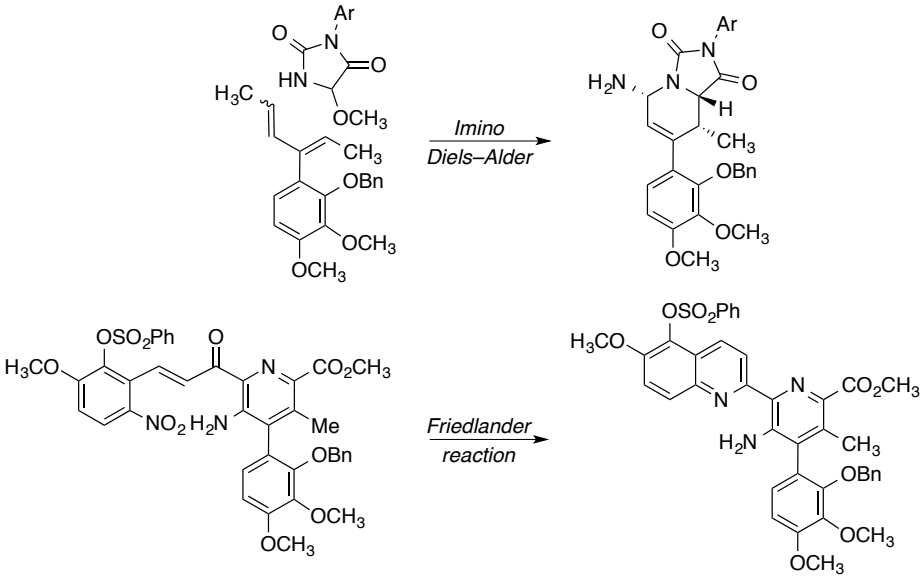

Figure 2-12. Key steps of Weinreb's total synthesis (34 steps, 0.013% yield)

A formal synthesis of **2.1** published by the Kende group in 1981 would allow access to **2.1** in 27 steps with a yield of 0.07%.[58] This route constructed the CD rings through a regiocontrolled condensation then also used a Friedlander synthesis to complete the AB-ring system (Figure 2-13).[44,58] Kende's route intersects with a late-stage intermediate of Weinreb's and the A-ring functionality could subsequently be installed taking advantage of Kende's improved end game strategy.[44]

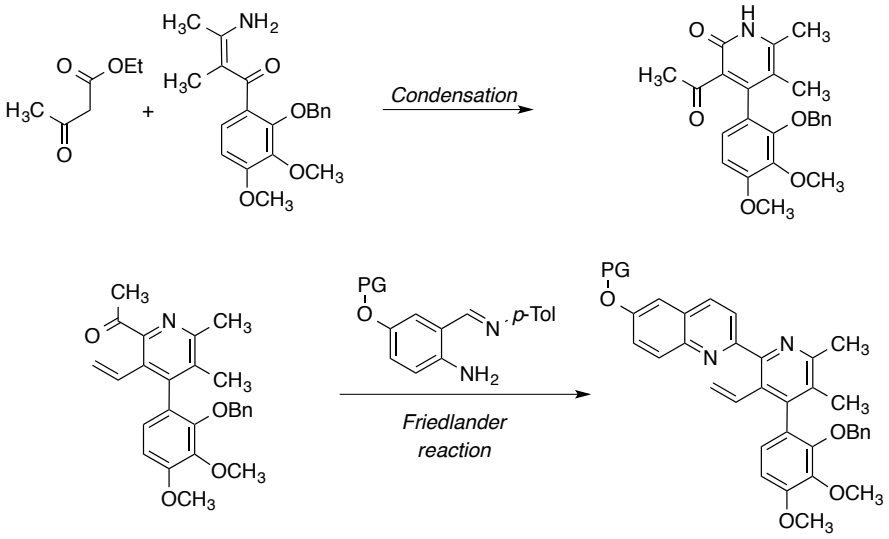

Figure 2-13. Key steps of Kende's formal synthesis (21 steps, 0.013% yield)

The Boger group published a formal synthesis of **2.1** shortly after.[59] The researchers employed a convergent 7-step synthesis of the tetracycle using two consecutive Diels–Alder reactions with inverse electron demand as key steps (Figure 2-14). Four additional steps provided a late stage Kende intermediate, completing a formal synthesis of **2.1** in 17 steps with an overall yield of 0.5%.

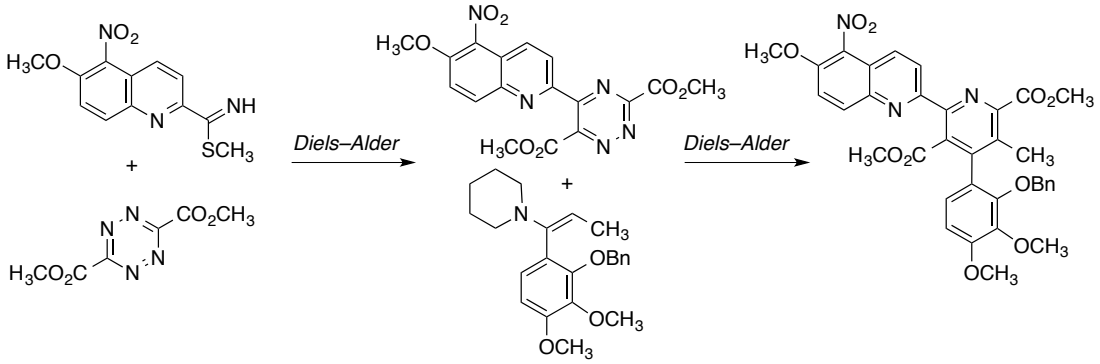

Figure 2-14. Key steps of Boger's formal synthesis (17 steps, 0.5% yield)

In the 25 years following, no additional total syntheses were published. Questions still remain regarding the mechanism of action including the cause of bone marrow depression. The potential to produce additional ABCD analogues and, for the first time, synthetically accessed enantioenriched structures inspired the project described herein.

2.2 Results and Discussion

The Donohoe group initiated a study towards a modern, improved total synthesis of **2.1**. An early route was designed by colleagues Dr. Chris Jones and Prof. Luiz Barbosa to obtain **2.1** in 14 linear steps and an overall yield of 11%.[60] In addition to improving the yield, step-count and operational simplicity compared to previous syntheses, the route was designed to allow easy access to full ABCD-ring model systems due to the late-stage biaryl linkages achieved through Suzuki and Stille couplings. This primary route is described in section 2.2.1 and was used and optimized in this work. Additionally, with the aim of constructing a novel library of streptonigrin analogues, we sought to advance and refine the route and explore a synthetic method to access enantiopure **2.1**.

2.2.1 Retrosynthesis and first route to key intermediate

The retrosynthetic analysis of **2.1** suggested an exciting application of methodology developed in the Donohoe group to form the pentasubsituted pyridine core **2.1** (Figure 2-15). Metal-catalyzed cross-coupling reactions would construct the two biaryl bonds by joining **2.16** to AB- and D-ring substructures (**2.17** and **2.18**, respectively, Figure 2-15). The generation of heteroaromatic compounds such as pyridone **2.19** utilizing a ring-closing metathesis (RCM) reaction as the cyclization step was well-precedented in Donohoe group literature.[61-63] RCM-precursor **2.20** was imagined either with inclusion of a protected amino substituent ($X = NR_2$) or with X = H for a simpler, less hindered RCM transformation with subsequent amine introduction (Figure 2-15).

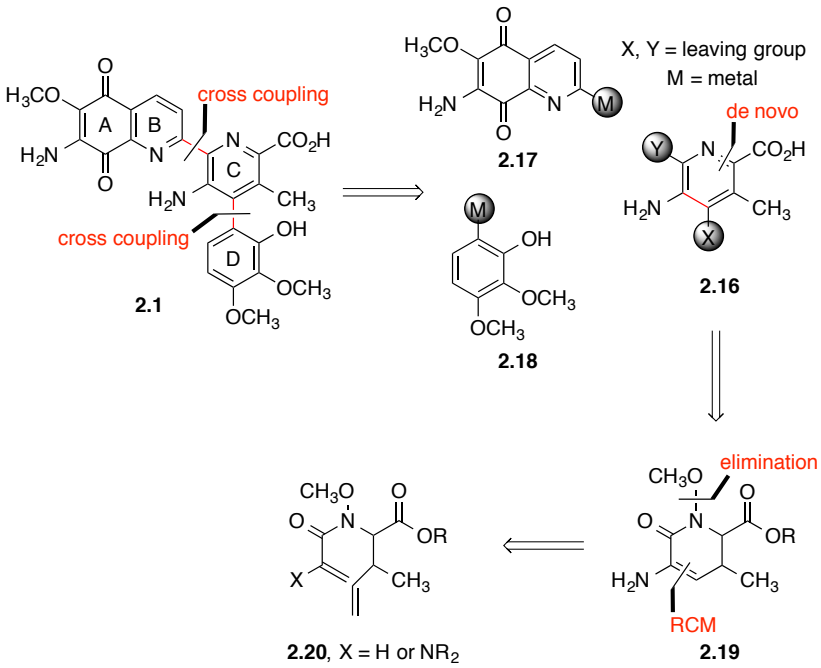

Figure 2-15. Retrosynthetic analysis to access **2.1** as designed in the Donohoe group

The route, as designed and optimized by Dr. Chris Jones and Prof. Luiz Barbosa proved fruitful in my hands, with yields from the 2011 communication indicated in the following schemes for comparison. Beginning from the simple and inexpensive starting material ethyl glyoxalate, **2.21**, condensation with methoxyamine hydrochloride furnished oxime **2.22** (Scheme 2-2a). This was subjected to a regioselective zinc-mediated crotylation to yield methoxyamine **2.23** in 78% yield over two steps. Phthalamide was chosen as the protecting group (PG) to introduce the desired protected amine functionality, as the imide-containing PG was found to be less nucleophilic and more stable than amide-containing groups such as the use of 2-acetamidoacrylic acid (PG screening performed by Dr. Chris Jones). *N*-Phthalimide-protected α-amino acrylic acid **2.24** was also easily formed from phthalic anhydride and DL-serine in 43% yield (Scheme 2-2b).[64] In situ formation of the acid chloride of **2.24** and addition of **2.23** gave RCM precursor **2.25** in 99% yield and 77% yield over these first three steps.

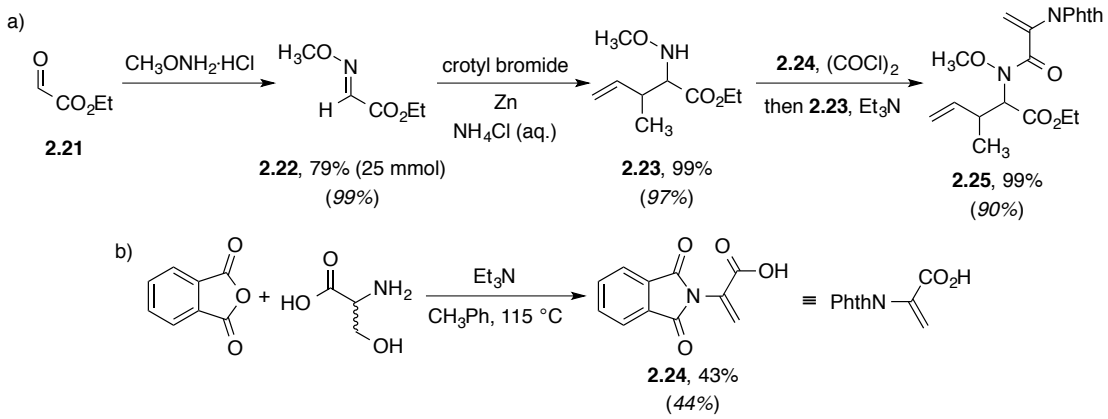

Scheme 2-2. (a) Synthesis of RCM-precursor **2.25** from ethyl glyoxalate; (b) synthesis of *N*-phthaloyldehydroalanine from DL-serine (yields in brackets indicate yields from Donohoe 2011[60])

The subsequent RCM was made challenging by the bulky 1,1-disubstituted alkene[61] containing an enamine moiety, which had not previously been employed in such reactions.[63] Optimization by Dr. Chris Jones led to the use of 5 mol% Hoveyda–Grubbs second-generation catalyst (G–H II, added through slow addition using a syringe pump) and the use of benzoquionone as an additive (to quench Ru–H species formed in situ) achieving RCM product **2.26** in 70% yield (4.4 mmol scale) with scaling up to 3.0 g (7.8 mmol scale) possible (Scheme 2-3). Subsequent deprotection of the amino group, transesterification to the methyl ester and methanol elimination to access pyridone **2.27** were achieved in one pot through the use of quinuclidine as base and followed by methylamine addition (which effected cleavage of the N-protecting group) (Scheme 2-3). The use of methanol as solvent enabled the route to converge with a late-stage intermediate from Weinreb's synthesis.[57] Thus, a three-transformation procedure afforded **2.27** in 80% yield from **2.26**. This primary route allowed the formation of key pyridione substrate (**2.27**) in 5 steps and 43% yield from commercially available **2.21**.

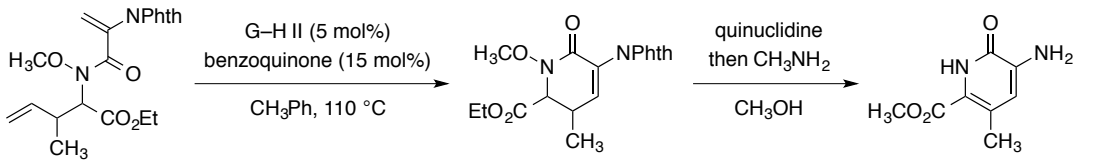

2.25 **2.26**, 70% (4.4 mmol) (*76% 0.20 mmol*) **2.27**, 80% (4.4 mmol) (*89%*)

Scheme 2-3. RCM and elimination reactions to form key pyridone intermediate **2.27**

2.2.2 Secondary route to pyridone intermediate

Key intermediate **2.27** was also accessible through a second route, envisioned using the simpler RCM precursor **2.20** (X = H, see Figure 2-15) for a predicted higher yielding RCM and subsequent amino group introduction accomplished through nitration and reduction. Despite the increased step-count as compared to the first route, the higher yield and improved operational convenience, especially with regards to the RCM, could allow more expedient access to **2.1**.

This secondary route was initiated from the same methoxyamine substrate as the previous route (**2.23**, see Scheme 2-2). Acylation with acryloyl chloride in my hands produced **2.28** in 96% yield and the subsequent RCM was achieved with lower catalyst loading (3.0 mol%) to give **2.29** in 99% yield (Scheme 2-4). This step was scaled to 2 g (8.3 mmol) and the catalyst loading could be lowered to 1.0 mol% without a drop in yield (necessitating 72 h instead of 24 h reaction time). Elimination of the methoxide protecting group was effected through use of 1,8-diazabicyclo[5.4.0]undec-7-ene (DBU) and use of methanol as solvent allowed transesterification to obtain a single methyl ester product **2.30** in 87% yield (Scheme 2-4).

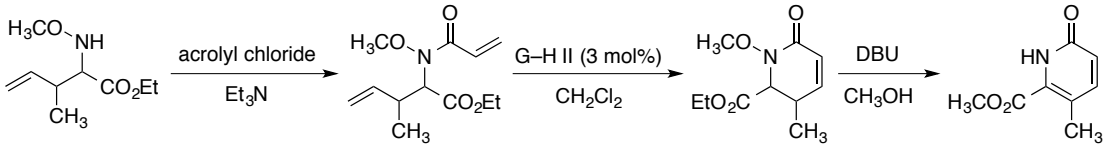

2.23 **2.28**, 76% **2.29**, 99% **2.30**, 87%

Scheme 2-4. Secondary route to pyridone core with simpler, higher yielding RCM step

The subsequent steps of nitration and reduction to converge with aminopyridone **2.27** required further development. By utilizing the inherent preference of pyridones to undergo electrophilic substitution at C-5, this transformation had been used in a previous synthesis of CD-ring analogues of **2.1**[65] and initial screening (by Prof. Luiz Barbosa) in the Donohoe group showed promise. Subjection of **2.30** to nitric acid with catalytic sulfuric acid[66,67] gave the highly polar nitropyridone **2.31** in 80% yield (Table 2-3, entry 1). Replications and scaling in my hands gave unpredictable yields, in part due to the difficulty of purifying the extremely polar **2.31**, with flash column chromatography (FCC) giving low yields (entry 2). Scaling up the reaction also proved difficult as increasing from 3 to 10 mmol led to a significant drop in yield, even prior to FCC (entry 3).

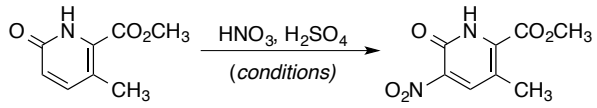

2.30

2.31: R = CH_3
2.32: R = H

entry	conditions	workup	purification	yield 2.31 (%)
1	RBF & condenser	filtration	FCC	80[a]
2	RBF & condenser	filtration	FCC	55
3[b]	RBF & condenser	filtration	crude	30
4	add portionwise HNO_3	filtration	FCC	22
5	add portionwise HNO_3	filtration	crude	>100
6	add portionwise HNO_3	extraction	crude	16
7	add portionwise HNO_3; add CH_3OH	extraction	crude	41

3 mmol **2.30**, 50 °C, 5–10 h, monitored by TLC to SM consumption; [a]performed by Dr. Luiz Barbosa; [b]10 mmol **2.30**

Table 2-3. Optimization of difficult nitration step

During the course of the five-hour reaction, nitrogen dioxide evolution was observed indicating that nitric acid was decomposing. In an effort to overcome this problem, nitric acid was added portionwise throughout the course of the reaction. Utilizing these conditions and a filtration collection gave low yields after FCC (entry 4) though some iterations gave a crude mass recovery greater than 100% (entry 5). In this latter case, the resulting crude product appeared clean by ^{1}H NMR spectroscopy,

but the IR spectrum revealed large broad peaks associated with the presence of inorganic impurities (2360 cm^{-1} and 1020 cm^{-1}).[68] A water wash removed the salts, but an aqueous workup did not prove to be reliable for this system (entry 6). This was discovered to be due to the presence of hydrolyzed byproduct **2.32** in the reaction and loss of this mass to the water layer. It was demonstrated that material lost by conversion to the acid could be recovered during the reaction upon addition of methanol to the heated mixture, but the yield remained low (entry 7).

The highly polar nature of **2.31** prompted more expedient optimization of the nitration through reduction of the nitro group to amine **2.27** and assessment of a two-step yield. The reduction had previously been performed using iron in acetic acid, but for ease of product purification, a hydrogenation with palladium on carbon was performed on clean **2.31** to yield **2.27** in 82% yield (Table 2-4, box). Thus, the two-step procedure was undertaken with direct reduction of the nitro group after nitration. Initially, the two-step procedure gave a maximum yield of 18% (Table 2-4, entry 1). Use of a closed reaction system showed dramatic improvements to 38% over two steps (entry 2). Pre-stirring the mixture of **2.30** and reagent acid before heating led to an additional increase in yield, likely due to formation of active nitrating species before decomposition which occurs upon heating, with a maximum of 88% yield observed over two steps (entry 3). Unfortunately, scaling this optimized procedure still proved capricious and increasing beyond 3 mmol led to a significant drop in yield (entry 4).

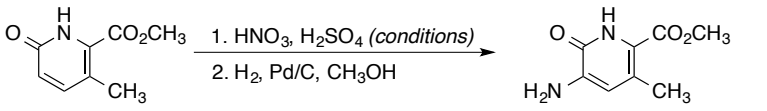

entry	conditions	workup	yield 2.27 (%) (two-step from 2.30)
1	RBF & condenser	filtration	18
2	sealed tube	extraction	38
3[a]	sealed tube	extraction	88
4[b]	sealed tube	extraction	22

3 mmol **2.30**, 7 equiv. HNO_3, 50 °C, 5.5 h; [a]pre-stir at 0 °C, 7 h; [b]10 mmol **2.30**

Table 2-4. Two-step optimization of nitration and reduction to aminopyridone **2.27**

Ultimately, this secondary route allowed access to **2.27**, converging with the primary route, in 7 steps and 45% yield compared to 43% yield in 5 steps from that route. Though this route provided an improved yield and ease of operation (with simpler transformations and lower catalyst loadings), the difficulty of scaling the nitration step led to the preference of the previous route for larger-scale synthesis.

2.2.3 Formation of key ABCD-ring framework of streptonigrin

With **2.26** in hand, the synthesis proceeded cleanly to install the two cross-coupling handles for B–C and C–D ring biaryl bond formation. It was hypothesized that C-ring C6 leaving group would be more reactive than C4 towards oxidative addition of Pd(0) and thus the order of biaryl couplings would be arranged to allow C6 then C4 coupling. The C6 triflate was easily installed using triflic anhydride and 2,6-di-*tert*-butyl-4-methylpyridine (DTBMP) to yield **2.32** in 73% yield (Scheme 2-5). A simple NBS bromination furnished pentasubstituted C-ring precursor **2.33** in 96% yield.

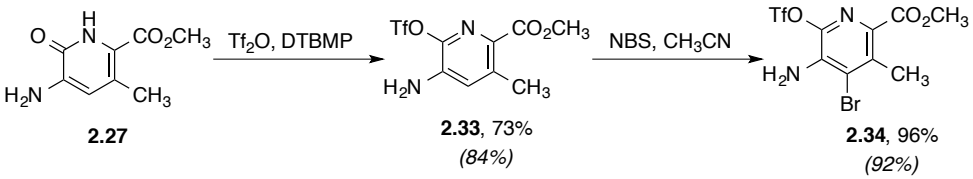

Scheme 2-5. Formation of key pentasubstituted pyridine

AB-ring stannane **2.35** was prepared in six steps from 2,4,5-trimethoxybenzaldehyde (Scheme 2-6), through subjection to nitration and reduction to form substituted aniline **2.37**. Coupling with **2.38** (prepared in one step) and acid-mediated quinolinone formation yielded **2.40** in 77% yield over two steps. The 2-chloroquinoline, **2.41**, was found to be the ideal substrate for 2-stannane formation (optimization performed by Dr. Chris Jones) and was accessed in my hands in 81% yield. **2.41** was transformed to trimethylstannane **2.42** and used without purification as it decomposed on silica gel.

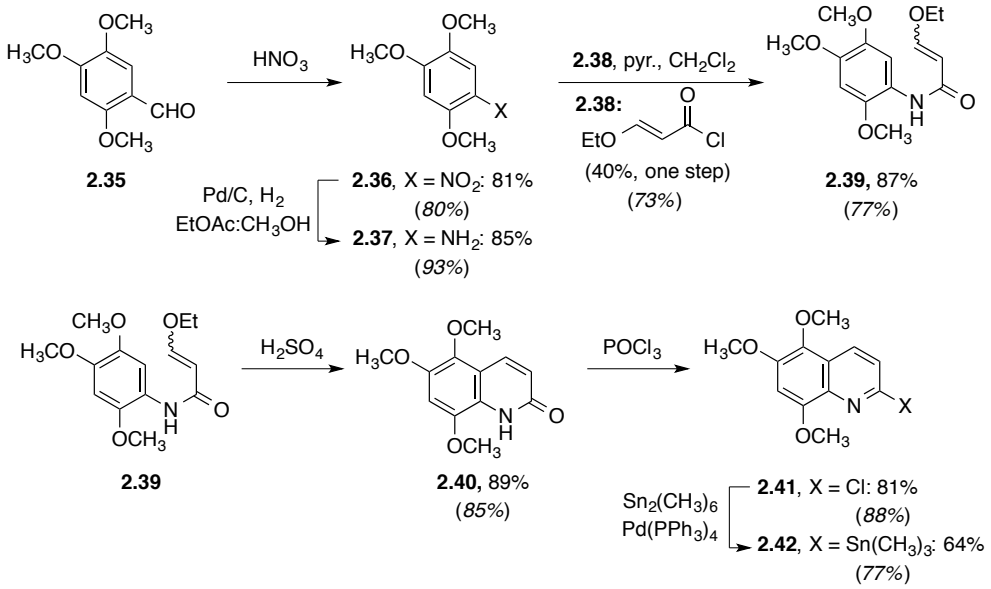

Scheme 2-6. AB-ring system formed and converted to stannane for Stille coupling

The Stille coupling of **2.34** and **2.42** proceeded smoothly to yield **2.43** and, as demonstrated previously,[60] there was no cross reactivity or byproducts observed from reaction at C6 (Scheme 2-7a). The subsequent Suzuki–Miyaura coupling joined **2.43** and boronate **2.46** (prepared in three steps and 51% yield, Scheme 2-7b) to give racemic **2.47** in 74% yield (Scheme 2-7a). Thus, this expedient synthesis allowed assembly of **2.47**, the tetracyclic core of **2.1**, in 17% yield over 9 steps (primary route) or 18% over 11 steps (secondary route).

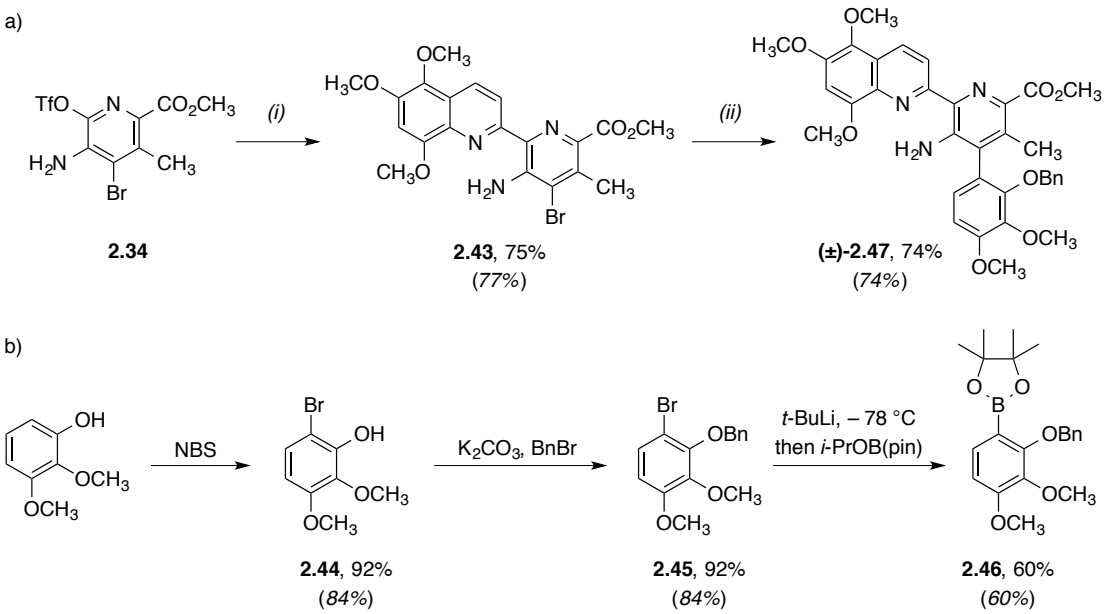

2.34

2.43, 75%
(*77%*)

(±)-2.47, 74%
(*74%*)

2.44, 92%
(*84%*)

2.45, 92%
(*84%*)

2.46, 60%
(*60%*)

Scheme 2-7. (a) Stille coupling and racemic Suzuki–Miyaura reaction to form tetracyclic core and (b) boronate ester coupling partner formation
Conditions: (i) 1.5 equiv. **2.42**, $Pd(PPh_3)_4$ (5 mol%), CuI (10 mol%), CsF, CH_3Ph, 110 °C ; (ii) 1.5 equiv. **2.46**, $Pd(PPh_3)_4$ (10 mol%), K_3PO_4, dioxane:water, 110 °C.

2.2.4 Asymmetric Suzuki–Miyaura coupling to form chiral C–D ring bond

The successful catalytic C–D ring bond formation encouraged the development of methodology to form a single atropisomer of the biaryl bond and enable late-stage synthetic access to enantiopure intermediates of **2.1** for the first time.

Typically, chiral compounds with non-centrochirality (unlike the typical example of a diversely substituted quaternary carbon) have been accessed in enantiomerically enriched forms by resolution of racemates or stoichiometric deriviatization from the appropriate enantiomerically enriched precursors. Examples of catalytic enantioselective induction of axial chirality are rare.[69] Though examples of asymmetric S_NAr,[70] catalytic Kumada[71,72] and Negishi[73] cross-coupling methods exist, the Suzuki–Miyaura (S–M) coupling has advantages including functional group tolerance and increased stability of the boronic acid coupling partner.

2.2.4.1 Precedence for asymmetric Suzuki–Miyaura reaction

Since the pioneering asymmetric catalytic S–M couplings published by Buchwald[74] and Cammidge,[75] method development in this area has pursued a variety of ligand classes including P-N ligands, monophosphines, diphosphines, dienes, phenyl bisoxazolines and heterocyclic carbenes (Scheme 2-16).[69,76,77] The transformations published have overwhelmingly focused on binapthyl couplings with very few biphenyl examples[78] and none involving a heterocycle. Though binapthyl products can find utility as ligands, there is limited applicability of this transformation to natural product and pharmaceutical syntheses. The reported yields and levels of enantioselectivity also varied greatly and thus the generality of this useful transformation was still lacking (Figure 2-16).[73,75,79-82]

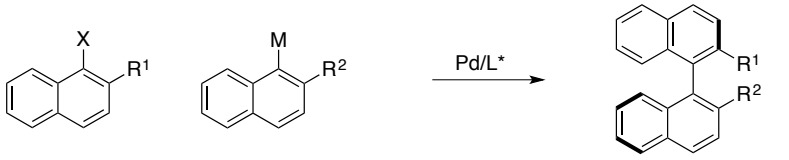

X	R^1	M	R^2	L*	yield (%), ee%
I	OCH_3	$B(OH)_2$	CH_3	(*S*)-(*R*)-ppfa	44%, 63%
I	OCH_3	$B(OH)_2$	OCH_3	(*R*)-BINAP	76%, 36%
Br	OCH_3	$B(OH)_2$	H	(*S*)-Cy-BINAP	17%, 84%
Br	CH_3	$B(OH)_2$	CH_3	(*S*)-(*R*)-ppfa	55%, 90%
Br	H	$B(OH)_2$	CH_3	**2.48**	54%, 46%
Br	CH_3	$B(OH)_2$	H	**2.49**	80%, 90%

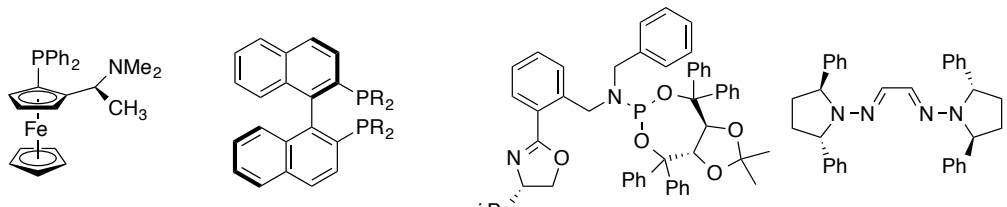

ppfa (*R*)-BINAP, R = Ph (*R*)-Cy-BINAP, R = C_6H_{11} **2.48** **2.49**

Figure 2-16. Summary of literature precedent for asymmetric S–M reactions (Adapted from Ogasawara 2009[69])

The difficulty of the asymmetric S–M transformation stems directly from the requirements for axial chirality. Atropisomerism is the term for chirality derived from hindered rotation about an axis (typically an aryl–aryl single bond).[3,83] A

configurationally stable biaryl bond requires a high barrier to rotation (defined as greater than 1000 sec by Oki)[84] which typically requires three *ortho* substituents, showing the following trend for high to low predicted hindrance: bromine >> methyl > chlorine > nitro > carboxylic acid > methoxy > fluorine.[85] Thus the catalytic system chosen for an asymmetric S–M reaction must achieve the coupling of two highly hindered coupling partners in sufficient conversion while also containing geometry to drive enantiocontrol. Thus, low coupling efficiency is often married to the requirement of stereoselectivity, and the desired reaction competes with hydrolytic deboronation or dehalogenation of starting substrates. When embarking on this project, no catalytic enantioselective S–M biaryl couplings had been employed in a natural product total synthesis. A synthesis of an analogue of the natural product (-)-rhazinilam was reported in 2003 by Baudoin and coworkers. This was also the only enantioselective S–M methodology to form biphenyls (Scheme 2-8).[78]

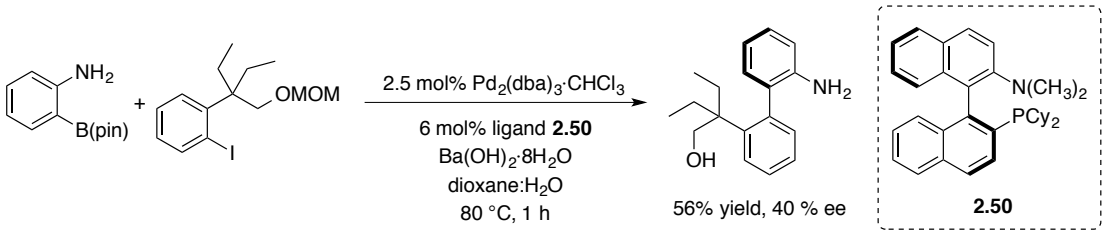

Scheme 2-8. Natural product analogue synthesized with enantioselective S–M method[78]

2.2.4.2 Initial asymmetric Suzuki–Miyaura coupling results

Preliminary investigations of an asymmetric coupling of ABC- and D-ring precursors **2.43** and **2.46** (see Scheme 2-7) were performed by Dr. Chris Jones. He showed that **2.47** could be produced with an enantiomeric excess (ee) of 22% using $Pd(OAc)_2$ and (*R*)-2,2'-bis(diphenylphosphino)-1,1'-binaphthalene (**2.51**, (*R*)-BINAP, Figure 2-17) at 65 °C. Chiral monodentate phosphine ligands, such as (*R*)-(+)-2-(diphenylphosphino)-2'-methoxy-1,1'-binaphthyl ((*R*)-MOP, **2.52**), gave racemic

product and chiral bidentate amino phosphine ligand (R_p)-1-[(1*S*)-(1-aminoethyl)]-2-(diphenylphosphino)ferrocene (**2.53**) reduced catalytic activity.

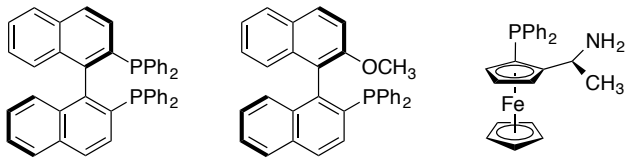

2.51: (*R*)-BINAP **2.52:** (*R*)-MOP, R = OCH_3 **2.53**

Figure 2-17. Chiral non-racemic ligands examined in preliminary asymmetric S–M screen

In my hands, the 22% ee observed using (*R*)-BINAP proved reproducible (Table 2-5, entry 1) and investigations to find conditions with increased enantioselectivity were undertaken. The low yield and low solubility of **2.47** impeded HPLC analysis and prompted optimization of the initial asymmetric S–M reaction before pursuit of increased enantioselectivity.

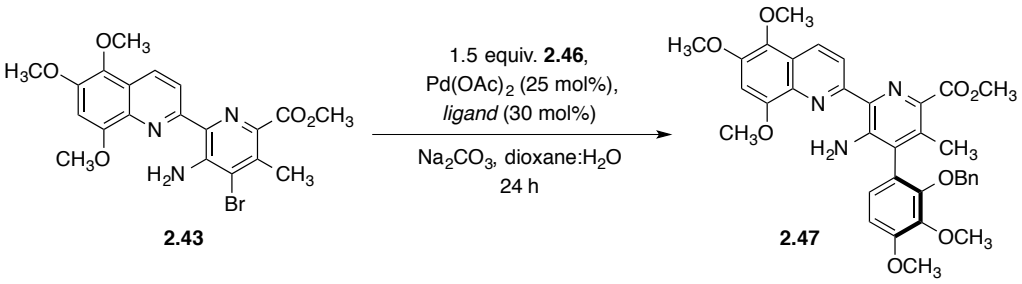

2.43 **2.47**

entry	ligand	temp (°C)	yield 2.67 (%)	ee (%)[a]
1	(*R*)-BINAP	60	65	22
2	(*R*)-BINAP	110	80	<10
3	(*R*)-BINAP	40	37	27
4	(*R*)-BINAP[b]	40	42	21
5	(*R*)-BINAP[b]	40	55	13
6	(*R*)-BINAP[c]	40	40	<10
7	(*R*)-BINAP[c]	40	51	<10

[a]Measured by analytical chiral HPLC; [b]Entry 4 run for 38 h, entry 5 for 48 h; [c]Entry 6 run using 1:1 metal:ligand and entry 7 run using 1:2 metal:ligand

Table 2-5. Optimization of asymmetric S–M reaction conditions to enable a ligand screen

Byproducts of the reaction included protodeboronated compound **2.54** and byproduct **2.55** which results from protonolysis of transmetallated **2.42** (Figure 2-18).

These were unsurprising given the high steric demands of the coupling bulky substrates and did not suggest clear alternative reaction conditions.

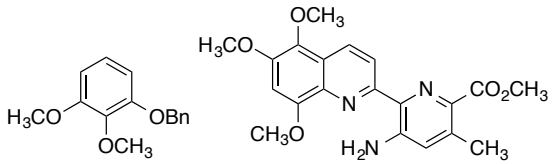

Figure 2-18. Compounds observed as byproducts of the asymmetric S–M reaction

Increasing the temperature of the S–M reaction resulted in lower levels of stereocontrol (Table 2-5, entry 2), while a lower temperature (40 °C) afforded some increase in enantioselectivity, though with a decrease in yield (entry 3). Increased reaction time led to higher conversion of starting materials to desired product, but with a lower observed ee (entries 4 & 5). This implied a loss of enantiocontrol or loss of enantioenrichment of **2.47** over the course of the reaction, though the latter is known to be slow at 40 °C.

The ratio of metal to ligand has been shown to affect the enantioselectivity in asymmetric S–M transformations.[79] The adjustment of metal:ligand to 1:1 and 1:2 in our system resulted in a decrease in ee in both cases (entries 6 & 7). Alternative bases and additives such as CsF,[86] Ag_2O[87] and CuI[88] yielded only returned starting materials (not shown in Table 2-5). Thus our best efforts gave only slightly improved yields but would allow sufficient conversion to screen additional ligands.

2.2.4.3 Ligand screen for increased enantioselectivity

Use of the reaction conditions described above allowed screening of the enantioselectivity resulting from use of bidentate phosphine ligands **2.56–2.61** (Table 2-6, entries 2–7).

entry	ligand	temp. (°C)	yield 2.47 (%)	ee (%)[a]
1	(*R*)-BINAP, **2.51**	40	65	(–) 27
2	(*R*)-Tol-BINAP, **2.56**	40	20	(–) 35
3	(*R*)-H_8-BINAP, **2.57**	40	43	(–) 27
4	(*R*)-DM-BINAP, **2.58**	40	25	(–) 36
5	(*R*)-SEGPHOS, **2.59**	40	41	(–) 13
6	(*R*)-DM-SEGPHOS, **2.60**	40	38	(–) 15
7	(*R*)-DTBM-SEGPHOS, **2.61**	40	15	(–) 22
8	precatalyst **2.64**	40	17	(+) 40
9	phosphino hydrazone **2.63**	40	65	(+) 42
10	phosphino hydrazone **2.63**	60	85	(+) 29
11	phosphino hydrazone **2.63**	110	54	(+) 8

[a]Measured by analytical chiral HPLC, absolute configuration unknown

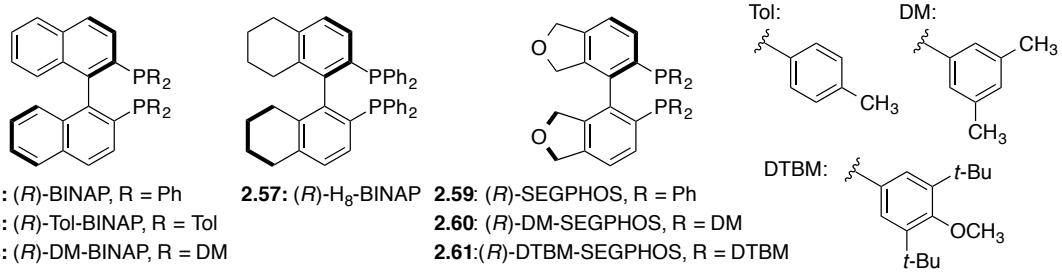

2.51: (*R*)-BINAP, R = Ph
2.56: (*R*)-Tol-BINAP, R = Tol
2.58: (*R*)-DM-BINAP, R = DM

2.57: (*R*)-H_8-BINAP

2.59: (*R*)-SEGPHOS, R = Ph
2.60: (*R*)-DM-SEGPHOS, R = DM
2.61:(*R*)-DTBM-SEGPHOS, R = DTBM

Table 2-6. Screen of ligands for asymmetric S–M reaction (with commercially available bidentate phosphine ligands shown, see Scheme 2-9 for synthesized **2.64**)

The highest enantioselectivity was achieved with functionalized versions of the BINAP core (ligands **2.56** and **2.58**, entries 2 and 4). However, this was observed with a concurrent decrease of yield from 65% (entry 1) to 20% and 25%, a trend demonstrated across the series of biphosphines tested. The SEGPHOS scaffold, with benzodioxole backbones replacing the naphthyl rings, gave the lowest enantioselectivities (entries 5–7).

The report of a new phosphino hydrazone precatalyst **2.64** for bulky binapthyl systems was pursued as a promising P-N ligand system.[89] The precatalyst was synthesized, as described in the publication by Lassaletta and coworkers, in five steps from commercially available diketone **2.62** (synthesis performed by Dr. Chris Jones, Scheme 2-9).

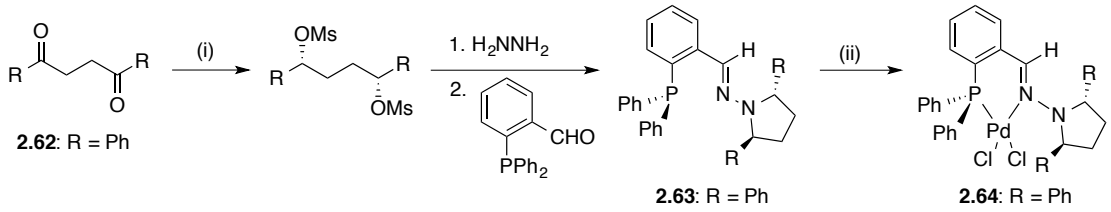

Scheme 2-9. Synthesis of precatalyst **2.64** (performed by Dr. Chris Jones)
Conditions (i) Asymmetric reduction; (ii) $PdCl_2(CH_3CN)_2$

The use of **2.64** in the asymmetric S–M reaction gave promising results showing an increase in enantioselectivity to 40% albeit with a lower yield (Table 2-6, entry 8). The resulting enriched enantiomer in the reaction using **2.64** was the opposite atropoisomer observed in entries 1–7. This is indicated by the (+) vs (–) designation, as the absolute configuration is not known. The use of the free phosphino hydrazine **2.63** with $Pd_2(dba)_3$ improved the yield to 65% coupled with 42% ee (entry 9). Increasing the temperature led to higher yields with a drop in enantiocontrol (entry 10 & 11).

A further increase of enantioselectivity was anticipated through the use of a bulkier substituent on the C2-symmetric pyrrolidine in **2.63**. Synthesis of a novel ligand was commenced, beginning through attempts to access diketone **2.69** (with R = anthracenyl, Scheme 2-10). The dimerization of 9-acetoanthrace **2.65** was attempted through S_N2 reaction of LDA enolate **2.67** with a synthesized α-bromine derivative (**2.66**) as well as oxidative enolate coupling using Cu(II) 2-ethylhexanoate (**2.68**) and the enolate **2.67** (Scheme 2-10). Unfortunately both routes failed in such a bulky system and the 1,4-diketone was not successfully synthesized, leading to the abandonment of this route to the proposed ligand.

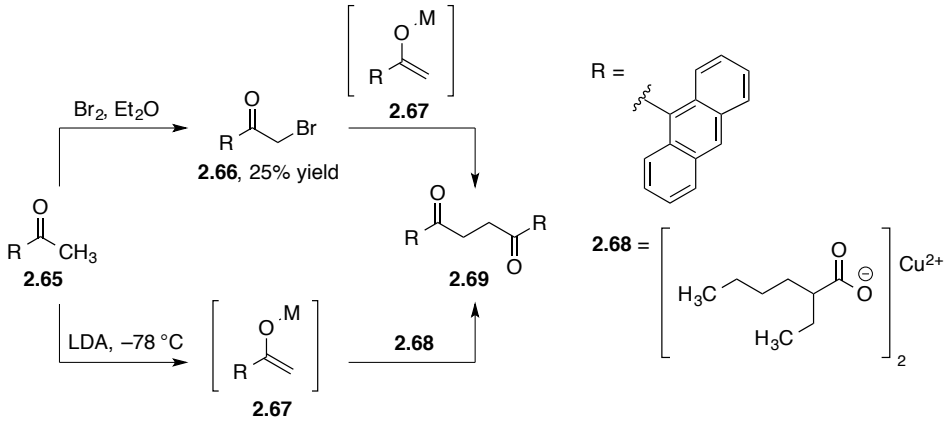

Scheme 2-10. Attempted 1,4-diketone formation to use in ligand synthesis protocol

2.2.4.4 Verification of enantiomeric excess

Methodological advancement was plagued by difficult HPLC analysis. This included low solubility of **2.47** in required solvents, broad peaks in the UV traces, and a persistent impurity overlapping with the peaks. The impurity was determined to be **2.55** (see Figure 2-18) by synthesis of a variety of presumed byproducts and comparison of retention times. The solubility of **2.47** was eventually increased through use of acetonitrile as loading solvent.

Alternative methods for determining enantioselectivity were also explored. NMR chiral agents such as Pirkle's alcohol ((*R*)-**2.70**, Scheme 2-11) are known to form diastereomeric solvates in solution.[90] However, upon addition of varying amounts of (*R*)-**2.70** to a racemic sample of **2.47** in $CDCl_3$, no peak splitting was observed in the ^1H NMR spectrum.

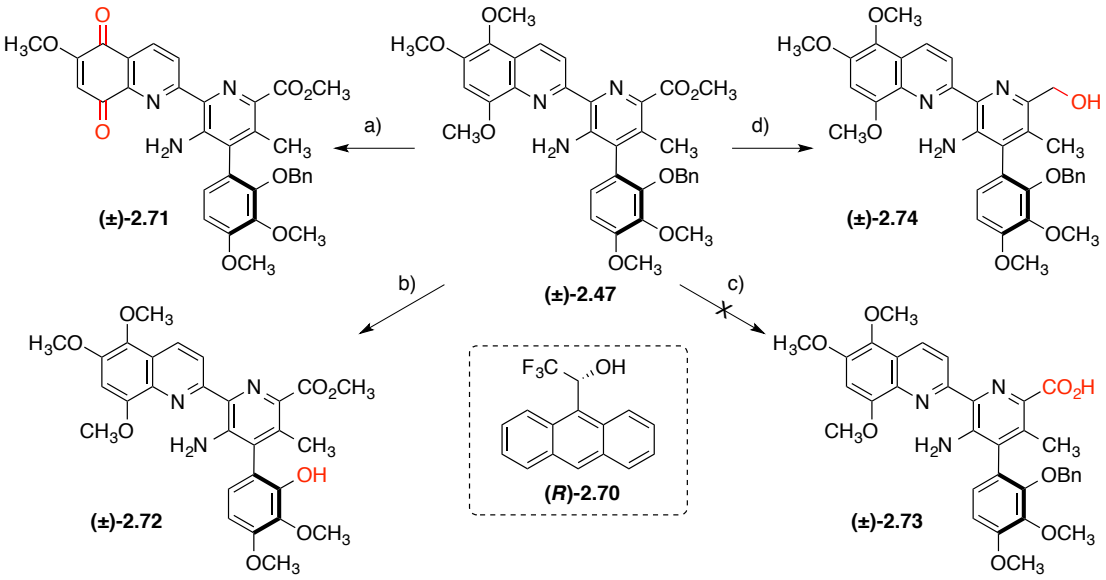

Scheme 2-11. Chemical derivatization of (±)-**2.47** to optimize a new ee determination method Conditions: a) CAN (aq. 0.04 M), CH_3CN, 25 °C, 90% yield; b) H_2, Pd/C, methanol:EtOAc, 25 °C, 38% yield; c) K_2CO_3, methanol:water, 25 °C, no reaction; d) $LiAlH_4$, THF, –30 to 0 °C, 46% yield;

It was proposed that chemical derivatization advancing the synthesis towards **2.1** (see section 2.2.4.5) could allow access to related structures, which might possess improved HPLC behavior. Oxidation of **2.47** to **2.71** by ceric ammonium nitrate (CAN, Scheme 2-11a) proved unproductive as (±)-**2.71** did not resolve into clear peaks by HPLC. Deprotection of the D-ring benzyl ether through hydrogenolysis with palladium on carbon gave poor yields of derivative (±)-**2.72** (Scheme 2-11b); moreover, the two enantiomer peaks overlapped in the HPLC chromatogram. Ester hydrolysis toward the synthesis of (±)-**2.73** gave only starting material after 48 hours at both 25 °C and 50 °C (Scheme 2-11c). Reduction of **2.47** with $LiAlH_4$ gave primary alcohol **2.74** in good yield, yet (±)-**2.74** did not show resolved peaks.

Instead, the corresponding Mosher's ester was synthesized from (±)-**2.74** and (*R*)-(+)-α-methoxy-α-trifluoromethylphenylacetic acid ((*R*)-(+)-MTPA) (**2.75**, Figure 2-19, entry 1).[91] The resulting diastereomers were inseparable by FCC, but showed distinct diastereomeric peaks in the ^{1}H and ^{19}F NMR spectra and allowed analysis of the diastereomeric ratio (dr) through integration (entry 1). An enantioenriched sample

of **2.47** showing 27% ee by HPLC (see Table 2-6, entry 1) was also brought through the two simple synthetic steps to give the corresponding Mosher's esters with a dr of 60:40 (corresponding to an ee of 20%, Figure 2-19, entry 2). This largely corroborates the previous data, although it did suggest that a slight overestimation of the atroposelectivity had resulted from chiral HPLC analysis.

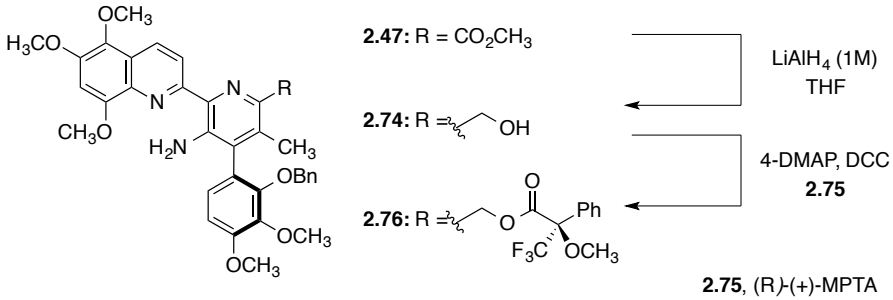

entry	2.74 source	2.74 ee (%)[a]	2.76 yield (%)	2.76 dr[b]
1	racemic	0	35	50:50
2	(*R*)-BINAP	(–) 27	40	60:40

[a]Measured by analytical chiral HPLC; [b]measured by NMR analysis of Mosher's ester

Figure 2-19. Synthesis of Mosher's ester from (*R*)-MTPA and resulting dr analysis by NMR

Enantioselectivity verification was repeated for two samples of **2.47** generated using the phosphine hydrazine ligand (see Table 2-6, entry 8 and 10). Reduction to **2.74** allowed acylation with the (*R*)-(–)-α-methoxy-α-trifluoromethylphenylacetyl chloride (**2.77**, (*R*)-(–)-MTPA Cl) which proved to be an easier and higher yielding transformation (Table 2-7). The (*R*)-MPTA Cl reagent contains the opposite configuration at the stereogenic carbon, due to differing priority assignments of acid vs acid chloride substituents, but this still allowed the verification of the ee% reported by HPLC. Again a 5–7% decrease of ee% (equivalent) was observed (Table 2-7).

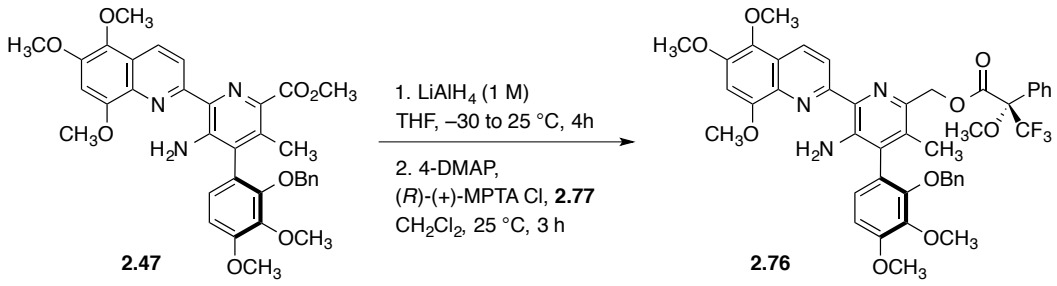

entry	2.47 S–M conditions	2.47 ee (%)[a]	2.76 yield (%)	2.76 dr[b]	2.76 ee equivalent
1	**2.64**, 40 °C	(+) 40	59	67.5:32.5	35%
2	**2.63**, 60 °C	(+) 29	78	81:59	22%

[a]Measured by analytical chiral HPLC; [b]measured by NMR analysis of Mosher's ester

Table 2-7. Synthesis of Mosher's ester from (*R*)-MTPA Cl and resulting analysis by NMR

The enantiomeric excess achieved through these studies allowed for temperature studies through NMR analysis to probe the rotational stability of the C–D bond. A sample of **2.76**, which was produced from a sample of **2.47** showing 27% ee, was monitored in variable temperature NMR while heating to 90 °C. No change was observed in the ratio of the two atropisomers after 1 hour. Heating to 165 °C in DMSO led to decomposition of the Mosher's ester reporter functional group.

The preparation of a late-stage tetracyclic streptonigrin intermediate **2.47** was thus achieved in 65% yield and with a moderate level of enantiocontrol (42% ee from chiral HPLC analysis), using a phosphino hydrazone ligand **2.63**. The route to **2.47** represents the first synthetic access to enantioenriched streptonigrin analogues.[92]

2.2.5 Final steps of streptonigrin total synthesis

The end game of the synthesis is presented here, as developed and performed by colleagues Dr. Chris Jones and Prof. Luiz Barbosa. (±)-**2.47** was subjected to a regioselective, ceric ammonium nitrate (CAN)-mediated oxidation, yielding quinoline-5,8-dione **2.71** in 90% yield (with none of the *o*-quinone or decomposition observed). The final steps required introduction of the C-7 amino group on ring A, removal of the D-ring benzyl ether, and hydrolysis of the pyridine methyl ester,

accomplished in 4 steps as shown in Scheme 2-12.

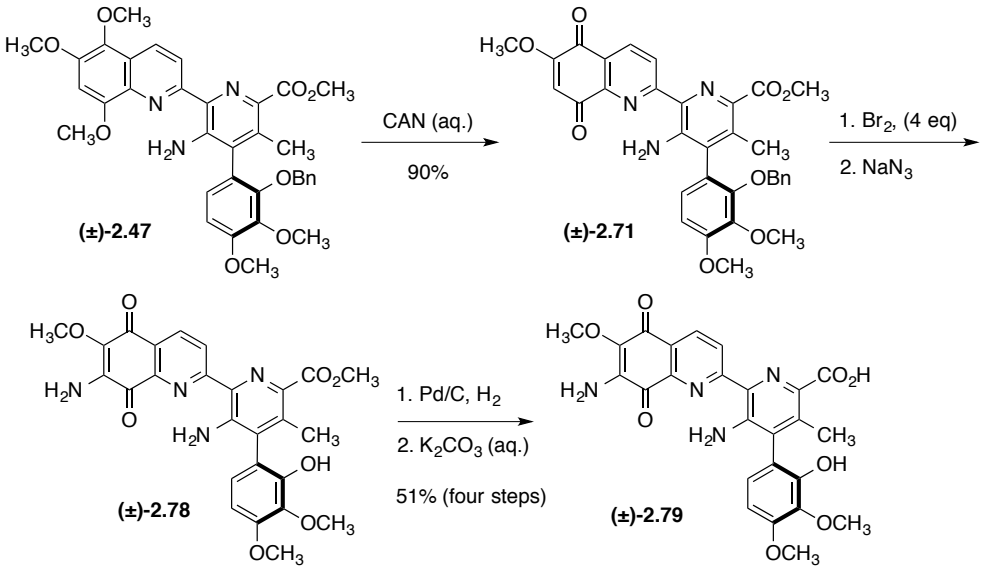

Scheme 2-12. Last steps of Donohoe total synthesis of **2.1** (final four experiments completed by Dr. Chris Jones)

2.3 Conclusion

The synthesis described herein allows for a concise and efficient synthesis of the antitumor agent (±)-streptonigrin. The showcased RCM methodology provides rapid generation of a complex substituted pyridine, which was accessed via two different pathways. The first route to pyridine **2.33** afforded C-ring precursor with a pre-installed amino group and leads to **2.1** in 14 steps and 11% overall yield. The second route, a simpler but slightly longer sequence, gave an increased overall yield (16 steps, 15% overall yield), but was limited to small-scale synthesis despite extensive optimization work described herein.

Overall, the method allowed preparation of the natural product and could allow easy access to late-stage analogues whose biological activity could be quickly evaluated, though this was not investigated further in the current work. Investigations into the use of chiral ligands to effect a challenging asymmetric Suzuki–Miyaura cross-coupling reaction revealed moderate levels of enantioselectivity in the presence of bidentate phosphino hydrazone and bisphosphine ligands. This represented the first purely synthetic access to an enantioenriched streptonigrin core and, though not presented in this thesis, could be used to enable the synthesis of enantioenriched streptonigrin.

2.4 Experimental

2.4.1 General experimental details

All solvents and reagents requiring purification were purified using standard laboratory techniques apart from CH_2Cl_2, THF and toluene which were dried by filtration through an activated alumina purification column. Petrol refers to petroleum ether in the boiling range 40–60 °C. Flash column chromatography was performed using Merck Kieselgel 60 (40–63 μm). ^{1}H nuclear magnetic resonance spectra (NMR) were recorded at 200 MHz, MHz or 500 MHz. ^{13}C NMR spectra were recorded at 100 MHz or 125 MHz as stated. Chemical shifts δ are quoted in parts per million (ppm) to the nearest 0.01 for ^{1}H and 0.1 for ^{13}C and reported using the solvent resonance internal standard ($CDCl_3$: ^{1}H NMR 7.27 ppm and ^{13}C NMR 77.0 ppm; DMSO-d_6: ^{1}H NMR 2.50 ppm and ^{13}C NMR 39.5 ppm; CD_3OD: ^{1}H NMR 3.31 ppm and ^{13}C NMR 49.0 ppm, toluene-d_8: ^{1}H NMR 2.08, 6.97, 7.01 and 7.09 ppm and ^{13}C NMR 137.5, 128.9, 128.0, 125.1, 20.4 ppm). Coupling constants *J* are quoted in Hz to the nearest 0.1 for ^{1}H and nearest integer for ^{13}C. Signal multiplicities are recorded as singlet (s), doublet (d), triplet (t), quartet (q) and quintet (qu). Broad (br) signals are specified and unresolvable multiplets (m) are quoted as ranges. Infrared spectra were recorded neat on a Bruker Tensor 27 FT-IR spectrometer equipped with Attenuated Total Reflectance sampling accessory. Absorption maxima are quoted in wavenumbers (cm^{-1}) and broad (br) signals are specified. High-resolution mass spectra (HRMS) were recorded on a Bruker MicroTof (resolution = 10000 FWHM) under electrospray ionization (ESI) and are given to four decimal places. All materials were purchased from commercial sources where available and used without further purification. All reactions were carried out in flame-dried glassware under an atmosphere of argon, unless otherwise specified. Molecular sieves were pre-activated using a Bunsen burner and under high vacuum.

2.4.2 Synthetic procedures and compound characterization

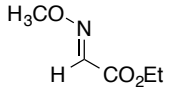

Compound 2.22, (*E*)-ethyl 2-(methoxyimino)acetate

Ethyl glyoxalate (50 wt% in toluene, 4.9 mL, 25 mmol) and methoxyamine hydrochloride (2.5 g, 30 mmol) were dissolved in ethanol (95 mL). Pyridine (2.2 mL, 27 mmol) was added dropwise and the reaction mixture was heated at reflux for 15 h. The mixture was cooled to 25 °C, concentrated and partitioned between CH_2Cl_2 (50 mL) and water (50 mL). The aqueous phase was extracted with CH_2Cl_2 (2×50 mL) and the combined organic extracts were dried with Na_2SO_4, filtered and concentrated to yield **2.22** as a colorless oil (2.5 g, 19 mmol, 79%) which was used in subsequent reactions without further purification. ^{1}H NMR (400 MHz, $CDCl_3$) δ 7.49 (s, 1H), 4.33 (q, J = 5.0 Hz, 2H), 4.07 (s, 3H), 1.35 (t, J = 5.0 Hz, 3H); ^{13}C NMR (100 MHz, $CDCl_3$) δ 161.9, 140.7, 63.5, 61.7, 14.1. Spectroscopic data were consistent with those previously reported.[60]

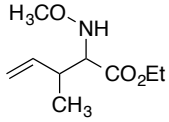

Compound 2.23, ethyl 2-(methoxyamino)-3-methylpent-4-enoate

Crotyl bromide (15.7 mL, 153 mmol) was added dropwise to a solution of **2.22** (9.10 g, 69.4 mmol) and zinc powder (9.52 g, 146 mmol) in THF/NH_4Cl (aqueous) (1:4, 350 mL total) and the resulting mixture was stirred at 25 °C for 40 h. The aqueous phase was extracted with EtOAc (3×100 mL) and the combined organic extracts were dried with Na_2SO_4, filtered and concentrated to yield **3.23** as a colorless oil (12.8 g, 68.4 mmol, 99%) and as an inseparable 3:2 mixture of diastereoisomers. The crude product was used in subsequent reactions without further purification. The ^{1}H and ^{13}C NMR spectroscopic data provided are for the major diastereoisomer. ^{1}H NMR (400

MHz, $CDCl_3$) δ 5.96 (br s, 1H), 5.75–5.68 (m, 1H), 5.08 (dd, *J* = 15.8, 1.0 Hz, 1H), 5.03 (dd, *J* = 10.4, 1.0 Hz, 1H), 4.24–4.17 (m, 2H), 3.56 (d, *J* = 6.6 Hz, 1H), 3.50 (s, 3H), 2.46–2.42 (m, 1H), 1.28 (t, *J* = 7.3 Hz, 3H), 1.09 (d, *J* = 6.7 Hz, 3H); ^{13}C NMR (100 MHz, $CDCl_3$) δ 173.0, 139.0, 115.9, 67.4, 61.5, 60.8, 38.8, 17.0, 14.3. Spectroscopic data were consistent with those previously reported.[60]

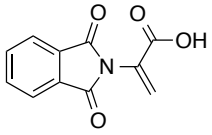

Compound 2.24, 2-(1,3-dioxoisoindolin-2-yl)acrylic acid

A solution of DL-serine (5.0 g, 48 mmol), phthalic anhydride (7.0 g, 48 mmol) and triethylamine (0.71 mL, 5.2 mmol) in toluene (250 mL) was refluxed, with azeotropic elimination of water using a Dean–Stark apparatus, for 4 h. The reaction mixture was cooled to 25 °C and concentrated. The resulting brown residue was dissolved in EtOAc (100 mL), washed with 1 M HCl (50 mL) and the aqueous phase was extracted with EtOAc (2×50 mL). The combined organic extracts were dried with Na_2SO_4, filtered and concentrated. The crude product was purified by flash column chromatography (SiO_2, 60% EtOAc/petrol) to afford **2.24** as a pink crystalline solid (4.4 g, 20 mmol, 43%). ^{1}H NMR (400 MHz, $CDCl_3$) δ 7.96–7.91 (m, 2H), 7.81–7.77 (m, 2H), 6.83 (s, 1H), 6.12 (s, 1H), 6.09 (br s, 1H); ^{13}C NMR (100 MHz, $CDCl_3$) δ 167.0, 166.3, 134.5, 131.7, 130.6, 128.5, 124.0; m.p. 171–173 °C [recrystallized from CH_2Cl_2]. Spectroscopic data were consistent with those previously reported.[60]

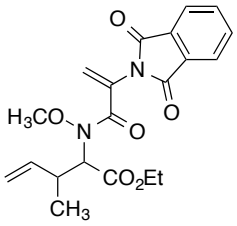

Compound 2.25, ethyl 2-(2-(1,3-dioxoisoindolin-2-yl)-*N*-methoxyacrylamido)-3-methylpent-4-enoate

Oxalyl chloride (2.19 mL, 25.8 mmol) was added dropwise to a solution of **2.24** (3.81 g, 17.3 mmol) and DMF (20 μL) in CH_2Cl_2 (44 mL) at 0 °C. The mixture was allowed to warm to 25 °C and stirred for a further 5 h. Excess oxalyl chloride and solvent were removed in vacuo to yield the crude acid chloride as a yellow solid, which was used immediately without further purification. A solution of **2.23** (1.49 g, 7.96 mmol) in CH_2Cl_2 (4.4 mL) was added dropwise to a solution of the crude acid chloride and triethylamine (3.7 mL, 26 mmol) in CH_2Cl_2 (40 mL) at 0 °C. The mixture was allowed to warm to 25 °C and stirred for a further 19 h. The reaction mixture was diluted with CH_2Cl_2 (25 mL) and washed with pH 7 buffer solution. The aqueous phase was extracted with CH_2Cl_2 (2×25 mL) and the combined organic extracts were washed with brine (50 mL), dried with Na_2SO_4, filtered and concentrated. The crude product was purified by flash column chromatography (SiO_2, 33–40% EtOAc/petrol gradient) to afford **2.25** as a white crystalline solid (3.07 g, 7.94 mmol, 99%) and as an inseparable 2:1 mixture of diastereoisomers. The ^{1}H and ^{13}C NMR spectroscopic data provided are for the major diastereoisomer. ^{1}H NMR (400 MHz, $CDCl_3$) δ 7.92–7.88 (m, 2H), 7.79–7.76 (m, 2H), 6.16 (s, 1H), 5.98 (s, 1H), 5.82–5.73 (m, 1H), 5.10 (dd, *J* = 17.1, 0.9 Hz, 1H), 5.01 (d, *J* = 10.3 Hz, 1H), 4.60 (br s, 1H), 4.16 (q, *J* = 6.6 Hz, 2H), 3.87 (s, 3H), 3.03 (q, *J* = 7.9 Hz, 1H), 1.24 (t, *J* = 7.0 Hz, 3H), 1.11 (d, *J* = 7.0 Hz, 3H); ^{13}C NMR (100 MHz, $CDCl_3$) δ 169.0, 166.2, 164.2, 139.1, 134.4, 131.7, 130.1, 123.8, 121.4, 116.1, 65.3, 64.3, 61.2, 37.7,

17.4, 14.0; m.p. 84–88 °C [recrystallized from CH_2Cl_2]. Spectroscopic data were consistent with those previously reported.[60]

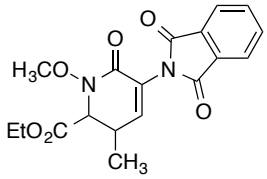

Compound 2.26, ethyl 5-(1,3-dioxoisoindolin-2-yl)-1-methoxy-3-methyl-6-oxo-1,2,3,6-tetrahydropyridine-2- carboxylate

A solution of Hoveyda–Grubbs second-generation catalyst (0.178 g, 0.219 mmol) in toluene (11 mL) was added dropwise over 10 h *via* a syringe pump to a refluxing solution of **2.25** (1.69 g, 4.37 mmol) and benzoquinone (0.071 g, 0.66 mmol) in toluene (40 mL). Once addition was complete, the reaction mixture was heated at reflux for a further 36 h. The reaction mixture was allowed to cool to 25 °C, treated with dimethylsulfoxide (1.16 mL, 16.3 mmol) and the resulting solution was stirred at 25 °C for 16 h. The crude mixture was pre-adsorbed onto SiO_2 and the solvent removed in vacuo. The product was then purified by flash column chromatography (SiO_2, 40% EtOAc/petrol) to afford **2.26** as a colorless oil (1.10 g, 3.07 mmol, 70%) and as an inseparable 2:1 mixture of diastereoisomers. The reaction was also scaled to 3 g (7.8 mmol) to give **2.25** in 56% yield. The ^{1}H and ^{13}C NMR spectroscopic data provided are for the major diastereoisomer. ^{1}H NMR (400 MHz, $CDCl_3$) δ 7.90–7.87 (m, 2H), 7.76–7.74 (m, 2H), 6.39 (d, J = 2.6 Hz, 1H), 4.46 (d, J = 7.3 Hz, 1H), 4.36–4.26 (m, 2H), 3.83 (s, 3H), 3.52 (dq, J = 7.3, 2.5 Hz, 1H), 1.33–1.31 (m, 6H); ^{13}C NMR (100 MHz, $CDCl_3$) δ 167.9, 166.9, 162.0, 143.0, 134.3, 131.9, 124.3, 123.7, 66.3, 62.5, 62.0, 32.5, 15.7, 14.1; Spectroscopic data were consistent with those previously reported.[60]

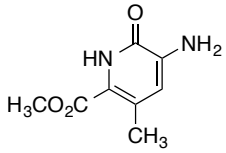

Compound 2.267 methyl 5-amino-3-methyl-6-oxo-1,6-dihydropyridine-2-carboxylate

From **2.26**: Quinuclidine (0.450 g, 4.05 mmol) was added to a solution of **2.26** (0.966 g, 2.70 mmol) and pre-activated 3 Å beaded molecular sieves in methanol (27 mL). The reaction mixture was stirred at 25 °C for 24 h, then additional quinuclidine (0.150 g, 1.35 mmol) and molecular sieves were added. After stirring for a further 36 h, methylamine (2 M in methanol, 4.04 mL, 8.08 mmol) was added and the resulting mixture was heated at 60 °C for 3 h. The crude mixture was allowed to cool to 25 °C, filtered, pre-adsorbed onto SiO_2 and concentrated. The product was then purified by flash column chromatography (SiO_2, 1% methanol/EtOAc) to afford **2.26** as a pale brown crystalline solid (0.397 g, 2.18 mmol, 80%). ^{1}H NMR (400 MHz, DMSO-d_6) δ 10.63 (br s, 1H), 6.28 (s, 1H), 6.07 (s, 2H), 3.74 (s, 3H), 2.27 (s, 3H); ^{13}C NMR (100 MHz, DMSO-d_6) δ 161.9, 155.4, 143.9, 125.3, 115.6, 112.3, 51.7, 18.8; Spectroscopic data were consistent with those previously reported.[60]

From **2.31**: A suspension of **2.31** (0.560 g, 2.64 mmol) and 10% Pd/C (0.056 g, 0.053 mmol) in methanol (100 mL) was stirred under a H_2 (g) atmosphere at 25 °C for 3 h. The reaction mixture was filtered through Celite®, eluting with methanol (100 mL) and then concentrated. The crude product was purified by flash column chromatography (SiO_2, EtOAc to 5% methanol/EtOAc gradient) to afford **2.27** as a pale brown crystalline solid (0.448 g, 2.46 mmol, 82%).

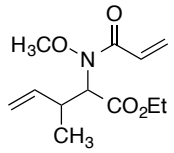

Compound 2.28, ethyl 2-(*N*-methoxyacrylamido)-3-methylpent-4-enoate

Acryloyl chloride (2.9 mL, 35 mmol) was added dropwise to a stirring solution of **2.23** (4.4 g, 24 mmol) and triethylamine (6.9 mL, 50 mmol) in CH_2Cl_2 (47 mL) at 0 °C. The mixture was allowed to warm to 25 °C and stirred for 16 h. The mixture was diluted with CH_2Cl_2 (50 mL) and quenched with the addition of water (50 mL). The aqueous phase was extracted with CH_2Cl_2 (3×20 mL) and the combined organic extracts were washed with brine (50 mL), dried with Na_2SO_4, filtered and concentrated. The crude product was purified by flash column chromatography (SiO_2, 11–20% EtOAc/petrol gradient), to afford **2.28** as a light yellow oil (4.4 g, 18 mmol, 76%), as a 2:1 mixture of diastereoisomers, which were not separated. The ^{1}H and ^{13}C NMR data provided are for the major diastereomer. ^{1}H NMR (400 MHz, $CDCl_3$) δ 6.71 (dd, *J* = 17.6, 10.4 Hz, 1H), 6.46 (dd, *J* = 17.0, 1.6 Hz, 1H), 5.83–5.67 (m, 2H), 5.13 (d, *J* = 17.3 Hz, 1H), 5.03 (d, *J* = 10.1 Hz, 1H), 4.82 (d, *J* = 9.8 Hz, 1H), 4.20–4.12 (m, 2H), 3.81 (s, 3H), 3.04–2.98 (m, 1H), 1.24 (t, *J* = 6.9 Hz, 3H), 1.03 (d, *J* = 6.7 Hz, 3H); ^{13}C NMR (100 MHz, $CDCl_3$) δ 169.9, 168.1, 139.5, 130.7, 126.1, 116.4, 64.9, 64.7, 61.4, 37.8, 17.5, 14.4. Spectroscopic data were consistent with those previously reported.[63]

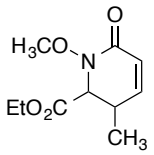

Compound 2.29, ethyl 1-methoxy-3-methyl-6-oxo-1,2,3,6-tetrahydropyridine-2-carboxylate

To a solution of Hoveyda–Grubbs second-generation catalyst (122 mg, 0.190 mmol) in CH_2Cl_2 (216 mL) was added a solution of **2.28** (1.56 g, 6.50 mmol) in CH_2Cl_2 (20

mL). The solution was refluxed for 24 h. Upon consumption of starting material, the reaction was cooled and DMSO (0.675 mL, 9.50 mmol) was added and the mixture stirred for an additional 24 h at 25 °C. The mixture was concentrated and purified by flash column chromatography (SiO_2, 50% EtOAc/petrol) to afford **2.29** as a light brown oil (1.37 g, 6.43 mmol, 99%) and as a 2:1 mixture of diastereoisomers which were not separated. The ^1H and ^{13}C NMR data provided are for the major diastereomer. ^1H NMR (400 MHz, $CDCl_3$) δ 6.16 (dd, J = 10.0, 1.4 Hz, 1H), 5.84 (dd, J = 9.9, 2.8 Hz, 1H), 4.33 (d, J = 7.3 Hz, 1H), 4.16 (q, J = 7.19 Hz, 2H), 3.77 (s, 3H), 3.29–3.21 (m, 1H), 1.26 (t, J = 7.3 Hz, 3H), 1.20 (d, J = 7.5 Hz, 3H); ^{13}C NMR (100 MHz, $CDCl_3$) δ 168.9, 166.3, 143.2, 123.9, 66.7, 63.2, 61.9, 34.5, 16.2, 14.5. Spectroscopic data were consistent with those previously reported.[63]

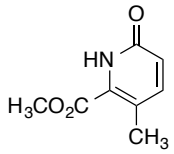

Compound 2.30, methyl 3-methyl-6-oxo-1,6-dihydropyridine-2-carboxylate

To a solution of **2.29** (1.69 g, 7.93 mmol) in methanol (23 mL) was added DBU (1.67 mL, 11.2 mmol). The mixture was stirred for 15 h at 25 °C. The reaction mixture was concentrated to yield the crude product which was purified by flash column chromatography (SiO_2, EtOAc to 10% methanol/EtOAc gradient) to afford **2.30** as a white solid (1.14 g, 6.82 mmol, 87%). ^1H NMR (400 MHz, $CDCl_3$) δ 9.84 (br s, 1H), 7.29 (d, J = 9.5 Hz, 1H), 6.71 (d, J = 9.2 Hz, 1H), 3.95 (s, 3H), 2.40 (s, 3H); ^{13}C NMR (100 MHz, $CDCl_3$) δ 162.2, 161.7, 145.8, 129.7, 126.9, 121.8, 53.4, 18.6; IR (neat) ν_{max} 2918 (br), 1731, 1673, 1604, 1524, 1432, 1343, 1274, 1212, 1050, 869, 791 cm^{-1}. The data are in accordance with the literature.[63]

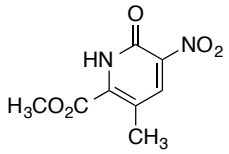

Compound 2.31, methyl 5-amino-3-methyl-6-oxo-1,6-dihydropyridine-2-carboxylate

Concentrated sulfuric acid (0.029 mL, 0.56 mmol) was added to a solution of **2.30** (0.031 g, 0.19 mmol) in 70% nitric acid (0.058 mL, 1.3 mmol) at 0 °C in a sealed tube. The mixture was allowed to warm to 25 °C and then heated to 50 °C for 6 h. The mixture was cooled and poured onto ice water. The aqueous phase was extracted with EtOAc (5×20 mL) and the combined organic extracts were dried with Na_2SO_4, filtered and concentrated. The crude yellow solid (**2.31**, R_f 0.33 in 10% EtOAc/petrol) was used without further purification. ^{1}H NMR (400 MHz, CD_3OD) δ 8.41 (s, 1H), 4.01 (s, 3H), 2.46 (s, 3H); ^{13}C NMR (125 MHz, DMSO-d_6) 162.1, 153.3, 141.0, 138.7, 118.8, 53.5, 17.1 (note: one carbon not observed in ^{13}C spectrum); IR (neat) ν_{max} 3054 (br), 2956, 2851, 1670, 1271, 1208 cm^{-1}; HRMS (ESI$^+$) *m/z* calculated for $C_8H_8N_2O_5$ [M+Na]$^+$: 235.0331, found: 235.0326.

Optimized conditions: Concentrated sulfuric acid (1.2 mL) was added dropwise to a screw-top tube containing a solution of pyridone **2.30** (0.500 g, 2.99 mmol) in concentrated nitric acid (2.0 mL) at 0 °C, and the reaction vessel was then sealed. After 5 min, the reaction mixture was allowed to warm to 25 °C and then heated at 50 °C. After 7 h, the reaction mixture was allowed to cool to 25 °C and then poured into ice water. The aqueous layer was extracted six times with EtOAc (until the yellow color had faded), and the combined organic layers were dried with Na_2SO_4, filtered, and concentrated. The product was then purified by flash column chromatography (SiO_2, 5% methanol/EtOAc) to afford **2.31** as a yellow solid (0.558 g, 88%).

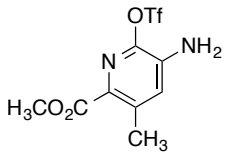

Compound 2.33, methyl 5-amino-3-methyl-6-(trifluoromethylsulfonyloxy)picolinate

Trifluoromethane sulfonic anhydride (0.125 mL, 0.741 mmol) was added dropwise to a solution of **2.27** (0.113 g, 0.624 mmol) and 2,6-di-*tert*-butyl-4-methylpyridine (0.191 g, 0.932 mmol) in CH_2Cl_2/hexafluoroisopropanol (25:1 by volume, 5.2 mL total) at –50 °C. The mixture was stirred at –50 °C for 1 h, then allowed to warm to 25 °C slowly over a further 3 h. The mixture was diluted with CH_2Cl_2 (10 mL) and washed with saturated aqueous $NaHCO_3$ (10 mL). The aqueous phase was extracted with CH_2Cl_2 (2×10 mL) and the combined organic extracts were washed with brine (10 mL), dried with Na_2SO_4, filtered and concentrated. The crude product was purified by flash column chromatography (SiO_2, 20% EtOAc/petrol) to afford **2.33** as a colorless crystalline solid (0.195 g, 0.620 mmol, 73%). ^{1}H NMR (400 MHz, $CDCl_3$) δ 7.01 (s, 1H), 4.31 (br s, 2H), 3.89 (s, 3H), 2.58 (3H, s); ^{13}C NMR (100 MHz, $CDCl_3$) δ 164.9, 139.8, 139.6, 136.2, 132.4, 127.1, 118.5 (q, J = 319 Hz, CF_3), 52.2, 19.9; m.p. 108–110 °C [recrystallized from CH_2Cl_2]. Spectroscopic data were consistent with those previously reported.[60]

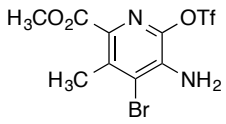

Compound 2.34, methyl 5-amino-4-bromo-3-methyl-6-(trifluoromethylsulfonyloxy)picolinate

N-Bromosuccinimide (0.145 g, 0.815 mmol) was added to a solution of **2.33** (0.232 g, 0.738 mmol) in acetonitrile (7.4 mL) at 0 °C. The reaction mixture was allowed to warm to 25 °C and stirred for 17 h before the solvent was removed. The crude reaction mixture was dissolved in CH_2Cl_2 (10 mL) and washed with 1 M HCl (10

mL), saturated aqueous $NaHCO_3$ (10 mL) and brine (10 mL). The organic phase was dried with Na_2SO_4, filtered and concentrated. The crude product was purified by flash column chromatography (SiO_2, 13% EtOAc/petrol) to afford **2.33** as an orange crystalline solid (0.278 g, 0.710 mmol, 96%). ^{1}H NMR (400 MHz, $CDCl_3$) δ 4.81 (br s, 2H), 3.92 (s, 3H), 2.71 (s, 3H); ^{13}C NMR (100 MHz, $CDCl_3$) δ 164.8, 138.8, 138.1, 135.0, 132.8, 123.0, 118.5 (q, J = 319 Hz, CF_3), 52.6, 19.5; m.p. 117–118 °C [recrystallized from CH_2Cl_2]. Spectroscopic data were consistent with those previously reported.[60]

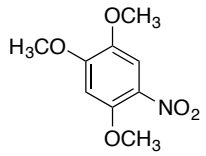

Compound 2.36, 1,2,4-trimethoxy-5-nitrobenzene

2,4,5-Trimethoxybenzaldehyde (6.15 g, 31.3 mmol) was added portionwise over 10 min to a mechanically stirred solution of 28% aq. nitric acid (120 mL) at −10 °C. The reaction mixture was stirred for 3 h at −10 °C then allowed to warm to 25 °C and diluted with CH_2Cl_2 (50 mL). The aqueous phase was extracted with CH_2Cl_2 (3×50 mL) and the combined organic extracts were washed with saturated aqueous $NaHCO_3$ (100 mL) and brine (100 mL), dried with $MgSO_4$, filtered and concentrated to yield **2.36** as a yellow solid (5.42 g, 25.4 mmol, 81%) which was used in subsequent reactions without further purification. ^{1}H NMR (400 MHz, $CDCl_3$) δ 7.59 (s, 1H), 6.58 (s, 1H), 3.99 (s, 3H), 3.98 (s, 3H), 3.90 (s, 3H); ^{13}C NMR (100 MHz, $CDCl_3$) δ 154.7, 150.4, 142.4, 130.9, 109.0, 97.5, 57.2, 56.5, 56.4; m.p. 123–124 °C. Spectroscopic data were consistent with those previously reported.[60]

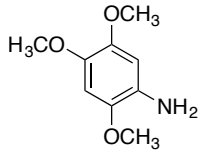

Compound 2.37, 2,4,5-trimethoxyaniline

A suspension of 2,4,5-trimethoxynitrobenzene **2.36** (4.27 g, 20.0 mmol) and 10% Pd/C (0.650 g, 0.611 mmol) in methanol/EtOAc (9:1 by volume, 300 mL total) was stirred under a H_2 (g) atmosphere at 25 °C for 14 h. The reaction mixture was filtered through Celite®, eluting with methanol (50 mL) and then concentrated. The crude product was purified by flash column chromatography (SiO_2, 50% EtOAc/petrol) to afford **2.37** as a white crystalline solid (3.11 g, 17.0 mmol, 85%). ^{1}H NMR (400 MHz, $CDCl_3$) δ 6.54 (s, 1H), 6.40 (s, 1H), 3.82 (d, *J* = 1.4 Hz, 3H), 3.80 (d, *J* = 1.3 Hz, 3H), 3.80 (d, *J* = 1.2 Hz, 3H), 3.55 (br s, 2H); ^{13}C NMR (100 MHz, $CDCl_3$) δ 143.7, 141.4, 140.8, 129.6, 101.8, 100.1, 57.2, 56.5 (2C); m.p. 89–90 °C. Spectroscopic data were consistent with those previously reported.[60]

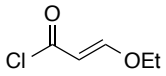

Compound 2.38, (*E*)-3-ethoxyacryloyl chloride

Ethyl vinyl ether (9.56 mL, 100 mmol) was added dropwise to oxalyl chloride (12.9 mL, 150 mmol) at 0 °C. The mixture was allowed to warm to 25 °C and stirred for 12 h. Excess oxalyl chloride was distilled off and the residue was heated at 120 °C for 30 min. The crude residue was purified by vacuum distillation to yield acid chloride **2.38** (5.34 g, 39.7 mmol, 40%) as a colorless oil. ^{1}H NMR (400 MHz, $CDCl_3$) δ 7.78 (d, *J* = 12.1 Hz, 1H), 5.51 (d, *J* = 12.1 Hz, 1H), 4.05 (q, *J* = 7.1 Hz, 2H), 1.40 (t, *J* = 7.1 Hz, 3H); ^{13}C NMR (100 MHz, $CDCl_3$) δ 168.1, 164.7, 102.9, 68.8, 14.4; b.p. 85–87 °C [20 mbar]. Spectroscopic data were consistent with those previously reported.[60]

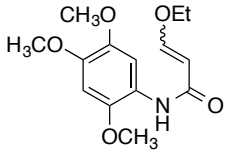

Compound 2.39, (*E*)-3-ethoxy-*N*-(2,4,5-trimethoxyphenyl)acrylamide & (*Z*)-3-ethoxy-*N*-(2,4,5-trimethoxyphenyl)acrylamide

A solution of (*E*)-3-ethoxyacryloyl chloride **2.38** (3.05 g, 22.6 mmol) in CH_2Cl_2 (10 mL) was added dropwise to a solution of aniline **2.37** (3.32 g, 18.1 mmol) and pyridine (4.38 mL, 54.4 mmol) in CH_2Cl_2 (180 mL) at 0 °C. The mixture was allowed to warm to 25 °C and stirred for 21 h. The solvent was removed and the residue was dissolved in EtOAc (100 mL), washed with 1 M HCl (75 mL), saturated aqueous $NaHCO_3$ (75 mL) and brine (75 mL), dried with $MgSO_4$, filtered and concentrated. The crude product was purified by flash column chromatography (SiO_2, 50–80% EtOAc/petrol gradient) to afford *trans*-aryl amide (*E*)-**2.39** and *cis*-aryl amide (*Z*)-**2.39** as a colorless crystalline solid (4.41 g, 15.7 mmol, 87%). For (*E*)-**2.39**: ^{1}H NMR (400 MHz, $CDCl_3$) δ 8.21 (br s, 1H), 7.62 (d, *J* = 12.0 Hz, 1H), 7.41 (s, 1H), 6.55 (s, 1H), 5.36 (d, *J* = 12.1 Hz, 1H), 3.96 (q, *J* = 6.8 Hz, 2H), 3.88 (s, 6H), 3.87 (s, 3H), 1.37 (t, *J* = 7.0 Hz, 3H); ^{13}C NMR (100 MHz, $CDCl_3$) δ 164.8, 160.6, 144.5, 142.9, 141.7, 121.4, 105.3, 99.4, 97.5, 67.2, 56.6 (2C), 56.3, 14.6. For (*Z*)-**2.39**: ^{1}H NMR (400 MHz, $CDCl_3$) δ 9.44 (s, 1H), 8.32 (s, 1H), 6.55 (s, 1H), 6.53 (d, *J* = 7.1 Hz, 1H), 4.97 (d, *J* = 7.1 Hz, 1H), 4.15 (q, *J* = 7.1 Hz, 2H), 3.88 (s, 3H), 3.87 (s, 3H), 3.86 (s, 3H), 1.47 (t, *J* = 7.1 Hz, 3H); ^{13}C NMR (100 MHz, $CDCl_3$) δ 163.5, 152.7, 144.3, 142.9, 141.7, 122.0, 105.2, 103.7, 97.8, 70.8, 56.7, 56.6, 56.3, 15.2; Spectroscopic data were consistent with those previously reported.[60]

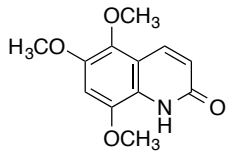

Compound 2.40, 5,6,8-trimethoxyquinolin-2(1*H*)-one

Compound **2.39** (1.57 g, 5.58 mmol) was dissolved in concentrated sulfuric acid (10.5 mL) at 0 °C. The reaction mixture was allowed to warm to 25 °C and stirred for 4 h. Ice water (20 mL) was slowly added and the mixture stirred for a further 1 h at 25 °C. The reaction mixture was extracted with CH_2Cl_2 (3×50 mL) and the combined organic extracts were washed with saturated aqueous $NaHCO_3$ (75 mL) and brine (75 mL), then dried with $MgSO_4$, filtered and concentrated. The crude product was purified by flash column chromatography (SiO_2, EtOAc to 5% methanol/EtOAc gradient) to afford **2.40** as a colorless crystalline solid (1.19 g, 5.06 mmol, 89%). ^{1}H NMR (400 MHz, $CDCl_3$) δ 9.02 (br s, 1H), 8.02 (dd, *J* = 9.8, 1.2 Hz, 1H), 6.73 (s, 1H), 6.66 (dd, *J* = 9.7, 1.0 Hz, 1H), 3.95 (d, *J* = 1.0 Hz, 3H), 3.92 (d, *J* = 1.1 Hz, 3H), 3.89 (d, *J* = 1.2 Hz, 3H); ^{13}C NMR (100 MHz, $CDCl_3$) δ 161.5, 146.4, 141.5, 138.4, 135.0, 123.0, 122.8, 115.0, 100.3, 61.8, 57.5, 56.3; m.p. 171–173 °C. Spectroscopic data were consistent with those previously reported.[60]

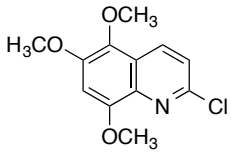

Compound 2.41, 2-chloro-5,6,8-trimethoxyquinoline

Phosphorus oxychloride (6.40 mL, 68.6 mmol) was added to a solution of **2.40** (2.69 g, 11.4 mmol), pyridine (0.303 mL, 3.77 mmol) and DMF (0.029 mL, 0.38 mmol) in chlorobenzene (100 mL) at 25 °C and the resulting mixture was heated at reflux for 3.5 h. The reaction mixture was allowed to cool to 25 °C and quenched upon slow addition of saturated aqueous $NaHCO_3$ (20 mL). The mixture was extracted with EtOAc (3×50 mL) and the combined organic extracts were washed

with brine (50 mL), dried with $MgSO_4$, filtered and concentrated. The crude product was purified by flash column chromatography (SiO_2, 40% EtOAc/petrol) to afford **2.41** as a colorless crystalline solid (2.35 g, 9.26 mmol, 81%). ^{1}H NMR (400 MHz, $CDCl_3$) δ 8.31 (dd, *J* = 8.8, 1.4 Hz, 1H), 7.35 (dd, *J* = 8.8, 1.4 Hz, 1H), 6.86 (s, 1H), 4.03 (d, *J* = 1.1 Hz, 3H), 4.00 (d, *J* = 1.3 Hz, 3H), 3.90 (d, *J* = 1.4 Hz, 3H); ^{13}C NMR (100 MHz, $CDCl_3$) δ 151.6, 148.8, 147.9, 135.4, 134.5, 133.0, 123.2, 123.0, 99.3, 61.4, 57.0, 56.2; m.p. 146–147 °C. Spectroscopic data were consistent with those previously reported.[60]

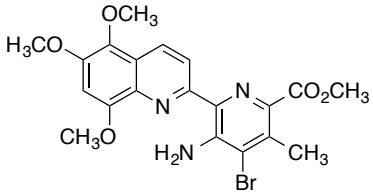

Compound 2.43, methyl 5-amino-4-bromo-3-methyl-6-(5,6,8-trimethoxyquinolin-2-yl)picolinate

A solution of chloroquinoline **2.41** (0.246 g, 0.970 mmol) and tetrakis(triphenylphosphine)palladium (0.056 g, 0.048 mmol) in toluene (9.7 mL) was degassed and refilled with argon five times. Hexamethylditin (0.221 mL, 1.07 mmol) was subsequently added and the resulting solution heated at 60 °C for 17 h. The reaction mixture was allowed to cool to 25 °C, diluted with Et_2O (20 mL) and washed with water (20 mL). The aqueous phase was extracted with Et_2O (2×10 mL) and the combined organic extracts were washed with brine (20 mL), dried with Na_2SO_4, filtered and concentrated. The crude product **2.42**, contaminated with triphenylphosphine oxide, was immediately used in the next step without any further purification.

Pyridine **2.34** (0.162 g, 0.412 mmol) was added to a solution of 2-stannyl quinoline **2.42** (0.224 g, 0.587 mmol), tetrakis(triphenylphosphine)palladium (0.022 g, 0.019 mmol), cesium fluoride (0.119 g, 0.783 mmol) and copper(I) iodide (7.4 mg,

0.39 mmol) in toluene (9 mL). The reaction mixture was degassed and refilled with argon five times, then heated at reflux for 21 h. The mixture was allowed to cool to 25 °C, filtered and concentrated. The crude product was purified by flash column chromatography (10% w/w SiO_2/K_2CO_3,[93] 25–40% EtOAc/petrol gradient) to afford **2.42** as a yellow solid (0.122 g, 0.263 mmol, 75%). ^{1}H NMR (400 MHz, $CDCl_3$) δ 8.76 (d, *J* = 9.0 Hz, 1H), 8.44 (d, *J* = 9.0, 1H), 6.83 (s, 1H), 4.05 (s, 3H), 4.03 (s, 3H), 3.98 (s, 3H), 3.95 (s, 3H), 2.73 (s, 3H); ^{1}H NMR (100 MHz, $CDCl_3$) δ 166.5, 154.4, 152.1, 149.0, 144.2, 136.6, 135.6, 134.3, 133.4, 132.7, 130.1, 123.3, 123.2, 120.6, 98.3, 61.5, 57.1, 56.1, 52.2, 20.2; m.p. 177–179 °C [recrystallized from CH_2Cl_2]. Spectroscopic data were consistent with those previously reported.[60]

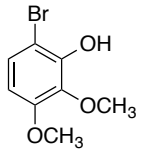

Compound 2.44, 6-bromo-2,3-dimethoxyphenol

N-bromosuccinimide (5.77 g, 32.4 mmol) was added to a solution of 2,3-dimethoxyphenol (5.00 g, 32.4 mmol) in THF (162 mL) at –78 °C. The resulting mixture was stirred at –78 °C for 4 h then allowed to warm to 25 °C and stirred for a further 16 h. The solvent was removed in vacuo, the residue was dissolved in CH_2Cl_2 (100 mL) and washed with water (50 mL) and brine (50 mL). The organic phase was dried with $MgSO_4$, filtered and concentrated. The crude product was purified by flash column chromatography (SiO_2, 5% EtOAc/petrol) to afford **2.44** as a colorless solid (6.90 g, 29.6 mmol, 91%). ^{1}H NMR (400 MHz, $CDCl_3$) δ 7.16 (d, *J* = 9.0 Hz, 1H), 6.43 (d, *J* = 9.0 Hz, 1H), 6.02 (s, 1H), 3.92 (s, 3H), 3.86 (s, 3H); ^{13}C NMR (100 MHz, $CDCl_3$) δ 152.0, 146.8, 136.4, 126.7, 105.1, 100.3, 61.0, 56.0; m.p. 43–45 °C [recrystallized from CH_2Cl_2]. Spectroscopic data were consistent with those previously reported.[60]

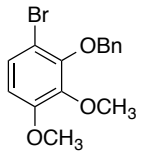

Compound 2.45, 2-(benzyloxy)-1-bromo-3,4-dimethoxybenzene

Benzyl bromide (1.68 mL, 14.1 mmol) was added dropwise to a solution of **2.44** (3.00 g, 12.9 mmol) and potassium carbonate (2.67 g, 19.3 mmol) in acetone (129 mL) at 25 °C and the resulting mixture stirred at reflux for 16 h. The reaction mixture was allowed to cool to 25 °C, the solvent was removed and the residue was dissolved in CH_2Cl_2 (100 mL). The organic phase was washed with water (50 mL) and brine (50 mL), then dried with $MgSO_4$, filtered and concentrated. The crude product was purified by flash column chromatography (SiO_2, 5% EtOAc/petrol) to afford **2.45** as a colorless solid (3.82 g, 11.8 mmol, 92%). ^{1}H NMR (400 MHz, $CDCl_3$) δ 7.59 (d, *J* = 7.6 Hz, 2H), 7.42 (t, *J* = 7.7 Hz, 2H), 7.36 (t, *J* = 7.7 Hz, 1H), 7.25 (dd, *J* = 9.0, 1.0 Hz, 1H), 6.62 (dd, *J* = 9.0, 0.6 Hz, 1H), 5.09 (s, 2H), 3.91 (d, *J* = 1.0 Hz, 3H), 3.88 (d, *J* = 0.7 Hz, 3H); ^{13}C NMR (100 MHz, $CDCl_3$) δ 153.3, 149.9, 143.8, 137.0, 128.5, 128.3, 128.1, 126.8, 108.8 (2C), 75.3, 61.1, 56.2; m.p. 68–70 °C. Spectroscopic data were consistent with those previously reported.[60]

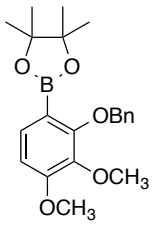

Compound 2.46, 2-(2-(benzyloxy)-3,4-dimethoxyphenyl)-4,4,5,5-tetramethyl-1,3,2-dioxaborolane

tert-Butyl lithium (1.6 M in pentane, 5.0 mL, 8.0 mmol) was added dropwise to a solution of **2.45** (1.46 g, 4.52 mmol) in THF (23 mL) at –78 °C. The resulting mixture was stirred at –78 °C for 25 min, before 2-isopropoxy-4,4,5,5-tetramethyl-1,3,2-dioxaborolane (1.38 mL, 6.76 mmol) was added dropwise to the mixture. The

solution was stirred at −78 °C for a further 3 h then allowed to warm to 25 °C and stirred for 7 h. The mixture was partitioned between EtOAc (50 mL) and water (50 mL), the organic phase washed with brine (50 mL), dried with Na_2SO_4, filtered and concentrated. The crude product was purified by flash column chromatography (SiO_2, 5% EtOAc/petrol) to afford **2.46** as a colorless solid (1.00 g, 2.70 mmol, 60%). The product was recrystallized from hot petrol to yield fine white crystals. ^{1}H NMR (400 MHz, $CDCl_3$) δ 7.61 (d, *J* = 7.0 Hz, 2H), 7.47 (dd, *J* = 8.3, 1.1 Hz, 1H), 7.38 (t, *J* = 7.2 Hz, 2H), 7.32 (t, *J* = 7.5 Hz, 1H), 6.72 (dd, *J* = 8.3, 1.0 Hz, 1H), 5.06 (s, 2H), 3.90 (d, *J* = 1.1 Hz, 3H), 3.88 (d, *J* = 1.3 Hz, 3H), 1.34 (s, 12H); ^{13}C NMR (100 MHz, $CDCl_3$) δ 157.9, 156.5, 142.3, 138.0, 131.7, 128.7, 128.1, 127.7, 112.5, 107.5, 83.3, 76.2, 61.0, 55.9, 24.8; m.p. 39–40 °C. Spectroscopic data were consistent with those previously reported.[60]

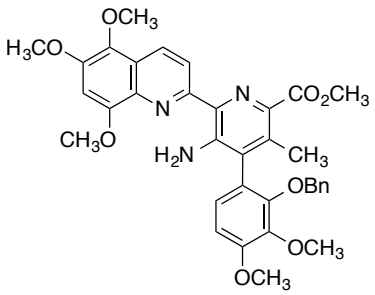

Compound 2.47, methyl 5-amino-4-(2-(benzyloxy)-3,4-dimethoxyphenyl)-3-methyl-6-(5,6,8-trimethoxyquinolin- 2-yl)picolinate

Racemic protocol: Aryl boronate ester **2.46** (0.120 g, 0.324 mmol) was added to a solution of **2.43** (0.100 g, 0.216 mmol), tetrakis(triphenylphosphine)palladium (0.025 g, 0.022 mmol) and potassium phosphate tribasic (0.138 g, 0.650 mmol) in dioxane/water (3:1 by volume, 2.2 mL total). The reaction mixture was degassed and refilled with argon five times, then heated at reflux for 24 h. The mixture was allowed to cool to 25 °C, diluted with EtOAc (4 mL) and washed with brine (4 mL). The organic phase was dried with Na_2SO_4, filtered and concentrated. The crude product

was purified by flash column chromatography (SiO_2, 33% EtOAc/petrol) to afford (±)-**2.47** as a yellow solid (79 mg, 0.13 mmol, 74%). ^{1}H NMR (400 MHz, $CDCl_3$) δ 8.88 (d, *J* = 9.1 Hz, 1H), 8.49 (d, *J* = 9.1 Hz, 1H), 7.12–7.10 (m, 3H), 7.05–7.01 (m, 2H), 6.88 (s, 2H), 6.83 (s, 1H), 4.93 (d, *J* = 11.0 Hz, 1H), 4.86 (d, *J* = 11.0 Hz, 1H), 4.04 (s, 3H), 4.01 (s, 6H), 3.97 (s, 6H), 3.95 (s, 3H), 2.29 (s, 3H); ^{13}C NMR (62.5 MHz, $CDCl_3$) δ 167.2, 155.7, 154.1, 152.1, 150.7, 148.7, 145.2, 143.4, 137.1, 136.6, 135.8, 134.4, 133.1, 133.0, 132.7, 130.0, 128.1 (2C), 128.0 (2C), 127.7, 125.1, 123.0, 122.1, 120.9, 108.4, 98.3, 75.2, 61.6, 61.1, 57.2, 56.1 (2C), 52.1, 17.5; m.p. 208–210 °C [recrystallized from CH_2Cl_2]. Spectroscopic data were consistent with those previously reported.[60]

Enantioenriched Protocol: A solution of the palladium source (0.008 mmol) and ligand (0.01 mmol) in dioxane (0.1 mL) was stirred at 25 °C for 30 min. A solution of aryl boronate ester **2.46** (0.049 mmol) and pyridine **2.43** (0.015 g, 0.032 mmol) in dioxane (0.22 mL) was subsequently added. The reaction mixture was degassed and refilled with argon five times, then treated with a solution of sodium carbonate (1 M, 0.10 mL). The mixture was degassed and refilled with argon five times again and then heated at 60 °C for 24 h. The mixture was allowed to cool to 25 °C, diluted with EtOAc (1 mL) and washed with brine (1 mL). The organic phase was dried with Na_2SO_4, filtered and concentrated. The crude product was purified by flash column chromatography (SiO_2, 33% EtOAc/petrol) to afford **2.47** as a yellow solid. Enantioselectivity was measured by chiral HPLC, see Appendix 1 for HPLC chromatogram. A sample obtained using phosphino hydrazone ligand **2.63** that afforded product **2.47** with 30% ee (by chiral HPLC analysis) gave $[\alpha]^{25}_{D}$ +51.5 (*c* = 0.29, $CHCl_3$).

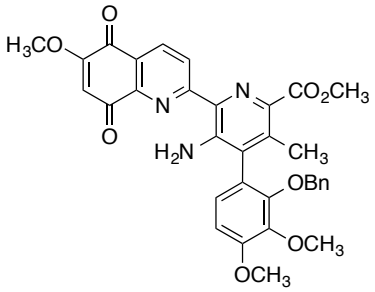

Compound 2.71, methyl 5-amino-4-(2-(benzyloxy)-3,4-dimethoxyphenyl)-6-(6-methoxy-5,8-dioxo-5,8- dihydroquinolin-2-yl)-3-methylpicolinate

An aqueous solution of ceric ammonium nitrate (0.04 M, 42.0 mL, 1.68 mmol) was added dropwise to a solution of quinoline **2.47** (0.350 g, 0.559 mmol) in acetonitrile (110 mL) in the dark at 0 °C. The reaction mixture was allowed to warm to 25 °C and stirred for 48 h. The crude mixture was diluted with EtOAc (40 mL), washed with water (40 mL) and brine (40 mL) then dried with Na_2SO_4, filtered and concentrated. The crude product was purified by flash column chromatography (SiO_2, 50% EtOAc/petrol) to afford **2.71** as a dark red crystalline solid (0.300 g, 0.503 mmol, 90%). ^{1}H NMR (400 MHz, $CDCl_3$) δ 9.02 (d, *J* = 8.5 Hz, 1H), 8.49 (d, *J* = 8.5 Hz, 1H), 7.13–7.07 (m, 3H), 7.02–6.98 (m, 2H), 6.87 (d, *J* = 8.7 Hz, 1H), 6.82 (d, *J* = 8.7 Hz, 1H), 6.28 (s, 1H), 4.96 (d, *J* = 11.2 Hz, 1H), 4.89 (d, *J* = 11.2 Hz, 1H), 3.99 (s, 3H), 3.96 (s, 3H), 3.94 (s, 6H), 2.24 (s, 3H); ^{13}C NMR (100 MHz, $CDCl_3$) δ 182.7, 179.3, 166.9, 163.0, 160.4, 154.3, 150.5, 146.2, 145.5, 143.4, 137.8, 137.1, 135.5, 134.3, 133.9, 130.4, 128.1 (2C), 127.9 (2C), 127.8, 125.4, 125.3, 124.8, 121.3, 109.8, 108.6, 75.1, 61.1, 56.6, 56.1, 52.2, 17.6; m.p. 242–246 °C [recrystallized from CH_2Cl_2]. Spectroscopic data were consistent with those previously reported.[60]

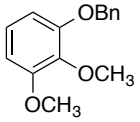

Compound 2.54, 1-(benzyloxy)-2,3-dimethoxybenzene

Benzyl bromide (0.054 mL, 0.45 mmol) was added dropwise to a solution of 2,3-dimethoxyphenol (0.064 g, 0.42 mmol) and potassium carbonate (0.086 g,

0.62 mmol) in acetone (4.1 mL) at 25 °C and the resulting mixture was stirred at reflux for 15 h. The reaction mixture was allowed to cool to 25 °C, the solvent was removed and the residue was dissolved in CH_2Cl_2 (5 mL). The organic phase was washed with water (5 mL) and brine (5 mL), then dried with $MgSO_4$, filtered and concentrated. The crude product was purified by flash column chromatography (SiO_2, 5% EtOAc/petrol) to afford **2.54** as a clear oil (0.091 g, 0.37 mmol, 90%). ^{1}H NMR ($CDCl_3$, 400 MHz) δ 7.47 (d, *J* = 7.3 Hz, 2H), 7.40 (t, *J* = 7.4 Hz, 2H), 7.33 (t, *J* = 7.3 Hz, 1H), 6.96 (t, *J* = 8.4 Hz, 1H), 6.65–6.60 (m, 2H), 5.16 (s, 2H), 3.92 (s, 3H), 3.88 (s, 3H). ^{13}C NMR ($CDCl_3$, 100 MHz) δ 153.7, 152.7, 138.9, 137.3, 128.5, 127.8, 127.2, 123.5, 107.5, 105.6, 71.0, 60.9, 56.1; IR (neat) ν_{max} 2936, 2835, 1597, 1494, 1476, 1380, 1298, 1257, 1175, 1103, 1009, 733 cm^{-1}; HRMS (ESI$^+$) *m/z* calculated for $C_{15}H_{16}O_3$ [M+Na]$^+$: 267.0992, found: 267.0992. See Appendix 1 for impurity identification and HPLC retention times.

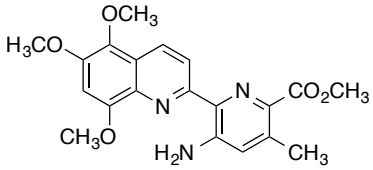

Compound 2.55, methyl 5-amino-3-methyl-6-(5,6,8-trimethoxyquinolin-2-yl)picolinate

A solution of chloroquinoline **2.41** (0.077 g, 0.30 mmol) and tetrakis(triphenylphosphine)palladium (0.018 g, 0.0020 mmol) in toluene (3.0 mL) was degassed and refilled with argon five times. Hexamethylditin (0.069 g, 0.33 mmol) was subsequently added, the reaction was degassed and refilled with argon five times, and the resulting solution heated at 60 °C for 16 h. The reaction mixture was allowed to cool to 25 °C, diluted with Et_2O (2.0 mL) and washed with water (2.0 mL). The aqueous phase was extracted with Et_2O (2×10 mL) and the combined organic extracts were washed with brine (5.0 mL), then dried with Na_2SO_4, filtered

and concentrated. The crude product **2.42**, contaminated with triphenylphosphine oxide, was immediately used in the next step without any further purification.

Trifluoromethanesulfonyl-substituted pyridine (**2.32**, 0.040 g, 0.13 mmol) was added to a solution of 2-stannyl quinoline **2.41** (0.070 g, 0.18 mmol), tetrakis(triphenylphosphine)palladium (0.007 g, 0.006 mmol), cesium fluoride (0.037 g, 0.24 mmol) and copper(I) iodide (0.002 g, 0.01 mmol) in toluene (1.8 mL). The reaction mixture was degassed and refilled with argon five times, then heated at reflux for 16 h. The mixture was allowed to cool to 25 °C, then was filtered and concentrated. The crude product was purified by flash column chromatography (10% w/w SiO_2/K_2CO_3, 25% EtOAc/petrol) to afford **2.55** as a pale brown solid (0.027 g, 0.069 mmol, 55%). ^{1}H NMR (400 MHz, $CDCl_3$) δ 8.78 (d, *J* = 9.0 Hz, 1H), 8.46 (d, *J* = 9.0 Hz, 1H), 6.89 (s, 1H), 6.85 (s, 1H), 4.06 (s, 3H), 4.04 (s, 3H), 3.98 (s, 3H), 3.95 (s, 3H), 2.60 (s, 3H); ^{13}C NMR (100 MHz, $CDCl_3$) δ 166.5, 155.3, 152.1, 148.8, 146.6, 138.4, 135.8, 134.0, 133.7, 133.1, 130.2, 125.8, 123.1, 120.6, 98.4, 61.6, 57.2, 56.2, 52.0, 20.6; IR (neat) ν_{max} 3423, 3243, 2926, 2848, 1698, 1601, 1572, 1492, 1462, 1439, 1363, 1310, 1263, 1246, 1192, 1179, 1144, 1111, 1071, 1002 cm^{-1}; HRMS (ESI$^+$) *m/z* calculated for $C_{20}H_{21}N_3O_5$ $[M+Na]^+$: 406.1373, found: 406.1358; See Appendix 1 for HPLC retention times.

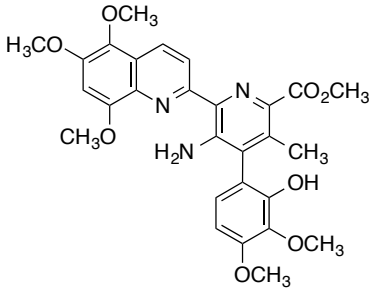

Compound 2.72, methyl 5-amino-4-(2-hydroxy-3,4-dimethoxyphenyl)-3-methyl-6-(5,6,8-trimethoxyquinolin-2-yl)picolinate

A suspension of **2.47** (11.8 mg, 0.0189 mmol) and 10% Pd/C (0.006 g, 0.006 mmol) in methanol/EtOAc (3:1 by volume, 5 mL total) was stirred under a H_2 (g) atmosphere at 25 °C for 36 h. The reaction mixture was filtered through Celite®, eluting with methanol (20 mL) and then concentrated. The crude product was purified by flash column chromatography (SiO_2, 33% EtOAc/petrol) to yield **2.72** as a yellow oil (3.8 mg, 0.0071 mmol, 38%). ^{1}H NMR (400 MHz, $CDCl_3$) δ 8.87 (d, *J* = 8.9 Hz, 1H), 8.49 (d, *J* = 9.0 Hz, 1H), 6.85 (d, *J* = 8.6 Hz, 1H), 6.84 (s, 1H), 6.68 (d, *J* = 8.6 Hz, 1H), 4.04 (s, 3H), 4.01 (s, 3H), 4.00 (s, 3H), 3.99 (s, 6H), 3.96 (s, 3H), 2.35 (s, 3H); ^{13}C NMR ($CDCl_3$, 100 MHz) δ 175.9, 175.1, 171.4, 152.1, 145.1, 136.7, 135.8, 133.2, 133.0, 132.8, 130.1, 128.2, 125.3, 123.1, 104.9, 99.6, 98.4, 87.8, 78.4, 63.5, 61.6, 61.2, 57.3, 56.1, 55.9, 55.8, 52.1, 17.4; IR (neat) ν_{max} 2926 (br), 1720, 1610, 1461, 1339, 1292, 1262, 1212, 1090 cm^{-1}; HRMS (ESI$^+$) *m/z* calculated for $C_{28}H_{29}N_3O_8$ $[M+Na]^+$: 558.1847, found: 558.1851.

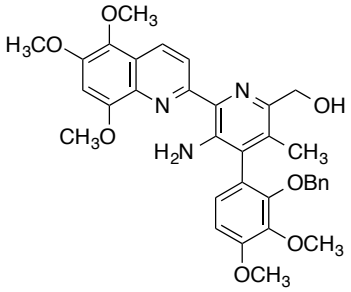

Compound 2.74, (5-amino-4-(2-(benzyloxy)-3,4-dimethoxyphenyl)-3-methyl-6-(5,6,8-trimethoxyquinolin-2-yl)pyridin-2-yl)methanol

To a solution of **2.47** (0.0106 g, 0.0169 mmol) in THF (0.10 mL) was added a solution of $LiAlH_4$ (1 M, 0.051 mL) at –30 °C. The mixture was warmed to 0 °C and stirred for 4 h. Upon completion by TLC, water (0.1 mL) was added, followed by a 15% solution of NaOH (0.1 mL) and additional water (0.4 mL).[36] The aqueous phase was extracted with EtOAc (3×5 mL) and the combined organic extracts were dried with Na_2SO_4, filtered and concentrated. The crude product was purified by flash column chromatography (SiO_2, 33–50% EtOAc/petrol gradient) to afford **2.74** as a yellow oil (0.0046 g, 0.0077 mmol, 46%). ^{1}H NMR (400 MHz, $CDCl_3$) δ 8.31 (d, *J* = 8.4 Hz, 1H), 8.09 (d, *J* = 8.4 Hz, 1H), 7.11–7.09 (m, 3H), 7.00–6.97 (m, 2H) 6.91 (d, *J* = 11.9 Hz, 1H), 6.88 (s, 1H), 6.87 (d, *J* = 11.9 Hz, 1H), 4.91 (m, 2H), 4.68 (m, 2H), 4.06 (s, 3H), 4.03 (s, 3H), 3.97 (s, 6H), 3.94 (s, 3H), 2.44 (s, 3H); ^{13}C NMR (100 MHz, $CDCl_3$) δ 155.8, 154.0, 152.1, 150.8, 148.5, 143.4, 142.7, 142.4, 137.3, 135.8, 133.9, 133.3, 131.2, 130.1, 129.9, 128.1, 127.9, 127.8, 125.0, 122.8, 122.3, 120.3, 108.4, 98.4, 75.3, 61.6, 61.2, 57.3, 56.1, 56.1, 14.0; IR (neat) ν_{max} 2918, 2850, 2360, 2339, 1737, 1600, 1525, 1488, 1462, 1424, 1367, 1292, 1260, 1231, 1098, 1004, 751 cm^{-1}; HRMS (ESI$^+$) *m/z* calculated for $C_{34}H_{35}N_3O_7$ $[M+H]^+$: 598.2548, found: 598.2548.

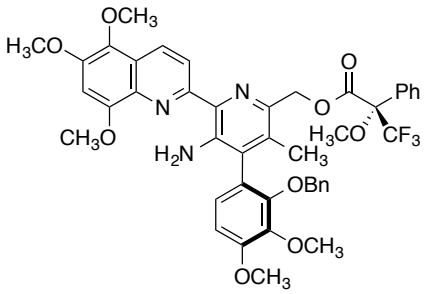

Compound 2.76, ((*R*)-5-amino-4-(2-(benzyloxy)-3,4-dimethoxyphenyl)-3-methyl-6-(5,6,8-trimethoxyquinolin-2-yl)pyridin-2-yl)methyl (*S*)-3,3,3-trifluoro-2-methoxy-2-phenylpropanoate

A solution of $LiAlH_4$ (1.0 M, 0.062 mL) was added to a solution of **2.47** (0.013 g, 0.021 mmol) in THF (0.20 mL) at –30 °C. The mixture was warmed to 25 °C and stirred for 4 h. A saturated aqueous solution of Na_2SO_4 was added until excess $LiAlH_4$ was quenched, and solid Na_2SO_4 had precipitated. The solution was then filtered and concentrated. The crude product **2.74** was used without further purification. DMAP (0.011 g, 0.086 mmol) and (*R*)-(–)-α-methoxy-α-(trifluoromethyl)phenylacetyl chloride (0.013 mL, 0.069 mmol) were added to a solution of **2.74** (0.0079 g, 0.013 mmol) in CH_2Cl_2 (0.13 mL). The reaction was stirred at 25 °C for 16 h or until TLC indicated consumption of the starting material. The reaction was filtered through a small SiO_2 plug and then purified by flash column chromatography (SiO_2, petrol to 33% EtOAc/petrol gradient) to afford **2.76** as a red solid (0.0087 mg, 0.010 mmol, 48%). Data given are for the major diastereomer from an enantioenriched sample (from P-N ligand). ^{1}H NMR (400 MHz, $CDCl_3$) δ 8.80 (d, *J* = 9.2 Hz, 1H), 8.42 (d, *J* = 9.2 Hz, 1H), 7.58–7.54 (m, 2H), 7.33–7.29 (m, 3H), 7.08–6.93 (m, 5H), 6.87 (s, 2H), 6.83 (s, 1H), 5.65–5.57 (m, 1H), 5.48–5.41 (m, 1H), 4.93–4.86 (m, 1H), 4.80–4.77 (m, 1H), 4.04 (s, 3H), 4.00 (s, 3H), 3.96 (s, 6H), 3.94 (s, 3H), 3.52 (s, 3H), 1.92 (s, 3H); ^{13}C NMR (125 MHz, toluene-d_8) δ 166.6 (2C), 156.9, 154.5 (2C), 152.5, 151.5, 151.4, 148.9, 144.3 (m, CF_3), 139.5, 139.4, 134.2, 133.7, 133.6, 133.5, 133.3 (2C), 133.2, 129.9, 123.5, 123.1 (2C), 121.2, 108.8, 99.8, 69.2, 68.9, 60.9, 60.7, 57.2,

55.6, 55.4, 14.4; ^{19}F NMR (472 MHz, toluene-d_8) δ 71.73, 71.76 (both diastereomers given); IR (neat) ν_{max} 3460, 3321, 2930, 2850, 1746, 1625, 1600, 1581, 1490, 1465, 1422, 1358, 1228 (br), 1169, 1098, 1069, 1001, 921, 719 cm^{-1}; HRMS (ESI$^+$) *m/z* calculated for $C_{44}H_{42}F_3N_3O_9$ [M+Na]$^+$: 836.2771, found 836.2736; m.p. 190–195 °C [recrystallized from CH_2Cl_2]. See Appendix 1 for additional data regarding the Mosher's ester synthesis and analysis for ee% determination.

2.5 References

1. Rao, K. V.; Cullen, W. P. *Antibiot. Annu.* **1959**, *7*, 950–953.
2. Bringmann, G.; Reichert, Y.; Kane, V. V. *Tetrahedron* **2004**, *60*, 3539–3574.
3. Bringmann, G.; Gulder, T.; Gulder, T. A. M.; Breuning, M. *Chem. Rev.* **2011**, *111*, 563–639.
4. Herlt, A. J.; Rickards, R.; Wu, J. P. *J. Antibiot.* **1985**, *38*, 516–518.
5. Rickards, R. W.; Wu, J. P. *J. Antibiot.* **1985**, *38*, 513–515.
6. Rao, K.; Biemann, K.; Woodward, R. B. *J. Am. Chem. Soc.* **1963**, *83*, 2532–2533.
7. Lown, J. W.; Begleiter, A. *Can. J. Chem.* **1974**, *52*, 2331–2336.
8. Gould, S. J.; Cane, D. E. *J. Am. Chem. Soc.* **1982**, *104*, 343–346.
9. Chiu, Y. Y.; Lipscomb, W. N. *J. Am. Chem. Soc.* **1975**, *97*, 2525–2530.
10. Harding, M. M.; Long, G. V.; Brown, C. L. *J. Med. Chem.* **1993**, *36*, 3056–3060.
11. Dholakia, S.; Gillard, R. *Tetrahedron* **1981**, *37*, 2929–2933.
12. Rickards, R.; Tennant, S. *Tetrahedron* **1997**, *53*, 15101–15114.
13. Bringmann, G.; Reichert, M.; Hemberger, Y. *Tetrahedron* **2008**, *64*, 515–521.
14. Cuyegkeng, M. A.; Mannschreck, A. *Chem. Ber.* **1987**, *120*, 803–809.
15. Long, G. V.; Harding, M. M. *J. Chem. Soc., Dalton Trans.* **1996**, 549.
16. Oleson, J.; Calderella, L. A.; Mjos, K. J.; Reith, A. R.; Thie, R. S.; Toplin, I. *Antibiot. Chemother.* **1961**, *11*, 158–164.
17. Wilson, W. L.; Labra, C.; Barris, E. *Antibiot. Chemother.* **1961**, *11*, 147–150.
18. Teller, M. N.; Wagshul, S. F.; Wooley, G. W. *Antibiot. Chemother.* **1961**, *11*, 165–173.
19. Reilly, H. C.; Sugiura, K. *Proc. Am. Assoc. Canc. Res.* **1960**, *3*, 144.
20. Livingston, R. B.; Carter, S. K. In *Single Agents in Cancer Chemotherapy*; Springer US: Boston, MA, **1970**; pp. 359–402.
21. Sullivan, R. D.; Miller, E.; Zurek, W. Z.; Rodriguez, F. R. *Cancer Chemother. Rep.* **1963**, *33*, 27–40.
22. Hackethal, C. A.; Golbey, R. B.; Tan, C. T.; Karnofsky, D. A.; Burchenal, J. H. *Antibiot. Chemother.* **1961**, *11*, 178–183.
23. Chirigos, M. A.; Pearson, J. W.; Papas, T. S.; Woods, W. A.; Wood, H. B.; Spahn, G. *Cancer Chemother. Rep.* **1973**, *57*, 305–309.
24. McBride, T.; Oleson, J. *Cancer Res.* **1966**, *26*, 727–732.
25. Harding, M. M.; Long, G. V. *Curr. Med. Chem.* **1997**, *4*, 405–420.
26. Take, Y.; Inouye, Y.; Nakamura, S.; Allaudeen, H. S.; Kubo, A. *J. Antibiot.* **1989**, *42*, 107–115.
27. Rivers, S. L.; Whitting, R. M.; Medrek, T. J. *Cancer* **1966**, *19*, 1377–1385.

28. Harris, M. N.; Medrek, T. J.; Golomb, F. M.; Gumport, S. L.; Postel, A. H.; Wright, J. C. *Cancer* **1965**, *18*, 49–57.

29. Hoff, Von, D. D.; Rozencweig, M.; Soper, W. T.; Helman, L. J.; Penta, J. S.; Davis, H. L.; Muggia, F. M. *Cancer Treat. Rep.* **1977**, *61*, 759–768.

30. Israel, L. *Recent Results Canc. Res.* **1976**, 189–195.

31. Bianchi, M.; Bolzan, A. *Mutat. Res.* **2001**, *488*, 25–37.

32. Ross, D.; Beall, H.; Traver, R. D.; Siegel, D.; Phillips, R. M.; Gibson, N. W. *Oncol. Res.* **1994**, *6*, 493–500.

33. Knuckley, B.; Jones, J. E.; Bachovchin, D. A.; Slack, J.; Causey, C. P.; Brown, S. J.; Rosen, H.; Cravatt, B. F.; Thompson, P. R. *Chem. Commun.* **2010**, *46*, 7175–7177.

34. Capranico, G.; Palumbo, M.; Tinelli, S.; Zunino, F. *J. Biol. Chem.* **1994**, *269*, 25004–25009.

35. Mizuno, N. S.; Gilboe, D. P. *Biochim. Biophys. Acta* **1970**, *224*, 319–327.

36. Hajdu, J. *Met. Ions Biol. Syst.* **1985**, *19*, 53–80.

37. Rao, K. V. *J. Heterocyclic Chem.* **1977**, *14*, 653–659.

38. Godard, A.; Rocca, P.; Fourquez, J. M.; Rovera, J. C.; Marsais, F.; Queguiner, G. *Tetrahedron Lett.* **1993**, *34*, 7919–7922.

39. McElroy, W. T.; DeShong, P. *Org. Lett.* **2003**, *5*, 4779–4782.

40. Boger, D. L.; Yasuda, M.; Mitscher, L. A.; Drake, S. D.; Kitos, P. A.; Thompson, S. C. *J. Med. Chem.* **1987**, *30*, 1918–1928.

41. Rao, K. V. *Cancer Chemother. Rep. 2* **1974**, *4*, 11–17.

42. Kremer, W. B.; Laszlo, J. *Cancer Chemother. Rep.* **1967**, *51*, 19–24.

43. Dhar, K.; Rosazza, J. P. N. *Appl. Environ. Microbiol.* **2000**, *66*, 4877–4882.

44. Kende, A. S.; Naegely, P.C. *Tetrahedron Lett.* **1978**, *19*, 4775–4778.

45. Lown, J. W.; Sim, S. K. *Can. J. Biochem.* **1976**, *54*, 446–452.

46. Lown, J. W.; Sim, S. K. *Can. J. Chem.* **1976**, *54*, 2563–2572.

47. Shaikh, I. A.; Johnson, F.; Grollman, A. P. *J. Med. Chem.* **1986**, *29*, 1329–1340.

48. Hafuri, Y.; Takemori, E.; Oogose, K.; Inouye, Y.; Nakamura, S.; Kitahara, Y.; Nakahara, S.; Kubo, A. *J. Antibiot.* **1988**, *41*, 1471–1478.

49. Harding, M. M.; Anderberg, P. *Anti-Cancer Drug Des.* **2001**, *16*, 143–153.

50. Inouye, Y.; Take, Y.; Kubo, A.; Takemori, E.; Nakamura, S.; Nishimura, T.; Suzuki, H.; Yamaguchi, H. *J. Antibiot.* **1989**, *42*, 968–976.

51. Kametani, T.; Ogasawara, K.; Kozuka, A. *Yakugaku Zasshi* **1966**, *86*, 815–822.

52. Cushman, M.; Mathew, J. *J. Org. Chem.* **1981**, *46*, 4921–4923.

53. Ciufolini, M. A.; Byrne, N. E. *J. Chem. Soc., Chem. Commun.* **1988**, 1230–1231.

54. Pomel, V.; Rovera, J.; Godard, A.; Marsais, F.; Queguiner, G. *J. Heterocyclic Chem.* **1996**, *33*, 1995–2005.

55. Fourquez, J. M.; Godard, A.; Marsais, F.; Queguiner, G. *J. Heterocyclic Chem.* **1995**, *32*, 1165–1170.

56. Godard, A.; Rovera, J.-C.; Marsais, F.; Plé, N.; Quéguiner, G. *Tetrahedron* **1992**, *48*, 4123–4134.

57. Basha, F. Z.; Hibino, S.; Kim, D.; Pye, W. E.; Wu, T. T.; Weinreb, S. M. *J. Am. Chem. Soc.* **1980**, *102*, 3962–3964.

58. Kende, A.; Lorah, D.; Boatman, R. *J. Am. Chem. Soc.* **1981**, *103*, 1271–1273.

59. Boger, D.; Panek, J. *J. Am. Chem. Soc.* **1985**, *107*, 5745–5754.

60. Donohoe, T. J.; Jones, C. R.; Barbosa, L. C. A. *J. Am. Chem. Soc.* **2011**, *133*, 16418–16421.

61. Donohoe, T. J.; Bower, J. F.; Basutto, J. A.; Fishlock, L. P.; Procopiou, P. A.; Callens, C. K. A. *Tetrahedron* **2009**, *65*, 8969–8980.

62. Donohoe, T. J.; Fishlock, L. P.; Basutto, J. A.; Bower, J. F.; Procopiou, P. A.; Thompson, A. L. *Chem. Commun.* **2009**, 3008–3010.

63. Donohoe, T. J.; Fishlock, L. P.; Procopiou, P. A. *Org. Lett.* **2008**, *10*, 285–288.

64. Yim, A. M.; Vidal, Y.; Viallefont, P.; Martinez, J. *Tetrahedron: Asymmetry* **2002**, *13*, 503–510.

65. McElroy, W. T.; DeShong, P. *Tetrahedron* **2006**, *62*, 6945–6954.

66. Cai, S.; Zhou, Z.; Huang, J.; Whittemore, E. R.; Egbuwoku, Z. O.; Hawkinson, J. E.; Woodward, R. M.; Weber, E.; Keana, J. *J. Med. Chem.* **1996**, *23*, 4682–4686.

67. Bode, H. M. *Angew. Chem.* **1936**, *49*, 486–489.

68. Marcus, R.; Fresco, J. *J. Chem. Phys.* **1957**, *27*, 564.

69. Ogasawara, M.; Watanabe, S. *Synthesis* **2009**, 1761–1785.

70. Shindo, M.; Koga, K.; Tomioka, K. *J. Am. Chem. Soc.* **1992**, *114*, 8732–8733.

71. Hayashi, T.; Hayashizaki, K.; Kiyoi, T.; Ito, Y. *J. Am. Chem. Soc.* **1988**, *110*, 8153–8156.

72. Colletti, S. L.; Halterman, R. L. *Tetrahedron Lett.* **1989**, *30*, 3513–3516.

73. Genov, M.; Fuentes, B.; Espinet, P.; Pelaz, B. *Tetrahedron: Asymmetry* **2006, *17*, 2593-2593**.

74. Buchwald, S. L.; Yin, J. *J. Am. Chem. Soc.* **2000**, *122*, 12051–12052.

75. Cammidge, A. N.; Crépy, K. V. L. *Chem. Commun.* **2000**, 1723–1724.

76. Baudoin, O. *Eur. J. Org. Chem.* **2005**, *2005*, 4223–4229.

77. Kozlowski, M. C.; Morgan, B. J.; Linton, E. C. *Chem. Soc. Rev.* **2009**, *38*, 3193–3207.

78. Herrbach, A.; Marinetti, A.; Baudoin, O.; Guénard, D.; Guéritte, F. *J. Org. Chem.* **2003**, *68*, 4897–4905.

79. Castanet, A.-S.; Colobert, F.; Broutin, P.-E.; Obringer, M. *Tetrahedron: Asymmetry* **2002**, *13*, 659–665.

80. Mikami, K.; Miyamoto, T.; Hatano, M. *Chem. Commun.* **2004**, 2082–2083.

81. Bronger, R. P. J.; Guiry, P. J. *Tetrahedron: Asymmetry* **2007**, *18*, 1094–1102.

82. Bermejo, A.; Ros, A.; Fernández, R.; Lassaletta, J. M. *J. Am. Chem. Soc.* **2008**, *130*, 15798–15799.

83. Christie, G. H.; Kenner, J. *J. Am. Chem. Soc.* **1922**, *1*, 614–620.

84. Oki, M. In *onlinelibrary.wiley.com*; Topics in Stereochemistry; John Wiley & Sons, Inc.: Hoboken, NJ, USA, **1983**; Vol. 14, pp. 1–81.

85. Adams, R.; Yuan, H. C. *Chem. Rev.* **1933**, *12*, 261–338.

86. Kishi, Y.; Uenishi, J.; Beau, J.-M.; Armstrong, R. W. *J. Am. Chem. Soc.* **1987**, *109*, 4756–4758.

87. Korenaga, T.; Sakai, T.; Kosaki, T.; Fukumura, R.; Ema, T. *Org. Lett.* **2005**, *7*, 4915–4917.

88. Sindkhedkar, M. D.; Mulla, H. R.; Wurth, M. A.; Cammers-Goodwin, A. *Tetrahedron* **2001**, *57*, 2991–2996.

89. Lassaletta, J. M.; Fernández, R.; Ros, A.; Estepa, B.; Bermejo, A.; Alvarez, E. *J. Org. Chem.* **2012**, *77*, 4740–4750.

90. Pirkle, W. H.; Sikkenga, D. L.; Pavlin, M. S. *J. Org. Chem.* **1977**, *42*, 384–387.

91. Zhang, F.; Liu, S.; Lu, X.; Guo, L.; Zhang, H.; Che, Y. *J. Nat. Prod.* **2009**, *72*, 1782–1785.

92. Donohoe, T. J.; Jones, C. R.; Kornahrens, A. F.; Barbosa, L. C. A.; Walport, L. J.; Tatton, M. R.; O'Hagan, M.; Rathi, A. H.; Baker, D. B. *J. Org. Chem.* **2013**, *78*, 12338–12350.

93. Harrowven, D. C.; Curran, D. P.; Kostiuk, S. L.; Wallis-Guy, I. L.; Whiting, S.; Stenning, K. J.; Tang, B.; Packard, E.; Nanson, L. *Chem. Commun.* **2010**, *46*, 6335–6337.

Chapter 3

Metal-catalyzed interrupted-hydrogen-borrowing reactions to form 1,5-diketones and pyridines

3.1 Introduction

Key to the success of the total synthesis of streptonigrin designed and executed in the Donohoe group and described in Chapter 2 was the formation of a key C-ring pyridine precursor through RCM methods developed in the group (see **2.26**, Scheme 2-3). This exemplifies the utility of synthetic method development, a key tenet of modern organic chemistry research (see Chapter 1). Innovation and discovery are driven through the repeated process of method development and application. This interplay motivates the re-examination of methods to push the boundaries of organic synthesis.

The prevalence of the pyridine scaffold in natural products and pharmaceutical targets[1,2] (see Figure 1-5) drives the development of methods to produce pyridines and their precursor pyridones (such as **2.26**). A key retrosynthetic target to produce pyridines **3.1** is the 1,5-diketone scaffold (**3.2**) and examples employing this logic include the Krohnke annulation, the Bohlmann–Rahtz synthesis, and the Hantzsch pyridine synthesis (Figure 3-1).

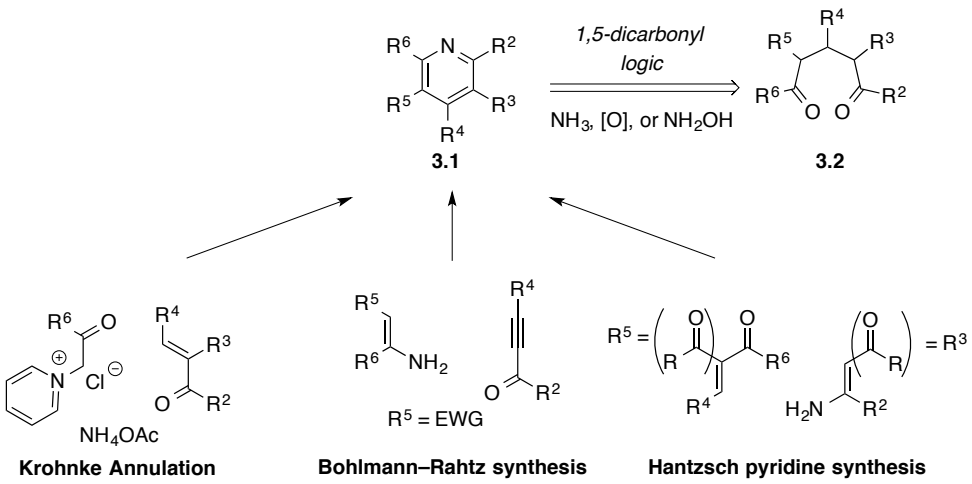

Figure 3-1. Methods to form diversely substituted pyridines using the 1,5-dicarbonyl logic

The target methodology pursued subsequently and detailed in this chapter enabled the synthesis of 1,5-diketones such as **3.2** through an application of the "hydrogen-borrowing" catalytic method.

3.1.1 Introduction to hydrogen-borrowing methodology

Hydrogen-borrowing (H-B) methodology uses transfer hydrogenation to enable reversible changes in the oxidation state of reaction partners. The resulting overall reaction would typically be difficult, costly or toxic by other more conventional methods. For example, direct S_N2 reactions of an alcohol with a nucleophile would require hydroxide displacement, a difficult feat as the strength of the C–O bond is ≈90 kcal mol^{-1}.[3] Instead, oxidation of the alcohol reaction partner to the corresponding aldehyde allows easier C–C bond formation, and subsequent "hydrogen returning" yields a product with the same oxidation state as the starting material.

Generally H-B methodology involves three main steps: (1) an H-B catalyst (**3.4**) oxidizes an alcohol substrate (**3.3**) by formally removing two hydrogen atoms and temporarily forming a reactive aldehyde intermediate (**3.6**) and a metal hydride (**3.5**); (2) subsequent attack by nucleophile (**3.7**) generates a new compound with C–C bond formation, **3.8**; (3) redelivery of the two hydrogen atoms from the catalyst reduces **3.8** to yield product **3.9** (Scheme 3-1). The transformation is thus performed with no net change in the oxidation state of the substrate and with catalyst regeneration.

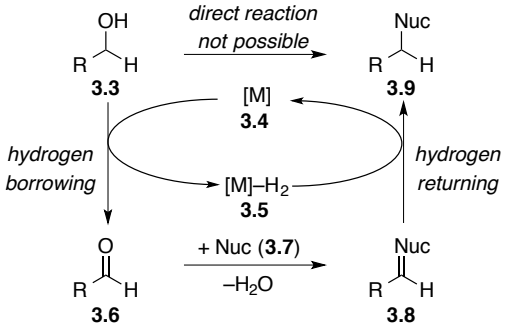

Scheme 3-1. General H-B catalytic cycle

The earliest example of H-B-type chemistry is the Guerbet reaction, which can be performed without a hydrogen-transfer catalyst (Scheme 3-2). In the original example from the late 19th century,[4] a primary alcohol (**3.10**) is dimerized to form β-branched primary alcohols (such as **3.11**) via oxidation, aldol reaction and reduction steps (Scheme 3-2a) sometimes using catalysts (e.g. Raney nickel or copper).[5] The high temperature and byproducts from Cannizzaro-type reactions (**3.12** and **3.13**) prompted development of a transition metal (TM)-catalyzed method using $[IrCp^*Cl_2]_2$ allowing increased yield of **3.11** (Scheme 3-2b)[6].

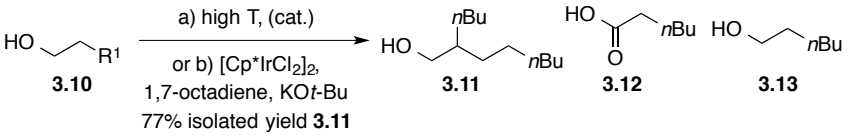

Scheme 3-2. Guerbet reaction: (a) traditional and (b) TM-catalyzed methods

One of the earliest uses of TM-catalysis to enable the use of alcohols as alkylation reagents in an H-B transformation was in 1981 by Grigg and coworkers (Scheme 3-3).[1-9] This method used Rh catalysis to alkylate arylacetonitriles **3.14** (a) and amines **3.19** (b) in good yields and relatively mild conditions exposing the potential of a robust α-alkylation protocol through transition metal H-B catalysis.

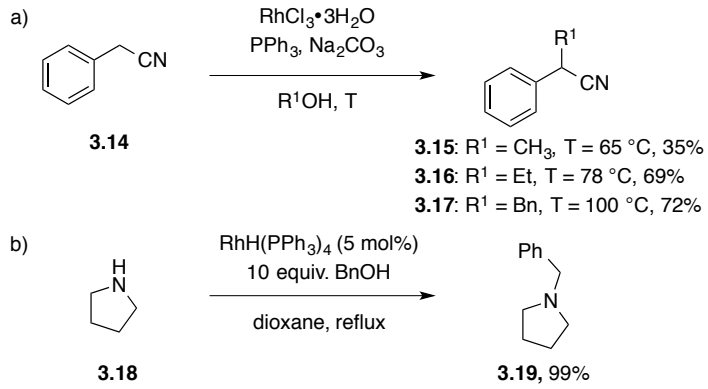

Scheme 3-3. Early TM-catalyzed H-B methodology by Grigg and coworkers

Many examples of TM-catalyzed H-B methodology enabling addition of alcohols to various nucleophiles have been disclosed (Figure 3-2) forming N–C and C–C bonds. The range of substrates includes anilines (**3.20**, **3.21**),[10] additional arylacetonitriles (**3.22**)[11] and other activated methylenes such as α-cyanoketones (**3.23**).[12] These methods use primary alcohols and ruthenium catalysts, though additional examples have been published using Ir (**3.24**)[13] and Os catalysts.[14]

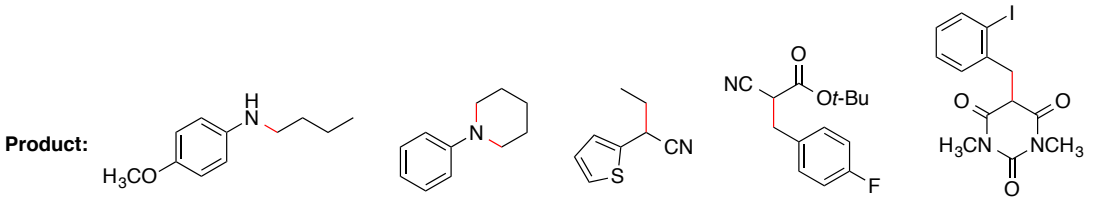

Figure 3-2. TM-catalyzed H-B reactions (with alcohols and catalysts shown)

Another related methodology utilizing similar hydrogen borrowing and returning steps is the transfer-hydrogenative (T-H) coupling methodology. T-H methodology allows the exchange of hydrogen between alcohols and π-unsaturated reactants to generate nucleophile-electrophile pairs (**3.25** and **3.26**, Scheme 3-4) which can subsequently react to form diverse products.

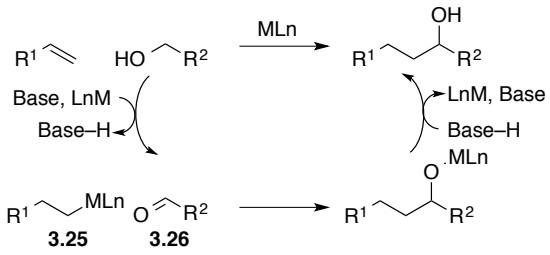

Scheme 3-4. Transfer-hydrogenative coupling method

Krishe and coworkers showed in their 2007 publication that hydrogen does not need to be added for this system to be effective, as it can be sourced through alcohol oxidation in situ.[15] This allowed reverse prenylation, crotylation and allylation of alcohols with allenes through use of a cationic Ir^{I} catalyst to give complex secondary alcohols such as **3.27** in good yields under relatively mild conditions (Scheme 3-5).

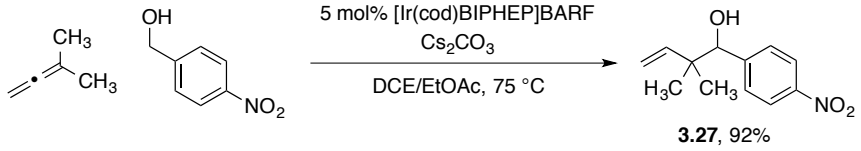

Scheme 3-5. Krische's transfer-hydrogenative coupling methodology

3.1.2 Hydrogen-borrowing methodology utilizing ketone substrates

A major class of activated methylene compounds are carbonyl-containing compounds. The ease of removing protons adjacent to carbonyl moieties allows enolates to act as nucleophilic partners for H-B methodology. Examples using esters and dimethylbarbituric acid were previously mentioned (Figure 3-2), but the use of ketones in H-B alkylation provides a powerful alternative to the traditional lithium enolate reactions used to α-alkylate ketones (**3.28** to **3.31**, Scheme 3-6a). The use of H-B methodology provides the same transformation without the restrictions of lithium enolate reactions: exclusion of moisture, use of stoichiometric high molecular weight strong bases (i.e. LDA), large leaving groups (halides or tosylates, often toxic) which all result in low atom economy and large amounts of waste. In contrast, H-B methodology has been shown to allow the use of alcohols in such alkylation reactions

with low loadings of catalysts, with high turnover numbers, at relatively low temperatures and with water as the only byproduct. The H-B reaction utilizing enolate nucleophiles (Scheme 3-6b) proceeds via oxidation of the alcohol to aldehyde **3.33** (with production of metal hydride, **3.5**), aldol reaction with ketone **3.28** to form intermediate **3.34** and subsequent reduction of this enone by the metal hydride to form alkylated product **3.31**.

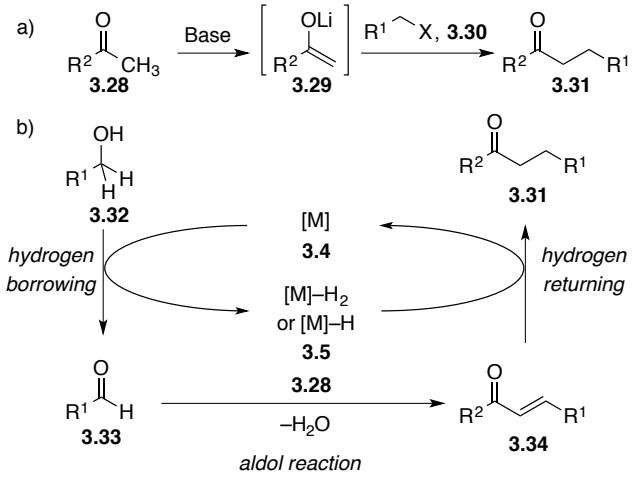

Scheme 3-6. Ketone α-alkylation by (a) lithium enolate and (b) H-B methods

The first α-alkyation of a ketone using transition metal-catalyzed H-B methodology was published in 2001.[16] The use of primary aliphatic and benzylic alcohols (at a threefold excess) with a Ru catalyst allowed alkylation of methyl ketones (**3.35**) and concomitant reduction of the ketone moiety to give secondary alcohols **3.36** and **3.37** (Scheme 3-7a). The methodology was also successfully applied to cyclic ketone **3.38** with *n*-butanol to give **3.39**, a rare example of an α-branched product utilizing simple ketones with H-B methodology (Scheme 3-7b).

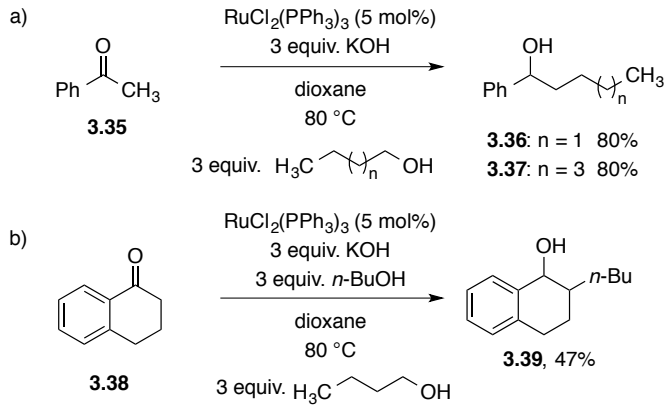

Scheme 3-7. Examples of ketone α-alkylation forming alcohols with H-B method

Expansion of the H-B methodology sought to access α-alkylated ketone products by preventing carbonyl reduction. Cho and coworkers demonstrated that the use of metal-hydride scavengers such as 1-dodecene[17] and 1-decene[18] (Scheme 3-8a–c) allowed the formation of alkyl, aryl and branched ketones (utilizing cyclic ketones **3.44** and **3.45**, in b). Yus and coworkers also demonstrated benzophenone would prevent ketone reduction (not shown).[19,20]

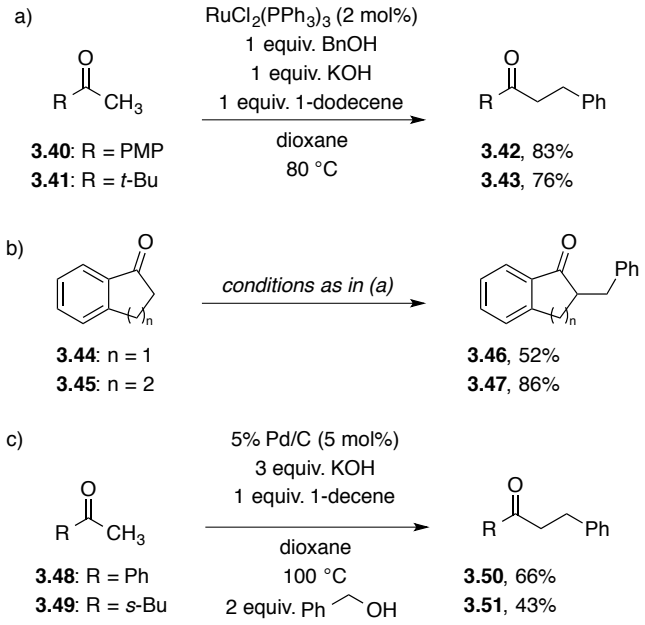

Scheme 3-8. Use of metal hydride quenchers for α-alkylated ketone formation

Other catalytic systems provided the oxidation of primary alcohols, nucleophilic addition and alkene hydrogenation without product or starting material

ketone reduction. Park and coworkers used Pd-nanoparticles and aluminum hydroxide (Pd/AlO(OH)) to achieve the α-alkylation of methyl ketone **3.52** using aliphatic, benzylic and heteroaromatic alcohols with an argon atmosphere (Scheme 3-9a).[21] Interestingly, using an oxygen environment instead yielded unreduced enone (**3.54)** as the primary product (Scheme 3-9b), suggesting that the metal hydride was consumed in solution. This suggests that another product family is accessible from ketones through interruption of the hydrogen returning step of H-B catalysis (see Section 3.2.1).

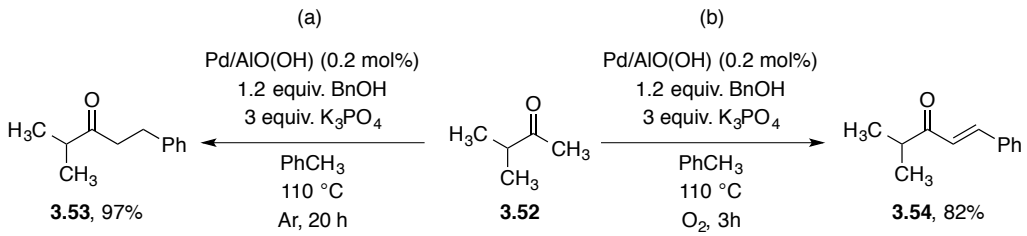

Scheme 3-9. Catalytic system allowing (a) ketone or (b) α,β-unsaturated ketone formation

Other examples of methodology that access alkylated ketones without reduction of the carbonyl utilized Pd,[15,22] Os,[14,16] and Ir,[23] using a variety of primary alcohols (Figure 3-3).[19,20] Many of these catalytic systems were previously demonstrated to enable alcohol oxidation with subsequent redelivery of hydride in the alkylation of nitriles or amines.

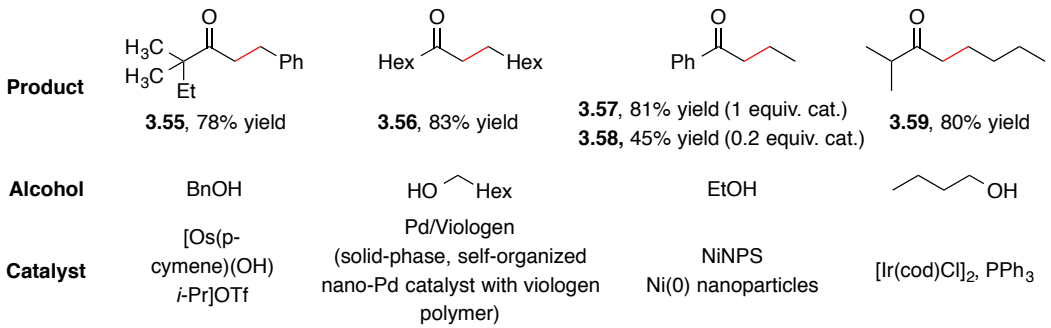

Figure 3-3. Examples of α-alkylated ketone products using various catalytic methods

The use of catalyst $[Ir(cod)Cl]_2$ with an arylphosphine was shown to enable α-alkylation and provide ketone products and unreduced starting material (Figure 3-3d).[23] Of note is that the use of P(*n*-Bu)$_3$ and PCy_3 led to over reduction, suggesting a more active metal hydride species. One additional substrate worth noting is **3.60** which was shown by Ishii and coworkers to give branched product **3.61**, the only prior example of branched ketone formation using an acyclic system and H-B methodology prior to the work of the Donohoe group (Scheme 3-10).

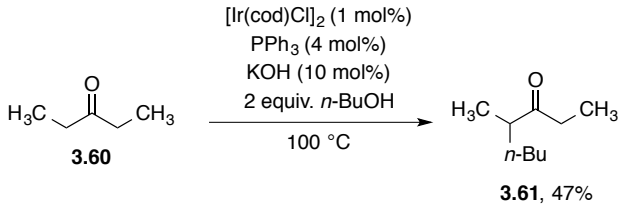

Scheme 3-10. Acyclic ketone used for branched α-alkylation

The scope of ketone substrates demonstrated by H-B methods was predominantly limited to methyl ketones at the inception of the Donohoe H-B methodology program. These formed linear products after monoalkylation with limited examples of the formation of α-branched products.

3.1.3 The use of methanol in hydrogen-borrowing methods

Existing methods of H-B alkylation lacked examples using short-chain alcohols such as methanol and instead used benzyl or long chain alcohols, with a few notable exceptions using amines or arylacetonitriles as described above. This is despite the great utility methanol provides in catalytic alcohol dehydrogenation reactions. Methanol is oxidized in situ in H-B methodology to formaldehyde, a reactive and unhindered electrophile which can undergo interesting and useful reactions. It also confers the ability to form branched products and allows the production of more complex products than in previous cases.

Methanol is an important and highly abundant feedstock chemical with 35 million tons of methanol produced industrially every year.[24,25] It is available from renewable sources such as gasification of industrial or municipal waste, or by carbon capture technologies. Greater utilization of methanol would contribute towards more green chemistry through avoiding pre-functionalization of methanol (to form CH_3I, CH_3OTf or $(CH_3)_2SO_4$, for example). Catalytic C–C bond forming methods using methanol have been used on an industrial scale, including the Monsanto and Cativa processes for the synthesis of acetic acid.[26]

The oxidation of methanol typically requires harsh conditions (>200 °C) due to the higher enthalpy of dehydrogenation of methanol $\Delta H_{dehydrogenation}(CH_3OH)$ = +84 kJ mol^{-1} (as compared to other alcohols: $\Delta H_{dehydrogenation}(EtOH)$ = +68 kJ mol^{-1}).[26] This could be in part due to the lack of strain relief of oxidizing methanol (as compared to the release of steric strain when oxidizing isopropanol, for example). Low temperature methods to achieve methanol dehydrogenation have been disclosed include Beller's Ru^{II}-pincer complex (**3.62)** to form hydrogen and carbon dioxide (Figure 3-4).[27] The use of **3.62** generated three molecules of H_2 per molecule of methanol, requiring only 1.6 ppm of catalyst at 95 °C.

Other examples include the Ru complex, disclosed by Milstein and coworkers, (**3.63**) which can activate methanol via dehydrogenation at very low temperatures.[28,29] Trincado and Grutzmacher published the Ru-$trop_2$dad complex (**3.64**) in the same year, which can effect production of H_2 with only 0.01 mol% of the catalyst, using Et_3N and $Ba(OH)_2$ with a THF/H_2O mixture at 90 °C.[30] The ligands of **3.64** are proposed to play a role in the mechanism, thereby assigning these complexes to the "non-innocent" family of catalysts.

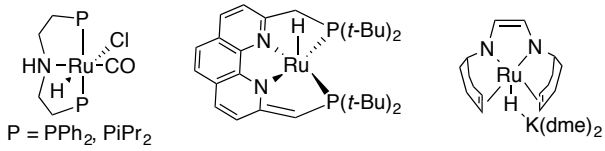

3.62 **3.63** **3.64**

Figure 3-4. Catalysts developed for methanol dehydrogenation

Examples using methanol as an alkylating reagent are few, with the methylation of nitriles and amines published first. Del Zotto's *N*-methylation provided dimethylation and monomethylation products (**3.66** and **3.68**, respectively) from cyclohexylamine (**3.65**) and piperidine (**3.67**) with 1 mol% $CpRuCl(PPh_3)_2$ and in very good yield (Scheme 3-11a–b).[31] *N*-monomethylation of aromatic primary amines, including arylamines (i.e. **3.69**), arylsulfonamides and amino-azoles, has also been demonstrated by Li and coworkers using $[IrCp^*Cl_2]_2$/NaOH (Scheme 3-11c).[32] Interestingly, the catalytic system $[Cp^*IrCl_2]_2$ (used in c) was shown to be incapable of dimethylating anilines, while $Cp^*RuCl(PPh_3)_2$ (seen in a) is incapable of aniline methylation at all suggesting fine tuning of catalytic systems (including choice of metal and the electronic/steric effects of ligands) can enable access to versatile products.

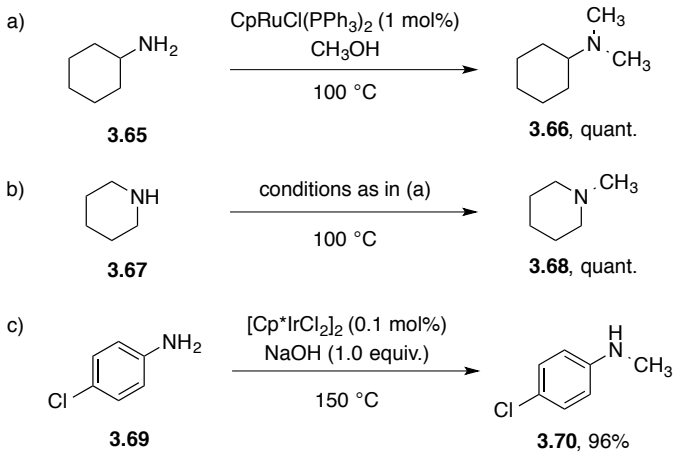

Scheme 3-11. Methylation of amines using methanol and H-B methods

Glorius demonstrated the synthesis of formamides using a ruthenium-*N*-heterocyclic carbene (NHC) complex, methanol and primary or secondary alcohols (Scheme 3-12) through the addition of formaldehyde to amine with loss of hydrogen to the sacrificial hydrogen acceptor styrene.[33]

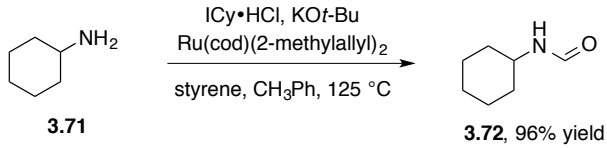

3.71 **3.72**, 96% yield

Scheme 3-12. Formylation of amines with Ru-NHC catalyst

Methanol was also utilized in an earlier example to methylate benzyl nitrile **3.14** to produce **3.16** using $RhCl_3•3H_2O$, triphenylphosphine and relatively low temperature (as in Scheme 3-3).[34] The use of ruthenium-grafted hydrotalcite (Ru/HT) allows efficient α-alkylation of nitriles with primary alcohols, with one example using methanol to again access **3.16** in increased yield (Scheme 3-13).[35]

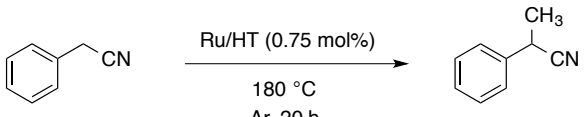

3.14 **3.16**, 65%

Scheme 3-13. Use of methanol to methylate benzyl nitrile

Other C–C bond formation methods using methanol dehydrogenation have also been reported. Krische and coworkers utilized T-H catalysis to form homoallylic alcohols from functionalized allenes, methanol and the *o*-cyclometallated π-allyl iridium complex **3.73** (Scheme 3-14). Only 15 equiv. of methanol and mild temperatures were required (80 °C) and it was determined that methanol dehydrogenation was the turnover-limiting step. Examples with higher order alcohols indicated instead that carbonyl addition was the turnover-limiting step.[26]

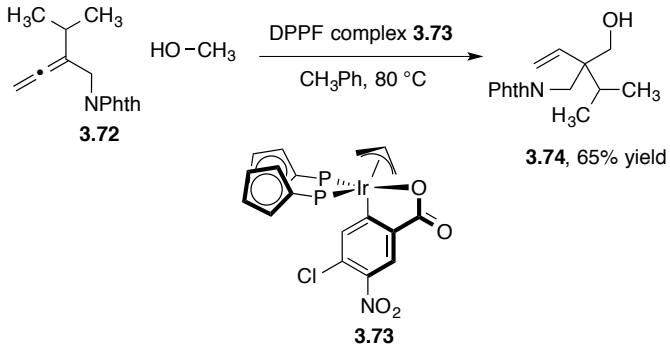

Scheme 3-14. C–C bond formation with methanol and T-H methodology

During the time the work presented in this chapter was being completed, and subsequent to the first Donohoe H-B publication,[36] Obora and coworkers published an iridium-catalyzed methylation of ketones with methanol.[37] The use of $[Cp^*IrCl]_2$ (5 mol%) and high temperatures (120 °C) allowed the formation of mono- and di-methylated, branched aryl- and alkyl-ketones. This methodology highlights the increased diversity of products accessible using methanol and H-B catalysis.

The untapped potential of the diverse products that can be formed from the dehydrogenation of methanol inspired the commencement of work in the Donohoe group to develop a H-B method using methanol to α-methylate ketones.

3.1.4 Hydrogen-borrowing methylation developed by the Donohoe group

The Donohoe group sought to enable α-methylation through H-B methodology using milder conditions and with a more expansive substrate scope. Preliminary results presented in 2014 gave methylated products in high yields using the commercially available catalyst $[RhCp^*Cl_2]_2$ and were optimized using valerophene (**3.75**) (Scheme 3-15).[36]

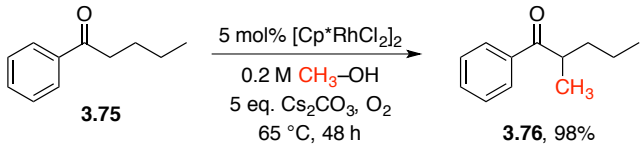

Scheme 3-15. Methylation H-B methodology developed in the Donohoe group

The methodology used methanol as the 1-C source to allow the α-methylation of a variety of ketones in a mild and relatively low temperature protocol using carbonate base. It was demonstrated that an oxygen atmosphere resulted in higher yields and shorter reaction times. The method was applied to a variety of ketones with available α-protons for enolate formation (Figure 3-5), tolerating a variety of electron-rich and -poor substituents (**3.77–3.81**) as well as heterocycles (**3.83**) and alkyl-alkyl ketones (**3.84, 3.85**) since alkylation does not occur at secondary centers. The method was also used to enable double methylation (α,α') of dialkyl ketones (**3.86**) and dimethylation (α,α) of some methyl ketone substrates (**3.87** and **3.88**).

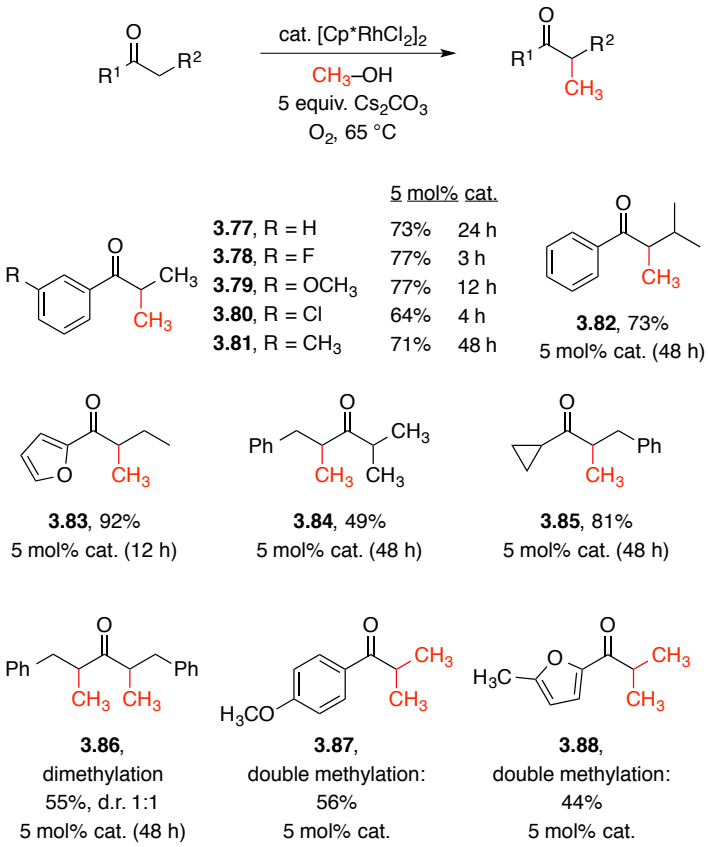

Figure 3-5. Substrate scope demonstrated in previous Donohoe H-B methylation method

The methodology was extended to a one-pot procedure allowing methylation of alkylated ketones using tandem alcohol alkylation reactions with a benzyl or primary alkyl alcohol and then with methanol (Figure 3-6). The second step simply

required addition of reagents to the reaction mixture (without purification or solvent removal) to allow access to double alkylated products in this one-pot process.

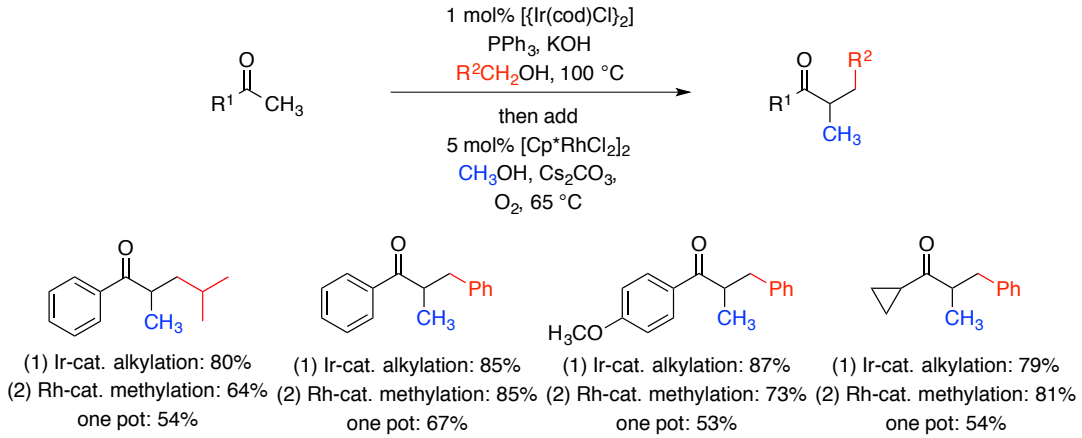

Figure 3-6. One-pot sequential Ir-/Rh-catalyzed dialkylations

The optimized H-B system allowed for exploration of the proposed mechanism and catalytic cycle. Intermediates isolated from the reaction included enone **3.89**, methoxy-adduct **3.90** and dimer **3.91** (Scheme 3-16). Upon re-subjection, the first two were converted to methylation product **3.76** in good yields, supplying evidence that they may be intermediates in the formation of **3.76**. The dimer **3.91** did not convert to **3.76** (c), which supports its assignment as a dead-end byproduct incapable of undergoing retro-aldol reaction to reform reactive intermediates. The proposed intermediate **3.92** (formed by reaction of starting material enolate with formaldehyde) was never isolated from the reaction conditions described above, but a sample was prepared from paraformaldehyde and **3.75**. Re-subjection of this aldol product to reaction conditions gave **3.76** in 82% yield, potentially indicating a higher rate of retro-aldol or dimer formation for this intermediate as compared to **3.90** (Scheme 3-16d).

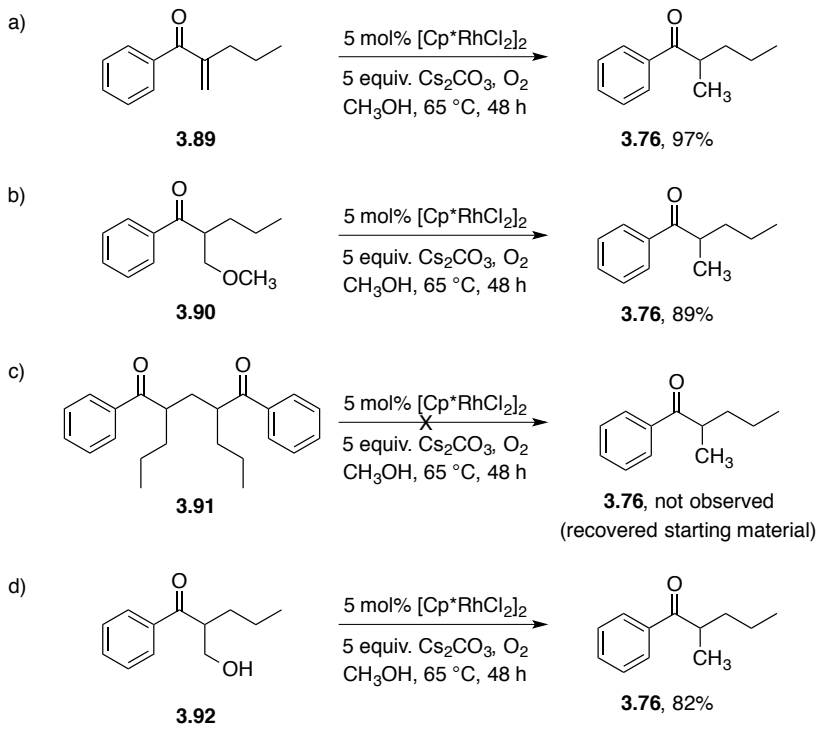

Scheme 3-16. Re-subjection of isolated or proposed reaction intermediates to probe mechanism

A mechanistic interpretation of these results was put forward (Scheme 3-17). Key steps include methanol oxidation to formaldehyde, reaction with enolate **3.93** to form aldol product **3.92** and elimination to form enone **3.89**. This intermediate can then undergo a Michael addition with nucleophiles such as reversible addition of CH_3O^- to form **3.90** or irreversible addition of **3.93** to form dimer **3.91**. Reduction by the metal hydride is competitive with these pathways, however, and in the Donohoe system gives unsaturated product **3.76** in exceptional yield. The role of oxygen was thought to be key in reoxidizing Rh^I species, formed by deprotonation and elimination of a leaving group from Rh^{III}–H, or in turning over deactivated catalyst, formed through over-oxidation of methanol to carbon monoxide.[38-40]

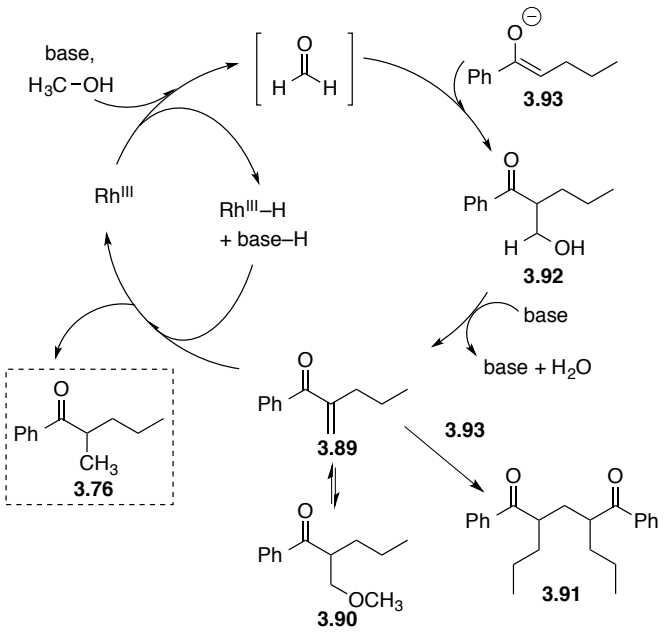

Scheme 3-17. Preliminary catalytic cycle proposed for Donohoe H-B methylation

This methodology was limited to methanol and was shown to be incompatible with more complex alcohols when using longer chain ketones than methyl ketones. The desire to access more complex branched products prompted the exploration of further optimization. Additionally, early results had indicated that an altered catalytic system might allow the expansion of the methodology through utilization of the activated Michael acceptor intermediate **3.89**. This formed the core of the goals of the project to be described herein.

3.2 Results and Discussion

The methodology detailed in section 3.1.4 was the pioneering example of α-methylation of ketones using H-B catalysis. The method required 5–10 mol% of rhodium metal which made it potentially costly and proved to be difficult to apply to more hindered alcohols. This latter downside made it difficult to form diverse branched products and was presumed to be due to adverse steric interactions in the aldol intermediates. In further efforts, we sought to improve the catalyst and catalytic loading and harness the enhanced reactivity of methanol to incorporate functionality beyond a methyl group. Work was performed in a team, with Darren Poole, Di Shen and Camilla Shotton, and reactions performed or optimized by these coworkers are indicated.

3.2.1 Interrupted-hydrogen-borrowing discovery

To expand the methodology developed previously, we sought to interrupt the hydrogen-borrowing process and access the intermediates formed from the addition of a methylene unit. The resulting formal "methylenation" product would be susceptible to the introduction of an external nucleophile by 1,4-addition, with the possibility of introducing this nucleophile in a one-pot, two-step transformation. This interrupted-hydrogen-borrowing (I-H-B) process (Scheme 3-18) would allow for the incorporation of other functionality beyond a methyl group to expand the α-functionalization of ketones.

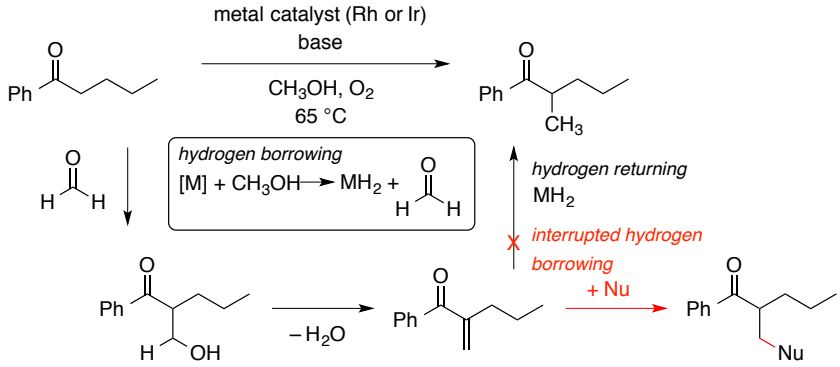

Scheme 3-18. Proposed interrupted-hydrogen-borrowing method (shown in red)

At the start of this program, there was limited precedent for I-H-B methodology as proposed in Scheme 3-18. The Pd/AlO(OH) catalytic system paired with oxygen described previously (see Scheme 3-9b) was shown by Park and coworkers to allow formation of *trans* enones (such as **3.94**) from methyl ketones and primary alcohols (Scheme 3-19a).[21] The use of the same highly porous aluminum oxyhydroxide with ruthenium nanoparticles (Ru/AlO(OH)) proved highly effective (when paired with sacrificial alkene **3.95**) at preventing reduction and allowed the interception of the aldehyde with Witting reagents to give α,β-unsaturated esters (**3.96**) in a one-pot process (Scheme 3-19b).[41] Pridmore and coworkers also used a hydrogen acceptor with $Ru(PPh_3)_3(CO)H_2$ and Xantphos to couple malonate half esters (**3.97**) and primary alcohols (**3.98**) to form esters (**3.99**) (Scheme 3-19c).[42] Another example by Owston and coworkers enabled a second oxidation (after methanol addition to the oxidized alcohol) to yield methyl esters such as **3.100** (3-19d).[43]

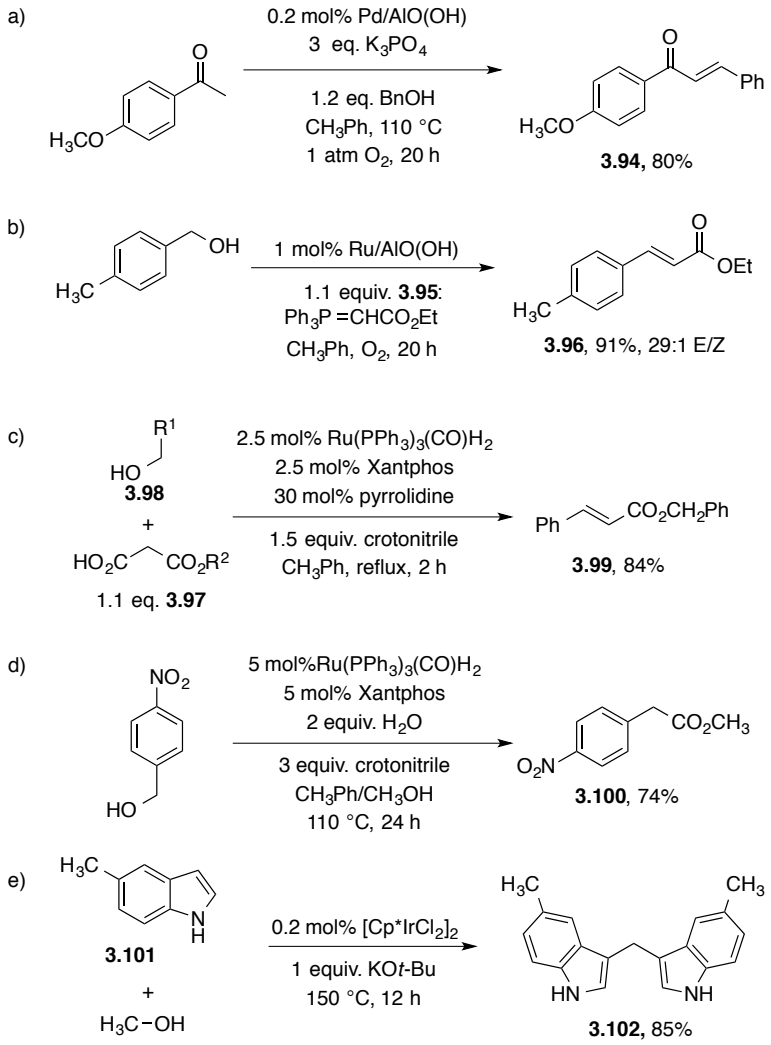

Scheme 3-19. IHB precedence generating unsaturated compounds or pseudo-homodimerizations

A self-coupling reaction of indoles (**3.101**) with formaldehyde (3-19e) was reported by Li in 2013 using $[Cp^*IrCl_2]_2$ and KO*t*-Bu to form 3,3'-bisindolylmethanes (**3.102**).[44] Only minor yields of the methylindole over-reduced byproducts were observed in a few cases and suggested that the active iridum species is regenerated through reaction with methanol. The proposed mechanism proceeds through a 1,4-addition of an equivalent of starting indole to the unsaturated intermediate, similar to the formation of symmetrical dimer **3.91** in the Donohoe system.[44] Control experiments using indole and paraformaldehyde supported the additional role of [Ir] species as Lewis acid catalyst for the Michael addition.

In the previously developed Donohoe methodology, described in Section 3.1.4, a screen of catalysts and conditions indicated the potential of some catalytic systems (Table 3-1, entries 2 and 7) to show increased levels of methylenated intermediates (**3.89** and **3.90**) over the dead-end products **3.76** and **3.91**.

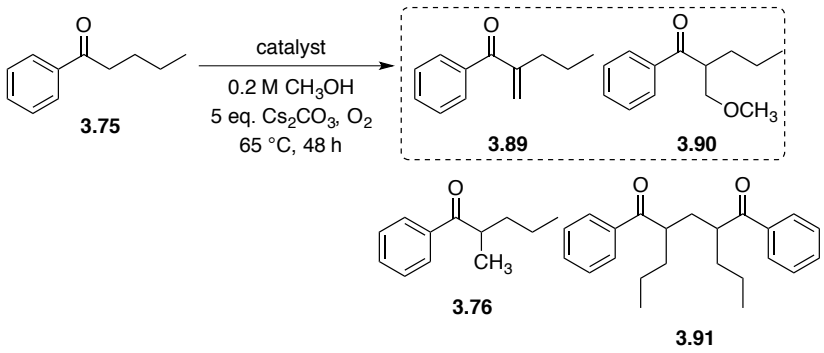

entry	catalyst	yield [3.89 + 3.90][a]	yield [3.76 + 3.91][a]
1	5 mol% $[Cp^*IrCl_2]_2$	41%	54%
2	5 mol% $[Cp^*RuCl_2]$	62%	21%
3	5 mol% $[Cp^*RhCl_2]_2$	n/o	98%
4	5 mol% $[Cp^*RhCl_2]_2$ (KOH)	n/o	86%
5	10 mol% $RhCl_3 \cdot 3H_2O$	48%	24%
6	10 mol% $RhCl_3 \cdot 3H_2O$, 10 mol% Cp*H	n/o	82%
7	10 mol% $RhCl_3 \cdot 3H_2O$, 10 mol% PPh_3	71%	27%
8	10 mol% $[RhCl(PPh_3)_3]$	n/o	23%
9	5 mol% $[Rh_2(OAc)_4]$	28%	22%

[a]Isolated yield

Table 3-1. Initial catalysts showing promise for I-H-B method (reactions performed by colleagues)

It was predicted that methoxy-adduct **3.90** interconverts with **3.89** under reaction conditions and this was confirmed by subjecting purified samples to reaction conditions with and without catalyst (Scheme 3-20a–b). The precise ratio of **3.89**/**3.90** depended on the reaction conditions, but the indication that **3.90** could undergo elimination to reform the enone allowed both intermediates to be considered useful Michael acceptor substrates. Thus optimization would aim for maximization of the combined yield of **3.89** and **3.90** with minimization of other byproducts.

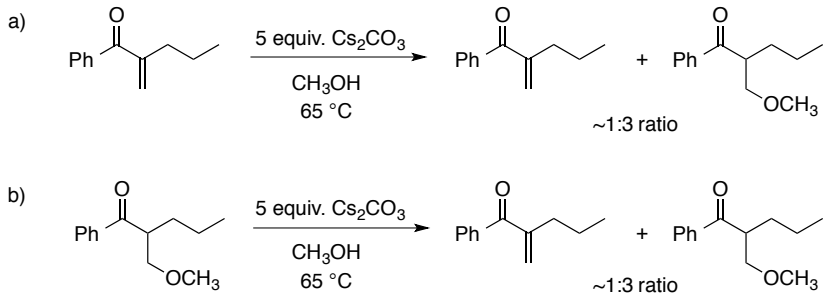

Scheme 3-20. Interconversion of enone and methoxy adduct intermediates

In the H-B mechanism, it is postulated that **3.89** and **3.90** are formed from the aldol adduct through elimination and methoxide addition (see Scheme 3-17). Optimization of this conversion with minimization of nucleophilic addition of the enolate to enone **3.89**, which instead forms dead-end dimer byproduct **3.91**, would be necessary to allow optimization of these desired intermediates (Table 3-2). The control reaction with **3.92** subjected to reaction conditions for 24 h gave only 33% isolated yield of desired products compared to 25% dimer (entry 1). An increase of base was proposed to encourage both the elimination to **3.89** and $^{(-)}OCH_3$ addition to **3.89** to form **3.90**. Pleasingly, increasing to 5 equiv. of sodium methoxide gave 88% yield of desired products with only 13% yield of the dimer (entry 2). A screen of solvent concentrations was completed and for shorter time periods to avoid any decomposition or loss of material to other byproducts and slight increases in the yield of desired products was seen for 0.3, 0.4 and 0.5 M (entries 3–5). This was paired with a concomitant slight decrease in dimer giving a >10:1 ratio of desired/undesired products with 0.4 M (entry 4). Lowering the concentration to 0.1 M gave a slight decrease in the yield but allowed an experiment proving the importance of the order of addition. These reaction were performed in a Biotage© vial with **3.75** added, then methanol and finally base. Upon switching the order of base and solvent, the ratio changed from 10:1 to 1:2 of desired to undesired products (entry 6 and 7). Running

the best conditions with optimized order of additon under O_2 for 2.5 h gave excellent yields with no observed dimer (entries 8 and 9).

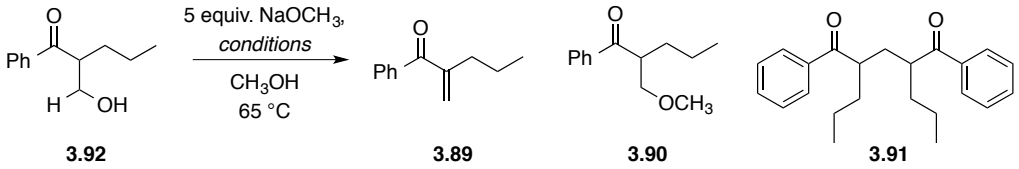

3.92 **3.89** **3.90** **3.91**

entry	conc. (M)	time (h)	yield 3.89[a]	yield 3.90[a]	yield 3.91[a]
1[b]	0.2	24	6%	27%	25%
2	0.2	0.5	60%	28%	13%
3	0.3	0.5	29%	59%	11%
4	0.4	0.5	30%	60%	8%
5	0.5	0.5	32%	54%	13%
6	0.1	0.5	19%	64%	8%
7	0.1[c]	0.5	28%	3%	68%
8[d]	0.2	2.5	12%	68%	n/o
9[d]	0.4	2.5	21%	57%	n/o

All reactions run with 0.3 mmol **3.75** in Biotage microwave vial (order of addition: **3.75**, CH_3OH, then base). [a]Isolated yield; [b]1.5 equiv. $NaOCH_3$, 10 mol% $[RuCp^*Cl_2]_n$ added and run under $O_{2(g)}$ environment; [c]Order of addition: **3.75**, base then CH_3OH; [d]run under $O_{2(g)}$ environment;

Table 3-2. Control reactions with aldol intermediate **3.92** to investigate desired transformation

Next, tuning of the catalytic system would provide a catalytic system that prevented enone reduction, allowing access to the methylenated intermediates in situ and allowing the addition of a variety of nucleophiles.

3.2.2 Optimization of desired activated intermediates

3.2.2.1 Optimization of I-H-B reaction using Ru catalyst and valerophenone

The initial promise of $[RuCp^*Cl]_n$ as a catalyst for I-H-B (see Table 3-2, entry 2) encouraged the further exploration of conditions to maximize the desired intermediates. Commercially available valerophenone **3.75** was used as a model substrate with sodium methoxide, as in Table 3-2, driving the reaction to desired methylenated intermediates. The desired high yields of **3.89** and **3.90** would need to be paired with a minimization of **3.76** and **3.91**. Initial conditions were screened using an internal standard and NMR yields to establish general trends (Table 3-3).

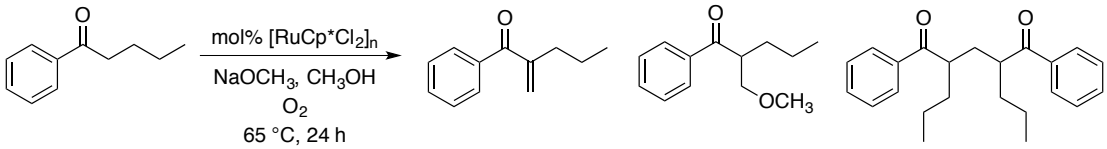

3.75 **3.89** **3.90** **3.91**

entry	equiv. $NaOCH_3$	conc. (M)	conditions	yield 3.89[a]	yield 3.90[a]	yield 3.91[a]
1	5	0.2	-	15%	37%	38%
2	5	0.2	anhydrous conditions, dry CH_3OH	16%	56%	22%
3[b]	5	0.2	freshly prepared $NaOCH_3$	9%	28%	46%
4[c]	2	0.2	-	22%	42%	26%
5	5	0.1	-	22%	56%	14%

0.3 mmol **3.75**; 10 mol% mol% $[RuCp^*Cl_2]_n$ [a]Determined by ^1H NMR with DMB as internal standard; All reactions showed complete consumption of **3.75** and negligible methylated product except [b]10% **3.76** observed and [c]5% RSM observed

Table 3-3 Screening of $[RuCp^*Cl]_n$ to optimize I-H-B intermediates of valerophenone

Initial conditions using 5 equiv. of base and an oxygen atmosphere at 65 °C showed promise with a combined yield of 52% of desired products achieved after 24 h of reaction, but with a moderate yield (38%) of undesired dimer **3.91** (Table 3-3, entry 1). Screening the effect of water through use of anhydrous conditions (flame dried glassware, anhydrous methanol) showed promise with an increase yield of desired products (72%) and only 22% yield of the dimer (entry 2). A reaction run under the same conditions (not shown) with the addition of 10 equiv. of water showed drastic decreases in the desired yields. Unfortunately, we recognized this would be a difficult system to pursue or employ since the mechanism proposed includes an equivalent of water produced for every elimination reaction to form the enone **3.89** from the aldol product **3.92**.

Producing sodium methoxide in situ (using Na(0) and methanol) would allow consumption of water and the use of rigorously dry base. Unfortunately, this system gave the largest proportion of dimer yet, with 46% yield of **3.91** compared to 37% combined yield of enone and masked enone products (entry 3). Interestingly, this reaction also showed a significant yield of methylated **3.76** (~10% by NMR, with yield determination made difficult by overlapping signals for **3.76** and the other

products). The difficulty of precisely portioning sodium metal suggests this reaction might have had a significantly varied amount of base and prompted the continued investigation using solid sodium methoxide.

Lowering the amount of base to only 2 equiv. showed promise with 64% desired products and only 26% dimer. NMR analysis indicated the reaction was incomplete (with 5% recovered starting material (RSM) observed) (entry 4). Instead, lowering the concentration to 0.1 M gave the best results with 76% yield of desired products and only 14% of dimer.

These conditions gave a >5:1 ratio of desired products to undesired, but would be more difficult to incorporate with a subsequent nucleophilic addition. Our one-pot, two-step reaction would need to incorporate conditions amenable to both the activated intermediate formation and the subsequent conjugate addition. This second transformation would require higher equivalents of base and would be encouraged in a higher concentration reaction. Thus, additional screening was done using 5 equiv. of base and a 0.2 M concentration in methanol.

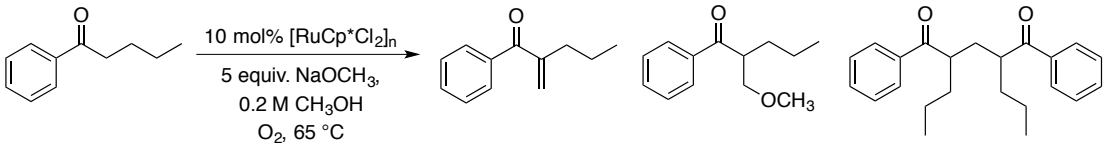

3.75, 0.3 mmol

3.89 5%*

3.90 31%

3.91 34%

*contaminated with 2% RSM

Scheme 3-21. I-H-B reaction of valerophenone

Repeating the reaction from entry 1 of Table 3-3 showed the difficulty of purification and product isolation for this system (Scheme 3-21). Only 5% and 31% of **3.89** and **3.90** were isolated, due to the co-elution of enone and RSM and the required slow and repeated flash column chromatography purifications (with only 72% total recovered mass). It is unclear whether the NMR yields gave over

exaggerated yields or if decomposition (by Ru, O_2 or during purification) and/or volatility are contributing factors to the low isolated yields.

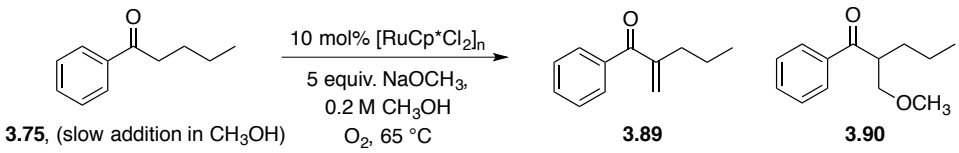

3.75, (slow addition in CH_3OH) **3.89** **3.90**

a) 0.3 mmol, 24 h	11%	43%
b) 1.5 mmol, 96 h	23%*	57%

*contaminated with 5% **3.76**

Scheme 3-22. Larger scale reaction of valerophenone to desired intermediates (using slow addition of **3.75**)

The slow addition of valerophenone **3.75** was predicted to reduce the side reaction of enolate with the activated intermediates by decreasing the concentration of enolate in solution. Pleasingly, the slow addition of **3.75** over 10 h allowed an increase in the ratio of desired to undesired isolated products (>5:1, see Scheme 3-22a), though overall mass recovery was again low. Scaling the reaction to 1.5 mmol (with increased reaction time) led to a good mass recovery and yields of desired activated intermediates, with no observed dimer (Scheme 3-22b). This exciting result allowed the exploration of a one-pot reaction with a secondary nucleophile (Scheme 3-23). The IHB reaction proceeded as described previously and then the vessel was cooled and stirred open for 2 h. Addition of 5 equiv. base and 1.05 equiv. of a second ketone (**3.103**) with subsequent heating gave desired product **3.104**. The symmetrical dimer of **3.103** was also formed (**3.105**) indicating that the catalyst was still active during the second portion of our one-pot reaction.

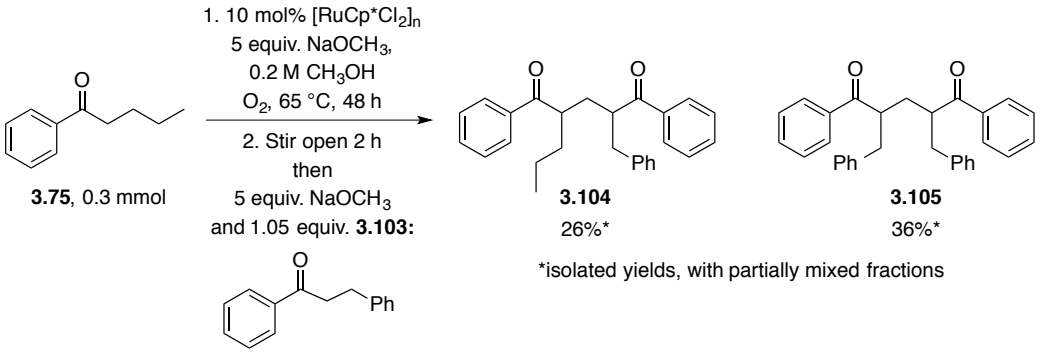

Scheme 3-23. One-pot I-H-B and conjugate addition reaction using $[RuCp^*Cl_2]_n$

3.2.2.2 Optimization of I-H-B using [Ir(cod)Cl]$_2$

The simultaneous discovery of the relatively inexpensive iridium(I) catalyst $[Ir(cod)Cl]_2$ (by colleague Di Shen) allowed lower loadings of the metal (1–2 mol%) for the previously examined methylation. This reaction gave high yields of **3.76** in 48 h at 65 °C in the presence of oxygen (Scheme 3-24).

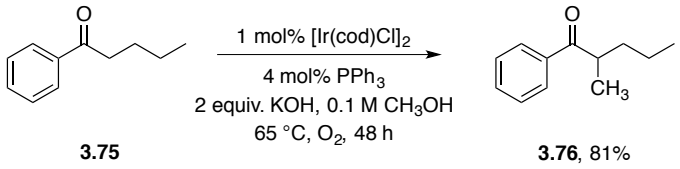

Scheme 3-24. Initial result showing the promise of $[Ir(cod)Cl]_2$ for H-B catalysis (reaction performed by Di Shen)

Replicating the optimized methylation reaction (in my hands) using only 1 mol% of $[Ir(cod)Cl]_2$, 2 equiv. of KOH and triphenyl phosphine ligand at 0.2 M concentration led to a pleasingly high yield of methylated product **3.76** (Table 3-4, entry 1). The catalytic system proved tunable with the nature of the phosphine ligand determining the product distribution. A screen performed by colleague Darren Poole identified PCy_3 and cataCXium® A as optimum targets, reactions not shown. The decreased loadings (1–2% vs 10%) and lower cost of Ir over Ru made this a preferred system for the I-H-B transformation and the $[RuCp^*Cl_2]_n$ system was abandoned. Further screening focused on the bulky phosphine ligand PCy_3 and use of the same

conditions as identified in Scheme 3-24 gave a promising ratio of desired and undesired products (>1:1), with only 5% of **3.76** isolated (Table 3-4, entry 2).

entry	phosphine (mol%)	KOH (equiv.)	yield 3.89[a] (%)	yield 3.90[a] (%)	yield 3.91[a] (%)	yield 3.76[a] (%)	product ratio
1[b]	PPh_3 (4%)	2	0	0	0	80	0
2	$P(Cy)_3$ (4%)	2	6	47	27	5	1.6
3[b]	$P(Cy)_3$ (4%)	2	7	39	43	9	0.9
4[b]	$P(Cy)_3$ (4%)	3	4	48	26	9	1.4
5[b]	$P(Cy)_3$ (4%)	4	1	33	39	0	0.9
6	$P(Cy)_3$ (4%)	3	8[d]	61	18	5	2.4
7	$P(Cy)_3$ (4%)	4	6	55	26	2	2.0
8	$P(Cy)_3$ (4%)	5	19[d]	56	20	4	1.9
9	$P(Cy)_3$ (2%)	5	6	41	44	10	1
10[c]	$P(Cy)_3$ (8%)	3	27	50	12	10	3.5

[a]Isolated yields with <5% RSM; [b]0.2 M in methanol; [c]Isolated with ~5% RSM; [d]2 mol% $[Ir(cod)Cl]_2$

Table 3-4. Use of $[Ir(cod)Cl]_2$ to effect I-H-B transformation of valerophenone Conditions: 0.3 mmol **3.75**, 1 mol% $[Ir(cod)Cl]_2$, KOH, 0.1 M methanol, 65 °C, O_2, 48 h;

Conditions explored included increasing the concentration to 0.2 M, with 2, 3 and 4 equiv. of KOH (entries 3–5) which gave poor or comparable yields, with a slight increase in the yield of methylated product observed. Maintaining 0.1 M concentration and increasing to 3 equiv. (entry 6), 4 equiv. (entry 7) and 5 equiv. (entry 8) of base showed a much more desirable trend with yields of desired products (61–69%) exceeding undesired (29–33%) by a factor of 2. Low concentration and low equivalents of base (entry 6) gave a higher proportion of RSM than seen previously, while 4 or 5 equiv. of base gave >25% of the dimer product. The challenge of maintaining conversion to desired product, while promoting aldol elimination without over reduction was apparent.

The ratio of [Ir] to phosphine was adjusted from the previously used 1:2 ratio, since the dimer of $[Ir(cod)Cl]_2$ provides 2 equiv. of [Ir] per equivalent of catalyst. A 1:1 ratio gave reduced yields of **3.89** and **3.90** (entry 9) with a concurrent increase in production of **3.91** and methylated product **3.76**. The latter is explained by the loss of the protective role of the bulky phosphine in preventing Ir–H production or reduction

of the intermediate enone. An increase of $[Ir(cod)Cl]_2$ to 2 mol% (with 8 mol% ligand to maintain the original ratio) gave 77% yield of desired products, with only 12% dimer (entry 10). The presence of 10% methylated product implied that the reaction pathway to **3.76** was encouraged under higher catalyst loadings as well.

Additional screening was undertaken to ensure other factors such as the addition or removal of water from the system, the choice of base and the order of addition were not determining factors to the varied ratio of desired and undesired products observed (Table 3-5). Conditions used (1 mol% $[Ir(cod)Cl]_2$, 4 mol% PCy_3, 5 equiv. KOH at 0.1 M methanol) are comparable to entry 8 of Table 3-4 (which gave a 62%:31% yield ratio of desired to undesired products). The use of anhydrous reaction conditions showed comparably good yields (Table 3-5, entry 1) while added water showed lower yields and higher levels of dimer observed (entry 2). Cesium carbonate gave comparable yields, though also yielding more dimer than with KOH (entry 3). Premixing the catalyst for 30 min without **3.75** gave very high levels of dimer (entry 4), while premixing $[Ir(cod)Cl]_2$ and PCy_3 without base or **3.75** led to a drastic increase in the yield of **3.76** with no observed **3.89** or **3.90** (entry 5). This indicates the importance of base in removing iridium hydride species from the reaction, even before the addition of substrate.

entry	conditions	yield 3.89[a] (%)	Yyeld 3.90[a] (%)	yield 3.91[a] (%)	yield 3.76[a] (%)	yield RSM[a]
1	anhydrous	7	62	15	3	5
2	+10 equiv. water	13	50	36	2	1
3	5 equiv. Cs_2CO_3	15	57	28	5	0
4	premix (without **3.75**)	5	45	42	1	2
5	premix (without base or **3.75**)	0	0	11	61	2

[a]Isolated yields

Table 3-5. Control I-H-B reactions using $[Ir(cod)Cl]_2$ and PCy_3
Conditions: 1 mol% $[Ir(cod)Cl]_2$, 4 mol% PCy_3, 5 equiv. KOH, 0.1 M methanol, 65 °C, O_2, 48 h;

Screening the previously optimized conditions with the bulky adamantyl-containing phosphine cataCXium® A (**3.106**) led to high yields using both (a) 2 equiv. and (b) 3 equiv. of KOH at 0.1 M concentration (Scheme 3-25).

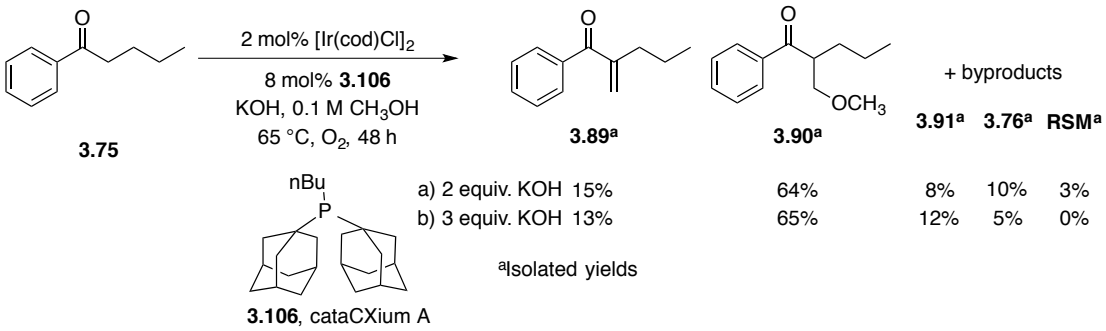

Scheme 3-25. Optimized conditions using cataCXium® A

Additional control reactions undertaken with cataCXium® A and 3 equiv. of base are shown in Table 3-6. Importantly, the removal of the oxygen environment, as in entry 2, gives predominantly **3.76**, with a larger portion of RSM than other reaction conditions. This is indicative of the two key roles of oxygen as we discovered in this system: (1) the oxygen environment (combined with bulky, electron-rich phosphines) removes hydride from the system (potentially through oxidation to water) and/or blocks reduction of the reactive intermediates in another way; and (2) oxygen accelerates the oxidation of methanol (which does occur under Ar, but is much slower, leading to increased RSM). Replacing oxygen with *N*-methylmorpholine *N*-oxide was attempted, in the presence of O_2, air and argon (entries 3–5) but did not improve the yield of desired products since any increase in enone and masked enone was observed concurrently with increased dimer formation. Ultimately, 2 mol% $[Ir(cod)Cl]_2$ with 8 mol% cataCXium® A and 3 equiv. KOH were chosen as the best conditions for the methylenation reaction.

entry	condition	Yield 3.89[a] (%)	Yield 3.90[a] (%)	Yield 3.91[a] (%)	Yield 3.76[a] (%)	Yield RSM[a]
1	24 h	11	40	6	6	41
2	no O_2	0	0	0	80	12
3	add NMO, O_2	27	44	24	6	0
4	add NMO, air	0	0	2	38	14
5	add NMO, argon	4	29	25	9	25
6	LiOH as base	8	56	8	4	25
7[b]	change Ir:P	21	66	8	4	1
8[c]	change Ir:P	11	71	10	6	2

[a]Isolated yields; [b]4 mol% ligand; [c]2 mol% $[Ir(cod)Cl]_2$, 16 mol% ligand

Table 3-6. Control reactions using Ir and cataCXium® A
Conditions: 0.3 mmol **3.75**, 2 mol% $[Ir(cod)Cl]_2$, 8 mol% cataCXium® A, 3 equiv. KOH, 0.1 M methanol, 65 °C, O_2, 48 h;

3.2.2.3 Mechanistic considerations for the I-H-B reaction

Additional mechanistic insight allowed for the proposal of a catalytic cycle for this I-H-B reaction (Scheme 3-26). It is clear that oxygen plays a critical role in the I-H-B process, just as in H-B, since loss of oxygen atmosphere led to an increase in the production of **3.76** (Table 3-6, entry 2). Experiments indicate that oxygen both enhances the efficiency of the methylenation reaction (increased yields of **3.89** and **3.90** with low levels of RSM) and halts the enone reduction (low yields of **3.76**). The precise mechanism is unknown, but it is proposed that oxygen can assist the I-H-B reaction in 3 ways: (i) the reoxidation of Ir^{I} to Ir^{III}; (ii) the regeneration of Ir^{I} from Ir–CO species; (iii) the removal of the metal–hydride through reaction with Ir–H and production of water. The observance of water during concentration of crude reaction mixtures lends support to the third proposed role.

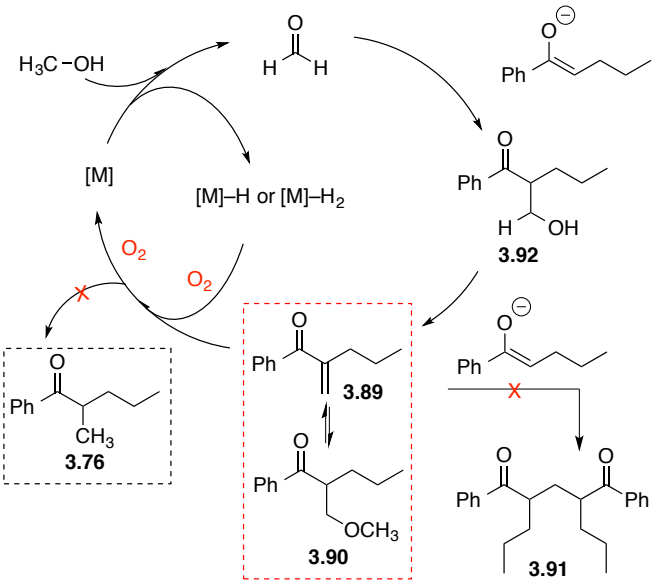

Scheme 3-26. Proposed catalytic cycle for I-H-B transformation

3.2.2.4 Extension of the I-H-B method to additional ketone substrates

The optimized conditions were extended to other substrates (Scheme 3-27) including (a) 3-phenylpropiophenone (**3.103**) and (b) long-chain alkyl ketone **3.107** (synthesized using Ishii alkylation conditions). The use of *p*-methoxyphenyl (PMP) ketones was proposed to allow expansion of the methodology to products at the ester oxidation level through Baeyer–Villiger reactions of the resulting ketones. Simultaneous work by Camilla Shotton (not shown) demonstrated that esters would otherwise be difficult to incorporate into our methodology.

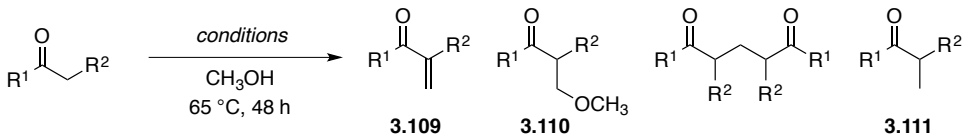

	3.109	3.110		3.111	RSM
a) 3.103: R^1 = Ph, R^2 = Bn	**a)** 23%	**a)** 55%	n/o	**a)** 2%	9%
b) 3.107 R^1 = PMP, R^2 = *n*-Pr	**b)** 21%	**b)** 55%	n/o	**b)** 4%	9%
c) 3.108 R^1 = PMP, R^2 = Bn	**c)** 6%	**c)** 63%	n/o	**c)** 5%	0%

Scheme 3-27. Substrate scope of I-H-B methodology using $[Ir(cod)Cl]_2$
Conditions: 0.3 mmol ketone, 2 mol% $[Ir(cod)Cl]_2$, 8 mol% cataCXium® A, 3 equiv. KOH, 0.1 M in methanol;

Access to a variety of reactive I-H-B intermediates in good yields provided the platform upon which to incorporate an in situ conjugate addition reaction. This would

allow the formation of 1,5-diketones in one pot through the addition of diverse ketone enolates, but required further optimization before achieving this desired transformation.

3.2.3 Conjugate addition of nucleophiles to activated methylenated inermediates

3.2.3.1 Screen of conjugate addition reaction conditions (to make symmetrical dimer)

Optimized conditions using the bulky adamantyl-containing ligand **3.106** and KOH provided the desired intermediates in consistently high yields using an oxygen atmosphere. Subsequent studies would determine the ideal conditions for the addition of a nucleophile to the reactive enone derived from **3.75**.

The utilization of pre-made and isolated intermediate **3.90** allowed the addition of ketone **3.75** to test ideal conditions for the conjugate addition (Table 3-7). Thus, the generation of 1,5-diketones was first examined with symmetrical compound formation, as this product dimer had been isolated in the previous studies and was well characterized. The production of dimers had already been observed to give a mixture of inseparable *anti* and *syn* diastereomers, further complicating the NMR analysis for novel or nonsymmetrical 1,5-diketones.

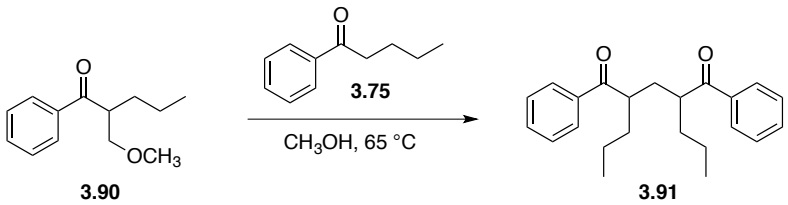

entry	base	time (h)	yield 3.91[a]
1	$NaOCH_3$[b]	48	<5%[c]
2	$NaOCH_3$	15	58%[c]
3	KOH	15	50%
4	K_2CO_3	15	31%
5	Cs_2CO_3	15	65%
6	Et_3N	15	5%
7[d]	$NaOCH_3$	15	50%[c]
8[d]	$NaOCH_3$	72	75%
9[e]	$NaOCH_3$	15	89%

[a]Isolated yield [b]1.05 equiv. base used; [c]Other material isolated was a mixture of **3.90** and enone **3.89**;[d]O_2 used; [e]0.4 M in CH_3OH

Table 3-7. Optimization of symmetrical 1,5-diketone formation
Conditions: 0.3 mmol **3.90**, 1.05 equiv. **3.75**, 5 equiv. base, 0.1 M in methanol, 65 °C;

The use of 1.05 equiv. of base showed >95% RSM (entry 1), so subsequent reactions used 5 equiv. which increased the yield to 58% upon the first attempt (entry 2). A screen of different bases included KOH, to align with I-H-B methodology, which gave 50% yield (entry 3), K_2CO_3 which gave 31% yield (entry 4) and Cs_2CO_3 (65% yield, entry 5). Triethylamine proved ineffective with a very low yield of desired dimer product (5%, entry 6). The addition of oxygen to the system did not show a significant difference in product isolation (entry 7) and extending the reaction to 72 h at 65 °C led to an increased yield of **3.91** (72%, entry 8), which indicates no significant decomposition or retro-aldol is occurring in these conditions. Increasing the concentration to 0.4 M was very favorable with an 89% isolated yield achieved with only 15 h reaction time (entry 9).

3.2.3.2 Screen of conjugate addition reaction conditions (to make nonsymmetrical dimer)

A nonsymmetrical 1,5-diketone (**3.104**) was accessed using these optimized conditions in quantitative yield using 5 equiv. sodium methoxide and ketone **3.103** (Scheme 3-28). The reaction showed tolerance to decreasing the loading of base, with

4 equiv. or 3 equiv. still producing **3.104** in 97% and 94% yield, respectively. Neither of the products of symmetrical dimerization was observed (**3.91** or **3.105**).

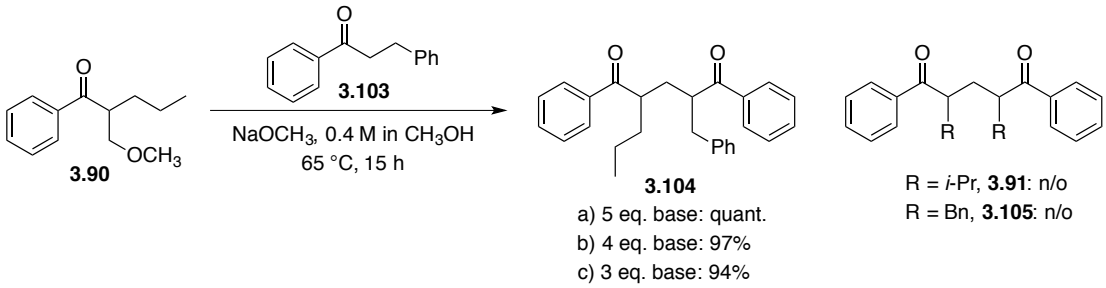

Scheme 3-28. Application of conjugate addition conditions to form nonsymmetrical 1,5-diketone

A mixture of activated intermediates were tested in order to more closely replicate the I-H-B reaction conditions (Scheme 3-29). The compounds were generated from a reaction of valerophenone and paraformaldehyde and were present in a 2.7:1 molar ratio (**3.90**/**3.89**). The reaction with ketone **3.103** gave 77% yield of the desired product in 15 h (Scheme 3-29). A small amount (13%) of a mixture of the symmetrical dimers (**3.91** and **3.105**) was observed in this case, indicating that retro-aldol and production of formaldehyde did occur.

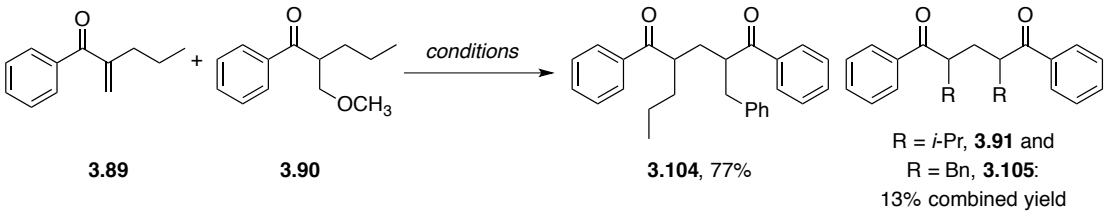

Scheme 3-29. Use of mixed intermediates to form nonsymmetrical 1,5-diketone
Conditions: 1.05 equiv. **3.103**, 5 equiv. $NaOCH_3$, 0.1 M in methanol, 65 °C, 15 h;

In the interest of aligning the base for the two steps of the desired one-pot procedure, we targeted the base chosen for use in the I-H-B reaction (KOH) with an additional screen of the nonsymmetrical dimer formation (Scheme 3-30). Using a 0.1 M concentration in methanol and 3 equiv. of KOH, the amount of **3.103** was varied

from 2 equiv. through 5 equiv. to give product in good to excellent yield (with 8% of **3.105** observed only for 2 equiv. of **3.103**).

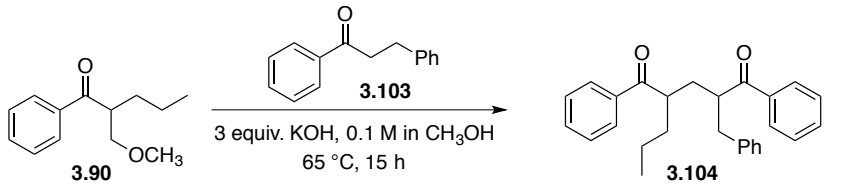

a) 2 equiv. **3.103**: 85% (+8% **3.105**)
b) 3 equiv. **3.103**: 94%
c) 4 equiv. **3.103**: 92%
d) 5 equiv. **3.103**: 98%

Scheme 3-30. Use of KOH in conjugate addition step to align with I-H-B methodology

As a model system to predict the difficulty of placing this reaction in line with the first I-H-B reaction, a conjugate addition reaction with added $[Ir(cod)Cl]_2$, cataCXium® A and O_2 was heated for 24 h (Scheme 3-31). The reaction gave a more complex mixture of products with **3.104** isolated (16%) as well as recovered starting materials (32%, mixture of **3.90** and **3.89**), methylated product **3.76** (15%) and the symmetrical dimer **3.105** (16%). Additional screening within the two-step process would be required to suppress these undesired byproducts.

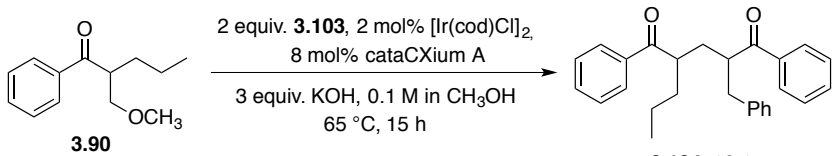

3.104, 16%
with [**3.90**+**3.89**] (32%),
3.76 (15%) and **3.105** (16%)

Scheme 3-31. Model system for one-pot I-H-B and conjugate addition reactions

3.2.3.3 I-H-B and conjugate addition reactions in a one-pot transformation

The use of the optimized conditions for forming reactive intermediates (see Scheme 3-27) and the successful formation of nonsymmetrical dimer **3.104** (Scheme 3-30) prompted the application of the Ir-catalyzed interrupted process to a one-pot

reaction sequence. This would allow an I-H-B reaction to form methylenated intermediates and a subsequent nucleophilic addition without isolation or purification.

The translation of this methodology to a one-pot procedure revealed the difficulty of shutting down the methanol oxidation potential of the catalytic system and the pervasive nature of formaldehyde in the reaction mixture. Initial studies using optimized I-H-B conditions and a simple 'quench' of the reaction (stirring open for 2 hours) before addition of additional base and the second ketone gave 57% yield of the product (Table 3-8, entry 1), but a mixture of byproducts made purification and isolation of the desired 1,5-diketone very prohibitive. Byproducts observed included **3.76**, from reduction of the reactive intermediates, the symmetrical dimerization of each participating ketone to form **3.91** and **3.105** and even the α-methylation product of the secondary ketone (**3.312**). The homo-aldol dimers co-eluted with **3.104** when purifying by flash column chromatography, which made isolation of the desired nonsymmetrical dimer difficult. Quenching the reaction with the addition of carbon tetrachloride (entry 4) led to a mixture of compounds, none of which were identifiable as product **3.104** or any byproducts.

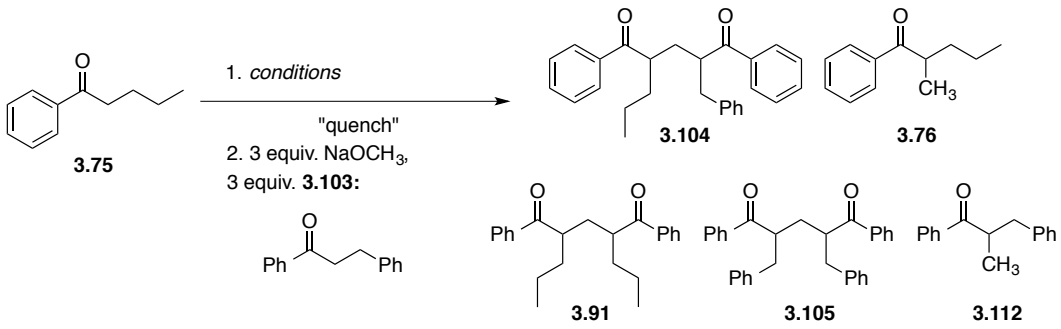

entry	reaction "quench" used	yield of isolated products				
		3.104	3.76	3.91	3.105[a]	3.112[a]
1	stir open 2 hours	57%	8%	28%	(45%)	(2%)
2	sonicate open 5 min	37%	12%	31%	(27%)	(12%)
3	sonicate open 15 min, use KOH	27%	29%	40%	(30%)	(34%)
4	add CCl_4	n/o	n/o	n/o	n/o	n/o
5	add O_2 for 2nd step	61%	n/o	5%	(7%)	n/o

[a]Yield indicates proportion with respect to mmol of **3.103** added, as these byproducts do not contribute to the overall conversion of **3.75**

Table 3-8. Translation of methodology to a one-pot, two-step method
Conditions (1): 0.3 mmol ketone, 2 mol% $[Ir(cod)Cl]_2$, 8 mol% cataCXium® A, 3 equiv. KOH, 0.1 M in methanol, O_2, 65 °C, 48 h

Control experiments showed the detrimental affect of formaldehyde, which is soluble in methanol and exists as various short polymers. An assay using Na_2SO_3 and HCl allowed the interrogation of reaction solutions to test for the presence of formaldehyde. The addition of sodium sulfite to formaldehyde forms a formaldehyde-sodium bisulfite adduct CH_2O_4SNa, which is an alkaline substance (Figure 3-7a). The addition of 2 equiv. of HCl can reform formaldehyde, with the evolution of $SO_{2(g)}$ (Figure 3-7b).

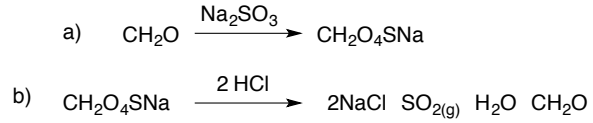

Figure 3-7. Test system using sodium sulfite/formaldehyde reactivity as a formaldehyde assay

A stock solution of formaldehyde was made by heating paraformaldehyde and KOH in methanol to 55 °C and then cooling slowly. A blank control solution (without formaldehyde) was created in the same way, without paraformaldehyde. The addition

of Na_2SO_3 to the stock solution of formaldehyde in methanol gave a solution with an alkaline pH (14), while the blank control upon addition of the Na_2SO_3 solution had a pH of 10 (and appeared cloudy). The system was also shown to be diagnostic for paraformaldehyde in water, with 1 M NaOH used to solubilize the substance and an equal volume of 1 M HCl used to neutralize the pH. Adding sodium sulfite to this neutral stock solution of formaldehyde yielded a solution with pH of 14, compared to 7 for the blank control in water.

To investigate formaldehyde removal from this system, three stock samples of formaldehyde were created and subjected to different test conditions: (i) evaporation on rotary evaporator for 5 min, (ii) sonication for 5 min or nothing. Sodium sulfite was added to each of these, post treatment, and to a fourth sample (a blank control, d). The pH and observations are summarized in Table 3-9. Treatment of the positive control formaldehyde solution gave a high pH and a clear solution with Na_2SO_3, while the blank gave a lower pH reading and showed precipitation of Na_2SO_3. The test conditions gave somewhat mixed results with high pH and precipitate observed for evaporated sample (a), while sonication gave the same results as the positive control, indicating some removal of formaldehyde in the first case (a) and none in the second (b).

sample	test	result (pH)	result (observation)
a) formaldehyde	i)	14	cloudy solution
b) formaldehyde	ii)	14	clear solution
c) formaldehyde	none	14	clear solution
d) blank (no formaldehyde)	none	10	cloudy solution

Table 3-9. Sodium sulfite assay to interrogate formaldehyde presence in solution
Test conditions: (i) evaporation for 5 min and (ii) open-air sonication for 5 min

To examine the formaldehyde left in solution after the I-H-B reaction, three additional models were created: (a) reaction conditions without substrate, heated to 65 °C [2 mg $[Ir(cod)Cl]_2$, 4 equiv. PCy_3, 17 mg KOH, 3 mL methanol, O_2]; (b)

reaction conditions as in (a), but at 25 °C; (c) a known quantity of paraformaldehyde heated to 65 °C [200 mg in 3 mL methanol with 17 mg KOH, O_2, 65 °C]. A blank containing only methanol and 17 mg of KOH was stirred for 24 h with the test conditions (a–c). After 24 hours, the samples were subjected to the formaldehyde assay through addition of HCl (to neutralize the pH), Na_2SO_3 and then an immediate pH test. Aliquots of the two I-H-B reaction mimics were also subjected to two test quench conditions before assaying [either (i) evaporation and/or (ii) sonication]. Observations and pH measurements are recorded in Table 3-10. The formaldehyde positive control gave a pH reading of 14, while the blank showed pH = 11. The room temperature samples had similar responses to the blank, both before and after a 'quench'. The I-H-B reaction conditions with heating gave a high pH reading at 24 h upon treatment with Na_2SO_3 (pH = 12). Both quenches reduced the level of formaldehyde observed with pH decreasing to (i) 10–11 and (ii) 11.

	sample	test	result (pH)	result (observation)
a)	I-H-B reaction (65 °C)	none	12	cloudy to clear
	I-H-B reaction (65 °C)	(i)	10–11	cloudy to clear
	I-H-B reaction (65 °C)	(ii)	11	cloudy
b)	I-H-B reaction (25 °C)	(i)	10	cloudy to clear
	I-H-B reaction (25 °C)	none	11	cloudy
c)	200 mg paraformaldehyde	none	14	clear
d)	none	none	11	cloudy then clear

Table 3-10. Sodium sulfite assay with I-H-B reaction model system
Test conditions: (i) evaporation for 5 min and (ii) open-air sonication for 5 min

Based on our studies, we predicted that sonication of the open reaction vessel would remove excess formaldehyde from the system, yet proved unsuccessful for the one-pot reaction (see Table 3-8, entry 2 and 3). Separately, efforts by colleague Darren Poole showed that open-air sonication was sufficient preparation to allow the addition of amines to enones in a one-pot reaction (not shown). Ultimately, running the second enolate-addition step under an oxygen atmosphere was undertaken. This proposal relies on the protective nature of the cataCXium® A ligand paired with an

oxygen environment to prevent metal-hydride reduction of the enone intermediates. This cannot prevent the methylenation of the external nucleophile (**3.103**), but we hoped reaction of **3.89** and **3.103** would occur preferentially. We were pleased to find that the addition of O_2 allowed a one-pot, two-step access to 1,5 diketone **3.104** in 61% yield without prohibitive amounts of symmetrical dimer **3.91** or **3.105** isolated (Table 3-8, entry 5).

Simultaneous work by colleague Darren Poole enabled the development of a higher yielding protocol using SiliaMetS DMT. This metal scavenging resin was added to the reaction crude from the I-H-B step and stirred open for 1 hour. It is proposed that the resin binds the iridium metal and prevents methanol oxidation or enone reduction during the second phase of the transformation. The open air stirring (found to be beneficial in Table 3-8, entry 1) also concentrated the reaction somewhat and may remove excess formaldehyde. The addition of base and external nucleophile allowed the formation of 1,5-diketones in good yield (Scheme 3-32) enabling a one-pot transformation of ketone **3.108** to 1,5-diketones **3.116** and **3.117** in good yield.

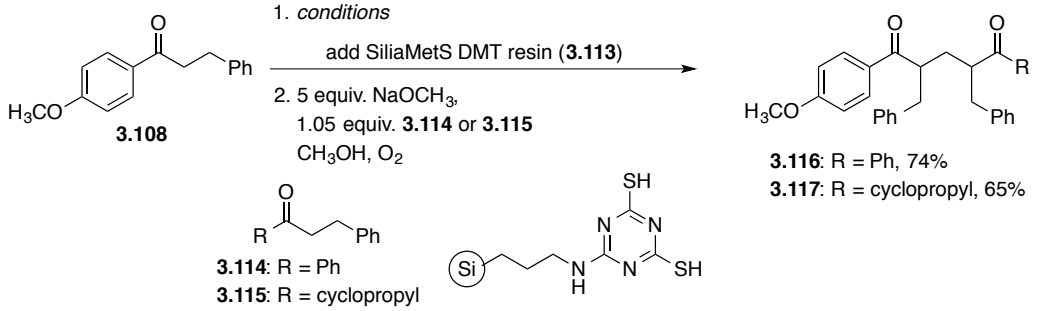

Scheme 3-32. Use of optimized one-pot reaction sequence to form dimer **3.116** and **3.117** (reactions run by Darren Poole)
Conditions (1): 0.3 mmol ketone, 2 mol% $[Ir(cod)Cl]_2$, 8 mol% cataCXium® A, 3 equiv. KOH, 0.1 M in methanol, O_2, 65 °C, 48 h

3.2.4 Utility of the new I-H-B methodology and applications to pyridine synthesis

Further application of this catalytic system was pursued to supplement the one-pot I-H-B and conjugate addition protocol described in section 3.2.3. The

methodology using $[Ir(cod)Cl]_2$ proved to be tunable with conditions described that achieved either a high yield of methylated product **3.76** (PPh_3, 2 equiv. KOH, O_2) or a maximized yield of methylenated intermediates **3.89** and **3.90** (PCy_3 or cataCXium® A, KOH, O_2). The re-examination of catalysts screened by previous collaborators on this project (Table 3-1) showed that an additional system would promote symmetrical dimer formation. Incorporating the dimer formation conditions optimized in previous studies led to the use of 0.5 mol% of $[Ir(cod)Cl]_2$ and 5 equiv. of Cs_2CO_3 in 0.4 M methanol to form symmetrical 1,5-diketone **3.118** in 83% yield, **3.105** in 70% yield and **3.91** in 66% yield (Scheme 3-33).

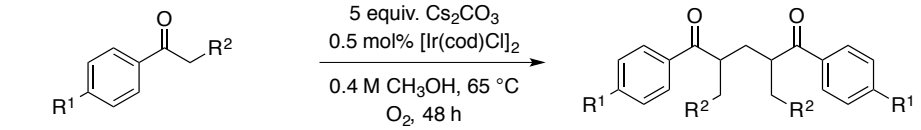

a) **3.108**, $R^1 = OCH_3$; R^2 = Bn
b) **3.103**, R^1 = H; R^2 = Bn
c) **3.75**, R^1 = H; R^2 = *n*-Pr

a) **3.118**, 83%
b) **3.105**, 70%
c) **3.91**, 66%

Scheme 3-33. Symmetrical dimer formation with 1 mol% [Ir]

The access to a diverse set of 1,5-diketones encouraged the formation of tetra-substituted pyridines through an oxidative (and aromatizing) transformation (Scheme 3-34). Reaction of diketone **3.105** with ammonium acetate and Cu^{II} proved promising with a yield of 77% of **3.119** isolated after 10 h of refluxing in acetic acid (Scheme 3-34).

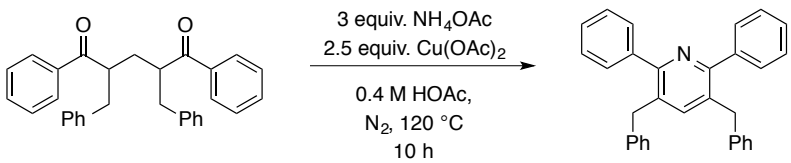

3.105

3.119, 81%

Scheme 3-34. Initial pyridine formation

Application of the same conditions to nonsymmetrical ketone **3.104** gave 85% yield of pyridine **3.120** (Table 3-11, entry 1). Increasing the reaction time to 24 h

led to a pleasing 96% yield (entry 2) with additional increase to 48 h showing a decrease in yield (55%, entry 3), presumably due to decomposition of product. Unfortunately, the super-stoichiometric levels of $Cu(OAc)_2$ made purification by flash column chromatography more difficult (due to difficulty of removing copper salts, despite an ammonium chloride wash during aqueous workup). Stoichiometric levels of copper had also been demonstrated to successfully allow the reaction to pyridines if the reaction is performed under an aerobic environment.[45] The reaction under air gave comparable yields to the use of 2.5 eq of Cu^{II} (entry 4 vs 1). Reacting with ammonium acetate in the absence of $Cu(OAc)_2$ was also precedented,[46] but in our system this led to a significant drop in the yield (entry 5). Additionally, the reaction with 1.0 or less equiv. of $Cu(OAc)_2$ proved to be much less pure and required multiple rounds of flash column chromatography to purify. Adjustment of solvent (including methanol, entry 6, to make this amenable to a one-pot synthesis) gave a low yield and did not improve purification, leading to the attempt of pyridine formation and oxidation with another reagent. [47,48]

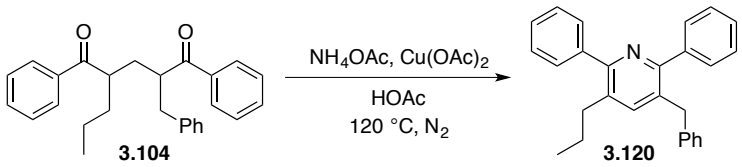

3.104 **3.120**

entry	$Cu(OAc)_2$ (equiv.)	time	yield (%)
1	2.5	10 h	85
2	2.5	24 h	95
3	2.5	48 h	55
4	1.1	10 h[a]	86
5	0	10 h	50
6	2.5	10 h[b]	55

[a]run in air; [b]run in HOAc:CH_3OH 1:1

Table 3-11. Optimization of formation of pyridine **3.120** from 1,5-diketone **3.104**

Symmetrical (**3.91**) and nonsymmetrical (**3.104**) diketones were both reacted with hydroxylamine hydrochloride in ethanol to form the corresponding tetra-

substituted pyridines with an ease of purification that gave this set of reagents an advantage (Scheme 3-35).

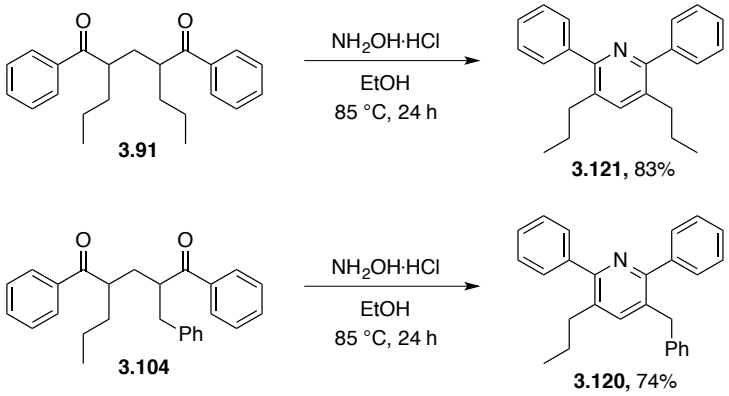

Scheme 3-35. Formation of tetra-substituted pyridines using hydroxylamine hydrochloride

Other 1,5-diketones were also carried through the ammonium acetate and $Cu(OAc)_2$ aromatization to yield additional tetra-substituted pyridines in good yields (Scheme 3-36).

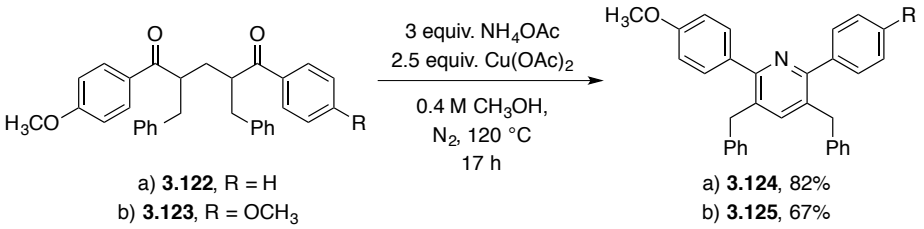

Scheme 3-36. Additional tetra-substituted pyridines accessed

To enable the synthesis of pyridines from IHB-synthesized 1,5-diketones in a one-pot transformation, the reaction would need to occur in the presence of methanol, known to be difficult as a 1:1 mixture of methanol and acetic acid gave low yields of desired pyridine product (Table 3-11, entry 6). The one-pot protocol was attempted by addition of NH_4OAc and $Cu(OAc)_2$ to a microwave vial after 1,5-diketone **3.122** was generated in the I-H-B and conjugate addition steps (Scheme 3-37). Dissolving this mixture in acetic acid and heating the sealed vial to 120 °C gave the desired pyridine in 18 hours and 40% yield over three steps (Scheme 3-37) (though the product was

contaminated with ~5% yield of **3.119**, formed from the diketone derived from **3.103**).

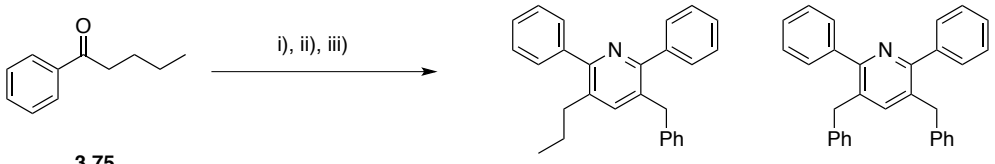

3.75

3.120, 56%*
(one-pot from **3.75**)
*contaminated with **3.119**

3.119

Scheme 3-37. One-pot, three-transformation conversion of alkyl ketone to substituted pyridine
Conditions: i) 2 mol% $[Ir(cod)Cl]_2$, 8 mol% CataCXium® A, 3 equiv. KOH, methanol, O_2, 65 °C, 48 h; ii) 5 equiv. ketone **3.103**, 3 equiv. KOH, O_2, 18 h; iii) 3 equiv. NH_4OAc, 2.5 equiv. $Cu(OAc)_2$, HOAc, 120 °C, N_2, 18 h;

The pyridine cyclization was also applied in a one-pot transformation to allow symmetrical dimer formation (see Scheme 3-33) and subsequent pyridine cyclization and aromatization to allow a one-pot, two-step procedure yielding symmetrical pyridines **3.121** and **3.119** (Scheme 3-38).

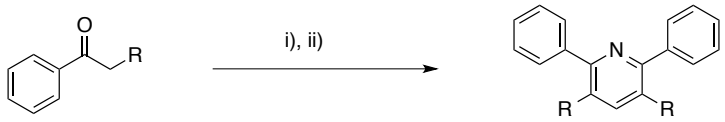

3.75: R = *n*-Pr
3.103: R = Bn

3.121: 47%
3.119: 58%

Scheme 3-38. Symmetrical 1,5-diketone and pyridine formation in one pot
Conditions: i) 0.5 mol% $[Ir(cod)Cl]_2$, 5 equiv. Cs_2CO_3, methanol, O_2, 65 °C, 48 h; ii) 3 equiv. NH_4OAc, 2.5 equiv. $Cu(OAc)_2$, HOAc, 120 °C, 18 h;

Regioselective Baeyer–Villiger reactions (performed by Camilla Shotton, Scheme 3-39) were also performed to access diverse products and exemplify the utility of this catalytic system. Subjection of PMP ketones which were methylated or functionalized with I-H-B reactions gave diverse products at the ester oxidation level.

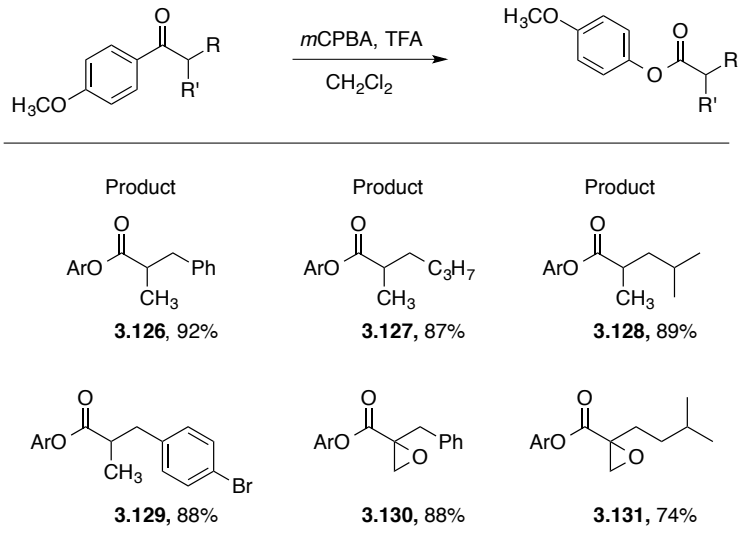

Scheme 3-39. Baeyer–Villiger reaction of PMP ketones (performed and optimized by Camilla Shotton)

3.3 Conclusion

The work described herein represents the expansion of promising Ir-catalyzed methanol hydrogen borrowing chemistry[36] to an α-methylenation method with a one-pot protocol to add external nucleophiles to activated intermediates.[49] Low metal loadings and relatively mild conditions allowed access to reactive intermediates from diverse ketones, and the 1,4-addition of a second ketone enolate gave access to 1,5-diketones. Subsequent (or one-pot) cyclization and aromatization to pyridines allows access to diverse tetra-substituted pyridines.

The desired expansion of this methodology included access to differently substituted pyridines with the use of masked esters to enable pyridone formation (and align with the work completed and detailed in Chapter 2). Additionally, the generation of secondary reactive nucleophiles in situ by a tandem oxidation/activation system was considered. These efforts were limited due to time constraints and my relocation to TSRI.

Additional efforts performed by colleagues and not covered in this chapter include the application of the methodology to other activated, carbonyl-containing substrates (i.e. esters, amides, nitriles) by Camilla Shotton. Darren Poole demonstrated the use of other nucleophiles for conjugate addition (i.e. 1,4-addition of nitro compounds and the use of *t*-BuOOH to form epoxides), and Di Shen designed an elegant improvement of the one-pot, dialkylation procedure (using higher order alcohols than methanol) which are covered in our publication.[49] A subsequent manuscript from the Donohoe group[50] demonstrated the application of this chemistry to direct alkylation of *o*-disubstituted phenyl and cyclopropyl ketones directly with higher order alcohols.

This work has not been applied to the synthesis of natural products or biologically active molecules, but the prominence of activated ketone moieties and the prevalence of target pyridines in these types of structures (see section 3.1) would suggest this is a worthy and likely target use. The method-enabled synthesis of such biologically relevant targets is the focus of my subsequent project at TSRI and will be covered in Chapter 4.

3.4 Experimental

3.4.1 General experimental details

See 2.3.1 for general details pertaining to this chapter.

3.4.2 General procedures

General procedure 3.A: Ir-catalyzed methylation

Under an open atmosphere, $[Ir(cod)Cl]_2$, KOH and PPh_3 were added to a Biotage® microwave vial equipped with a stir bar, followed by methanol (not anhydrous) and starting ketone. The vial was sealed with a microwave vial cap (containing a ResealTM septum) and a balloon of O_2 was inserted via a needle through the septum. The reaction was heated to 65 °C for the period of time stated. The reaction was quenched by diluting with Et_2O and filtering through a pad of SiO_2. Purification by flash column chromatography afforded the desired product.

General procedure 3.B: Ir-catalyzed methylenation

Under an open atmosphere, $[Ir(cod)Cl]_2$, KOH and cataCXium® A were added to a Biotage® microwave vial equipped with a stir bar, followed by methanol (not anhydrous) and starting ketone. The vial was sealed with a microwave vial cap (containing a ResealTM septum) and degassed via a needle with a balloon of O_2. The reaction was heated to 65 °C for the period of time stated with the O_2 balloon attached. The reaction was quenched by diluting with Et_2O and filtering through a pad of silica gel. Purification by flash column chromatography afforded desired product. (Note: It is important to keep the balloon properly attached. The reaction mixture turning from green to brown indicates insufficient O_2 atmosphere.)

General procedure 3.C: Symmetrical dimer formation

Under an open atmosphere, $[Ir(cod)Cl]_2$ and Cs_2CO_3 were added to a Biotage® microwave vial equipped with a stir bar, followed by methanol (not anhydrous) and starting ketone. The vial was sealed with a microwave vial cap (containing a ResealTM septum) and a balloon of O_2 was inserted via a needle through the septum.

The reaction was heated to 65 °C for 48 h. The reaction was quenched by dilution with Et_2O and filtering, first through a cotton filter and then through a pad of silica gel. Purification by flash column chromatography afforded symmetrical dimer products (as an inseparable mixture of diastereomers).

General procedure 3.D: Pyridine formation (using $NH_2OH \bullet HCl$)

Under an open atmosphere, starting diketone (1 equiv.) and hydroxylamine hydrochloride (3 equiv.) were added to a Biotage® microwave vial equipped with a stir bar, followed by ethanol (0.15 mL). The vial was sealed with a microwave vial cap (containing a ResealTM septum) and was heated to 80 °C for 24 h. The reaction was quenched by adding $NaHCO_3$ (sat.), extracted with CH_2Cl_2, then washed with brine, dried over Na_2SO_4, filtered and concentrated in vacuo. Purification by flash column chromatography afforded the desired pyridines.

General procedure 3.E: Pyridine formation (using NH_4OAc)

Under an open atmosphere, starting diketone (30 mg, 1 equiv.), NH_4OAc (3 equiv.) and copper (II) acetate monohydrate (2.5 equiv.) were added to a Biotage® microwave vial equipped with a stir bar, followed by HOAc (0.16 mL). The vial was sealed with a microwave vial cap (containing a ResealTM septum), degassed with argon and heated to 120 °C for 24 h. The reaction was quenched by adding ammonia solution (28%–30%, 0.7 mL), extracted with EtOAc, then washed with brine, dried over Na_2SO_4, filtered, concentrated in vacuo. Purification by flash column chromatography afforded the desired product.

3.4.3 Synthetic procedures and compound characterization

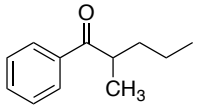

Compound 3.76, 2-methyl-1-phenylpentan-1-one

1-phenylpentan-1-one (**3.75**, 49.3 μL, 0.300 mmol), $[Ir(cod)Cl]_2$ (2.0 mg, 0.0030 mmol), KOH (33.7 mg, 0.602 mmol), PPh_3 (3.2 mg, 0.012 mmol) and methanol (1.5 mL) were subjected to general procedure 3.A for 48 h. Purification by flash column chromatography (SiO_2, 11% Et_2O/petrol) afforded **3.76** (60.9 mg, 0.239 mmol, 80%) as a colorless oil. ^1H NMR (400 MHz, $CDCl_3$) δ 7.92–7.84 (m, 2H), 7.52–7.34 (m, 3H), 3.41 (sext, J = 6.8 Hz, 1H), 1.78–1.66 (m, 1H), 1.42–1.13 (m, 3H), 1.12 (d, J = 6.9 Hz, 3H), 0.83 (t, J = 7.2 Hz, 3H); ^{13}C NMR (100 MHz, $CDCl_3$) δ 204.6, 136.8, 132.8, 128.6, 128.2, 40.3, 35.9, 20.6, 17.2, 14.2. Spectroscopic data are consistent with those previously reported.[36]

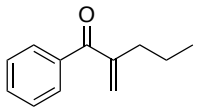

Compound 3.89, 2-methylene-1-phenylpentan-1-one

1-phenylpentan-1-one (**3.75**, 49.3 μL, 0.300 mmol), $[Ir(cod)Cl]_2$ (4.0 mg, 0.0060 mmol), KOH (50.0 mg, 0.893 mmol), cataCXium® A (8.4 mg, 0.024 mmol) and methanol (3.0 mL) were subjected to general procedure 3.B for 48 h. Purification by flash column chromatography (SiO_2, 20% Et_2O/petrol) afforded **3.89** (6.8 mg, 0.039 mmol, 13%) as a colorless oil. ^1H NMR (400 MHz, $CDCl_3$) δ 7.80–7.74 (m, 2H), 7.60–7.54 (m, 1H), 7.47–7.42 (m, 2H), 5.83 (s, 1H), 5.59 (s, 1H), 2.46 (t, J = 6.9 Hz, 2H), 1.54 (sext, J = 6.9 Hz, 2H), 0.98 (t, J = 6.9 Hz, 3H); ^{13}C NMR (150 MHz, $CDCl_3$) δ 198.5, 148.3, 138.0, 132.2, 129.5, 128.2, 125.3, 34.4, 21.4, 13.8. Spectroscopic data were consistent with those previously reported.[36]

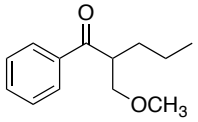

Compound 3.90, 2-(methoxymethyl)-1-phenylpentan-1-one

1-phenylpentan-1-one (**3.75**, 49.3 μL, 0.300 mmol), $[Ir(cod)Cl]_2$ (4.0 mg, 0.0060 mmol), KOH (50.0 mg, 0.893 mmol), cataCXium® A (8.4 mg, 0.024 mmol) and methanol (3.0 mL) were subjected to general procedure 3.B for 48 h. Purification by flash column chromatography (SiO_2, 20% Et_2O/petrol) afforded **3.90** (40.2 mg, 0.195 mmol, 65%) as a colorless oil. ^1H NMR (400 MHz, $CDCl_3$) δ 8.01–7.96 (m, 2H), 7.59–7.54 (m, 1H), 7.50–7.44 (m, 2H), 3.81–3.69 (m, 2H), 3.55–3.48 (m, 1H), 3.30 (s, 3H), 1.77–1.69 (m, 1H), 1.57–1.47 (m, 1H), 1.30 (sext, J = 7.8 Hz, 2H), 0.88 (t, J = 7.2 Hz, 3H); ^{13}C NMR (150 MHz, $CDCl_3$) δ 203.1, 137.7, 132.9, 128.6, 128.3, 74.3, 59.1, 46.5, 32.0, 20.6, 14.2. Spectroscopic data were consistent with those previously reported.[36]

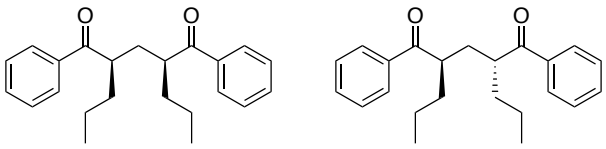

syn-**3.91** *anti*-**3.91**

Compound 3.91, 1,5-diphenyl-2,4-dipropylpentane-1,5-dione

Compound **3.91** (as an inseparable mixture of *syn*-**3.91** and *anti*-**3.91**) was isolated as a byproduct of procedure 3.B (during optimization) and synthesized using procedure 3.C as follows. 1-phenylpentan-1-one (**3.75**, 49.3 μL, 0.300 mmol), $[Ir(cod)Cl]_2$ (2.0 mg, 0.0030 mmol), Cs_2CO_3 (293 mg, 0.901 mmol) and methanol (0.75 mL) were subjected to general procedure 3.C for 48 h. Purification by flash column chromatography (SiO_2, 20% Et_2O/petrol) afforded **3.90** (33.7 mg, 0.0990 mmol, 66%) as a colorless oil. Dimers *anti*-**3.90** and syn-**3.90** were isolated as a 1:1 mixture of inseparable diastereoisomers. *Anti*-**3.90** ^1H NMR (400 MHz, $CDCl_3$) δ 7.72–7.68 (m, 4H), 7.46–7.39 (m, 2H), 7.31–7.23 (m, 4H), 3.42–3.33 (m, 2H), 2.10–2.04 (m, 2H),

1.80–1.58 (m, 4H), 1.49–1.37 (m, 2H), 1.36–1.11 (m, 2H), 0.85 (t, J = 7.3 Hz, 6H); ^{13}C NMR (100 MHz, $CDCl_3$) δ 204.9, 137.4, 132.8, 128.5, 128.0, 43.7, 36.2, 34.4, 20.5, 14.1.

Syn-**3.90** ^{1}H NMR (400 MHz, $CDCl_3$) δ 8.04–7.98 (m, 4H), 7.61–7.55 (m, 2H), 7.53–7.47 (m, 4H), 3.57–3.49 (m, 2H), 2.34–2.25 (m, 1H), 1.79–1.69 (m, 1H), 1.49–1.37 (m, 2H), 1.36–1.11 (m, 6H), 0.79 (t, J = 7.3 Hz, 6H); ^{13}C NMR (100 MHz, $CDCl_3$) δ 203.9, 137.2, 133.0, 128.7, 128.3, 43.4, 36.2, 34.0, 20.4, 14.1. Spectroscopic data were consistent with those previously reported.[36]

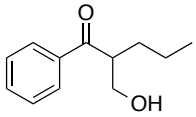

Compound 3.92, 2-(hydroxymethyl)-1-phenylpentan-1-one

A stirred solution of 1-phenylpentan-1-one (**3.75**, 1.00 mL, 6.10 mmol) in methanol (40 mL) was treated with paraformaldehyde (185 mg, 6.10 mmol) and K_2CO_3 (84 mg, 0.61 mmol). The mixture was stirred at 25 °C for 72 h. The solvent was removed, 1 M HCl was added and the mixture was extracted with $CHCl_3$. The combined organic phase was dried over $MgSO_4$, filtered and concentrated. Purification by flash column chromatography (SiO_2, $CHCl_3$ to 10% methanol in $CHCl_3$) afforded **3.92** (774 mg, 4.02 mmol, 66%) as a colorless oil. ^{1}H NMR (400 MHz, $CHCl_3$) δ 8.00–7.93 (m, 2H), 7.62–7.56 (m, 1H), 7.52–7.46 (m, 2H), 3.97 (dd, J = 11.1, 6.9 Hz, 1H), 3.86 (dd, J = 11.1, 3.8 Hz, 1H), 3.67–3.59 (m, 1H), 2.25 (br s, 1H), 1.74–1.56 (m, 2H), 1.47–1.30 (m, 2H), 0.92 (t, J = 7.3 Hz, 3H); ^{13}C NMR (100 MHz, $CHCl_3$) δ 204.7, 136.8, 133.3, 128.7, 128.3, 62.9, 47.9, 31.3, 20.6, 14.1. Spectroscopic data were consistent with those previously reported.[36]

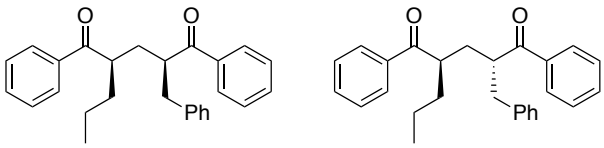

syn-**3.104** *anti*-**3.104**

Compound 3.104, (±)-(2*RR*,4*RS*)-2-benzyl-1,5-diphenyl-4-propylpentane-1,5-dione

1-phenylpentan-1-one (**3.75**, 49.3 μL, 0.300 mmol), $[Ir(cod)Cl]_2$ (4.0 mg, 0.0060 mmol), KOH (50.0 mg, 0.893 mmol), cataCXium® A (8.4 mg, 0.024 mmol) and methanol (3.0 mL) were subjected to general procedure 3.B for 48 h. The reaction was cooled, opened and sonicated for 15 min before 1,3-diphenylpropan-1-one (315 mg, 1.51 mmol) and KOH (50 mg, 0.89 mmol) were added. The vial was sealed and heated at 65 °C for 48 h. The crude mixture was diluted with Et_2O, filtered through SiO_2 and concentrated. Purification by flash column chromatography (SiO_2, 20% Et_2O/petrol) afforded **3.104** as an oil (69.6 mg, 0.181 mmol, 61%). Dimers *anti*-**3.104** and *syn*-**3.104** were isolated as a 1:1 mixture of inseparable diastereoisomers. ^{1}H NMR (400 MHz, $CDCl_3$) δ 7.85 (d, J = 7.3 Hz, 8H), 7.55–7.22 (m, 4H), 7.16–6.90 (m, 18H), 3.79–3.62 (m, 2H), 3.51–3.37 (m, 1H), 3.31–3.20 (m, 1H), 3.12–2.81 (m, 2H), 2.66 (dd, J = 22.4, 13.7 Hz, 2H), 2.26 (dt, J = 14.1, 7.1 Hz, 1H), 2.02 (dd, J = 20.8, 10.5 Hz, 2H), 1.66–1.43 (m, 3H), 1.35–1.03 (m, 6H), 0.72 (t, J = 7.3 Hz, 3H), 0.67 (t, J = 7.3 Hz, 3H); ^{13}C NMR (100 MHz, $CDCl_3$) δ 204.4, 204.3, 203.8, 203.3, 139.5, 139.0, 137.4, 137.2, 137.2, 136.9, 133.2, 133.2, 133.0, 133.0, 129.0, 129.0, 128.9, 128.8, 128.7, 128.5, 128.4, 128.4, 128.4, 128.3, 128.1, 128.0, 126.4, 126.3, 46.0, 45.7, 43.7, 43.5, 40.0, 38.2, 36.1, 34.6, 34.5, 34.4, 20.6, 20.5, 14.2, 14.2.

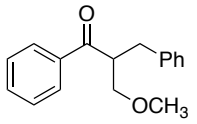

Compound 3.110a, 2-benzyl-3-methoxy-1-phenylpropan-1-one

1,3-diphenylpropan-1-one (**3.103**, 63.0 mg, 0.300 mmol), $[Ir(cod)Cl]_2$ (4.0 mg, 0.0060 mmol), KOH (16.7 mg, 0.893 mmol), cataCXium® A (8.4 mg, 0.024 mmol) and methanol (3.0 mL) were subjected to general procedure 3.B for 48 h. Purification by flash column chromatography (SiO_2, 20% Et_2O/petrol) afforded **3.110a** (41.9 mg, 0.165 mmol, 55%) as a colorless oil. Compound **3.109a** was also isolated (15.0 mg, 0.0670, 22%) but not characterized. ^{1}H NMR (400 MHz, $CDCl_3$) δ 7.79 (d, *J* = 7.7 Hz, 2H), 7.46–7.40 (m, 1H), 7.35–7.29 (m, 2H), 7.17–7.11 (m, 2H), 7.08 (d, *J* = 7.3 Hz, 3H), 3.97–3.88 (m, 1H), 3.66–3.60 (m, 1H), 3.43 (dd, *J* = 9.0, 5.3 Hz, 1H), 3.18 (s, 3H), 2.98 (dd, *J* = 13.7, 7.4 Hz, 1H), 2.80 (dd, *J* = 13.7, 6.8 Hz, 1H).

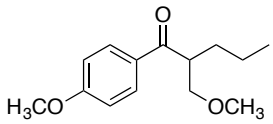

Compound 3.110b, 2-(methoxymethyl)-1-(4-methoxyphenyl)hexan-1-one

1-(4-methoxyphenyl)pentan-1-one (**3.107**, 61.9 mg, 0.300 mmol), $[Ir(cod)Cl]_2$ (4.0 mg, 0.0060 mmol), KOH (50.0 mg, 0.893 mmol), cataCXium® A (8.4 mg, 0.024 mmol) and methanol (3.0 mL) were subjected to general procedure 3.B for 48 h. Purification by flash column chromatography (SiO_2, 20% Et_2O/petrol) afforded **3.110b** (41.4 mg, 0.165 mmol, 55%) as a colorless oil. Compound **3.109b** was also isolated (13.7 mg, 0.00630 mmol, 20%) but not characterized. ^{1}H NMR (400 MHz, $CDCl_3$) δ 7.98 (d, *J* = 8.8 Hz, 2H), 6.95 (d, *J* = 8.8 Hz, 2H), 3.87 (s, 3H), 3.71–3.68 (m, 2H), 3.52–3.46 (m, 1H), 3.29 (s, 3H), 1.72–1.67 (m, 1H), 1.56–1.50 (m, 1H), 1.27–1.24 (m, 2H), 0.84 (t, *J* = 6.8 Hz, 3H); ^{13}C NMR (125 MHz, $CDCl_3$) δ 201.5, 163.5, 130.7, 129.9, 113.8, 74.4, 59.1, 55.4, 46.3, 29.6, 22.9, 13.9.

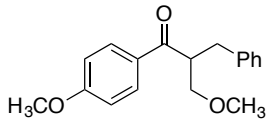

Compound 3.110c, 2-benzyl-3-methoxy-1-(4-methoxyphenyl)propan-1-one

1-(4-methoxyphenyl)-3-phenylpropan-1-one (**3.108**, 72.1 mg, 0.300 mmol), $[Ir(cod)Cl]_2$ (4.0 mg, 0.0060 mmol), KOH (50.0 mg, 0.893 mmol), cataCXium® A (8.4 mg, 0.024 mmol) and methanol (3.0 mL) were subjected to general procedure 3.B for 48 h. Purification by flash column chromatography (SiO_2, 20% Et_2O/petrol) afforded **3.110c** (53.7 mg, 0.189 mmol, 65%) as a colorless oil. Compound **3.109c** was also isolated (2.4 mg, 0.0095, 3%) but was not characterized. ^{1}H NMR (500 MHz, $CDCl_3$) δ 7.89 (d, *J* = 8.8 Hz, 2H), 7.25–7.15 (m, 5H), 6.89 (d, *J* = 9.0 Hz, 2H), 3.98 (td, *J* = 7.1, 1.9 Hz, 1H), 3.84 (s, 3H), 3.72 (dd, *J* = 9.0, 7.4 Hz, 1H), 3.51 (dd, *J* = 9.0, 5.4 Hz, 1H), 3.28 (s, 3H), 3.06 (dd, *J* = 13.8, 7.5 Hz, 1H), 2.88 (dd, *J* = 13.8, 6.7 Hz, 1H); ^{13}C NMR (125 MHz, $CDCl_3$) δ 200.5, 163.5, 139.3, 130.7, 130.4, 129.0, 128.4, 126.3, 113.7, 73.7, 59.1, 55.4, 48.3, 35.5.

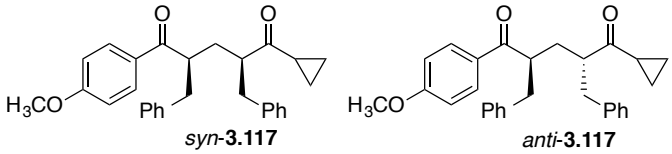

syn-**3.117** *anti*-**3.117**

Compound 3.117, (±)(2*RS*,4*SS*)-2,4-Dibenzyl-1-cyclopropyl-5-(4-methoxyphenyl)pentane-1,5-dione[1]

Under an open atmosphere, $[Ir(cod)Cl]_2$ (13.3 mg, 0.0200 mmol), KOH (167 mg, 3.00 mmol) and cataCXium® A (28.0 mg, 0.0800 mmol) were added to a Biotage® microwave vial equipped with a stir bar, followed by methanol (10 mL, not anhydrous) and 1-(4-methoxyphenyl)-3-phenylpropan-1-one (**3.108**, 240.0 mg, 1.000 mmol). The vial was sealed with a microwave vial cap (containing a ResealTM septum) and a balloon of O_2 was inserted via a needle through the septum. The reaction was heated to 65 °C for 48 h before being concentrated to 0.4 M (stream of

[1] Reaction performed by Darren Poole

Ar) and SiliaMetS DMT (257 mg, 0.160 mmol) was added. The mixture was stirred at 25 °C open to air for 1 h before 1-cyclopropyl-3-phenylpropan-1-one (**3.115**, 523 mg, 3.00 mmol) and KOH (167 mg, 3.00 mmol) were added. The vial was sealed and heated at 65 °C under O_2 for 21 h. The reaction was cooled, another 2 equiv. of KOH (112.0 mg, 1.000 mmol) was added and the reaction was heated for another 24 h. The crude mixture was diluted with Et_2O, filtered through SiO_2 and concentrated in vacuo. Purification by flash column chromatography (SiO_2, 20% Et_2O/petrol) afforded **3.117** as a light yellow oil (277 mg, 0.650 mmol, 65%). ^{1}H NMR (500 MHz, $CDCl_3$) δ 7.89 (d, *J* = 8.8 Hz, 2H), 7.84 (d, *J* = 9.0 Hz, 2H), 7.30–7.10 (m, 18H), 7.06–7.02 (m, 2H), 6.92 (d, *J* = 8.8 Hz, 2H), 6.88 (d, *J* = 8.8 Hz, 2H), 3.86–3.82 (m, 3H), 3.81–3.77 (m, 3H), 3.77–3.64 (m, 2H), 3.14–2.87 (m, 6H), 2.80–2.69 (m, 3H), 2.63 (dd, *J* = 6.7, 13.5 Hz, 1H), 2.36 (td, *J* = 7.1, 14.1 Hz, 1H), 2.14–2.05 (m, 1H), 2.04–1.96 (m, 1H), 1.94–1.84 (m, 1H), 1.67 (td, *J* = 6.6, 13.8 Hz, 1H), 1.57–1.48 (m, 1H), 1.07–0.92 (m, 2H), 0.91–0.79 (m, 3H), 0.79–0.71 (m, 1H), 0.65–0.51 (m, 2H); ^{13}C NMR (125 MHz, $CDCl_3$) δ 213.7, 213.1, 202.0, 201.4, 163.6, 163.5, 139.6, 139.4, 139.2, 138.9, 130.7, 130.6, 130.5, 129.8, 129.0, 129.0, 129.0, 128.5, 128.4, 128.4, 126.4, 126.3, 113.9, 113.8, 55.5, 55.4, 52.8, 52.6, 45.7, 45.3, 39.9, 39.3, 38.3, 38.1, 33.8, 33.7, 20.9, 20.7, 11.7, 11.5, 11.5, 11.5 (4 aromatic carbons were not observed due to overlapping); IR (neat) ν_{max} 3062, 3027, 2934, 2841, 1598, 1259, 1169, 699 cm^{-1}; HRMS (ESI)$^+$ *m/z* calculated for $C_{29}H_{30}O_3$ $[M+H]^+$ 427.2268, found 427.2259 (Δ –2.1 ppm).

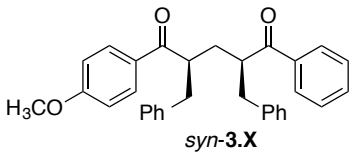

syn-**3.X**

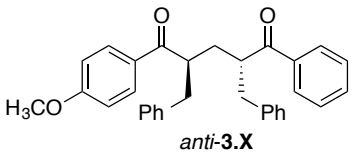

anti-**3.X**

Compound 3.116, (±)(2*SS*,4*RS*)-2,4-dibenzyl-1-(4-methoxyphenyl)-5-phenylpentane-1,5-dione[2]

Under an open atmosphere, $[Ir(cod)Cl]_2$ (13.3 mg, 0.0200 mmol), KOH (167 mg, 3.00 mmol) and cataCXium® (28.0 mg, 0.0800 mmol) were added to a Biotage® microwave vial equipped with a stir bar, followed by methanol (10 mL, not anhydrous) and 1-(4-methoxyphenyl)-3-phenylpropan-1-one (**3.108**, 240.0 mg, 1.000 mmol). The vial was sealed with a microwave vial cap (containing a ResealTM septum) and a balloon of O_2 was inserted via a needle through the septum. The reaction was heated to 65 °C for 48 h. It was then cooled and concentrated to 0.4 M (stream of Ar) before SiliaMetS DMT (257 mg, 0.161 mmol) was added. The mixture was stirred at 25 °C open to air for 1 h before 3-phenylpropiophenone (630 mg, 3.00 mmol) and KOH (167 mg, 3.00 mmol) were added. The vial was sealed and heated at 65 °C for 24 h under O_2 and another 1 equiv. KOH was added (56 mg, 1.0 mmol) then heated for another 18 h. The crude mixture was diluted with Et_2O, filtered through SiO_2 and concentrated. Purification by flash column chromatography (SiO_2, 20% Et_2O/petrol) afforded **3.116** as a light yellow oil (333 mg, 0.721 mmol, 72%). Dimers *anti*-**3.116** and *syn*-**3.116** were isolated as a 1:1 mixture of inseparable diastereoisomers. ^{1}H NMR (500 MHz, $CDCl_3$) δ 7.90–7.87 (m, 4H), 7.58–7.51 (m, 5H), 7.46–7.43 (m, 2H), 7.39–7.35 (m, 1H), 7.22–7.08 (m, 18H), 7.01–6.99 (m, 4H), 6.94–6.92 (m, 2H), 6.64–6.63 (m, 2H), 3.87 (s, 3H), 3.84–3.66 (m, 4H), 3.74 (s, 3H), 3.07–2.98 (m, 4H), 2.75–2.63 (m, 4H), 2.43–2.38 (m, 1H), 2.15–2.12 (m, 2H), 1.77–1.72 (m, 1H); ^{13}C NMR (125 MHz, $CDCl_3$) δ 203.9, 203.2, 202.3, 201.5, 163.6, 163.3, 139.5, 139.3, 139.1, 138.8, 137.2, 136.8, 133.1, 132.7, 130.7, 130.4, 129.8,

[2] Reaction performed by Darren Poole.

129.0, 128.9, 128.9, 128.7, 128.5, 128.4, 128.4, 128.4, 128.4, 128.3, 128.0, 126.4, 126.3, 126.3, 113.9, 113.5, 55.5, 55.4, 46.0, 45.6, 45.5, 45.2, 39.9, 39.9, 38.5, 38.3, 34.9, 34.5 (3 carbon signals are not observed due to overlapping); IR (neat) ν_{max} 3061, 3027, 2923, 2851, 2361, 2341, 1674, 1599, 1259, 1245, 1171, 699 cm^{-1}; HRMS (ESI^+) *m/z* calculated for $C_{32}H_{30}O_3$ $[M+H]^+$ 463.2268, found 463.2260 (Δ –1.6 ppm).

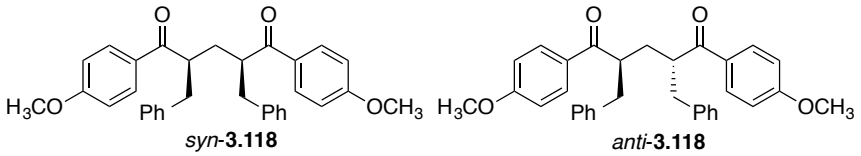

syn-**3.118** *anti*-**3.118**

Compound 3.118, (2*RR*,4*RS*)-2,4-dibenzyl-1,5-bis(4-methoxyphenyl)pentane-1,5-dione

1-(4-methoxyphenyl)-3-phenylpropan-1-one (**3.108**, 72.1 mg, 0.300 mmol), $[Ir(cod)Cl]_2$ (2.0 mg, 0.0030 mmol), Cs_2CO_3 (489 mg, 0.893 mmol) and methanol (0.75 mL) were subjected to general procedure 3.C for 48 h. Purification by flash column chromatography (SiO_2, 20% Et_2O/petrol) afforded **3.118** (61.0 mg, 0.124 mmol, 83%) as a colorless oil. Dimers *anti*-**3.118** and syn-**3.118** were isolated as a 1:1 mixture of inseparable diastereoisomers. ^1H NMR (400 MHz, $CDCl_3$) δ 7.88 (d, *J* = 8.7 Hz, 4H), 7.50 (d, *J* = 8.8 Hz, 4H), 7.21–7.07 (m, 16H), 6.99 (d, *J* = 7.1 Hz, 4H), 6.92 (d, *J* = 9.0 Hz, 4H), 6.61 (d, *J* = 8.6 Hz, 4H), 3.86 (s, 6H), 3.74 (s, 6H), 3.76–3.71 (m, 2H), 3.67–3.60 (m, 2H), 3.06–3.02 (m, 2H), 3.01–2.97 (m, 2H), 2.74–2.69 (m, 2H), 2.67–2.62 (m, 2H), 2.41–2.35 (m, 1H), 2.12 (t, *J* = 7.1 Hz, 2H), 1.75–1.69 (m, 1H); ^{13}C NMR (100 MHz, $CDCl_3$) δ 202.4, 201.6, 163.6, 163.2, 139.6, 139.2, 130.8, 130.4, 130.4, 129.9, 129.0 (2C), 128.5, 128.4, 126.3, 126.7, 113.9, 113.5, 55.6, 55.3, 45.6, 45.2, 40.2, 38.5, 35.5, 34.8; IR (neat) ν_{max} 2933, 2839, 1667, 1598, 1510, 1246, 1170, 1030, 836, 749, 700 cm^{-1}; HRMS (ESI^+) *m/z* calculated for $C_{33}H_{32}O_4$ $[M+H]^+$ 493.2373, found 493.2367 (Δ –1.3 ppm).

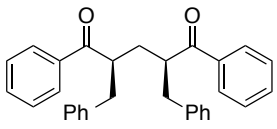

syn-**3.105**

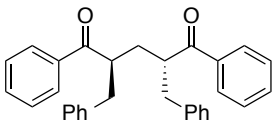

anti-**3.105**

Compound 3.105, (±)-(2*RR*,4*RS*)-2,4-dibenzyl-1,5-diphenylpentane-1,5-dione

Compound **3.105** (as a mixture of *syn*- and *anti*-**3.105**) was isolated as a byproduct from reaction of **3.103** (general procedure 3.B) and was also synthesized using procedure 3.C as follows. 1,3-diphenylpropan-1-one (**3.103**, 63.1 mg, 0.300 mmol), $[Ir(cod)Cl]_2$ (2.0 mg, 0.0030 mmol), Cs_2CO_3 (489 mg, 0.893 mmol) and methanol (0.75 mL) were subjected to general procedure 3.C for 48 h. Purification by flash column chromatography (SiO_2, 10% Et_2O/petrol) afforded **3.105** (45.6 mg, 0.105 mmol, 70%) as a colorless oil. Dimers *anti*-**3.105** and syn-**3.105** were isolated as a 1:1 mixture of inseparable diastereoisomers. ^{1}H NMR (400 MHz, $CDCl_3$) δ 7.80–7.73 (m, 4H), 7.51–7.41 (m, 6H), 7.41–7.31 (m, 2H), 7.31–7.24 (m, 4H), 7.14–7.02 (m, 16H), 7.02–6.97 (m, 4H), 6.91–6.84 (m, 4H), 3.65 (dq, J = 30.2, 7.0 Hz, 4H), 2.94 (td, J = 13.7, 7.3 Hz, 4H), 2.59 (ddd, J = 29.2, 13.7, 6.7 Hz, 4H), 2.31 (dt, J = 14.1, 7.1 Hz, 1H), 2.06–2.01 (m, 2H), 1.70–1.60 (m, 1H), 0.86–0.76 (m, 2H); ^{13}C NMR (100 MHz, $CDCl_3$) δ 203.8, 203.1, 139.2, 138.8, 137.2, 136.8, 133.1, 132.8, 128.9, 128.9, 128.7, 128.5, 128.4, 128.4, 128.4, 128.0, 126.4, 126.3, 45.9, 45.6, 39.7, 38.3, 34.6, 34.3.

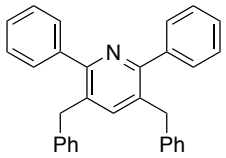

Compound 3.119, 3,5-dibenzyl-2,6-diphenylpyridine

Compound **3.105** (43.0 mg, 0.0994 mmol) was subjected to general procedure 3.E with NH_4OAc (23.1 mg, 0.300 mmol) and $Cu(OAc)_2$ (45.0 mg, 0.248 mmol) in HOAc (0.25 mL). The mixture was heated for 48 h, cooled then subjected to aqueous workup to yield crude product, which was purified by flash column chromatography (SiO_2,

toluene to 2% Et_2O/petrol gradient) to yield **3.119** (33.3 mg, 0.809 mmol, 81%) as a colorless oil.

Compound **3.119** was also synthesized through a one-pot procedure (using modified general methods 3.C, 3.E): 1,3-diphenylpropan-1-one (**3.103**, 63.0 mg, 0.300 mmol), $[Ir(cod)Cl]_2$ (2.0 mg, 0.0030 mmol), Cs_2CO_3 (489 mg, 0.893 mmol) and methanol (0.75 mL) were added to a Biotage® microwave vial equipped with a stir bar. The vial was sealed with a microwave vial cap (containing a ResealTM septum) and a balloon of O_2 was inserted via a needle through the septum. The reaction was heated to 65 °C for 24 h. The reaction was purged with N_2 and HOAc (0.75 mL), $Cu(OAc)_2$ (68.0 mg, 0.374 mmol) then NH_4OAc (35.0 mg, 0.454 mmol) were added. The vial was sealed under an N_2 atmosphere and stirred at 120 °C for 24 h. The reaction was cooled and subjected to an aqueous workup. Crude material was purified by flash column chromatography (SiO_2, 1–8% Et_2O/petrol gradient) to yield **3.119** (35.7 mg, 0.0867 mmol, 82%). ^1H NMR (400 MHz, $CDCl_3$) δ 7.42 (d, J = 6.4 Hz, 4H), 7.33–7.25 (m, 7H), 7.17–7.08 (m, 6H), 6.90 (d, J = 7.1 Hz, 4H), 3.94 (s, 4H); ^{13}C NMR (100 MHz, $CDCl_3$) δ 156.6, 141.2, 140.5, 132.5, 129.3, 128.8, 128.5, 128.5, 128.2, 128.0, 126.2, 38.2.

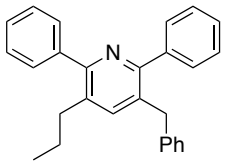

Compound 3.120, 3-benzyl-2,6-diphenyl-5-propylpyridine

Compound **3.104** (77.7 mg, 0.0202 mmol) was subjected to general procedure 3.E with NH_4OAc (46.7 mg, 0.606 mmol) and $Cu(OAc)_2$ (91.8 mg, 0.505 mmol) in HOAc (0.50 mL). The mixture was heated for 24 h, cooled then subjected to aqueous workup to yield crude product which was purified by flash column chromatography (SiO_2, petrol to 20% Et_2O/petrol gradient) to yield **3.120** (73.0 mg, 0.0202 mmol, quant.).

Compound **3.120** was also synthesized through a one-pot procedure: 1-phenylpentan-1-one (**3.75**, 49.3 μL, 0.300 mmol), $[Ir(cod)Cl]_2$ (4.0 mg, 0.0060 mmol), KOH (50.0 mg, 0.893 mmol) and methanol (3.0 mL) were added to a Biotage® microwave vial equipped with a stir bar. The vial was sealed with a microwave vial cap (containing a ResealTM septum) and a balloon of O_2 was inserted via a needle through the septum. The reaction was heated to 65 °C for 48 h. The reaction was purged with N_2 and **3.103** (315.4 mg, 1.500 mmol), KOH (50 mg, 0.89 mmol) were added and the vial was resealed with a balloon of O_2. The reaction was heated for 18 h then cooled and purged with N_2. HOAc (1.5 mL), $Cu(OAc)_2$ (136 mg, 0.745 mmol) then NH_4OAc (69.0 mg, 0.895 mmol) were added. The vial was sealed under an N_2 atmosphere and stirred at 120 °C for 16 h. The reaction was cooled and subjected to an aqueous workup. Crude material was purified by flash column chromatography (SiO_2, petrol to 15% Et_2O/petrol gradient) to yield **3.120** (63.7 mg, 0.100 mmol, 56%). ^1H NMR (400 MHz, $CDCl_3$) δ 7.49–7.39 (m, 4H), 7.39–7.10 (m, 10H), 6.99 (d, J = 7.3 Hz, 2H), 3.99 (s, 2H), 2.59–2.49 (m, 2H), 1.52–1.35 (m, 2H), 0.77 (t, J = 7.3 Hz, 3H).

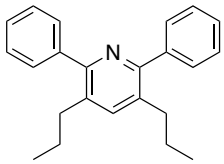

Compound 3.121, 2,6-diphenyl-3,5-dipropylpyridine

Compound **2.91** was subjected to general procedure 3.D with NH_2OH•HCl (13.0 mg, 0.187 mmol) in EtOH (0.95 mL) and heated for 12 h. Aqueous workup and purification by flash column chromatography (SiO_2, petrol to 10% Et_2O/petrol gradient) yielded **3.121** (33.1 mg, 0.105 mmol, 56% yield) as a colorless oil.

Compound **3.121** was also synthesized through a one-pot procedure: 1-phenylpentan-1-one (**3.75**, 49.3 μL, 0.300 mmol), $[Ir(cod)Cl]_2$ (2.0 mg, 0.0030 mmol), Cs_2CO_3 (489

mg, 0.893 mmol) and methanol (0.75 mL) were added to a Biotage® microwave vial equipped with a stir bar. The vial was sealed with a microwave vial cap (containing a ResealTM septum) and a balloon of O_2 was inserted via a needle through the septum. The reaction was heated to 65 °C for 24 h. The reaction was purged with N_2 and HOAc (0.75 mL), $Cu(OAc)_2$ (68.0 mg, 0.374 mmol) then NH_4OAc (35.0 mg, 0.454 mmol) were added. The vial was sealed under an N_2 atmosphere and stirred at 120 °C for 24 h. The reaction was cooled and subjected to an aqueous workup. Crude material was purified by flash column chromatography (SiO_2, 3–9% Et_2O/petrol gradient) to yield **3.121** (22.4 mg, 0.0710 mmol, 47%). ^{1}H NMR (400 MHz, $CDCl_3$) δ 7.44 (d, *J* = 6.9 Hz, 5H), 7.33 (t, *J* = 7.3 Hz, 4H), 7.29–7.25 (m, 2H), 2.57 (d, *J* = 7.7 Hz, 4H), 1.59–1.44 (m, 4H), 0.82 (t, *J* = 7.3 Hz, 6H); ^{13}C NMR (100 MHz, $CDCl_3$) δ 155.8, 140.9, 138.7, 133.8, 129.2, 128.0, 127.5, 34.2, 24.2, 14.1. Data were in accordance with the literature.[51]

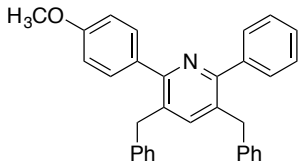

Compound 3.124, 3,5-dibenzyl-2-(4-methoxyphenyl)-6-phenylpyridine

Compound **3.122** (66.2 mg, 0.143 mmol) was subjected to general procedure 3.E with NH_4OAc (33.1 mg, 0.429 mmol) and $Cu(OAc)_2$ (52.4 mg, 0.358 mmol) in HOAc (0.36 mL). The mixture was heated for 24 h, cooled then subjected to aqueous workup to yield crude product which was purified by flash column chromatography (SiO_2, petrol to 10% Et_2O/petrol gradient) to yield **3.124** (51.7 mg, 0.117 mmol, 82%). ^{1}H NMR (500 MHz, $CDCl_3$) δ 7.42 (d, *J* = 7.6 Hz, 2H), 7.38 (d, *J* = 7.9 Hz, 2H), 7.33–7.24 (m, 4H), 7.15 (q, *J* = 8.0 Hz, 4H), 7.12–7.08 (m, 2H), 6.93 (d, *J* = 7.6 Hz, 2H), 6.90 (d, *J* = 7.4 Hz, 2H), 6.83 (d, *J* = 8.4 Hz, 2H), 3.96 (s, 2H), 3.93 (s, 2H), 3.74 (s, 3H); ^{13}C NMR (125 MHz, $CDCl_3$) δ 159.5, 156.5, 156.3, 141.2, 140.6, 140.2, 132.7,

140.5, 132.2, 132.0, 130.6, 129.3, 128.8, 128.8, 128.5, 128.5, 128.1, 127.9, 126.2, 126.2, 113.6, 55.4, 38.3, 38.2; IR (neat) ν_{max} 3060, 3026, 2932, 2836, 1609, 1434, 1248, 1175, 728, 699 cm^{-1}; HRMS (ESI^+) *m/z* calculated for $C_{32}H_{27}NO$ $[M+H]^+$ 442.2165, found 442.2157 (Δ –1.97 ppm).

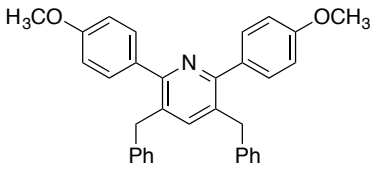

Compound 3.125, 3,5-dibenzyl-2,6-bis(4-methoxyphenyl)pyridine

Compound **3.123** (56.8 mg, 0.115 mmol) was subjected to general procedure 3.E with NH_4OAc (26.7 mg, 0.346 mmol) and $Cu(OAc)_2$ (52.4 mg, 0.288 mmol) in HOAc (0.30 mL). The mixture was heated for 24 h, cooled then subjected to aqueous workup to yield crude product which was purified by flash column chromatography (SiO_2, petrol to 10% Et_2O/petrol gradient) to yield **3.125** (36.6 mg, 0.0776 mmol, 67%). ^1H NMR (400 MHz, $CDCl_3$) δ 7.48 (d, *J* = 8.6 Hz, 4H), 7.34 (s, 1H), 7.25 (t, *J* = 7.7 Hz, 4H), 7.18 (t, *J* = 6.8 Hz, 2H), 7.02 (d, *J* = 7.6 Hz, 4H), 6.93 (d, *J* = 8.6 Hz, 4H), 4.04 (s, 4H), 3.83 (s, 6H); ^{13}C NMR (100 MHz, $CDCl_3$) δ 159.6, 156.3, 141.4, 140.8, 132.9, 131.9, 130.7, 128.8, 128.6, 126.2, 113.6, 55.4, 38.4; IR (neat) ν_{max} 3015, 2970, 1609, 1511, 1434, 1294, 1175, 1031, 839 cm^{-1}; HRMS (ESI^+) *m/z* calculated for $C_{33}H_{29}NO_2$ $[M+H]^+$: 472.2271, found 472.2264 (Δ –1.6 ppm).

3.5 References

1. Baumann, M.; Baxendale, I. R.; Ley, S. V.; Nikbin, N. *Beilstein J. Org. Chem.* **2011**, *7*, 442–495.
2. Alford, P. E. *Prog. Heterocycl. Chem.* **2011**, *23*, 329–369.
3. Guillena, G.; Ramón, D. J.; Yus, M. *Angew. Chem. Int. Ed.* **2007**, *46*, 2358–2364.
4. Guerbet, M. *C.R. Acad. Sci. Paris* **1899**, *128*, 5.
5. Carlini, C.; Di Girolamo, M.; Macinai, A.; Marchionna, M.; Noviello, M.; Galletti, A.; Sbrana, G. *J. Mol. Catal. A: Chem.* **2003**, *200*, 137–146.
6. Matsu-ura, T.; Sakaguchi, S.; Obora, Y.; Ishii, Y. *J. Org. Chem.* **2006**, *71*, 8306–8308.
7. Grigg, R.; Mitchell, T. R. B.; Sutthivaiyakit, S. *Tetrahedron* **1981**, *37*, 4313–4319.
8. Grigg, R.; Mitchell, T.; Sutthivaiyakit, S.; Tongpenyai, N. *J. Chem. Soc., Chem. Commun.* **1981**, 611–612.
9. Grigg, R.; Mitchell, T. R.; Sutthivaiyakit, S. *Tetrahedron Lett.* **1979**, *20*, 1067–1068.
10. Watanabe, Y.; Tsuji, Y.; Ige, H.; Ohsugi, Y.; Ohta, T. *J. Org. Chem.* **1984**, *49*, 3359–3363.
11. Motokura, K.; Nishimura, D.; Mori, K.; Mizugaki, T.; Ebitani, K.; Kaneda, K. *J. Am. Chem. Soc.* **2004**, *126*, 5662–5663.
12. Slatford, P. A.; Whittlesey, M. K.; Williams, J. M. J. *Tetrahedron Lett.* **2006**, *47*, 6787–6789.
13. Löfberg, C.; Grigg, R.; Whittaker, M. A.; Keep, A.; Derrick, A. *J. Org. Chem.* **2006**, *71*, 8023–8027.
14. Buil, M. L.; Esteruelas, M. A.; Herrero, J.; Izquierdo, S.; Pastor, I. M.; Yus, M. *ACS Catal.* **2013**, *3*, 2072–2075.
15. Bower, J. F.; Skucas, E.; Patman, R. L.; Krische, M. J. *J. Am. Chem. Soc.* **2007**, *129*, 15134–15135.
16. Cho, C. S.; Kim, B. T.; Kim, T.-J.; Shim, S. C. *J. Org. Chem.* **2001**, *66*, 9020–9022.
17. Cho, C. S.; Kim, B. T.; Kim, T.-J.; Chul Shim, S. *Tetrahedron Lett.* **2002**, *43*, 7987–7989.
18. Cho, C. S. *J. Mol. Catal. A: Chem.* **2005**, *240*, 55–60.
19. Martínez, R.; Ramón, D. J.; Yus, M. *Tetrahedron* **2006**, *62*, 8988–9001.
20. Martínez, R.; Brand, G. J.; Ramón, D. J.; Yus, M. *Tetrahedron Lett.* **2005**, *46*, 3683–3686.
21. Kwon, M. S.; Kim, N.; Seo, S. H.; Park, I. S.; Cheedrala, R. K.; Park, J. *Angew. Chem. Int. Ed.* **2005**, *44*, 6913–6915.
22. Yamada, Y. M. A.; Uozumi, Y. *Org. Lett.* **2006**, *8*, 1375–1378.

23. Taguchi, K.; Nakagawa, H.; Hirabayashi, T.; Sakaguchi, S.; Ishii, Y. *J. Am. Chem. Soc.* **2004**, *126*, 72–73.

24. Palo, D. R.; Dagle, R. A.; Holladay, J. D. *Chem. Rev.* **2007**, *107*, 3992–4021.

25. Maitlis, P. M.; Haynes, A.; Sunley, G. J.; Howard, M. J. *J. Chem. Soc., Dalton Trans.* **1996**, 2187–2196.

26. Moran, J.; Preetz, A.; Mesch, R. A.; Krische, M. J. *Nat. Chem.* **2011**, *3*, 287–290.

27. Nielsen, M.; Alberico, E.; Baumann, W.; Drexler, H.-J.; Junge, H.; Gladiali, S.; Beller, M. *Nature* **2013**, *495*, 85–89.

28. Langer, R.; Fuchs, I.; Vogt, M.; Balaraman, E.; Diskin-Posner, Y.; Shimon, L. J. W.; Ben-David, Y.; Milstein, D. *Chem. Eur. J.* **2013**, *19*, 3407–3414.

29. Gunanathan, C.; Milstein, D. *Acc. Chem. Res.* **2011**, *44*, 588–602.

30. Rodríguez-Lugo, R. E.; Trincado, M.; Vogt, M.; Tewes, F.; Santiso-Quinones, G.; Grützmacher, H. *Nat. Chem.* **2013**, *5*, 342–347.

31. Del Zotto, A.; Baratta, W.; Sandri, M.; Verardo, G.; Rigo, P. *Eur. J. Inorg. Chem.* **2004**, 524–529.

32. Li, F.; Xie, J.; Shan, H.; Sun, C.; Chen, L. *RSC Adv.* **2012**, *2*, 8645–8652.

33. Ortega, N.; Richter, C.; Glorius, F. *Org. Lett.* **2013**, *15*, 1776–1779.

34. Grigg, R.; Mitchell, T. R. B.; Sutthivaiyakit, S.; Tongpenyai, N. *Tetrahedron Lett.* **1981**, *22*, 4107–4110.

35. Motokura, K.; Fujita, N.; Mori, K.; Mizugaki, T.; Ebitani, K.; Jitsukawa, K.; Kaneda, K. *Chem. Eur. J.* **2006**, *12*, 8228–8239.

36. Chan, L. K.; Poole, D. L.; Shen, D.; Healy, M. P.; Donohoe, T. J. *Angew. Chem. Int. Ed.* **2014**, *53*, 761–765.

37. Ogawa, S.; Obora, Y. *Chem. Commun.* **2014**, *50*, 2491–2493.

38. Gabrielsson, A.; van Leeuwen, P.; Kaim, W. *Chem. Commun.* **2006**, 4926–4927.

39. Jiang, B.; Feng, Y.; Ison, E. A. *J. Am. Chem. Soc.* **2008**, *130*, 14462–14464.

40. Iwashita, Y.; Hayata, A. *J. Am. Chem. Soc.* **1969**, *91*, 2525–2528.

41. Lee, E. Y.; Kim, Y.; Lee, J. S.; Park, J. *Eur. J. Org. Chem.* **2009**, *2009*, 2943–2946.

42. Hall, M. I.; Pridmore, S. J.; Williams, J. *Adv. Synth. Catal.* **2008**, *350*, 1975–1978.

43. Owston, N. A.; Parker, A. J.; Williams, J. M. J. *Chem. Commun.* **2008**, 624–625.

44. Sun, C.; Zou, X.; Li, F. *Chem. Eur. J.* **2013**, *19*, 14030–14033.

45. Bell, T. W.; Rothenberger, S. D. *Tetrahedron Lett.* **1987**, *28*, 4817–4820.

46. Boivin, J.; Carpentier, F.; Jrad, R. *Synthesis* **2006**, 1664–1672.

47. Gill, N. S.; James, K. B.; Lions, F.; Potts, K. T. *J. Am. Chem. Soc.* **1952**, *74*,

4923–4928.

48. Sielemann, D.; Keuper, R.; Risch, N. *J. Prakt. Chem.* **1999**, *341*, 487–491.

49. Shen, D.; Poole, D. L.; Shotton, C. C.; Kornahrens, A. F.; Healy, M. P.; Donohoe, T. J. *Angew. Chem. Int. Ed.* **2015**, *54*, 1642–1645.

50. Frost, J. R.; Cheong, C. B.; Akhtar, W. M.; Caputo, D. F. J.; Stevenson, N. G.; Donohoe, T. J. *J. Am. Chem. Soc.* **2015**, *137*, 15664–15667.

51. Kaiser, S.; Smidt, S. P.; Pfaltz, A. *Angew. Chem. Int. Ed.* **2006**, *45*, 5194.

Chapter 4

Activated benzothiadiazin-3-one 1,1-dioxides and benzoxathiazin-3-one 1,1-dioxides targeting serine hydrolase inhibition

4.1 Introduction

Harnessing the power of chemistry towards biologically relevant discovery is the backbone of modern, interesting and successful programs within the field of organic chemistry. Herein, I disclose the initial work on a powerful chemical design to develop a new class of serine hydrolase inhibitors.

4.1.1 Introduction to serine hydrolases

Serine hydrolases are exciting and important targets in the post-genomic era. This family of enzymes consists of more than 1% of predicted proteins, making it one of the largest and most diverse classes of mammalian enzyme families.[1-7] Additionally, serine hydrolases play important roles in both physiological and pathophysiological processes.[8,9] The more than 200 human serine hydrolases include lipases, peptidases, esterases, thioesterases, and amidases that hydrolyze esters and amides found in small molecules, signaling lipids, peptides or post-translational ester and thioester protein modifications. Importantly, a large percentage of the serine hydrolases remain uncharacterized or unannotated, lacking a known role or endogenous substrate, and many more lack specific inhibitors.

An established program in the Boger group has focused on the serine hydrolase fatty acid amide hydrolase (FAAH). The discovery of FAAH, its endogenous substrates, its biological role, and the use of potent and selective FAAH inhibitors exemplify the potential of investigating serine hydrolases. FAAH was discovered along with its endogenous substrates, oleamide (**4.1**) and anandamide (**4.2**) (Figure 4-1) and is known to degrade these neuromodulatory fatty acid amides (through hydrolysis to acids **4.3** and **4.4**, respectively) at their site of action, thus controlling the intensity and duration of their effects. FAAH has been validated as a therapeutic target for the treatment of a wide range of disorders including pain, inflammation, and sleep disorders.[1,10-13]

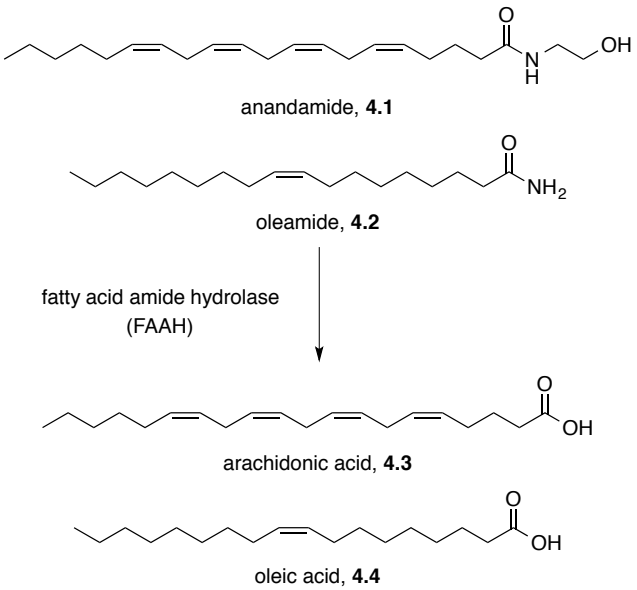

Figure 4-1. Two endogenous fatty acid amide substrates hydrolyzed by FAAH

The mechanism of serine hydrolase activity is derived from the key serine nucleophile in the conserved active site catalytic triads of each member of the family. The active site usually also contains acidic (aspartate/glutamate) and basic (histidine/lysine) residues that take part in the enzymatic hydrolysis process via proton relay. FAAH contains a Ser241–Ser217–Lys142 catalytic triad that upon nucleophilic attack of Ser241 on the carbonyl of the substrate anandamide generates a tetrahedral intermediate (**4.5**, Figure 4-2). Collapse of the intermediate yields ethanolamine (**4.6**) and the enzyme-bound arachidonoyl-intermediate **4.7**. Lys142 acts as a general base-general acid and serves to deprotonate Ser241 and protonate the leaving group during this process. The enzyme-substrate bond is hydrolyzed in a water-mediated deacylation to release the product carboxylic acid (**4.3**) with simultaneous regeneration of the enzyme.

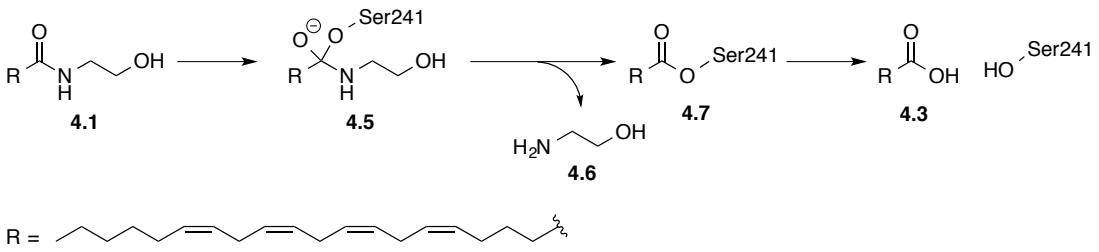

Figure 4-2. Mechanism of action of FAAH on endogenous substrate anandamide (**4.1**)

A similar mechanism is preserved by all serine hydrolases and informs the search for probes and selective inhibitors for this class of enzymes.

4.1.2 Covalent serine hydrolase inhibitors

Early studies identified the endogenous, sleep-inducing molecule 2-octyl α-bromoacetoacetate (**4.8**) as a potent, reversible FAAH inhibitor (K_i = 0.8 μM)[1,3,14,15] (Figure 4-3). Subsequent successful inhibitors designed to target this family of enzymes incorporated an electrophilic carbonyl, with notable exceptions including fluorophosphonates and sulfonyl fluorides,[8,16-22] to harness the serine-mediated mechanism through covalent modification of the active site.[15,23-29]

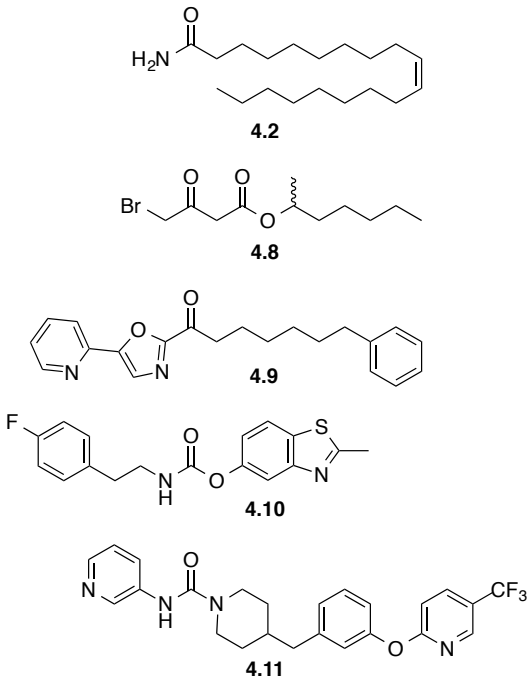

Figure 4-3. Inhibitors of FAAH (with reactive carbonyl moeities aligned with that of endogenous FAAH substrate oleamide **4.2**, included for comparison)

Library synthesis and substrate-based design have produced inhibitors with therapeutic potential including selective, reversible and irreversible covalent inhibitors, with most FAAH inhibitors falling into two generalized mechanistic classes. The first is a class of α-ketoheterocycle-based inhibitors[30-35] (e.g. **4.9**, Figure 4-3), which form a reversible hemiketal with the active site catalytic serine.[36-38] The libraries of α-ketoheterocycle inhibitors include nearly a thousand examples and have resulted in inhibitors for FAAH including OL-135 (**4.9**), extraordinarily selective over other serine hydrolases. They have also been shown to be efficacious analgesics in vivo.[5,6,39-45]

The second class is that of activated carbamates[2,8,17,46,47] (such as **4.10**) and ureas[1,3-7,48,49] (such as **4.11**), which form a carbonate or carbamate, respectively, upon reaction with the active site serine. These acylation products are more difficult to hydrolyze (carbamate > carbonate >> ester) and typically lead to irreversible acylation. This class of FAAH inhibitors includes potent inhibitors such as WWL65[8,35,50] (**4.10**, IC_{50} = 0.008 μM) and PF-3845[1,28,33] (**4.11**, K_i = 0.23 μM). High selectivity has been achieved for some irreversible urea and carbamate inhibitors; however, the more promiscuous inhibition displayed by others in this class can complicate their development as drug candidates. However, such potent and less selective inhibition provides the opportunity for developing exploratory probes for examining and identifying unannotated serine hydrolases.

Small molecule libraries have been prepared that include compounds incorporating an electrophilic carbonyl including ureas[1,3,15,51] and carbamates,[8,17,33] as well as others not covered herein including activated trifluoromethyl ketones,[23,24,26,28,52] lactones,[30,53] lactams[36,54] and others,[39-41,55] which also act through covalent modification of the serine nucleophile. The success of the FAAH inhibitor classes is exemplified in

identification and pursuit of potential new therapeutics, some of which are currently undergoing clinical trials.[56,57] Additionally, inhibitors of other serine hydrolases have been developed and approved to treat obesity, diabetes, microbial infections and Alzheimer's disease.[58]

The successful program that created such potent inhibitors for FAAH is indicative of the success that novel chemotypes can have in the development of new covalent serine hydrolase inhibitors. Library synthesis and inhibitor identification has been applied to many members of the serine hydrolase family. In addition to therapeutics, these tools have contributed greatly to a biological understanding of the role of unannotated serine hydrolases, with many more still remaining to be elucidated.

4.1.3 Activity-based protein profiling

The use of activity-based protein profiling (ABPP)[48,49,59,60] paired with such exquisitely designed inhibitor classes has allowed the rapid analysis of target serine hydrolases and monitoring of enzyme activity in complex systems. ABPP offers a distinct set of chemical tools with probes developed for many specific enzyme classes, such as fluorophosphonate-rhodamine[35,50] for selective serine hydrolase labeling. Thus, rapid identification of inhibitor targets, assessment and optimization of inhibitor selectivity, and functional assignment of uncharacterized enzymes[28,33,54] can occur without recombinant enzyme expression, purification of protein and the development of specific substrate assays, as required by traditional methods of inhibitor examination. This method was first exemplified in the expedited development of **4.9**,[51,62] an exceptional inhibitor which selectively (>100-fold) and potently ($K_i < 4$ nM) inhibits FAAH. OL-135 exhibited in vivo efficacy[33,63] and was used to validate FAAH as a new therapeutic target for the treatment of pain.

ABPP permits the discovery of new inhibitors and evaluation of compound libraries through rapid and comprehensive, proteome-wide screening of enzymes in a variety of states, including in vitro and in vivo,[52,64] and simultaneously probes the potency and selectivity of any discovered inhibitor. The assessment of all potential competitive enzymes is conducted without expressed or purified enzymes, without a competitive substrate and without inhibitor modifications such as a click tag or appended fluorophore. The relative potency for competitive enzymes can be quantified, even for hydrolases lacking known substrates or function, permitting the design and examination of novel chemical groups to harness different reactivity and inhibit new targets in the serine hydrolase family.

4.1.4 A new serine hydrolase-targeted chemotype

In order to explore new chemotypes and discover new targets accessible through chemical interrogation, a new irreversible inhibitor class was required that would exhibit high specificity for a particular serine hydrolase. The body of work on irreversible inhibitors of serine, cysteine and threonine proteases provides inspiration.[53,65] Specifically, tethered reactive moieties that acylate, phosphonylate, and sulfonylate the serine in the active site were of particular interest (Figure 4-4). The saccharin family of serine protease inhibitors (**4.12**) is described here as a model of tethered sulfonamide-containing inhibitors that provides a related examples to our novel serine protease inhibitor design.

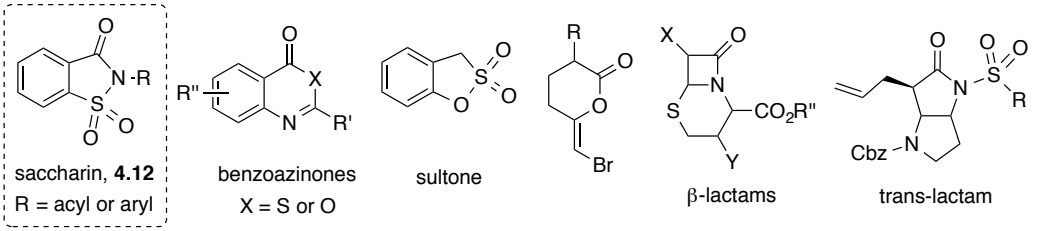

Figure 4-4. Irreversible inhibitors of proteases with tethered electrophiles

This family of 1,2-benzisothiazol-3-one 1,1-dioxides were designed and tested for their activity against serine proteases such as human leukocyte elastase (HLE)[54] and human mast cell tryptase[55] that act through acylation of the nucleophilic serine active site residue. The mechanism of action involves attack on the activated amide bond of the heterocyclic ring of **4.12** (Figure 4-5) by the active site serine, which upon collapse of the tetrahedral intermediate **4.13** forms an acyl enzyme intermediate in the form of an ester **4.14**, with concurrent release of the sulfonamide moiety as the leaving group (Figure 4-5a). This mechanism is supported by labeling studies showing preference for attack at the amide carbonyl over the sulfonamide.[58] The side chain (R) was originally designed as an acyl or aryl group (**4.12a**), and early *N*-arylsaccharins such as **4.15** inhibit HLE with IC_{50} values on the order of 1 μM[62] while *N*-furoyl saccharin was found to be affective at preventing the development of experimental emphysema in vivo.[59,60] Further studies led to the discovery of suicide inhibitors[58,61] with the general structure **4.12b** and with a leaving group (LG) that can participate in the inhibition mechanism. This is proposed to occur through a second addition of a nucleophilic residue to intermediates such as **4.16**, forming cross-linked acyl enzyme derivatives (**4.17**). This class has produced potent inhibitors such as 4-isopropyl-6-methoxybenzisothiazolone derivatives (e.g. **4.18**) that show potent HLE inhibition (K_i = 14 pM) and increased human blood stability ($t_{1/2}$ = 110 min).[54]

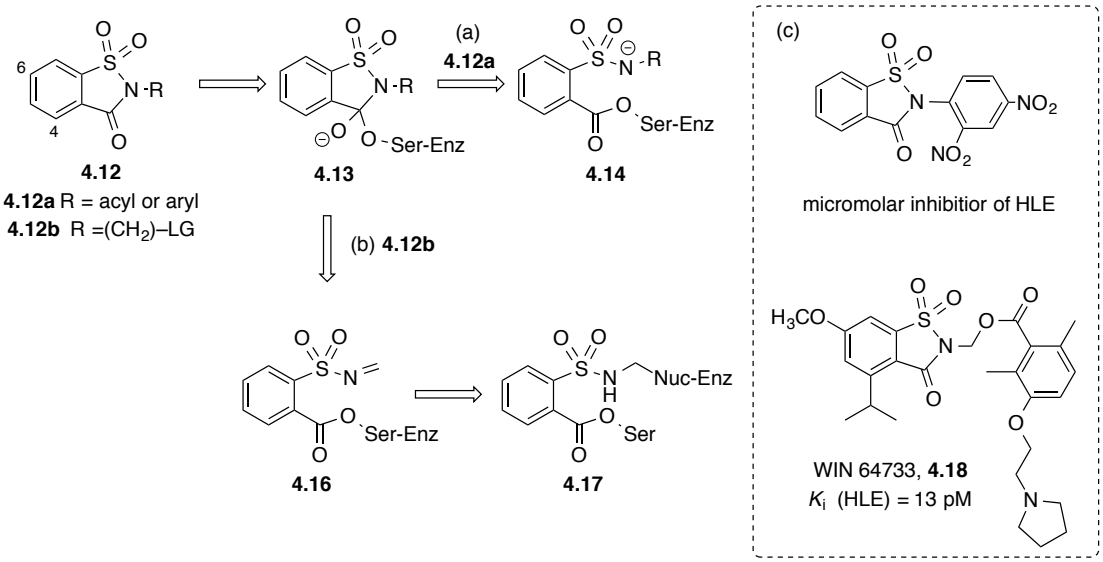

Figure 4-5. Saccharin inhibitors and mechanism of action for (a) acyl or aryl saccharins and (b) suicide saccharins; (c) a representative example of both classes of saccharin inhibitors[54, 62]

Structure-activity relationship (SAR) studies have shown that the potency and stability of saccharin derivatives depend on the leaving group R, with **4.12a** requiring strongly electron-withdrawing acyl groups. Similarly, the activity of the enzyme-activated inhibitors **4.12b** shows a strong dependence on the electronic features of the leaving group. The choice of C-4 and C-6 substitution of the aromatic ring (numbering shown in Figure 4-5) was shown to affect activity through interaction with the recognition pocket of serine hydrolases (for C-4 substitution) and through influence of the inactivation rate, reactivation rate, hydrogen-bonding effects and in vivo stability (for C-6 substitution).[62]

Limitations of saccharin inhibitors include the structural and synthetic constraints as indicated by the SAR results. The potency and irreversibility of potent inhibitors have relied heavily on the use of a leaving group moiety which is enzyme activated. This limits the modulation of potency and recognition elements that can be incorporated. Additionally, the acyl bond formed with simpler acyl- or aryl-saccharins

yields a serine ester, which is more susceptible to deacylation than the carbonates and carbamates formed with carbamate and urea inhibitors (see Section 4.1.2).

The potential to design and examine a new chemotype and scaffold for serine hydrolyse inhibition is the focus of the project described herein. The established program investigating FAAH inhibition in the Boger group, the use of ABPP methods and the inspiration of the saccharin family of inhibitors enabled the pursuit of a novel class of activated carbamate- and urea-containing inhibitors.

4.2 Results and Discussion

The proposed inhibitor scaffold pursued is a modification of the saccharin parent ring system with an α-insertion of a heteroatom (O, N) adjacent to the carbonyl (**4.19**, Figure 4-6). The mechanism of inhibition proposed is initiated by nucleophilic attack of an active site serine on the inhibitor carbonyl (Figure 4-6). Collapse of the tetrahedral intermediate **4.20** and release of the leaving group sulfonamide provides a covalently bound inhibitor **4.21**. The scaffold design provides the formation of a carbamate or carbonate bond, depending on the choice of heteroatom (X). This increases the stability of this enzyme-inhibitor complex by and increases the time until enzyme recovery through hydrolysis.

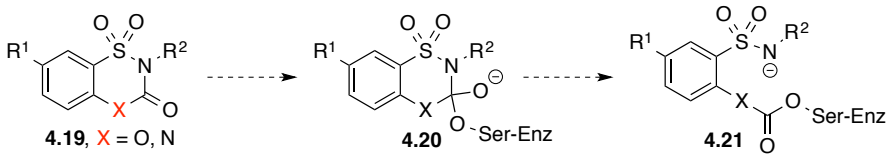

Figure 4-6. Inspired new scaffold with electrophilic carbamate and urea moieties

The proposed synthesis (Figure 4-7) relies on a known one-pot addition and cyclization of anilines and phenols (**4.23**) with chlorosulfonyl isocyanate (**4.24**)[63] to produce unsubstituted benzoxathiazin-3-one 1,1-dioxides (**4.22**, X = O) or benzothiadiazin-3-one 1,1-dioxides (**4.22**, X = NH) poised for *N*-alkylation. This would allow facile electronic tuning of the reactivity and introduction of active site recognition and binding features through substitution of the aromatic ring (R^1) and side chain *N*-alkylation (R^2) introduction. A range of R^1 substituents at position 7 on the aromatic ring would allow examination and modulation of electronic effects on the reactivity of the carbonyl. The easily modified R^2 moiety would allow incorporation of specific structural features to enable more selective enzyme active site targeting.

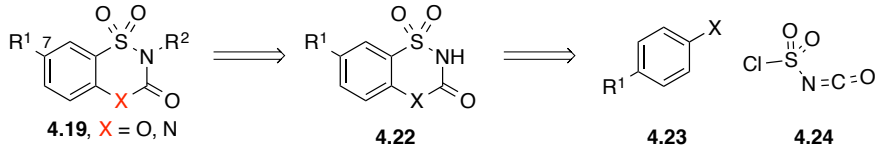

R^1 = screen for effect on carbonyl reactivity; OCH_3, H, and CN targeted
R^2 = side chain to allow enzyme specificity; H, Bn and $(CH_2)_5Ph$ targeted

Figure 4-7. Synthetic design to access the desired inhibitor class

The inclusion of a side chain similar to that found in OL-135 ($R^2 = (CH_2)_5Ph$) was proposed to allow validation of the new chemotype by initial screening for FAAH inhibition. Proteome-wide evaluation by gel-based ABPP would subsequently allow the identification of new and uncharacterized targets with the full inhibitors, whereas the core structures (R^2 = H) would allow fragment-based screening and analysis of the broader promiscuity of the scaffold. The scaffold provides a template that may be easily expanded. Gel-based ABPP will allow rapid screening and subsequent lead optimization to determine selective serine hydrolase inhibition and broad trends across serine hydrolase and other enzyme classes.

4.2.1 First-generation scaffold: benzothiadiazin-3-one 1,1-dioxides

Benzothiadiazin-3-one 1,1-dioxides (**4.19**, X = NH) were targeted first as an easy, two-step synthesis was known for similar compounds and would allow access to the desired set of potential inhibitors quickly and efficiently.[64] Interestingly, a select number of benzothiadiazin-3-one 1,1-dioxide core compounds and substituted derivatives have exhibited biological activity including hypoglycemic (**4.25**)[65] and sedative (**4.27**).[66] Additional family members have been demonstrated as HIV replication inhibitors (**4.26** and **4.28**)[67,68] as well as fusion inhibitors for respiratory syncytial virus (RSV) (**4.29**, Figure 4-8).[69]

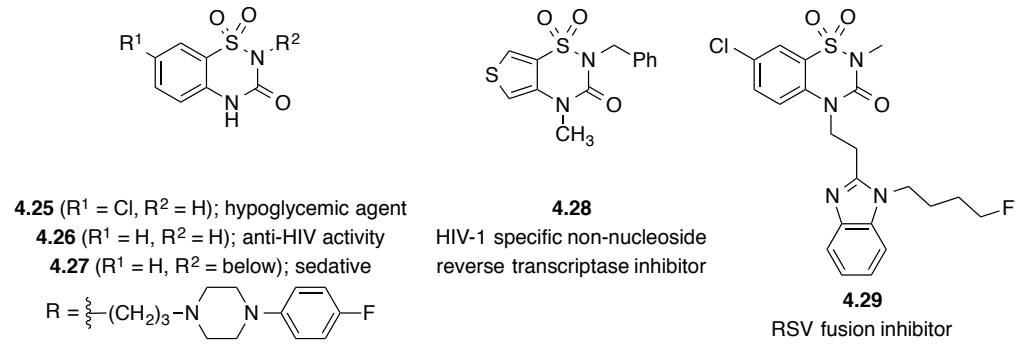

4.25 (R^1 = Cl, R^2 = H); hypoglycemic agent
4.26 (R^1 = H, R^2 = H); anti-HIV activity
4.27 (R^1 = H, R^2 = below); sedative

4.28
HIV-1 specific non-nucleoside reverse transcriptase inhibitor

4.29
RSV fusion inhibitor

Figure 4-8. Precedented benzothiadiazin-3-one 1,1-dioxides which displayed biological activity

The substitution on the aromatic ring proposed (R^1 = OCH_3, H, CN) was included to determine the electronic impact of the *p*-substituent on the intrinsic reactivity of the candidate inhibitors. The use of reported synthetic methods with chlorosulfonyl isocyanate and $AlCl_3$ gave promising results with electron-rich anilines **4.30** and **4.31**, forming **4.35** and **4.36**, respectively, in good yields (Scheme 4-1). The same method failed when using 4-aminobenzonitrile (**4.32**). Instead, after successful amine addition to the isocyanate to form intermediate **4.34** (R^1 = CN), attempts to promote electrophilic aromatic substitution led only to isolation of the 4-cyanophenylurea (**4.39**) despite a screen of Lewis acids (LA), temperatures, and solvents. The successful application of the method to *p*-bromoaniline (**4.33**) and formation of the 7-bromo benzothiadiazin-3-one 1,1-dioxide core **4.37** allowed the exploration of a cyanation reaction for the preparation of **4.38** from **4.37**. A variety of conditions were screened, and the use of non-toxic potassium ferrocyanide with catalytic copper iodide[70] was found to produce **4.38** in 69% yield (Scheme 4-1). Evidence of a small amount of **4.37** indicated less than full conversion and unfortunately proved to be inseparable from the desired product.

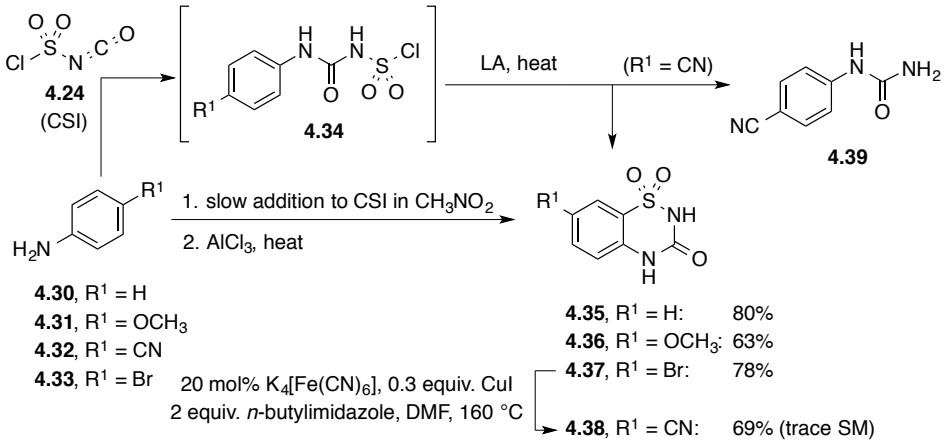

Scheme 4-1. Synthetic access to benzothiadiazin-3-one 1,1-dioxides cores (showing the intermediate formed in the reaction, **4.34**, and the byproduct formed from *p*-cyanoaniline, **4.39**)

The four core urea-containing scaffolds were then subjected to *N*-alkylation to incorporate varied R^2 substituents (Figure 4-9a). Preliminary experiments with the simplest scaffold **4.35** (R^1 = H), with use of NaH and benzyl bromide, yielded a mixture of two products (**4.40A** and **4.40B**) that were separable by flash column chromatography and yet gave identical masses by LCMS. The presumed products were the *O*- and *N*-benzyl products. The ^{1}H and ^{13}C NMR chemical shifts for the benzylic CH_2 revealed small differences. The faster eluting compound exhibited signals at δ_H 4.98 (C$\underline{H}_2$) and δ_C 44.0 ($\underline{C}H_2$) and the slower eluting compound showed signals at δ_H 5.37 (C$\underline{H}_2$) and δ_C 70.2 ($\underline{C}H_2$), suggesting *N*-benzylation and *O*-benzylation (with increased deshielding from O vs N). Ultimately, single crystal X-ray structures confirmed these assignments (**4.40A** and **4.40B**, Figure 4-9b).

a)

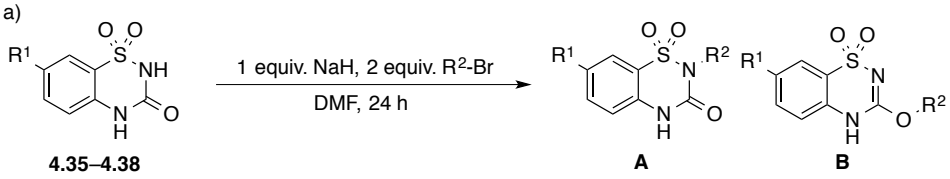

4.35–4.38 A B

starting material	product	R^2 = Bn R^1 =	isolated yield A	B	product	R^2 = $(CH_2)_5Ph$ R^1 =	isolated yield RSM	A	B
4.35	**4.40**	H	52%	22%	**4.44**	H	40%	31%	9%
4.36	**4.41**	OCH_3	54%	19%	**4.45**	OCH_3	46%	20%	10%
4.37	**4.42**	Br	64%	20%	**4.46**	Br	35%	23%	10%
4.38	**4.43**	CN	47%[a]	14%	**4.47**	CN	70%	3%	n/o

[a]**4.43A** isolated with trace amounts of **4.42B**

b)

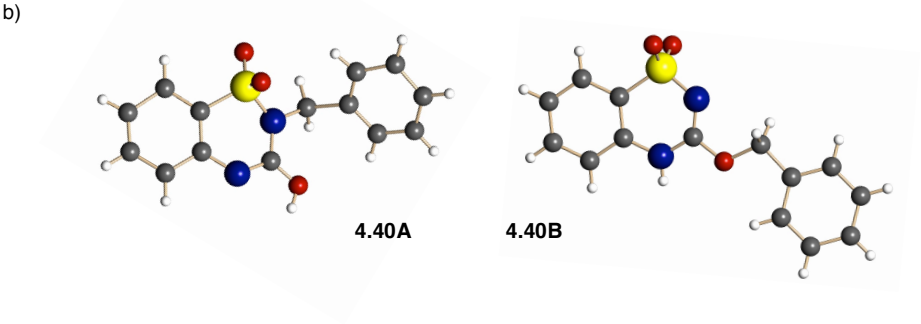

Figure 4-9. (a) Alkylation of benzothiadiazin-3-one 1,1-dioxides cores and (b) X-ray structures of **4.40A** and **4.40B** showing *N*- and *O*-benzylation, respectively

The application of this method to **4.36** and **4.37** proceeded smoothly to give **4.41A** and **4.42A** in 54% and 64% yield, with **4.41B** and **4.42B** also isolated (Figure 4-9). The reaction of **4.38** gave **4.43A** in 47% yield, but this desired product was isolated along with the *O*-benzylated 7-bromo substrate **4.42B**. Preparative HPLC provided a pure sample of **4.43A** for testing. The synthesis was also easily applied to access the second desired R^2 series using NaH and 5-phenyl-1-bromopentane to yield **4.44A**–**4.47A**, albeit in lower yields due to lower overall conversion (Figure 4-9).

4.2.2 Biological evaluation of the first-generation scaffold

Access to the nine originally targeted potential inhibitors along with three additional 7-bromo substituted compounds (summarized in Figure 4-10a) permitted examination of these benzothiadiazin-3-one 1,1-dioxides for inhibition of the enzymatic activity of purified FAAH[14] (Figure 4-10b, assay performed by Dan Brody). The unsubstituted scaffolds showed no activity (K_i > 100 μM) and the only

benzyl benzothiadiazin-3-one 1,1-dioxides to show activity were those with the more electron-withdrawing R^1 substitution (**4.42A** and **4.43A**). For the pentylphenyl series, the compounds exhibited the expected electronic effect, albeit with low activity overall. Despite this, the increasingly electron-withdrawing substituents did show greater potency (**4.46A** and **4.47A** compared to **4.44A** and **4.45A**). The most potent inhibitor (**4.46A**) was subjected to the FAAH assay with variation of the inhibitor incubation time (0, 3 and 6 h), which did not increase the inhibition potency and is characteristic of reversible enzyme inhibition.

Additionally, the full library was incubated with brain membrane and soluble proteome and labeled with IA-rhodamine or FP-rhodamine (Fig. 4-10c–d) to examine cysteine and serine hydrolase inhibition. The former gel examination indicated that there was some reactivity of our potential inhibitors with cysteine containing enzymes. Further investigations (performed by Keriann Backus) by competetive isoTOP-ABPP[71] showed no appreciable competition of iodoacetamide alkyne labeling, indicative of minimal global cysteine reactivity. The reactivity with lysine-containing enzymes was also explored through use of a KiNativ™ kit (Appendix 2), yet ultimately none of the above gel-based ABPP studies showed clear targets. Reactivity profiling of this series showed >24 h stability of the urea moiety in methanol, DMSO and organic solvents as well as weakly acidic and basic aqueous media, indicating a lack of hydrolytic reactivity of the carbonyl. These results encouraged the further examination of additional inhibitors, with the second-generation benzoxathiazin-3-one 1,1-dioxides (**4.19**, X = O) targeted next.

a)

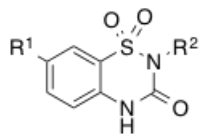

b)

compound	R^1	R^2	K_i[a]
4.36	OCH_3	H	no activity[b]
4.35	H	H	no activity
4.37	Br	H	no activity
4.38	CN	H	no activity
4.41A	OCH_3	Bn	no activity
4.40A	H	Bn	no activity
4.42A	Br	Bn	80 ± 1 μM
4.43A	CN	Bn	57.5 ± 0.7 μM
4.45A	OCH_3	$(CH_2)_5Ph$	71 ± 1 μM
4.44A	H	$(CH_2)_5Ph$	47.8 ± 0.5 μM
4.46A[c]	Br	$(CH_2)_5Ph$	29.3 ± 0.7 μM
4.47A	CN	$(CH_2)_5Ph$	45 ± 6 μM

[a]preincubation = 0 h; [b]No activity defined as K_i >100 μM; [c]Also run at 3 h and 6 h preincubation to give 47.1 ± 0.5 μM and 82.1 ± 0.1 μM

c)

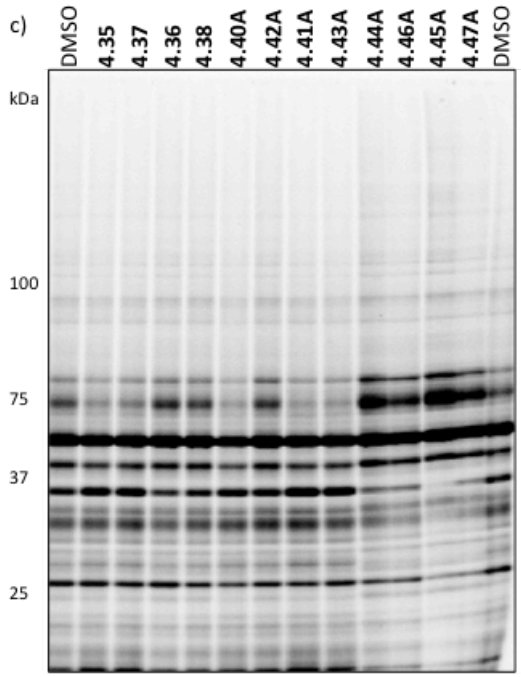

d)

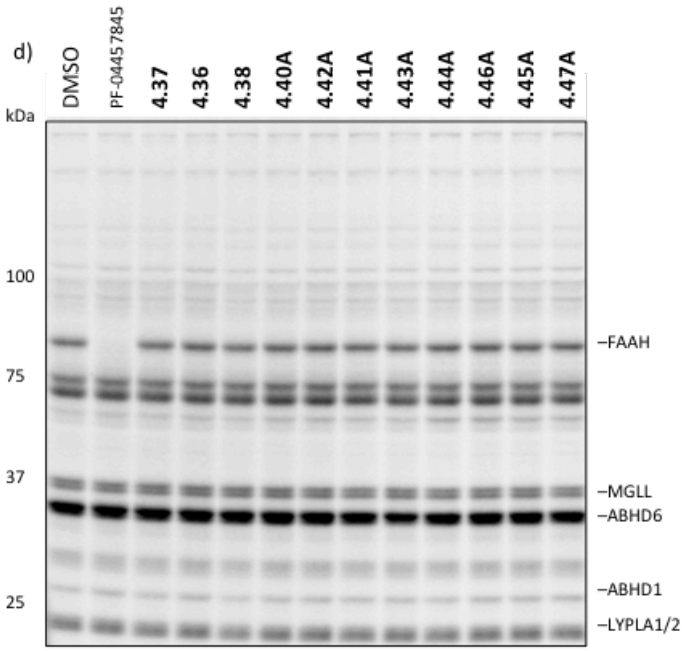

Figure 4-10. a) Structure of synthesized potential inhibitors; b) FAAH inhibition activity of benzothiadiazin-3-one 1,1-dioxides; c) Competitive gel-based ABPP of benzothiadiazin-3-one 1,1-dioxides. Mouse brain soluble proteomes were treated with known FAAH inhibitor (PF-04457845) and compounds (20 μM, 30 min incubation) then IA-rhodamine (2 μM, 1 h). Fluorescent images shown in gray scale; d) Competitive gel-based ABPP as in (c) with brain membrane proteome samples and FP-rhodamine (1 μM, 0.5 h)

4.2.3 Second-generation scaffold: benzoxathiazin-3-one 1,1-dioxides

The benzoxathiazin-3-one 1,1-dioxide core (**4.19**, X = O) has only one synthetic example reported in literature using chlorosulfonyl isocyanate and this is

with the substrate *p*-cresol ($R^1 = CH_3$).[72a] There are very limited examples of any substituted derivatives ($R^2 \neq H$) or the examination of biological activity of any of the benzoxathiazin-3-one 1,1-dioxides.[72]

p-Bromophenol (**4.48**) was chosen as a model substrate for initial studies of this route. In the reported synthesis, the benzoxathiazin-3-one 1,1-dioxide product of *p*-cresol was isolated as a byproduct during targeted sulfonylisocyanate formation. Attempts to repeat the synthesis on **4.48** were unsuccessful (Scheme 4-2a) yielding only recovered starting material, 4-bromophenyl carbamate (**4.49**) and 4-bromophenyl sulfamate (**4.50**), the product of nucleophilic addition to the sulfonyl chloride instead of the isocyanate of CSI. Isolation of sulfamoyl chloride intermediate **4.51** (Scheme 4-2b) allowed resubjection of this intermediate to a variety of reaction conditions and Lewis acids to form desired product **4.52**, yet only the byproduct **4.49** was observed. This indicated that the desired cyclization of **4.51** through electrophilic aromatic substitution of the aromatic ring with the sulfamoyl chloride was not occurring in this system.

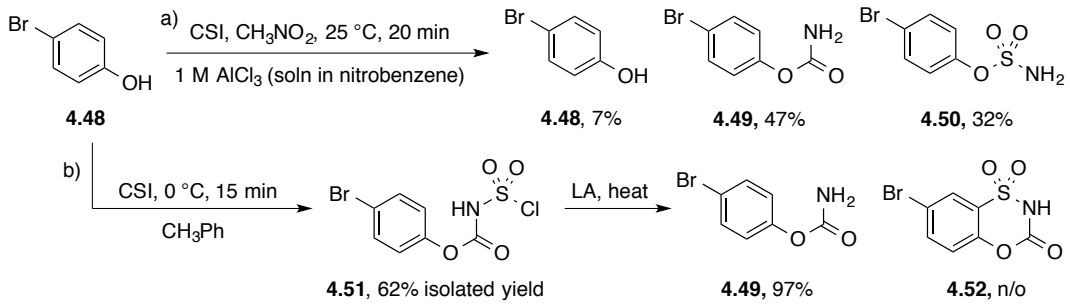

Scheme 4-2. Attempted synthesis of benzoxathiazin-3-one 1,1-dioxides (using CSI)

A stepwise approach to form **4.52** via 2-hydroxybenzenesulfonamide **4.56** was pursued (Scheme 4-3). The penultimate intermediate **4.56** was successfully formed in three steps from *p*-bromoanisole (**4.53**), as the chlorosulfonylation of (**4.48**) failed to

give clean product with 68% overall yield. The final cyclization step was attempted with triphosgene, phosgene and 4-nitrobenzoyl chloride yet did not lead to product **4.52** under any conditions examined. The highly polar, acidic, and reactive nature of the product led us to examine an alternative route that provides intermediates with increased organic solubility and decreased water solubility.

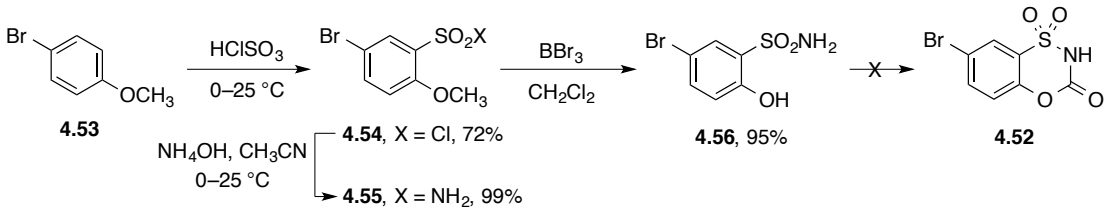

Scheme 4-3. Attempted stepwise synthesis of benzoxathiazin-3-one 1,1-dioxide core

Alkylation of **4.55**, with a methyl ether serving as a phenol protecting group to prevent *O*-alkylation, proceeded to give benzylated precursor **4.57** in 31% yield (Scheme 4-4a). The reaction was low yielding with recovered starting material and dialkylated product accounting for the remaining materials, but allowed material to be subjected to protecting group deprotection with boron tribromide to yield **4.59** in 92% yield (Scheme 4-4a). Formation of benzoxathiazin-3-one 1,1-dioxide was successful utilizing phosgene and NaH to yield **4.63** in 89% yield (Scheme 4-4b). This indicated the potential of this route to form alkylated benzoxathiazin-3-one 1,1-dioxides and was applied to the additional desired alkylation product (R^2 = $(CH_2)_5Ph$), which proceeded even more smoothly to form **4.64** in 42% over 3 steps (Scheme 4-4). Application of the route to the other substituents was straightforward, with hydrogenation of 7-bromo compounds **4.59** and **4.60** proceeding smoothly to yield the unsubstituted (R^1 = H) precursors **4.61** and **4.62** in 92% and 91% yield, respectively (Scheme 4-4a) and subsequent carbamate formation yielding **4.65** and **4.66** (Scheme 4-4b).

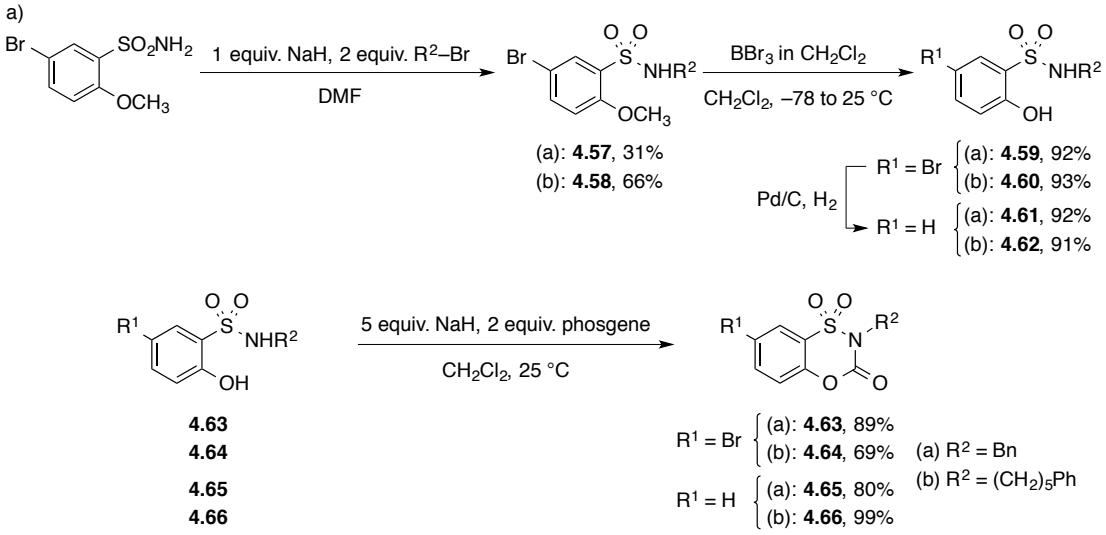

Scheme 4-4. Synthesis of benzoxathiazin-3-one 1,1-dioxide (a) precursors and (b) substituted final compounds with R^1 = Br and H

The cyanation conditions used previously to access the aryl nitriles (R^1 = CN, see Scheme 4-1) led to debrominated products when applied to this system using both **4.57** and **4.59** (attempts not shown). Instead, chlorosulfonylation of a precursor with a masked nitrile, 4-methoxybenzamide (**4.67**, Scheme 4-5a) and subsequent dehydration of **4.68** gave the cyano-substituted sulfonyl chloride **4.69**. Similarly, chlorosulfonylation of 1,4-dimethoxybenzene (**4.70**) was successfully utilized to access the required methoxy-substituted precursor **4.71** (Scheme 4-5b).

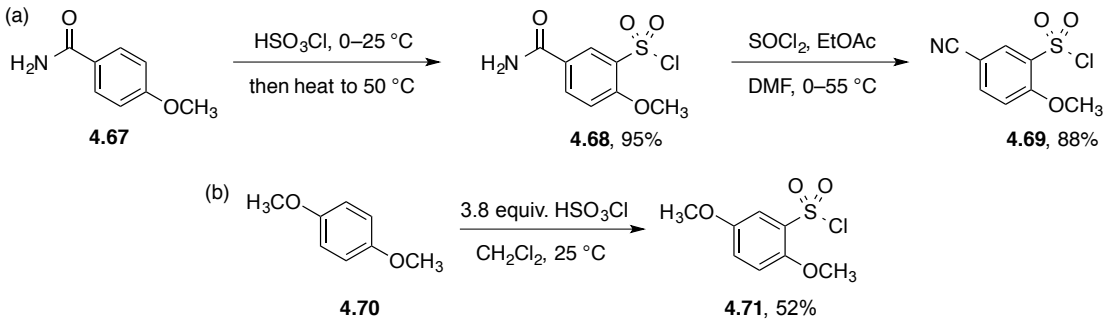

Scheme 4-5. Formation of (a) *p*-cyano and (b) *p*-methoxy intermediates **4.69** and **4.71**

To improve and streamline the route, a direct addition of the desired amine to the sulfonyl chloride was pursued (Scheme 4-6). Benzylamine and 5-phenylpentylamine (synthesized in two steps from 5-phenylpentanoic acid) were

reacted with **4.69** and **4.71** in a high yielding and facile manner to produce substituted sulfonamides **4.72–4.75** (Scheme 4-6). Deprotection of the methyl ether protecting group for the *p*-cyano series required stronger conditions (LiCl, 140 °C, DMF) to yield **4.76** and **4.77**, while the remaining compounds were obtained by subjection to the previously optimized boron tribromide conditions to give **4.78** and **4.79** (Scheme 4-6).

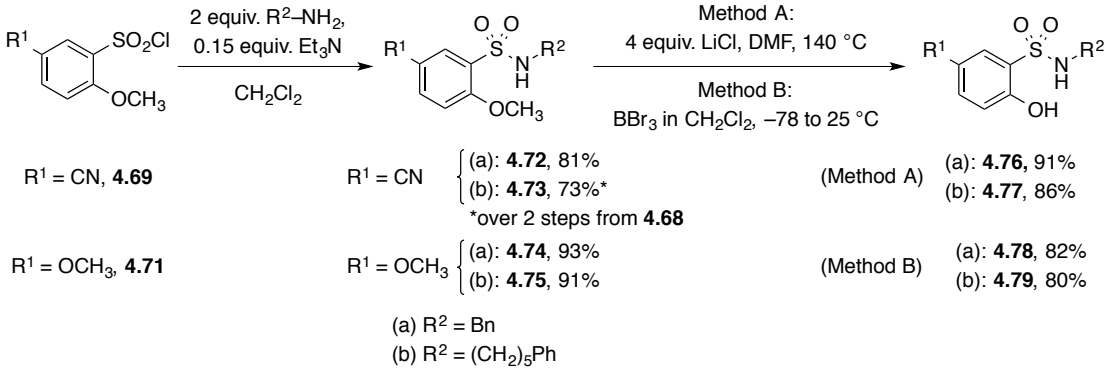

Scheme 4-6. Synthesis of cyano- and methoxy-containing scaffold precursors

Preparation of the four additional benzoxathiazin-3-one 1,1-dioxides (**4.80–4.83**) proceeded with the addition of phosgene and NaH and subsequent silica gel chromatography purification of the isolated products (Scheme 4-7). The structure of the designed inhibitors was confirmed through single crystal X-ray structure determination of **4.80** (Scheme 4-7).

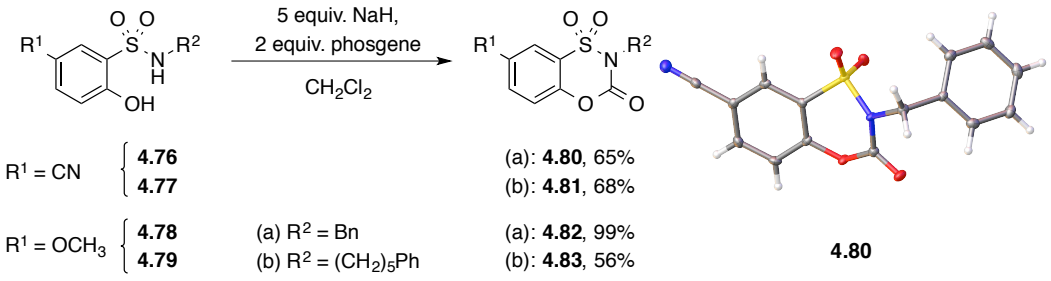

Scheme 4-7. Synthesis of 7-cyano and 7-methoxy benzoxathiazin-3-one 1,1-dioxides derivatives and X-ray structure of benzylated potential inhibitor **4.80**

4.2.4 Biological evaluation of the second-generation scaffold

Access to the six carbamates as originally designed and the additional two 7-bromo-substituted compounds, though not the core scaffold (R^2 = H) due to its polarity and acidity, allowed the examination of this second series by gel-based ABPP. The use of mouse brain tissue (cytosol and membrane fractions of proteome) and FP-rhodamine labeling showed clear inhibition of the serine hydrolase ABHD10 (Figure 4-11) through comparison to the known ABHD10 inhibitor ABL303a.

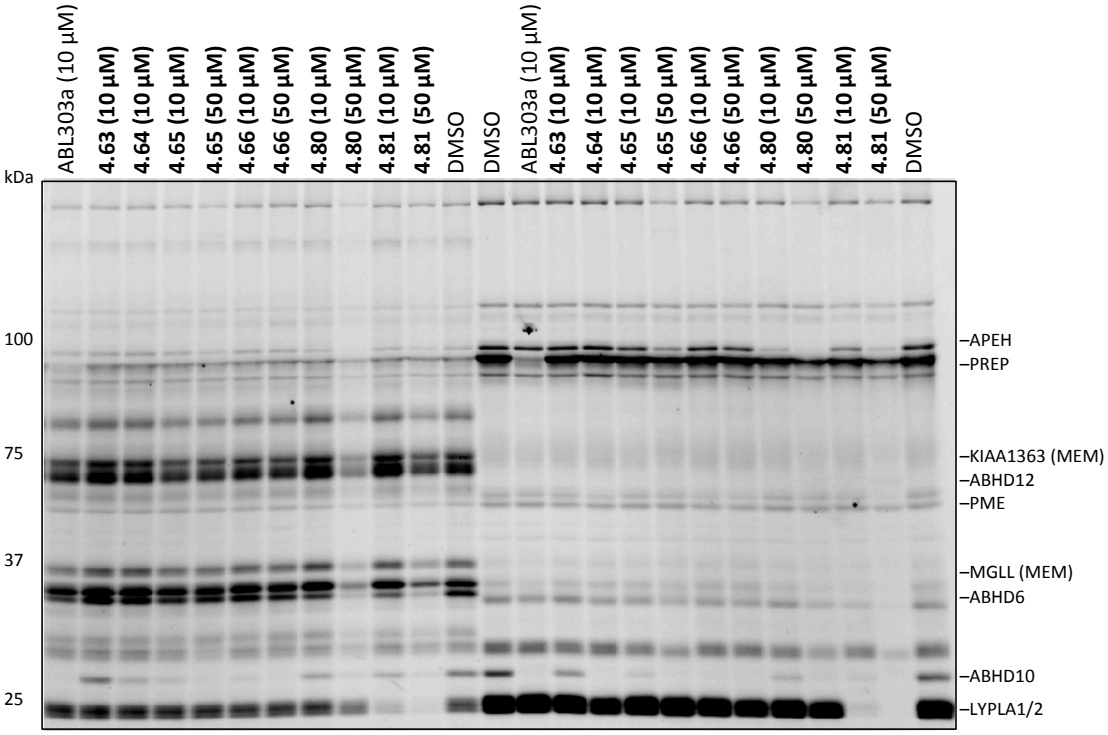

Figure 4-11. Competitive gel-based ABPP of benzoxathiazin-3-one 1,1-dioxides. Mouse brain membrane (left) and soluble (right) proteomes treated with compounds (at 10 µM and 50 µM, 30 min incubation) then FP-rhodamine (1 µM, 30 min). Fluorescent images shown in gray;

Screening at a series of concentrations allowed determination of approximate IC_{50} values for ABHD10 inhibition for the series, as well as quantification of low micromolar activity against LYPLA1/2 by **4.81** (summarized in Table 4-1, additional gels shown in Appendix 2). The results from this initial gel-based screen show interesting trends, with very low micromolar inhibition by **4.64** and **4.63**, the 7-bromo

compounds, similar to the comparatively high potency observed for the bromo-containing compounds from the first series (see section 4.2.2). Surprisingly, the trend of ABHD10 inhibition shows the 7-cyano compounds with the lowest levels of inhibition, despite containing the most electron-withdrawing, and presumably the most activating, substituent. However, the cyano-containing compound **4.81** is also the only compound of the set of eight which shows LYPLA1/2 inhibition. Further exploration of both the chemical and biochemical stability and reactivity of these compounds was conducted to establish the electronic effects of the varied substituents.

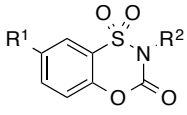

compound	R^1	R^2	IC_{50} (ABHD10)
4.82	OCH_3	Bn	9 μM
4.65	H	Bn	11 μM
4.63	Br	Bn	4 μM
4.80	CN	Bn	>50 μM
4.83	OCH_3	$(CH_2)_5Ph$	3 μM
4.66	H	$(CH_2)_5Ph$	10 μM
4.64	Br	$(CH_2)_5Ph$	0.5 μM
4.81*	CN	$(CH_2)_5Ph$	45 μM

*Also showed inhibition of LYPLA1/2: IC_{50} = 7 μM

Table 4-1. Approximate IC_{50} values calculated from gel-based ABPP

Additional gel-based ABPP screens were also performed with cysteine- and lysine-selective activity-based probes IA-rhodamine and AlexaFluor, respectively, but no reactivity was observed (see Appendix 2 for additional gels). Further investigation of the benzoxathiazin-3-one 1,1-dioxides was initiated with probing of the chemical and solvolytic stability and reactivity.

4.2.5 Stability and reactivity of benzoxathiazin-3-one 1,1-dioxides

The stability and reactivity studies were initially conducted using the compound **4.63** (R^1 = Br, R^2 = Bn) and **4.80** (R^1 = CN, R^2 = Bn) and both were stable in DPBS, H_2O, THF and ethanol at 25 °C for over 24 h (Table 4-2). Degradation (to unknown products) was observed in Tris-HCl buffer (in less than 1 h at 25 °C) and in DMEM buffer (to the hydrolysis products **4.59** or **4.76**) in 1–6 h at 25 °C or 37 °C

(Table 4-2). Samples of **4.63** and **4.80** dissolved in DMSO showed conversion to the hydrolysis products **4.59** and **4.76** at both 25 °C (50% conversion in approximately 7 or 14 days, respectively) and –78 °C (50% conversion in approximately 14 or 21 days, respectively).

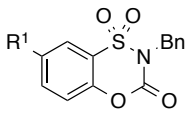

R^1 = Br, **4.63**
R^1 = CN, **4.80**

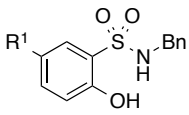

4.59
4.76

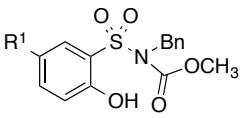

4.84
4.85

Conditions	Stability (at 25 °C)[a] **4.80** R^1 = CN, R^2 = Bn	Stability (at 25 °C)[a] **4.63** R^1 = Br, R^2 = Bn
H_2O	>24 h	>24 h
EtOH	>24 h	>24 h
CH_3OH	1 h[b]	4 h[b]
DMSO	7 days	14 days
DMSO (–78 °C)	14 days	21 days
DPBS	>24 h	>24 h
Tris-HCl	1 h	1 h
DMEM	2 h	6 h
DMEM (37 °C)	<2 h	2 h

[a]Time indicated is time to approximately 50% conversion to either the open-form **4.59** or **4.76,** or to an unknown product; [b]Product observed was instead **4.84** and **4.85**

Table 4-2. Stability and reactivity of **4.63** and **4.80**

The use of methanol as solvent provided a different reaction product, shown to be **4.84** or **4.85** by NMR studies. This provided the first indication of the propensity of the phenol to act as the leaving group (over $–SO_2NHR^2$). By subjecting the set of $Ph(CH_2)_5$-substituted compounds (with R^1 = OCH_3, H and CN) to the methanol reaction, a more direct comparison of the effect of the 7-substitution on the reactivity of the carbonyl (Table 4-3) was permitted. The compounds reacted in a predictable manner, where the compound with the electron-withdrawing substituent exhibited the greatest reactivity and that with the electron-donating substituent exhibited the lowest reactivity, displaying a clear electronic effect (Table 4-3).

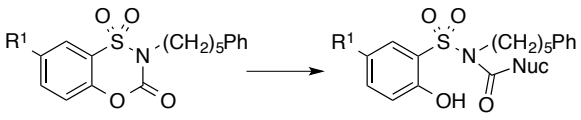

4.66, 4.81, 4.83 **4.86**

Nuc–H	Reactivity (at 25 °C)[a]		
	4.81 (R^1 = CN)	**4.66** (R^1 = H)	**4.83** (R^1 = OCH_3)
CH_3OH	32 h	>72 h (5 h)[b]	>72 h (>18 h)[b]
$BnNH_2$	<0.1 h	0.5 h	3.1 h
BnOH	>24 h	> 24 h	> 24 h
BnSH	>24 h	> 24 h	> 24 h

[a]Time until 75% conversion to **4.86;** [b]Time in bracket indicates result at 37 °C

Table 4-3. Reactivity of substituted inhibitors

The reactivity toward nucleophiles was also studied through subjection of the same series to reactions with benzylamine, benzyl alcohol and benzyl mercaptan (Table 4-3). The reactions were performed in an NMR tube in deuterated chloroform with dibromomethane as an internal standard and analyzed by ^{1}H NMR to determine the reaction time until 75% conversion to products **4.86** (Table 4-3). Neither benzyl alcohol nor benzyl mercaptan reacted with the compounds under these conditions. The reactivity profile with benzylamine shows a clear trend (Table 4-3), with a very rapid reaction observed with the 7-cyano derivative **4.81** (75% conversion in <5 min and full conversion in 30 min) and a slower reaction observed for the scaffold with an unsubstituted aromatic ring (**4.66**, R^1 = H, 30 min to 75% conversion and 2.75 h to full conversion). The 7-methoxy derivative **4.83** showed an even slower rate of reaction, with 75% conversion taking over 3 h and full conversion not observed until 12 h.

Subsequent studies investigated the irreversibility of serine hydrolase inhibition through a gel-base ABPP experiment. After 30 min of incubation of brain membrane proteome and compound **4.81**, filtration through a desalting column removed excess compound and allowed isolation of the enzyme-inhibitor complex. Aliquots of the complex were subjected to FP-rhodamine labeling at various time

points to show the persistence of inhibition of LYPLA1/2, indicating that binding is covalent, since the complex survives column filtration, and irreversible over the time scale since the enzyme reactivation was not observed over 4 hours post-filtration (Figure 4-12).

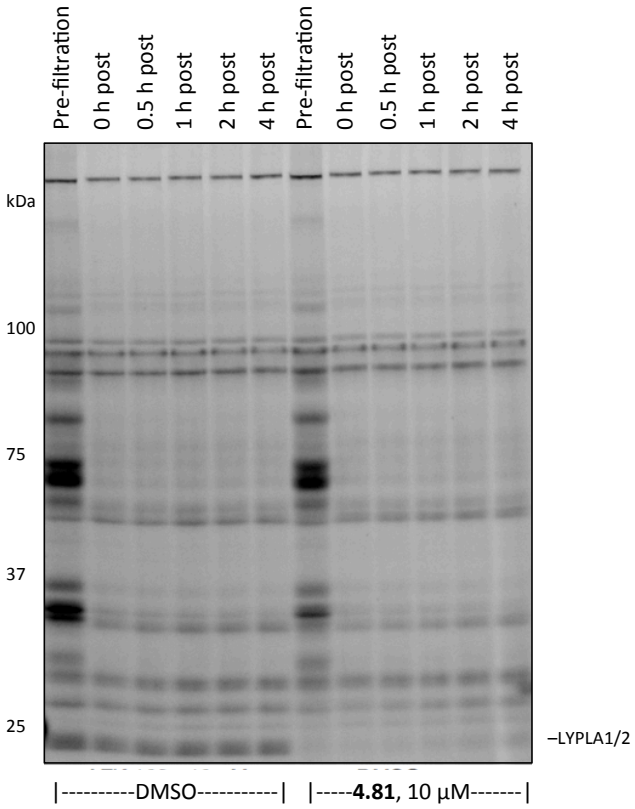

Figure 4-12. Demonstration of the irreversibility of the inhibition of LYPLA1/2 by **4.81**; Incubation of mouse brain membrane proteome with **4.81** (10 µM, 30 min) and desalting column filtration led to covalent complex which was then subjected to FP-rhodamine labeling (1 µM, 30 min) at various time points post-filtration, as indicated.

Additional proteome-wide screens of the compounds allowed the comparison of reactivity in vitro, by examining ABHD10 activity in cell lysate proteomic samples from mouse neuroblastomas (Neuro 2A or N2A cells, Figure 4-13a) and human embryonic kidney cells (HEK cells, Figure 4-13b). The three lead compounds were used at 1, 50 and 100 µM and showed a clear trend of strongest inhibition with **4.81** (R^1 = CN), and less with **4.66** (R^1 = H) and **4.83** (R^1 = OCH_3) (Figure 4-13)

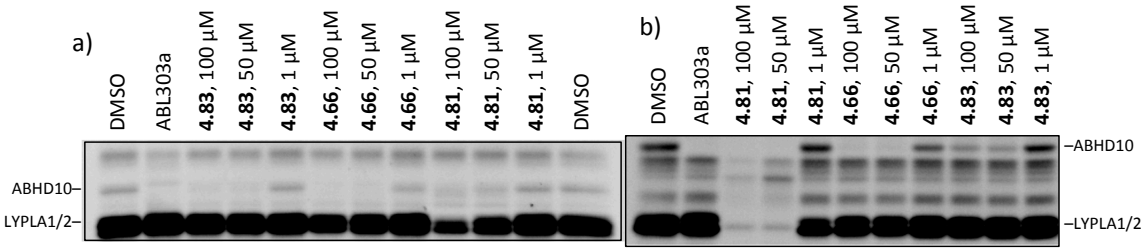

Figure 4-13. In vitro analysis of lead compounds (**4.83**, **4.66**, **4.81**) with (a) soluble proteome from N2A cell lysates (b) soluble proteome for HEK cell lysates; Proteome samples were treated with known ABHD10 inhibitor (10 µM) and compounds for 30 min, then FP-rhodamine (1 µM, 30 min).

The three lead compounds were analyzed by the ABPP/MudPIT protocol (Figure 4-14).[17,73] This entailed incubating whole cell proteomic samples from isotopically labeled HEK cell lysates with compounds (at 25 µM) or DMSO control and then the activity-based probe FP-biotin. The FP-biotin-labeled enzymes were enriched by avidin chromatography then subjected to an on-bead trypsin digestion. The resulting tryptic peptide mixture was analyzed by multidimensional liquid chromatography–tandem mass spectrometry (LC/LC-MS/MS). Comparison of spectral counts for serine hydrolases in DMSO-treated samples versus compound-treated samples allowed generation of the data in Figure 4-14 (experiment performed by Armand Cognetta). The corresponding gel with HEK cell lysates and compound treatment at 25 µM can be found in Appendix 2. The greatest inhibition spectrum was seen with the 7-cyano substituted inhibitor **4.81**, with ten enzymes inhibited at greater than 50% (Figure 4-14a), while only three enzymes were inhibited at this level by **4.66** (Figure 4-14b) and selective inhibition of only one protein (PNPLA4) was observed for **4.83** (Figure 4-14c). This clearly shows the electronic effect of the 7-substitution on the reactivity of the carbonyl of the benzoxathiazin-3-one 1,1-dioxides. Additionally, the selectivity of **4.81** for LYPLA1/2 was verified in the screen, with no inhibition of these enzymes seen with **4.83** and **4.66** (Figure 4-14).

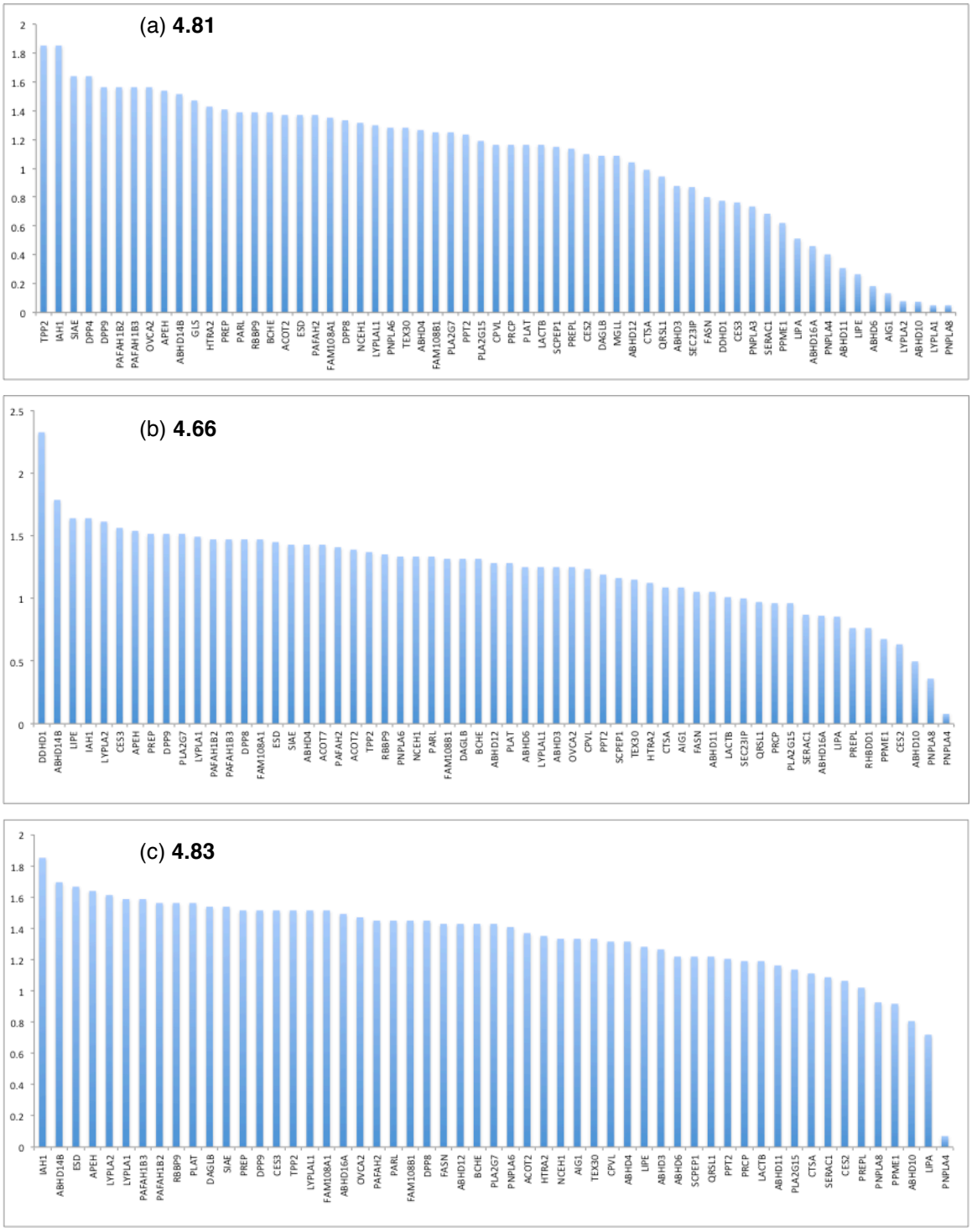

Figure 4-14. MudPIT analysis of lead compounds showing electronic effect of substituents on biological activity; the vertical axis shows SILAC ratios (observed serine hydrolases of the compound-treated vs the DMSO-treated samples)

In situ assays with N2A cells (mouse) and HEK cells (human) did not indicate facile translation to an in cell system, as low to no activity was observed for the potent

inhibitor **4.81**, even when running compounds at ten-fold higher concentrations than used in vitro. The discovery of DMEM reactivity for **4.63** and **4.80** (after initiation of in cell studies, see Table 4-2) led to the subjection of the three 5-phenylpentyl-susbtituted inhibitors to DMEM media for a 2 h incubation at 37 °C (which are the conditions used for incubation in the in situ assay). The expected trend was again observed, with full reaction to the hydrolysis product **4.77** observed for the 7-cyano substituted inhibitor **4.81**, partial reaction (to the hydrolysis product **4.62**) observed for **4.66** (approximately 50% in 2 h) and <10% reaction (to the hydrolysis product **4.79**) in 2 h for the 7-methoxy derivative **4.83**. Further investigations using **4.83** (R^1 = OCH_3) explored the potential of in situ work with this more stable scaffold.

The use of overexpressed PNPLA4 in HEK cells (provided by Armand Cognetta) allowed selective PNPLA4 inhibition with **4.83** to be observed with whole cell lysates and membrane proteome fractions, with a calculated IC_{50} of 800 nM (Figure 4-15a). Subjection of these same HEK cell to treatment with **4.83** in FBS-free media, provided potent in-cell inhibition (Figure 4-15b, cell treatments performed by Armand Cognetta).

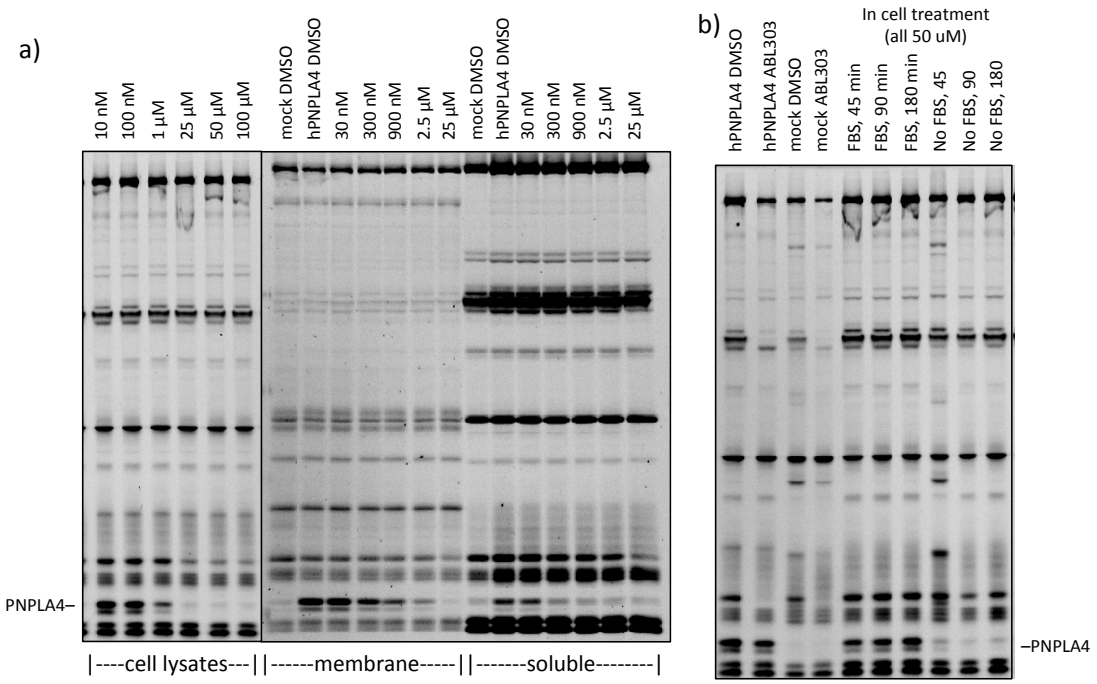

Figure 4-15. (a) IC_{50} determination of selective PNPLA4 inhibition by **4.83** using HEK cell lysates (whole cell, membrane and soluble fractions) and (b) in cell treatment of transfected HEK cells with **4.83** (cell treatment performed by Armand Cognetta, processing by Anne Kornahrens)

The use of a clickable probe, synthesized in three steps as shown in Scheme 4-8, allowed examination of this scaffold with rhodamine-N_3 (in vitro and in situ, see Appendix 2). No additional enzymatic targets were identified, but studies will be extended to explore possible cross-family targets.

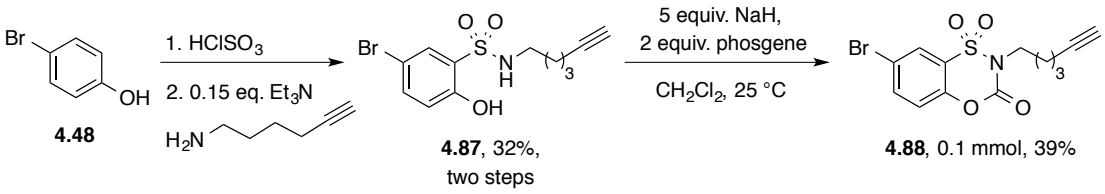

Scheme 4-8. Synthesis of alkyne-containing probe

4.3 Conclusion

The design and testing of a new family of serine hydrolase inhibitors was successfully performed to enable the covalent, irreversible inhibition of serine hydrolases. The predicted reactivity modulation of the tethered carbonyl by the backbone aromatic substitution was confirmed in chemical reactivity assays and through ABPP using gel and mass spectrometry analysis. The selective inhibition by **4.83** of the unannotated serine hydrolase PNPLA4 is a remarkable and exciting discovery and suggests this new family of inhibitors has the potential for affinity as well as tunable reactivity.

Further work on this new class of discovered inhibitors will continue to explore the potential of the activity and reactivity observed thus far. Additionally, the synthesis of various side chain lengths (n = 2–8) will complement the $-(CH_2)_5Ph$ substituted scaffold to allow examination of the effect of R^2 on biological activity, chemical reactivity and general stability. Lastly, the exploration of exciting PNPLA4 (patatin-like phospholipase domain-containing protein)-selective activity by **4.83** and the use of gel-based ABPP analysis (with overexpressed cell lysates) will allow the optimization and development of a selective inhibitor for this unannotated serine hydrolase.[74-76] The validation of our new scaffold through exploration of the biological and chemical activity and reactivity provides the basis for the expansion of this class and the continued efforts to target serine hydrolases.

4.4 Experimental

4.4.1 General experimental details

All commercial reagents were used without further purification unless otherwise noted. All reactions were performed in oven-dried (200 °C) glassware and under an inert atmosphere of anhydrous N_2 unless otherwise noted. Column chromatography was performed with silica gel 60. TLC was performed on silica gel (250 μm) F_{254} glass plates from EMD and spots were visualized by UV (254 or 366 nm). Preparative HPLC was performed using a Shimadzu HPLC on semi-preparative Diacel ChiralCel OD column (2×25 cm) with a flow rate of 10 mL/min with UV detection at 254 nm. ^{1}H and ^{13}C NMR were recorded on Bruker DRX-500 and DRX-600 MHz spectrometers. Chemical shifts are reported in ppm from an internal standard of residual $CHCl_3$ (7.26 for ^{1}H). Coupling constants (*J*) (H,H) are given in Hz. Coupling patterns are designated as singlet (s), doublet (d), triplet (t), quadruplet (q), multiplet (m), or broad singlet (br). High resolution mass spectra were obtained on an Agilent Technologies high resolution LC/MSD-TOF, and the detected masses given as *m/z* with *m* representing the molecular ion. The purity of tested compounds were confirmed to >95% by ^{1}H NMR.

4.4.2 General procedures

General procedure 4.A: Alkylation of benzothiadiazin-3-one 1,1-dioxide cores

A solution of the benzothiadiazin-3-one 1,1-dioxide core in DMF (0.5 M) was treated with NaH (60% in oil, 2 equiv.) followed by alkyl bromide (1 equiv.) at 25 °C. The reaction mixture was stirred for 24 h at 25 °C before the reaction was quenched with the addition of water, and extracted three times with EtOAc. The combined organic layers were dried with Na_2SO_4 and concentrated to yield a crude mixture of *N*- and *O*-alkylated products, which was purified by flash column chromatography (SiO_2, EtOAc/hexanes) to yield alkylated products.

General procedure 4.B: Substituted sulfonamide synthesis (using alkyl bromides)

A solution of substituted 2-methoxyphenylsulfonamide in DMF (0.25 M) was treated with alkyl bromide (2 equiv.) and triethylamine (1 equiv.) at 25 °C. The reaction mixture was stirred at 25 °C until sufficient conversion was observed (monitored by TLC) before the reaction was quenched by the addition of water. The aqueous layer was extracted three times with EtOAc, and the combined organic layers were washed with saturated aqueous NaCl, dried with Na_2SO_4 and concentrated. The crude material was purified by flash column chromatography to yield pure product.

General procedure 4.C: Substituted sulfonamide synthesis (using primary amines)

A solution of sulfonyl chloride in CH_2Cl_2 (0.5 M) was treated with primary amine (2 equiv.) and triethylamine (0.15 equiv.) at 0 °C. The reaction mixture was stirred at 25 °C until completion (monitored by TLC) before the reaction was quenched by the addition of water. The aqueous layer was extracted three times with EtOAc, and the combined organic layers were washed with saturated aqueous NaCl, dried with Na_2SO_4 and concentrated. The crude material was purified by flash column chromatography to yield pure product.

General procedure 4.D: Phenol deprotection (using boron tribromide)

A solution of the 2-methoxybenzenesulfonamides in anhydrous CH_2Cl_2 was cooled to the specified temperature and then slowly subjected to boron tribromide (1 M solution in CH_2Cl_2, 1–1.5 equiv.). Upon warming to 25 °C and stirring for the duration of the reaction (as monitored by TLC), the solution was carefully quenched with the addition of water. The aqueous layer was extracted three times with EtOAc and the combined organic layers were dried with Na_2SO_4 and concentrated to yield crude product, which was then purified by flash column chromatography.

General procedure 4.E: Cyclic carbamate formation

The 2-hydroxybenzenesulfonamides in CH_2Cl_2 (0.25 M) was treated with NaH (60% in oil, 5 equiv.) at 0 °C and the solution was stirred for 5 min. Phosgene (15% in toluene, 1.9 equiv.) was added to the sealed solution and the mixture was stirred while allowing to warm to 25 °C. The reaction was quenched (carefully!) with the addition water and then extracted three times with EtOAc, dried with Na_2SO_4 and concentrated to provide the crude product. The desired compound was purified by flash column chromatography.

4.4.3 Synthetic procedures and compound characterization

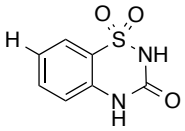

Compound 4.35, 2*H*-benzo[*e*][1,2,4]thiadiazin-3(4*H*)-one 1,1-dioxide

A solution of chlorosulfonyl isocyanate (**4.24**, CSI) (0.48 mL, 5.6 mmol) in nitromethane (5.6 mL) was treated with a solution of aniline (**4.30**, 0.46 mL, 5 mmol) in nitromethane (3.7 mL) dropwise at –40 °C. The reaction mixture was stirred for 15 min before $AlCl_3$(s) (740 mg, 5.6 mmol) was added and the reaction mixture was heated to 110 °C for 45 min. The resulting clear brown mixture was cooled and poured onto ice. The precipitate that formed was collected by filtration and dried to yield **4.35** (791 mg, 80%). The compound was purified by dissolving in saturated aqueous $NaHCO_3$, treating with charcoal, filtering over Celite® and re-acidifying to pH 1, affording **4.35** as a fine white solid (465 mg, 47%). ^{1}H NMR (400 MHz, DMSO-d_6) δ 12.67 (br s, 1H), 11.23 (s, 1H), 7.77 (d, J = 7.7 Hz, 1H), 7.64 (t, J = 8.4 Hz, 1H), 7.31–7.24 (m, 2H); ^{13}C NMR (150 MHz, DMSO-d_6) δ 151.5, 135.9, 134.8, 124.3, 123.4, 122.9, 117.9; IR (neat) ν_{max} 3202, 2980, 1680, 1599, 1381, 1309, 1158, 1134, 759, 583, 423 cm^{-1}; Data in accordance with literature.[77]

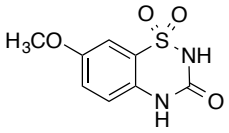

Compound 4.36, 7-methoxy-2*H*-benzo[*e*][1,2,4]thiadiazin-3(4*H*)-one 1,1-dioxide

A solution of chlorosulfonyl isocyanate (**4.24**, CSI) (0.776 mL, 8.9 mmol) in nitromethane (9.7 mL) was treated with a solution of *p*-methoxyaniline (**4.31**, 1.0 g, 8.1 mmol) in nitromethane (6.4 mL) dropwise at –40 °C. The reaction mixture was stirred for 30 min before $AlCl_3$(s) (740 mg, 5.6 mmol) was added and reaction mixture was heated to 110 °C for 1 h. The resulting purple solution was cooled and poured onto ice. The precipitate that formed was collected by filtration and dried to yield **4.36** as a purple solid (1.28 g, 69%). ^{1}H NMR (600 MHz, DMSO-d_6) δ 11.09 (br s, 1H), 7.27–7.25 (dd, J = 2.8, 9.1 Hz, 1H), 7.22 (d, J = 2.7 Hz, 1H), 7.19 (d, J = 9.0 Hz, 1H), 3.81 (s, 3H); ^{13}C NMR (150 MHz, DMSO-d_6) δ 155.1, 150.9, 128.5, 123.0, 121.7, 118.7, 104.6, 55.9; IR (neat) ν_{max} 3017, 1692, 1317, 1165 cm^{-1}; Data in accordance with literature.[64]

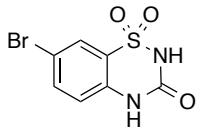

Compound 4.37, 7-bromo-2*H*-benzo[*e*][1,2,4]thiadiazin-3(4*H*)-one 1,1-dioxide

A solution of chlorosulfonyl isocyanate (**4.24**, CSI) (0.48 mL, 4.8 mmol) in nitromethane (4.8 mL) was treated with a solution of *p*-bromoaniline (**4.33**, 688 mg, 4 mmol) in nitromethane (3.2 mL) dropwise at –5 °C. The reaction mixture was stirred for 15 min before $AlCl_3$ (5.2 mL, 1 M in nitrobenzene, 5.2 mmol) was added and the mixture was heated to 100 °C for 45 min. The resulting clear brown mixture was cooled and poured onto ice. The precipitate that formed was collected by filtration and dried to yield **4.37** (571 mg, 51%). The compound was purified by dissolving in a saturated solution of $NaHCO_3$ in 1:1 H_2O/methanol, treating with charcoal, filtering

over Celite® and re-acidifying to pH 1, affording **4.37** as a fine white solid (523 mg, 47%). ^{1}H NMR (600 MHz, DMSO-d_6) δ 11.38 (br s, 1H), 7.91 (s, 1H), 7.82 (d, J = 9.0 Hz, 1H), 7.19 (d, J = 8.6 Hz, 1H); ^{13}C NMR (150 MHz, DMSO-d_6) δ 151.1, 136.5, 134.5, 124.3, 123.9, 119.3, 114.5; IR (neat) ν_{max} 3117, 1679, 1312, 1148 cm^{-1}.

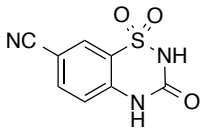

Compound 4.38, 3-oxo-3,4-dihydro-2*H*-benzo[*e*][1,2,4]thiadiazine-7-carbonitrile 1,1-dioxide

A solution of **4.37** (139 mg, 0.5 mmol) in DMF (0.5 mL) in a microwave vial was treated with CuI (29 mg, 0.15 mmol), $K_4[Fe(CN)_6]$ (dried for 12 h at 80 °C) (42 mg, 0.10 mmol) and *n*-butylimidazole (131 μL, 1.0 mmol). The mixture was purged with N_2, capped and heated at 160 °C for 24 h at which time the dark black mixture was transferred to a centrifuge tube with 5 mL CH_2Cl_2 and spun at 4000 rpm at 5 °C for 15 min. This was repeated twice with CH_2Cl_2 and then twice with 5 mL of a saturated aqueous solution of NH_4Cl. The solution was dissolved in DMF and filtered through a nylon microfilter (pore size 0.45 μM), and concentrated to provide **4.38** (139 mg) as a brown solid, which was used without further purification. ^{1}H NMR (500 MHz, DMSO-d_6) δ 9.96 (s, 1H), 7.85 (s, 1H) 7.71 (d, J = 8.5 Hz, 1H), 7.21 (br s, 1H) 7.08 (d, J = 8.5 Hz, 1H); ^{13}C NMR (100 MHz, DMSO-d_6) δ 153.6, 141.9, 134.6, 127.4, 123.6, 118.8, 116.2, 102.2; IR (neat) ν_{max} 3017 (w), 2359, 2330, 6111, 1328, 1140 cm^{-1}.

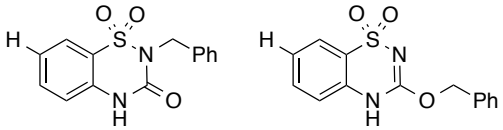

Compound 4.40A, 2-benzyl-3-hydroxy-2*H*-benzo[*e*][1,2,4]thiadiazine 1,1-dioxide and 4.40B, 3-(benzyloxy)-2*H*-benzo[*e*][1,2,4]thiadiazine 1,1-dioxide

Compound **4.35** (150 mg, 0.76 mmol) was subjected to general procedure 4.A with NaH (30 mg, 0.76 mmol) and benzyl bromide (180 μL, 1.5 mmol) in DMF (1.5 mL) at 25 °C for 24 hours. The 2:1 crude mixture of *N*- and *O*-alkylated products was purified by flash column chromatography (SiO_2, 0–50% EtOAc/hexanes gradient) to yield **4.40A** (114 mg, 52%) and **4.40B** (49 mg, 26%) as white solids. For **4.40A**: ^{1}H NMR (500 MHz, DMSO-d_6) δ 11.49 (s, NH), 7.88 (d, J = 7.8 Hz, 1H), 7.72 (t, J = 7.5 Hz, 1H), 7.35–7.30 (m, 6H), 7.26 (t, J = 7.0 Hz, 1H), 4.98 (s, 2H); ^{13}C NMR (125 MHz, DMSO-d_6) δ 149.7, 136.5, 134.9, 134.5, 128.4, 127.7, 127.6, 123.5, 122.08, 122.04, 117.2, 43.5; IR (neat) ν_{max} 3056, 2908, 1693, 1352, 1181, 721 cm^{-1}; HRMS-ESI-TOF m/z 289.0644 ($C_{14}H_{13}N_2O_3S+H^+$ requires 289.0647). For **4.40B**: ^{1}H NMR (500 MHz, DMSO-d_6) δ 7.79 (d, J = 8.0 Hz, 1H), 7.64 (t, J = 8.0 Hz, 1H), 7.52 (d, J = 7.1 Hz, 2H), 7.46–7.35 (m, 4H), 7.25 (d, J = 8.0 Hz, 1H), 5.37 (s, 2H); ^{13}C NMR (125 MHz, DMSO-d_6) δ 153.3, 134.7, 134.4, 133.3, 128.8, 128.7, 128.6, 125.1, 123.4, 121.4, 117.0, 69.7; IR (neat) ν_{max} 3243, 2919, 2849, 1607, 1253, 1169, 681 cm^{-1}; HRMS-ESI-TOF m/z 289.0644 ($C_{14}H_{13}N_2O_3S+H^+$ requires 289.0647).

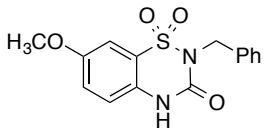

Compound 4.41A, 2-benzyl-7-methoxy-2*H*-benzo[*e*][1,2,4]thiadiazin-3(4*H*)-one 1,1-dioxide

Compound **4.36** (150 mg, 0.66 mmol) was subjected to general procedure 4.A with NaH (26 mg, 0.66 mmol) and benzyl bromide (156 μL, 1.3 mmol) in DMF (1.31 mL) at 25 °C for 24 h. The 3:1 crude mixture of *N*- and *O*-alkylated products was purified

by flash column chromatography (SiO_2, 0–100% EtOAc/hexanes gradient) to yield **4.41A** (112 mg, 54%) as a light brown solid. ^{1}H NMR (500 MHz, DMSO-d_6) δ 7.34–7.32 (s, 6H), 7.30–7.19 (m, 2H), 4.97 (s, 2H), 3.83 (s, 3H); ^{13}C NMR (125 MHz, DMSO-d_6) δ 163.6, 155.9, 150.4, 129.3, 128.5, 128.4, 123.6, 123.5, 119.9, 105.4, 56.9, 44.3; IR (neat) ν_{max} 2923, 1686, 1494, 1385, 1163 cm^{-1}.

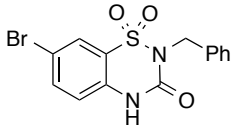

Compound 4.42A, 2-benzyl-7-bromo-3-hydroxy-3,4-dihydro-2*H*-benzo[*e*][1,2,4]thiadiazine 1,1-dioxide

Compound **4.37** (150 mg, 0.54 mmol) was subjected to general procedure 4.A with NaH (22 mg, 0.54 mmol) and benzyl bromide (129 μL, 1.08 mmol) in DMF (1.08 mL) at 25 °C for 24 h. The 3:1 crude mixture of *N*- and *O*-alkylated products was purified by flash column chromatography (SiO_2, 0–33% EtOAc/hexanes gradient) to yield **4.42A** (93 mg, 64%) as a white solid. ^{1}H NMR (500 MHz, CD_3OD) δ 7.98 (s, 1H), 7.80 (d, J = 8.8 Hz, 1H), 7.40 (d, J = 6.7 Hz, 2H), 7.32–7.25 (m, 3H), 7.15 (d, J = 8.2 Hz, 1H), 5.02 (s, 2H); ^{13}C NMR (150 MHz, CD_3OD) δ 151.7, 138.8, 137.8, 135.5, 129.6, 129.5, 129.0, 126.1, 125.9, 120.3, 116.4, 45.5; IR (neat) ν_{max} 2918, 1687, 1349, 1172, 593 cm^{-1}.

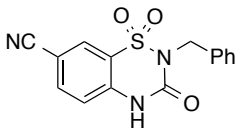

Compound 4.43A, 2-benzyl-3-oxo-3,4-dihydro-2*H*-benzo[*e*][1,2,4]thiadiazine-7-carbonitrile 1,1-dioxide

Compound **4.38** (150 mg, 0.54 mmol) was subjected to general procedure 4.A with NaH (22 mg, 0.54 mmol) and benzyl bromide (129 μL, 1.08 mmol) in DMF (1.08 mL) at 25 °C for 24 h. The 9:1 crude mixture of *N*- and *O*-alkylated products was purified by flash column chromatography (SiO_2, 20–80% EtOAc/hexanes gradient) to

yield **4.43A** (33 mg, 35%) as an off-white solid. **4.43A** was slightly impure (contaminated with **4.42B**) and was subjected to additional purification by semipreparative HPLC (ChiralCel OD column, 2×25 cm, 50% *i*-PrOH–hexane, 10 mL/min). ^{1}H NMR (600 MHz, DMSO-d_6) δ 11.98 (s, 1H), 8.50 (s, 1H), 8.12–8.10 (m, 1H), 7.44–7.27 (m, 6H), 4.99 (s, 2H); ^{13}C NMR (150 MHz, DMSO-d_6) δ 149.3, 138.3, 138.1, 136.1, 128.5, 127.8, 127.7, 127.5, 122.6, 118.41, 117.34, 105.9, 44.15.

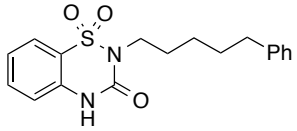

Compound 4.44A, 2-(5-phenylpentyl)-2*H*-benzo[*e*][1,2,4]thiadiazin-3(4*H*)-one 1,1-dioxide

Compound **4.35** (150 mg, 0.76 mmol) was subjected to general procedure 4.A with NaH (30 mg, 0.76 mmol) and 1-bromo-5-phenylpentane (280 μL, 1.52 mmol) in DMF (1.52 mL) at 25 °C for 48 h. The crude mixture was purified by flash column chromatography (SiO_2, 10–75% EtOAc/hexane to 20% MeOH in EtOAc) to yield **4.44A** (80 mg, 31%) as a white solid. ^{1}H NMR (400 MHz, $CDCl_3$) δ 10.26 (br s, 1H), 7.73 (d, *J* = 7.9 Hz, 1H), 7.43 (t, *J* = 7.8 Hz, 1H), 7.16 (t, *J* = 7.5 Hz, 3H), 7.10–6.99 (m, 4H), 3.86 (t, *J* = 8.1 Hz, 2H), 2.53 (t, *J* = 8.1 Hz, 2H), 1.76 (p, *J* = 7.6 Hz, 2H), 1.58 (p, *J* = 7.6 Hz, 2H), 1.35 (p, *J* = 7.6 Hz, 2H); ^{13}C NMR (125 MHz, $CDCl_3$) δ 152.0, 142.5, 134.5, 134.2, 128.5, 128.41, 128.39, 125.8, 123.9, 122.7, 117.1, 41.9, 35.8, 31.0, 29.3, 26.3; IR (neat) ν_{max} 2927, 1686, 1601, 1337, 1262, 715 cm^{-1}.

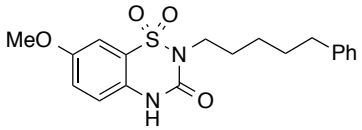

Compound 4.45A, 7-methoxy-2-(5-phenylpentyl)-2*H*-benzo[*e*][1,2,4]thiadiazin-3(4*H*)-one 1,1-dioxide

Compound **4.35** (150 mg, 0.66 mmol) was subjected to general procedure 4.A with NaH (26 mg, 0.66 mmol) and 1-bromo-5-phenylpentane (243 μL, 1.31 mmol) in

DMF (1.31 mL) at 25 °C for 48 h. The crude mixture was purified by flash column chromatography (SiO_2, 10–50% EtOAc/hexane gradient) to yield **4.45A** (58 mg, 25%) as a brown solid. ^{1}H NMR (500 MHz, $CDCl_3$) δ 8.81 (br s, 1H), 7.30–7.25 (m, 3H), 7.19–7.13 (m, 4H), 7.00 (d, *J* = 8.9 Hz, 1H), 3.92 (t, *J* = 7.6 Hz, 2H), 3.87 (s, 3H), 2.64 (t, *J* = 7.9 Hz, 2H), 1.84 (p, *J* = 7.7 Hz, 2H), 1.69 (p, *J* = 7.7 Hz, 2H), 1.44 (p, *J* = 7.7 Hz, 2H); ^{13}C NMR (125 MHz, $CDCl_3$) δ 155.4, 151.3, 141.9, 128.0, 127.9, 127.1, 125.3, 122.5, 122.2, 118.2, 104.4, 55.6, 41.3, 35.2, 30.4, 28.8, 25.8; IR (neat) ν_{max} 2932, 1681, 1503, 1163, 827, 570 cm^{-1}.

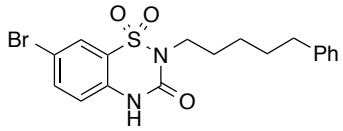

Compound 4.46A, 7-bromo-2-(5-phenylpentyl)-2*H*-benzo[*e*][1,2,4]thiadiazin-3(4*H*)-one 1,1-dioxide

Compound **4.37** (150 mg, 0.54 mmol) was subjected to general procedure 4.A with NaH (22 mg, 0.54 mmol) and 1-bromo-5-phenylpentane (200 μL, 1.08 mmol) in DMF (1.08 mL) at 25 °C for 48 h. The crude mixture was purified by flash column chromatography (SiO_2, 10–100% EtOAc/hexane gradient) to yield **4.46A** (39 mg, 17%) as a white solid. ^{1}H NMR (500 MHz, $CDCl_3$) δ 9.48 (s, 7H), 7.27 (d, *J* = 1.8 Hz, 1H), 6.92 (dd, *J* = 8.6, 1.9 Hz, 1H), 6.62–6.53 (m, 3H), 6.48 (t, *J* = 8.7 Hz, 3H), 6.30 (d, *J* = 8.6 Hz, 3H), 3.24 (t, *J* = 7.5 Hz, 2H), 1.94 (t, *J* = 7.7 Hz, 2H), 1.15 (p, *J* = 7.8 Hz, 2H), 1.00 (p, *J* = 7.7 Hz, 1H), 0.74 (p, *J* = 7.7 Hz, 1H); ^{13}C NMR (125 MHz, $CDCl_3$) δ 151.4, 142.4, 137.5, 133.1, 128.52, 128.45, 125.9, 125.4, 124.2, 118.7, 116.2, 42.3, 35.8, 31.0, 29.3, 26.3; IR (neat) ν_{max} 2921, 1697, 1330, 1170, 594 cm^{-1}.

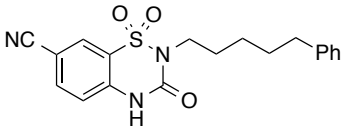

Compound 4.47A, 3-oxo-2-(5-phenylpentyl)-3,4-dihydro-2*H*-benzo[*e*][1,2,4]thiadiazine-7-carbonitrile 1,1-dioxide

Compound **4.38** (100 mg, 0.45 mmol) was subjected to general procedure 4.A with NaH (18 mg, 0.45 mmol) and 1-bromo-5-phenylpentane (165 μL, 0.90 mmol) in DMF (0.90 mL) at 25 °C for 48 h. The crude mixture was purified by flash column chromatography (SiO_2, 10–75% EtOAc/hexane gradient) to yield **4.47A** (11 mg, 17%) as a white solid. ^{1}H NMR (500 MHz, $CDCl_3$) δ 8.15 (s, 1H), 7.79 (d, J = 10.1 Hz, 1H), 7.29–7.26 (m, 2H), 7.22 (d, J = 8.5 Hz, 1H), 7.19–7.13 (m, 3H), 3.93 (t, J = 7.9 Hz, 2H), 2.63 (d, J = 7.9 Hz, 2H), 1.88–1.79 (m, 2H), 1.74–1.63 (m, 2H), 1.47–1.39 (m, 2H); ^{13}C NMR (150 MHz, DMSO-d_6) δ 149.6, 142.5, 138.6, 128.7, 128.6, 127.8, 126.1, 123.0, 118.7, 117.8, 106.14, 41.7, 35.3, 30.8, 29.0, 26.0 (one carbon not observed in ^{13}C NMR due to overlapping signals).

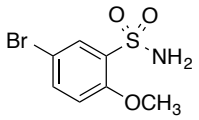

Compound 4.55, 5-bromo-2-methoxybenzenesulfonamide

Commercially available 2-methoxybenzenesulfonyl chloride (595 mg, 2.88 mmol) was dissolved in acetonitrile (15 mL) and cooled to 0 °C. NH_4OH (1.14 mL, 28.8 mmol) was added slowly and the reaction mixture was stirred for 2 h at 25 °C. The solvent was evaporated and the product was collected by filtration to yield **4.55** (501 mg, 2.67 mmol, 93%) as a white solid. ^{1}H NMR (400 MHz, DMSO-d_6) δ 7.80–7.75 (m, 2H), 7.27 (s, 2H), 7.21 (d, J = 8.8 Hz, 1H), 3.91 (s, 3H); ^{13}C NMR (150 MHz, DMSO-d_6) δ 155.4, 136.1, 133.0, 129.7, 115.3, 110.7, 56.5. The data were in accordance with literature.[78]

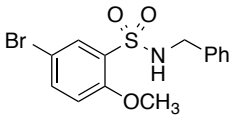

Compound 4.57, *N*-benzyl-5-bromo-2-methoxybenzenesulfonamide

Compound **4.55** (200 mg, 0.75 mmol) was subjected to general procedure 4.B with benzyl bromide at 25 °C for 5.5 h. Crude product was purified by flash column chromatography (SiO_2, 10–100% EtOAc/hexane gradient) to yield **4.57** (82 mg, 31%) as a white solid. ^{1}H NMR (500 MHz, $CDCl_3$) δ 8.06 (s, 1H), 7.63 (dd, *J* = 8.8, 2.5 Hz, 1H), 7.35–7.23 (m, 3H), 7.17 (m, 2H), 6.83 (d, *J* = 8.8 Hz, 1H), 5.28 (s, 1H), 4.17 (d, *J* = 6.3 Hz, 2H), 3.86 (s, 3H); ^{13}C NMR (125 MHz, $CDCl_3$) δ 155.2, 137.1, 136.1, 132.9, 129.4, 128.7, 128.0, 113.9, 112.9, 56.6, 47.9.

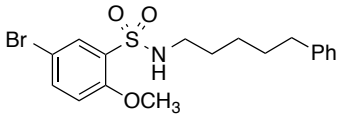

Compound 4.58, 5-bromo-2-methoxy-*N*-(5-phenylpentyl)benzenesulfonamide

Compound **4.55** (100 mg, 0.376 mmol) was subjected to general procedure 4.B with 5-bromo-1-phenylpentane at 25 °C for 16 h. Crude product was purified by flash column chromatography (SiO_2, 10–50% EtOAc/hexane gradient) to yield **4.58** (102 mg, 66%). ^{1}H NMR (500 MHz, $CDCl_3$) δ 8.10 (d, *J* = 2.4 Hz, 1H), 7.70 (dd, *J* = 8.8, 2.4 Hz, 1H), 7.37–7.32 (m, 2H), 7.25 (t, *J* = 7.4 Hz, 1H), 7.21 (d, *J* = 7.3 Hz, 2H), 6.98 (d, *J* = 8.8 Hz, 1H), 4.93 (t, *J* = 6.1 Hz, 1H), 3.42 (s, 3H), 2.97 (q, *J* = 6.7 Hz, 2H), 2.64 (t, *J* = 7.6 Hz, 2H), 1.64 (p, *J* = 8.0 Hz, 2H), 1.56 (p, *J* = 7.3 Hz, 2H), 1.37 (p, *J* = 7.6 Hz, 2H); ^{13}C NMR (125 MHz, $CDCl_3$) δ 155.3, 142.3, 137.1, 133.0, 129.3, 128.48, 128.45, 125.9, 114.0, 113.0, 56.8, 43.6, 35.8, 31.0, 29.5, 26.3.

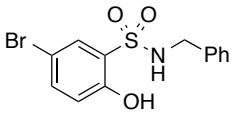

Compound 4.59, *N*-benzyl-5-bromo-2-hydroxybenzenesulfonamide

Compound **4.57** (101 mg, 0.284 mmol) in CH_2Cl_2 (0.1 M) at –78 °C was subjected to general procedure 4.D (1.5 equiv. BBr_3) for 16 h. Purification by flash column chromatography (SiO_2, 50% EtOAc/hexane gradient) gave **4.59** (82 mg, 84%) as a white solid. ^{1}H NMR (400 MHz, $CDCl_3$) δ 8.62 (br s, 1H), 7.71 (d, *J* = 2.4 Hz, 1H), 7.53 (dd, *J* = 8.8, 2.4 Hz, 1H), 7.32–7.26 (m, 3H), 7.22–7.19 (m, 2H), 6.91 (d, *J* = 8.8 Hz, 1H), 4.96 (br s, 1H), 4.19 (d, *J* = 6.1 Hz, 2H); ^{13}C NMR (125 MHz, $CDCl_3$) δ 154.2, 138.2, 135.3, 130.7, 129.0, 128.5, 128.0, 124.5, 120.9, 112.3, 47.4.

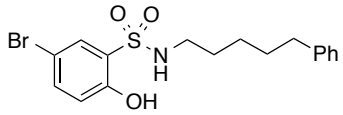

Compound 4.60, 5-bromo-2-hydroxy-*N*-(5-phenylpentyl)benzenesulfonamide

Compound **4.58** (95 mg, 0.23 mmol) in CH_2Cl_2 (0.1 M) at –78 °C was subjected to general procedure 4.D (1.5 equiv. BBr_3) for 13 h. Purification by flash column chromatography (SiO_2, 50% EtOAc/hexane gradient) gave **4.60** (85 mg, 93%) as a brown oil. ^{1}H NMR (600 MHz, $CDCl_3$) δ 8.69 (s, 1H), 7.78 (d, *J* = 2.3 Hz, 1H), 7.56 (dd, *J* = 8.8, 2.0 Hz, 1H), 7.30 (t, *J* = 7.5 Hz, 2H), 7.21 (t, *J* = 7.3 Hz, 1H), 7.17 (d, *J* = 7.4 Hz, 2H), 6.95 (d, *J* = 8.8 Hz, 1H), 4.79 (br s, 1H), 3.00 (q, *J* = 6.7 Hz, 2H), 2.60 (t, *J* = 7.7 Hz, 2H), 1.60 (p, *J* = 7.7 Hz, 2H), 1.54 (p, *J* = 7.3 Hz, 2H), 1.36–1.31 (m, 2H); ^{13}C NMR (150 MHz, $CDCl_3$) δ 154.2, 142.2, 138.1, 130.6, 128.48, 128.45, 125.9, 124.4, 120.9, 112.2, 43.2, 35.8, 30.9, 29.4, 26.1.

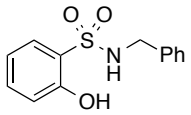

Compound 4.61, *N*-benzyl-2-hydroxybenzenesulfonamide

A solution of **4.59** (20 mg, 0.058 mmol) in methanol (0.29 mL) at 25 °C was treated with Pd/C (1.9 mg, 10 wt%, 0.03 mmol) and placed under a balloon atmosphere of H_2. The reaction mixture was stirred for 24 h and then filtered through Celite®. Purification of the crude material by flash column chromatography (SiO_2, 10–50% EtOAc/hexane gradient) gave **4.61** (14 mg, 92%) as a white solid. ^{1}H NMR (400 MHz, $CDCl_3$) δ 8.68 (s, 1H), 7.65 (d, *J* = 9.0 Hz, 1H), 7.49 (t, *J* = 8.1 Hz, 1H), 7.31–7.26 (m, 3H), 7.21–7.17 (m, 2H), 7.02 (m, 2H), 5.00 (br s, 1H), 4.17 (d, *J* = 6.1 Hz, 2H); ^{13}C NMR (100 MHz, $CDCl_3$) δ 155.1, 135.5, 135.4, 128.8, 128.4, 128.2, 127.9, 122.4, 120.6, 118.9, 47.2.

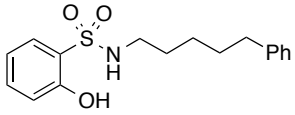

Compound 4.62, 2-hydroxy-*N*-(5-phenylpentyl)benzenesulfonamide

A solution of **4.60** (53 mg, 0.13 mmol) in methanol (0.66 mL) at 25 °C was treated with Pd/C (4.2 mg, 10 wt%, 0.004 mmol) and placed under a balloon atmosphere of H_2. The reaction mixture was stirred for 15 h and then filtered through Celite®. Purification of the crude material by flash column chromatography (SiO_2, 10–50% EtOAc/hexanes gradient) gave **4.62** (31 mg, 91%) as a clear oil. ^{1}H NMR (600 MHz, $CDCl_3$) δ 8.74 (s, 1H), 7.66 (dd, *J* = 8.0, 1.6 Hz, 1H), 7.48 (t, *J* = 8.6 Hz, 1H), 7.32–7.27 (m, 2H), 7.21 (t, *J* = 7.4 Hz, 1H), 7.16 (d, *J* = 7.0 Hz, 2H), 7.07–7.00 (m, 2H), 4.86 (t, *J* = 5.9 Hz, 1H), 2.98 (q, *J* = 6.2 Hz, 4H), 2.58 (t, *J* = 7.8 Hz, 2H), 1.57 (p, *J* = 8.1 Hz, 2H), 1.50 (p, *J* = 8.1 Hz, 2H), 1.35–1.29 (m, 2H); ^{13}C NMR (150 MHz, $CDCl_3$) δ 155.0, 142.1, 135.1, 128.3, 128.2, 125.7, 122.4, 120.4, 118.7, 42.9, 35.5, 30.7, 29.1, 25.9.

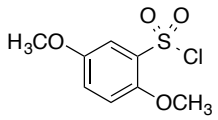

Compound 4.71, 2,5-dimethoxybenzenesulfonyl chloride

Compound 4.71 was synthesized following a literature procedure.[79] A solution of 1,4-dimethoxybenzene (**4.70**, 1.65 g, 11.9 mmol) in CH_2Cl_2 (10 mL) was cooled to 0 °C in an open round bottom flask. Chlorosulfonic acid (3 mL, 3.8 mmol) was added slowly and the reaction mixture was stirred for 5 min. Water (20 mL) was added slowly and the two phases were separated. The aqueous phase was extracted three times with CH_2Cl_2, and the combined organic layers were washed with saturated aqueous NaCl and dried with Na_2SO_4 to yield **4.71** (1.48 g, 52%) as a yellow solid which was used without further purification. ^{1}H NMR (600 MHz, $CDCl_3$) δ 7.48 (d, *J* = 3.1 Hz, 1H), 7.26 (dd, *J* = 9.1, 3.1 Hz, 1H), 7.09 (d, *J* = 9.1 Hz, 1H), 4.04 (s, 3H), 3.85 (s, 3H); ^{13}C NMR (150 MHz, $CDCl_3$) δ 152.6, 151.5, 131.8, 123.8, 114.7, 113.3, 57.0, 56.1.

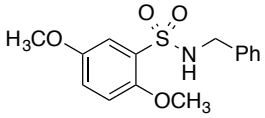

Compound 4.74, *N*-benzyl-2,5-dimethoxybenzenesulfonamide

Compound **4.71** (157 mg, 0.66 mmol) was subjected to general procedure 4.C with benzylamine (at 25 °C) for 20 hours. Purification (by flash column chromatography, elution solvent = 1:1 hexane/EtOAc) gave **4.74** (190 mg, 93%) as a yellow solid. ^{1}H NMR (400 MHz, $CDCl_3$) δ 7.48 (d, *J* = 3.1 Hz, 1H), 7.30–7.23 (m, 3H), 7.21–7.14 (m, 2H), 7.07 (dd, *J* = 9.0, 3.1 Hz, 1H), 6.90 (d, *J* = 9.0 Hz, 1H), 5.20 (t, *J* = 6.0 Hz, 1H), 4.10 (d, *J* = 6.2 Hz, 2H), 3.83 (d, *J* = 8.1 Hz, 6H); ^{13}C NMR (150 MHz, $CDCl_3$) δ 153.2, 149.9, 136.2, 128.5, 127.8, 127.7, 120.4, 114.5, 113.5, 56.6, 56.0, 47.7.

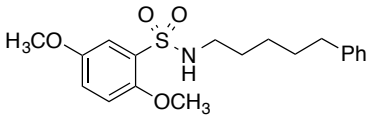

Compound 4.75, 2,5-dimethoxy-*N*-(5-phenylpentyl)benzenesulfonamide

Compound **4.71** (174 mg, 0.74 mmol) and triethylamine (103 μL, 1 equiv.) in CH_2Cl_2 (at 25 °C) was subjected to general procedure 4.C with 5-phenylpentylamine (241 mg, 2 equiv.) for 17 h. Purification by flash column chromatography (SiO_2, 10–100% EtOAc/hexanes gradient) gave **4.75** (242 mg, 91%) as a yellow solid. ^{1}H NMR (400 MHz, $CDCl_3$) δ 7.46 (d, *J* = 3.1 Hz, 1H), 7.28 (t, *J* = 7.4 Hz, 2H), 7.17 (m, 3H), 7.08 (dd, *J* = 9.0, 3.1 Hz, 1H), 6.97 (d, *J* = 9.0 Hz, 1H), 4.96 (t, *J* = 6.2 Hz, 1H), 3.91 (s, 3H), 3.82 (s, 3H), 2.89 (q, *J* = 6.8 Hz, 2H), 2.57 (t, *J* = 7.6 Hz, 2H), 1.64–1.43 (m, 4H), 1.31 (p, *J* = 7.7 Hz, 2H); ^{13}C NMR (100 MHz, $CDCl_3$) δ 153.4, 150.2, 142.3, 128.44, 128.38, 128.0, 125.8, 120.4, 114.7, 113.8, 57.0, 56.1, 43.6, 35.8, 31.0, 29.4, 26.3.

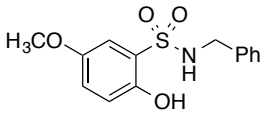

Compound 4.78, *N*-benzyl-2-hydroxy-5-methoxybenzenesulfonamide

Compound **4.74** (25 mg, 0.081 mmol) in CH_2Cl_2 (0.024 M) at –30 °C was subjected to general procedure 4.C for 15 min. Purification of the crude material by flash column chromatography (SiO_2, 2–10% EtOAc/CH_2Cl_2 gradient) gave **4.78** (20 mg, 82%) as a yellow oil. ^{1}H NMR (400 MHz, $CDCl_3$) δ 8.20 (s, 1H), 7.30–7.27 (m, 3H), 7.22–7.19 (m, 2H), 7.11–7.03 (m, 2H), 6.97 (d, *J* = 8.8 Hz, 1H), 4.97 (t, *J* = 5.7 Hz, 2H), 4.17 (d, *J* = 6.1 Hz, 2H), 3.76 (s, 3H); ^{13}C NMR (100 MHz, $CDCl_3$) δ 153.2, 149.3, 135.7, 128.9, 128.3, 128.0, 123.3, 122.3, 120.2, 111.0, 56.1, 47.3; IR (neat) ν_{max} 3306 (br), 2929, 1493, 1150, 1035 cm^{-1}.

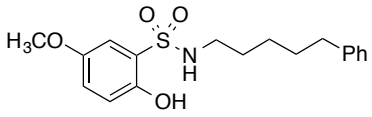

Compound 4.79, 2-hydroxy-5-methoxy-*N*-(5-phenylpentyl)benzenesulfonamide

Compound **4.75** (100 mg, 0.28 mmol) in CH_2Cl_2 (0.1 M, at 25 °C) was subjected to general procedure 4.C (1.5 equiv. BBr_3) for 30 min. Purification of the crude material by flash column chromatography (SiO_2, 2% EtOAc/hexanes gradient) gave **4.79** (77 mg, 80%) as a brown oil. ^{1}H NMR (400 MHz, $CDCl_3$) δ 8.23 (s, 1H), 7.37–7.26 (m, 2H), 7.22–7.11 (m, 4H), 7.07 (dd, *J* = 9.0, 3.0 Hz, 1H), 6.98 (d, *J* = 9.0 Hz, 1H), 4.69 (br s, 1H), 3.79 (s, 3H), 2.99 (q, *J* = 6.8 Hz, 2H), 2.58 (t, *J* = 7.6 Hz, 2H), 1.55 (m, 4H), 1.36–1.28 (m, 2H); ^{13}C NMR (100 MHz, $CDCl_3$) δ 153.1, 149.2, 142.3, 128.47, 128.45, 125.9, 123.0, 122.3, 120.1, 111.0, 56.1, 43.2, 35.8, 30.9, 29.4, 26.2.

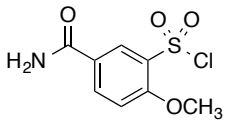

Compound 4.68, 5-carbamoyl-2-methoxybenzenesulfonyl chloride

4-Methoxybenzamide (**4.67**, 1.51 g, 10 mmol) was cooled to 0 °C in an open round bottom flask. Chlorosulfonic acid (9.97 mL, 150 mmol) was added slowly and the reaction was stirred for 12 h, while allowed to warm to 25 °C. The reaction was then heated to 50 °C for 3 h. The reaction was cooled and then quenched by slowly adding ice to the mixture (carefully!). The milky solution was dissolved in water and EtOAc and the two phases were separated. The aqueous phase was extracted three times with EtOAc, and the combined organic layers were washed with water, saturated aqueous NaCl and dried with Na_2SO_4 to yield **4.68** (2.27 g, 91%) as a white solid, which was used without further purification. ^{1}H NMR (400 MHz, DMSO-d_6) δ 8.23 (d, *J* = 2.4 Hz, 1H), 7.84 (dd, *J* = 8.5, 2.4 Hz, 1H), 7.00 (d, *J* = 8.6 Hz, 1H), 3.80 (s, 3H); ^{13}C NMR (150 MHz, DMSO-d_6) δ 167.5, 158.6, 135.0, 129.9, 128.5, 125.0, 111.1, 55.6.

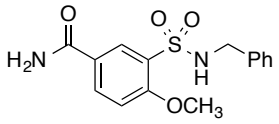

3-(*N*-benzylsulfamoyl)-4-methoxybenzamide

Compound **4.68** (100 mg, 0.401 mmol) was subjected to general procedure 4.C with benzylamine (at 25 °C) for 10 h. Purification by flash column chromatography (SiO_2, 50–100% EtOAc/hexane gradient) gave **4.68** (100 mg, 80%) as a white solid. ^{1}H NMR (500 MHz, $CDCl_3$) δ 8.24 (s, 1H), 8.15 (dd, *J* = 8.7, 2.3 Hz, 2H), 7.27 (s, 3H), 7.12 (d, *J* = 7.4 Hz, 2H), 7.00 (d, *J* = 8.7 Hz, 1H), 5.16 (t, *J* = 7.5 Hz, 1H), 4.14 (d, *J* = 6.2 Hz, 2H), 3.90 (s, 3H); ^{13}C NMR (150 MHz, $CDCl_3$) δ 158.9, 138.1, 135.7, 134.3, 129.4, 128.5, 128.0, 127.9, 117.5, 112.7, 104.5, 56.7, 47.7.

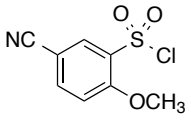

Compound 4.69, 5-cyano-2-methoxybenzenesulfonyl chloride

A solution of **4.68** (100 mg, 0.401 mmol) and DMF (1.5 μL) in anhydrous EtOAc (1.21 mL) at 0 °C was treated with thionyl chloride (145 μL, 2.00 mmol). The reaction mixture was heated to 55 °C and stirred for 3 h. Upon completion, the solvent was evaporated, the mixture was dissolved in EtOAc, and the organic layer was washed with water, saturated aqueous NaCl and dried with Na_2SO_4 to yield **4.69** (82 mg, 88%) as a slightly yellow oil, which was used without further purification. ^{1}H NMR (600 MHz, $CDCl_3$) δ 8.28 (d, *J* = 2.2 Hz, 1H), 7.97 (dd, *J* = 8.8, 2.1 Hz, 1H), 7.25 (d, *J* = 8.7 Hz, 1H), 4.16 (s, 3H); ^{13}C NMR (150 MHz, $CDCl_3$) δ 159.6, 140.0, 133.5, 132.1, 116.2, 113.7, 104.1, 56.9.

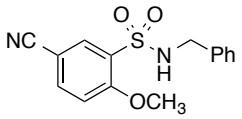

Compound 4.72, *N*-benzyl-5-cyano-2-methoxybenzenesulfonamide

A solution of 3-(*N*-benzylsulfamoyl)-4-methoxybenzamide (205 mg, 0.639 mmol) and DMF (2.5 μL) in anhydrous EtOAc (1.94 mL) at 0 °C was treated with thionyl chloride (232 μL, 3.20 mmol). The reaction mixture was heated to 55 °C and stirred for 5 h. Upon completion, the solvent was evaporated. The brown mixture was dissolved in EtOAc, and the organic layer was washed with water, saturated aqueous NaCl and dried with Na_2SO_4. The crude mixture was purified by flash column chromatography (SiO_2, 20–100% EtOAc/hexanes gradient) to yield **4.72** (181 mg, 93%) as a yellow solid. **4.72** was also synthesized from **4.69** (51 mg, 0.22 mmol) using general procedure 4.C with triethylamine (4.6 μL, 0.033 mmol) and benzyl amine (76 μL, 0.44 mmol) in CH_2Cl_2 (0.44 mL) at 25 °C for 19 h. The crude product was purified by flash column chromatography (SiO_2, 50–100% EtOAc/hexane gradient) to yield **4.72** (54 mg, 81%). ^{1}H NMR (400 MHz, $CDCl_3$) δ 8.17 (d, *J* = 2.0 Hz, 1H), 7.76 (dd, *J* = 8.7, 2.0 Hz, 1H), 7.24–7.18 (m, 3H), 7.11–7.06 (m, 2H), 6.94 (d, *J* = 8.7 Hz, 1H), 5.26 (br s, 1H), 4.18 (d, *J* = 6.3 Hz, 2H), 3.90 (s, 3H); ^{13}C NMR (150 MHz, $CDCl_3$) δ 159.2, 138.5, 136.0, 134.7, 129.8, 128.9, 128.4, 128.2, 117.8, 113.0, 105.0, 57.1, 48.1.

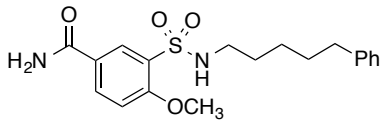

4-Methoxy-3-(*N*-(5-phenylpentyl)sulfamoyl)benzamide

Compound **4.68** (119 mg, 0.475 mmol) was subjected to general procedure 4.C with 5-phenylpentylamine at 25 °C for 5 h. Purification by flash column chromatography (SiO_2, 50–100% EtOAc/hexanes gradient) gave the title compound (131 mg, 73%) as

an off-white solid. ^{1}H NMR (400 MHz, $CDCl_3$) δ 8.30 (s, 1H), 8.18 (d, *J* = 10.3 Hz, 1H), 7.32–7.22 (m, 2H), 7.20–7.15 (m, 1H), 7.16–7.05 (m, 3H), 4.00 (s, 3H), 2.90 (t, *J* = 6.8 Hz, 2H), 2.56 (t, *J* = 7.6 Hz, 2H), 1.65–1.42 (m, 4H), 1.35–1.17 (m, 2H); ^{13}C NMR (150 MHz, $CDCl_3$) δ 167.6, 159.1, 142.5, 135.4, 129.4, 128.70, 128.68, 127.6, 126.1, 126.0, 112.7, 57.1, 43.8, 36.1, 31.2, 29.8, 26.5.

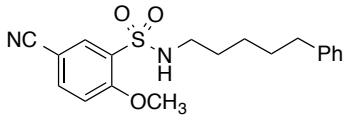

Compound 4.73, 5-cyano-2-methoxy-*N*-(5-phenylpentyl)benzenesulfonamide

A solution of 4-methoxy-3-(*N*-(5-phenylpentyl)sulfamoyl)benzamide (100 mg, 0.27 mmol) and DMF (1 μL) in anhydrous EtOAc (0.80 mL) at 0 °C was treated with thionyl chloride (96 μL, 1.3 mmol). The reaction mixture was heated to 55 °C and stirred for 13 h. Upon completion, the solvent was evaporated and the mixture was dissolved in EtOAc. The organic layer was washed with water, saturated aqueous NaCl and dried with Na_2SO_4. The crude mixture was purified by flash column chromatography (SiO_2, 20–100% EtOAc/hexanes gradient) to yield **4.73** (77 mg, 81%) as a white solid. ^{1}H NMR (400 MHz, $CDCl_3$) δ 8.22 (d, *J* = 2.2 Hz, 1H), 7.84 (dd, *J* = 8.7, 2.2 Hz, 1H), 7.30–7.26 (m, 4H), 7.19 (t, *J* = 7.5 Hz, 1H), 7.17–7.10 (m, 3H), 5.06 (br s, 1H), 4.02 (s, 3H), 2.92 (q, *J* = 6.7 Hz, 2H), 2.57 (t, *J* = 7.6 Hz, 2H), 1.63–1.45 (m, 4H), 1.34–1.27 (m, 2H); ^{13}C NMR (100 MHz, $CDCl_3$) δ 159.3, 142.2, 138.3, 134.5, 129.2, 128.42, 128.41, 125.9, 117.6, 113.0, 104.7, 57.0, 43.5, 35.8, 30.9, 29.5, 26.2.

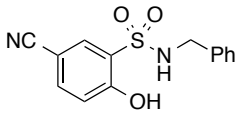

Compound 4.76, *N*-benzyl-5-cyano-2-hydroxybenzenesulfonamide

Compound **4.72** (75 mg, 0.29 mmol) in anhydrous DMF (0.475 mL, 0.6 M) at 0 °C was treated with LiCl (48 mg, 1.1 mmol). The solution was heated to 140 °C for 22 h. Upon cooling, the solvent was evaporated and the mixture was dry-loaded onto silica gel and purified by flash column chromatography (SiO_2, 2–40% EtOAc/CH_2Cl_2 gradient with 1% HOAc) to give **4.76** (75 mg, 91%) as an yellow/orange amorphous solid. ^{1}H NMR (400 MHz, $CDCl_3$) δ 9.20 (s, 1H), 7.86 (s, 1H), 7.67 (d, *J* = 10.5 Hz, 1H), 7.36–7.26 (m, 3H), 7.20–7.16 (m, 2H), 7.09 (d, *J* = 8.7 Hz, 1H), 5.03 (s, 1H), 4.25 (d, *J* = 6.0 Hz, 2H); ^{13}C NMR (150 MHz, $CDCl_3$) δ 158.1, 137.8, 134.7, 133.4, 128.8, 128.4, 127.8, 124.5, 120.0, 117.3, 104.1, 47.3.

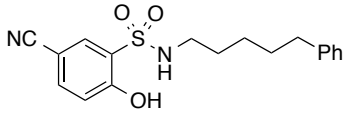

Compound 4.77, 5-cyano-2-hydroxy-*N*-(5-phenylpentyl)benzenesulfonamide

Compound **4.73** (78 mg, 0.22 mmol) in anhydrous DMF (0.36 mL, 0.6 M) at 0 °C was treated with LiCl (37 mg, 0.87 mmol). The solution was heated to 140 °C for 15 h. Upon cooling, the solvent was evaporated and the mixture was dry-loaded onto silica gel and purified by flash column chromatography (SiO_2, 2–100% EtOAc/CH_2Cl_2 gradient with 1% HOAc) to give **4.77** (64 mg, 86%) as a yellow oil. ^{1}H NMR (500 MHz, $CDCl_3$) δ 8.05 (s, 1H), 7.77 (d, *J* = 8.6 Hz, 1H), 7.38–7.34 (m, 2H), 7.27 (t, *J* = 7.4 Hz, 1H), 7.20 (dd, *J* = 16.1, 8.0 Hz, 3H), 4.90 (br s, 1H), 3.07 (s, 2H), 2.66 (t, *J* = 7.5 Hz, 2H), 1.77–1.52 (m, 4H), 1.47–1.30 (m, 2H); ^{13}C NMR (150 MHz, $CDCl_3$) δ 157.9, 141.5, 137.5, 132.8, 127.9, 127.9, 125.4, 123.8, 119.8, 116.9, 104.0, 42.7, 35.1, 30.2, 28.9, 25.5; IR (neat) ν_{max} 3291 (br), 2934, 2858, 2229, 1603, 1321, 1150 cm^{-1}.

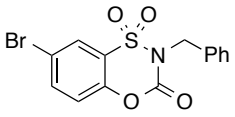

Compound 4.63, 2-benzyl-7-bromobenzo[*e*][1,4,3]oxathiazin-3(2*H*)-one 1,1-dioxide

Compound **4.59** (152 mg, 0.44 mmol) was subjected to general procedure 4.E with NaH (89 mg, 2.22 mmol) and phosgene (15% in toluene, 601 μL, 0.84 mmol) in CH_2Cl_2 (1.77 mL) at 0 °C. The reaction mixture was stirred for 9 h at 25 °C. The crude product was purified by flash column chromatography (SiO_2, hexanes then 2–100% EtOAc/CH_2Cl_2 gradient) to yield **4.63** (144 mg, 88%) as a white solid. ^{1}H NMR (600 MHz, $CDCl_3$) δ 8.00 (s, 1H), 7.80 (dd, *J* = 8.8, 2.1 Hz, 1H), 7.50–7.48 (m, 2H), 7.38–7.29 (m, 3H), 7.27–7.23 (m, 1H), 5.06 (s, 2H); ^{13}C NMR (125 MHz, $CDCl_3$) δ 146.6, 138.6, 134.3, 129.3, 128.9, 128.8, 125.7, 125.5, 120.7, 118.7, 46.9 (one carbon not observed in ^{13}C NMR due to overlapping signals); HRMS-ESI-TOF *m/z* 366.9514 ($C_{14}H_{10}BrNO_4S+H^+$ requires 367.9592).

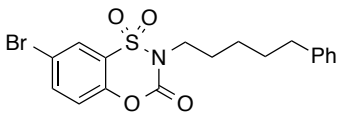

Compound 4.64, 7-bromo-2-(5-phenylpentyl)benzo[*e*][1,4,3]oxathiazin-3(2*H*)-one 1,1-dioxide

Compound **4.60** (124 mg, 0.31 mmol) was subjected to general procedure 4.E with NaH (62 mg, 1.6 mmol) and phosgene (15% in toluene, 421 μL, 0.59 mmol) in CH_2Cl_2 (1.60 mL) at 0 °C. The reaction mixture was stirred for 6 h at 25 °C. The crude product was purified by flash column chromatography (SiO_2, hexanes then 0–2% EtOAc/CH_2Cl_2 gradient) to yield **4.64** (91 mg, 69%) as a white solid. ^{1}H NMR (600 MHz, $CDCl_3$) δ 8.00 (d, *J* = 2.3 Hz, 1H), 7.83 (dd, *J* = 8.8, 2.3 Hz, 1H), 7.32–7.28 (m, 2H), 7.22–7.19 (m, 3H), 3.93 (t, *J* = 8.2 Hz, 2H), 2.66 (t, *J* = 7.7 Hz, 2H), 1.88 (p, *J* = 7.7 Hz, 2H), 1.71 (p, *J* = 7.7 Hz, 2H), 1.45 (p, *J* = 7.7 Hz, 3H); ^{13}C NMR (150 MHz, $CDCl_3$) δ 146.6, 146.5, 142.3, 138.5, 128.5, 128.4, 125.9, 125.5, 125.4,

120.6, 118.6, 77.4, 77.2, 77.0, 44.2, 35.7, 30.9, 28.6, 26.2; IR (neat) ν_{max} 2925, 2855, 1756, 1468, 1355, 1174, 736, 594 cm^{-1}; HRMS-ESI-TOF *m/z* 426.0128 ($C_{18}H_{18}BrNO_4S+H^+$ requires 426.0198).

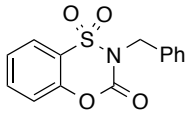

Compound 4.65, 2-benzylbenzo[*e*][1,4,3]oxathiazin-3(2*H*)-one 1,1-dioxide

Compound **4.61** (51 mg, 0.19 mmol) was subjected to general procedure 4.E with NaH (39 mg, 0.97 mmol) and phosgene (15% in toluene, 262 μL, 0.37 mmol) in CH_2Cl_2 (0.97 mL) at 0 °C and stirred for 9 h at 25 °C. The crude product was purified by flash column chromatography (SiO_2, hexanes then 0–50% EtOAc/CH_2Cl_2 gradient) to yield **4.65** (45 mg, 80%) as a white solid. ^1H NMR (400 MHz, $CDCl_3$) δ 7.89 (d, *J* = 9.0 Hz, 1H), 7.71 (t, *J* = 7.9 Hz, 1H), 7.51 (d, *J* = 7.6 Hz, 2H), 7.45 (t, *J* = 7.7 Hz, 1H), 7.40–7.29 (m, 4H), 5.07 (s, 2H); ^{13}C NMR (125 MHz, $CDCl_3$) δ 147.5, 147.0, 135.6, 134.6, 129.2, 128.8, 128.6, 126.0, 124.2, 122.9, 118.9, 46.6; IR (neat) ν_{max} 1754, 1351, 1190, 761 cm^{-1}; HRMS-ESI-TOF *m/z* 290.0482 ($C_{14}H_{11}NO_4S+H^+$ requires 290.0477).

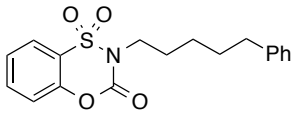

Compound 4.66, 2-(5-phenylpentyl)benzo[*e*][1,4,3]oxathiazin-3(2*H*)-one 1,1-dioxide

Compound **4.62** (32 mg, 0.101 mmol) was subjected to general procedure 4.E with NaH (20 mg, 0.51 mmol) and phosgene (15% in toluene, 128 μL, 0.193 mmol) in CH_2Cl_2 (0.404 mL) at 0 °C. The reaction mixture was stirred for 9 h at 25 °C. The crude product was purified by flash column chromatography (SiO_2, hexanes then 0–50% EtOAc/CH_2Cl_2 gradient) to yield **4.66** (34 mg, 97%) as a clear oil. ^1H NMR (400 MHz, $CDCl_3$) δ 7.87 (d, *J* = 7.6 Hz, 1H), 7.73 (t, *J* = 7.7 Hz, 1H), 7.46 (t, *J* = 7.7 Hz,

1H), 7.38 (d, *J* = 8.3 Hz, 1H), 7.29–7.27 (m, 2H), 7.20–7.18 (m, 3H), 3.92 (t, *J* = 8.1 Hz, 2H), 2.63 (t, *J* = 7.6 Hz, 2H), 1.91–1.83 (m, 2H), 1.76–1.63 (m, 2H), 1.49–1.38 (m, 2H); ^{13}C NMR (100 MHz, $CDCl_3$) δ 147.6, 147.0, 142.3, 135.5, 128.5, 128.4, 126.0, 125.8, 124.1, 122.9, 118.8, 43.9, 35.8, 31.1, 28.7, 26.2; IR (neat) ν_{max} 2931, 2858, 1757, 1352, 1214, 761 cm^{-1}; HRMS-ESI-TOF *m/z* 346.1104 ($C_{18}H_{19}NO_4S+H^+$ requires 346.1107).

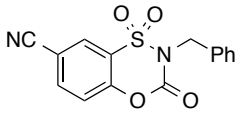

Compound 4.76, 2-benzyl-3-oxo-2,3-dihydrobenzo[*e*][1,4,3]oxathiazine-7-carbonitrile 1,1-dioxide

Compound **4.72** (70 mg, 0.24 mmol) was subjected to general procedure 4.E with NaH (49 mg, 1.21 mmol) and phosgene (15% in toluene, 329 μL, 0.46 mmol) in CH_2Cl_2 (0.96 mL) at 0 °C. The reaction mixture was stirred at 25 °C for 5.5 h. The crude product was purified by flash column chromatography (SiO_2, hexanes then 0–4% EtOAc/CH_2Cl_2 gradient) to yield **4.76** (47 mg, 65%) as a white solid. ^{1}H NMR (600 MHz, $CDCl_3$) δ 8.20 (s, 1H), 7.97 (d, *J* = 8.6 Hz, 1H), 7.49 (d, *J* = 7.0 Hz, 4H), 7.36 (d, *J* = 7.2 Hz, 3H), 5.07 (s, 2H); ^{13}C NMR (150 MHz, $CDCl_3$) δ 150.1, 145.8, 138.8, 133.9, 129.4, 129.00, 128.96, 127.6, 125.7, 120.5, 116.0, 110.7, 47.3; IR (neat) ν_{max} 2922, 2361, 1757, 1171, 702 cm^{-1}; HRMS-ESI-TOF *m/z* 337.0966 ($C_{15}H_{10}N_2O_4S+Na^+$ requires 337.0966).

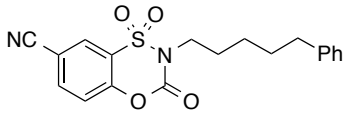

Compound 4.77, 3-oxo-2-(5-phenylpentyl)-2,3-dihydrobenzo[*e*][1,4,3]oxathiazine-7-carbonitrile 1,1-dioxide

Compound **4.73** (68 mg, 0.20 mmol) was subjected to general procedure 4.E with NaH (39 mg, 0.58 mmol) and phosgene (15% in toluene, 266 μL, 0.22 mmol) in

CH_2Cl_2 (0.79 mL) at 0 °C. The reaction mixture was stirred at 25 °C for 9 h. The crude product was purified by flash column chromatography (SiO_2, hexanes then 0–50% EtOAc/CH_2Cl_2 gradient) to yield **4.77** (50 mg, 68%) as a white solid. ^{1}H NMR (600 MHz, $CDCl_3$) δ 8.17 (d, *J* = 1.9 Hz, 1H), 7.98 (dd, *J* = 8.6, 1.9 Hz, 1H), 7.50 (d, *J* = 8.6 Hz, 1H), 7.28 (t, *J* = 7.4 Hz, 2H), 7.21–7.15 (m, 3H), 3.92 (t, *J* = 7.8 Hz, 2H), 2.63 (t, *J* = 7.7 Hz, 2H), 1.86 (p, *J* = 7.7 Hz, 2H), 1.69 (p, *J* = 7.7 Hz, 2H), 1.42 (p, *J* = 7.8 Hz, 2H); ^{13}C NMR (150 MHz, $CDCl_3$) δ 150.2, 145.7, 142.2, 138.7, 128.52, 128.46, 127.5, 125.9, 125.6, 120.4, 116.1, 110.6, 44.6, 35.8, 30.9, 28.6, 26.2; IR (neat) ν_{max} 2929, 1764, 1605, 1499, 1211, 1172, 703 cm^{-1}; HRMS-ESI-TOF *m/z* 371.1076 ($C_{19}H_{18}N_2O_4S$+H$^+$ requires 371.1066).

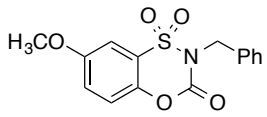

Compound 4.78, 2-benzyl-7-methoxybenzo[*e*][1,4,3]oxathiazin-3(2*H*)-one 1,1-dioxide

Compound **4.74** (32 mg, 0.104 mmol) was subjected to general procedure 4.E with NaH (22 mg, 0.55 mmol) and phosgene (15% in toluene, 148 μL, 0.21 mmol) in CH_2Cl_2 (0.42 mL) at 0 °C. The reaction was stirred at 25 °C for 5.5 h. The crude product was purified by flash column chromatography (SiO_2, hexanes then 0–50% EtOAc/CH_2Cl_2 gradient) to yield **4.78** (38 mg, quant) as a white solid. ^{1}H NMR (400 MHz, $CDCl_3$) δ 7.50 (d, *J* = 6.5 Hz, 1H), 7.42–7.19 (m, 2H), 5.07 (s, 1H), 3.90 (s, 1H); ^{13}C NMR (150 MHz, $CDCl_3$) δ 157.1, 147.3, 141.2, 134.7, 129.2, 128.8, 128.6, 124.4, 123.0, 120.3, 105.3, 56.4, 46.5; HRMS-ESI-TOF *m/z* 320.0586 ($C_{15}H_{13}NO_5S$+H$^+$ requires 320.0587).

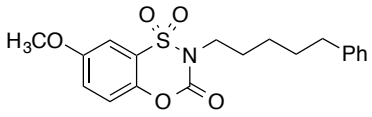

Compound 4.79, 7-methoxy-2-(5-phenylpentyl)benzo[*e*][1,4,3]oxathiazin-3(2*H*)-one 1,1-dioxide

Compound **4.75** (55 mg, 0.16 mmol) was subjected to general procedure 4.E with NaH (31 mg, 0.78 mmol) and phosgene (15% in toluene, 213 μL, 0.30 mmol) in CH_2Cl_2 (0.63 mL) at 0 °C. The reaction mixture was stirred at 25 °C for 7 h. The crude product was purified by flash column chromatography (SiO_2, hexanes then 0–50% EtOAc/CH_2Cl_2 gradient) to yield **4.79** (33 mg, 56%) as a slightly brown oil. ^{1}H NMR (600 MHz, $CDCl_3$) δ 7.31–7.26 (m, 4H), 7.25–7.22 (m, 1H), 7.22–7.16 (m, 3H), 3.94–3.88 (m, 5H), 2.64 (t, J = 8.4 Hz, 2H), 1.87 (p, J = 7.7 Hz, 2H), 1.70 (p, J = 7.7 Hz, 2H), 1.44 (p, J = 7.7 Hz, 2H); ^{13}C NMR (150 MHz, $CDCl_3$) δ 157.1, 147.2, 142.4, 141.4, 128.5, 128.4, 125.9, 124.2, 123.0, 120.2, 105.2, 56.4, 43.9, 35.8, 31.0, 28.7, 26.3; IR (neat) ν_{max} 2931, 2857, 1752, 1492, 1350, 1173 cm^{-1}; HRMS-ESI-TOF m/z 376.1216 ($C_{19}H_{21}NO_5S+H^+$ requires 376.1213).

4.4.4 Biological assay procedures

FAAH inhibition assay (performed by Dan Brody)

^{14}C-labeled oleamide was prepared from ^{14}C-labeled oleic acid as described.[80] The truncated rat FAAH (rFAAH) was expressed in *E. coli* and purified as described.[14] The purified recombinant rFAAH was used in the inhibition assays as described.[80] The enzyme reaction was initiated by mixing 1 nM of rFAAH (800, 500, or 200 pM rFAAH for inhibitors with $K_i \leq$ 1–2 nM) with 20 μM of ^{14}C-labeled oleamide in 500 μL of reaction buffer (125 mM TrisCl, 1 mM EDTA, 0.2% glycerol, 0.02% Triton X-100, 0.4 mM Hepes, pH 9.0) at room temperature in the presence of three different concentrations of inhibitor. The enzyme reaction was terminated by transferring 20 μL of the reaction mixture to 500 μL of 0.1 N HCl at three different time points. The

^{14}C-labeled oleamide (substrate) and oleic acid (product) were extracted with EtOAc and analyzed by TLC. The K_i of the inhibitor was calculated using a Dixon plot.

Preparation of mouse tissue proteomes

Mouse brains were Dounce-homogenized on ice in DPBS (pH 7.5) followed by a low-speed spin (1,400 × g, 5 min) to remove debris. After sonication, the supernatant was then centrifuged (100,000 × g, 45 min) to provide the cytosolic fraction in the supernatant and the membrane fraction as a pellet. The pellet was washed and re-suspended in PBS by sonication. Protein concentrations were determined using a protein assay kit (Bio-Rad). Samples were stored at –80 °C until use.

In vitro competitive activity-based protein profiling

Proteomes (brain membrane or soluble fractions or cell lysates) (50 μL, 1.0 mg/mL total protein concentration in DPBS) were preincubated with varying concentrations of inhibitors at 37 °C. After 30 min, FP-Rh (1.0 μL, 50 μM in DMSO) was added, and the mixture was incubated for another 30 min at room temperature. Reactions were quenched with SDS loading buffer (20 μL) and run on SDS-PAGE. Following gel imaging, serine hydrolase activity was determined by measuring fluorescent intensity of gel bands with ImageJ software.

In situ treatment of N2A and HEK cells

Neuro2A murine neuroblastoma (N2A) cells and human embryonic kidney (HEK) cells were grown in DMEM media supplemented with 10% fetal bovine serum and 2 mM L-glutamine in a humidified 5% CO_2 incubator at 37 °C.

Cells were treated with compound at the indicated concentrations (15 μL of a 200× DMSO stock) in a 6 cm dish (3 mL total media volume). Cells were harvested and separated into membrane and soluble fractions. Total protein concentrations of each fraction were adjusted to 1 mg/mL in PBS (50 μL total reaction volume), labeled with FP-Rh and analyzed as described above. The percentage of activity remaining was

quantified by measuring the integrated optical density of the individual serine hydrolase band relative to a DMSO-only (no compound) control using ImageJ software.

4.5 References

1. Ahn, K.; Johnson, D. S.; Mileni, M.; Beidler, D.; Long, J. Z.; McKinney, M. K.; Weerapana, E.; Sadagopan, N.; Liimatta, M.; Smith, S. E.; Lazerwith, S.; Stiff, C.; Kamtekar, S.; Bhattacharya, K.; Zhang, Y.; Swaney, S.; Van Becelaere, K.; Stevens, R. C.; Cravatt, B. F. *Chem. Biol.* **2009**, *16*, 411–420.
2. Bachovchin, D. A.; Cravatt, B. F. *Nat. Rev. Drug Discov.* **2012**, *11*, 52–68.
3. Adibekian, A.; Martin, B. R.; Wang, C.; Hsu, K.-L.; Bachovchin, D. A.; Niessen, S.; Hoover, H.; Cravatt, B. F. *Nat. Chem. Biol.* **2011**, *7*, 469–478.
4. Mileni, M.; Johnson, D. S.; Wang, Z.; Everdeen, D. S.; Liimatta, M.; Pabst, B.; Bhattacharya, K.; Nugent, R. A.; Kamtekar, S.; Cravatt, B. F.; Ahn, K.; Stevens, R. C. *Proc. Natl. Acad. Sci. U.S.A.* **2008**, *105*, 12820–12824.
5. Booker, L.; Kinsey, S. G.; Abdullah, R. A.; Blankman, J. L.; Long, J. Z.; Ezzili, C.; Boger, D. L.; Cravatt, B. F.; Lichtman, A. H. *Br. J. Pharmacol.* **2012**, *165*, 2485–2496.
6. Kinsey, S. G.; Long, J. Z.; O'Neal, S. T.; Abdullah, R. A.; Poklis, J. L.; Boger, D. L.; Cravatt, B. F.; Lichtman, A. H. *J. Pharm. Exp. Ther.* **2009**, *330*, 902–910.
7. Johnson, D. S.; Stiff, C.; Lazerwith, S. E.; Kesten, S. R.; Fay, L. K.; Morris, M.; Beidler, D.; Liimatta, M. B.; Smith, S. E.; Dudley, D. T.; Sadagopan, N.; Bhattachar, S. N.; Kesten, S. J.; Nomanbhoy, T. K.; Cravatt, B. F.; Ahn, K. *ACS Med. Chem. Lett.* **2011**, *2*, 91–96.
8. Bachovchin, D. A.; Ji, T.; Li, W.; Simon, G. M.; Blankman, J. L.; Adibekian, A.; Hoover, H.; Niessen, S.; Cravatt, B. F. *Proc. Natl. Acad. Sci. U.S.A.* **2010**, *107*, 20941–20946.
9. Long, J. Z.; Cravatt, B. F. *Chem. Rev.* **2011**, *111*, 6022–6063.
10. Schmid, H. H. O.; Schmid, P. C.; Natarajan, V. *Prog. Lipid Res.* **1990**, *29*, 1–43.
11. Schlosburg, J. E.; Boger, D. L.; Cravatt, B. F.; Lichtman, A. H. *J. Pharm. Exp. Ther.* **2009**, *329*, 314–323.
12. Karsak, M.; Gaffal, E.; Date, R.; Wang-Eckhardt, L.; Rehnelt, J.; Petrosino, S.; Starowicz, K.; Steuder, R.; Schlicker, E.; Cravatt, B.; Mechoulam, R.; Buettner, R.; Werner, S.; Di Marzo, V.; Tüting, T.; Zimmer, A. *Science* **2007**, *316*, 1494–1497.
13. Martin, B. R.; Mechoulam, R.; Razdan, R. K. *Life Sci.* **1999**, *65*, 573–595.
14. Patricelli, M. P.; Patterson, J. E.; Boger, D. L.; Cravatt, B. F. *Bioorg. Med. Chem. Lett.* **1998**, *8*, 613–618.
15. Otrubova, K.; Ezzili, C.; Boger, D. L. *Bioorg. Med. Chem. Lett.* **2011**, *21*, 4674–4685.
16. DePetrocellis, L.; Melck, D.; Ueda, N.; Maurelli, S.; Kurahashi, Y.; Yamamoto, S.; Marino, G.; DiMarzo, V. *Biochem. Biophys. Res. Commun.* **1997**, *231*, 82–88.
17. Li, W.; Blankman, J. L.; Cravatt, B. F. *J. Am. Chem. Soc.* **2007**, *129*, 9594–9595.

18. Deutsch, D. G.; Lin, S.; Hill, W.; Morse, K. L.; Salehani, D.; Arreaza, G.; Omeir, R. L.; Makriyannis, A. *Biochem. Biophys. Res. Commun.* **1997**, *231*, 217–221.

19. Deutsch, D. G.; Omeir, R.; Arreaza, G.; Salehani, D.; Prestwich, G. D.; Huang, Z.; Howlett, A. *Biochem. Pharmacol.* **1997**, *53*, 255–260.

20. Edgemond, W. S.; Greenberg, M. J.; Mcginley, P. J.; Muthian, S.; Campbell, W. B.; Hillard, C. J. *J. Pharm. Exp. Ther.* **1998**, *286*, 184–190.

21. Fernando, S. R.; Pertwee, R. G. *Br. J. Pharmacol.* **1997**, *121*, 1716–1720.

22. Du, W.; Hardouin, C.; Cheng, H.; Hwang, I.; Boger, D. L. *Bioorg. Med. Chem. Lett.* **2005**, *15*, 103–106.

23. Koutek, B.; Prestwich, G. D.; Howlett, A. C.; Chin, S. A.; Salehani, D.; Akhavan, N.; Deutsch, D. G. *J. Biol. Chem.* **1994**, *269*, 22937–22940.

24. Patterson, J. E.; Ollmann, I. R.; Cravatt, B. F.; Boger, D. L.; Wong, C. H.; Lerner, R. A. *J. Am. Chem. Soc.* **1996**, *118*, 5938–5945.

25. Vandevoorde, S. *Curr. Top. Med. Chem.* **2008**, *8*, 247–267.

26. Boger, D. L.; Sato, H.; Lerner, A. E.; Austin, B. J.; Patterson, J. E.; Patricelli, M. P.; Cravatt, B. F. *Bioorg. Med. Chem. Lett.* **1999**, *9*, 265–270.

27. Seierstad, M.; Breitenbucher, J. G. *J. Med. Chem.* **2008**, *51*, 7327–7343.

28. Leung, D.; Hardouin, C.; Boger, D. L.; Cravatt, B. F. *Nat. Biotechnol.* **2003**, *21*, 687–691.

29. Deng, H. *Expert Opin. Drug Discov.* **2010**, *5*, 961–993.

30. Bottcher, T.; Sieber, S. A. *Angew. Chem. Int. Ed.* **2008**, *47*, 4600–4603.

31. Otrubova, K.; Boger, D. L. *ACS Chem. Neurosci.* **2012**, *3*, 340–348.

32. Duncan, K. K.; Otrubova, K.; Boger, D. L. *Bioorg. Med. Chem.* **2014**, *22*, 2763–2770.

33. Leung, D.; Du, W.; Hardouin, C.; Cheng, H.; Hwang, I.; Cravatt, B. F.; Boger, D. L. *Bioorg. Med. Chem. Lett.* **2005**, *15*, 1423–1428.

34. Liu, Y. S.; Patricelli, M. P.; Cravatt, B. F. *Proc. Natl. Acad. Sci. U.S.A.* **1999**, *96*, 14694–14699.

35. Patricelli, M. P.; Giang, D. K.; Stamp, L. M.; Burbaum, J. J. *Proteomics* **2001**, *1*, 1067–1071.

36. Kluge, A. F.; Petter, R. C. *Curr. Opin. Chem. Biol.* **2010**, *14*, 421–427.

37. Boger, D. L.; Miyauchi, H.; Hedrick, M. P. *Bioorg. Med. Chem. Lett.* **2001**, *11*, 1517–1520.

38. Kidd, D.; Liu, Y.; Cravatt, B. F. *Biochemistry* **2001**, *40*, 4005–4015.

39. Wang, X.; Sarris, K.; Kage, K.; Zhang, D.; Brown, S. P.; Kolasa, T.; Surowy, C.; Kouhen, El, O. F.; Muchmore, S. W.; Brioni, J. D.; Stewart, A. O. *J. Med. Chem.* **2009**, *52*, 170–180.

40. Min, X.; Thibault, S. T.; Porter, A. C.; Gustin, D. J.; Carlson, T. J.; Xu, H.; Lindstrom, M.; Xu, G.; Uyeda, C.; Ma, Z.; Li, Y.; Kayser, F.; Nigel P. C.

Walker; Wang, Z. *Proc. Natl. Acad. Sci.* **2011**, *108*, 7379–7384.

41. Tian, G.; Paschetto, K. A.; Gharandaghi, F.; Gordon, E.; Wilkins, D. E.; Luo, X.; Scott, C. W. *Biochemistry* **2011**, *50*, 6867–6878.

42. Lichtman, A. H. *J. Pharm. Exp. Ther.* **2004**, *311*, 441–448.

43. Garfunkle, J.; Ezzili, C.; Rayl, T. J.; Hochstatter, D. G.; Hwang, I.; Boger, D. L. *J. Med. Pharm. Chem.* **2008**, *51*, 4392–4403.

44. Guimarães, C. R. W.; Boger, D. L.; Jorgensen, W. L. *J. Am. Chem. Soc.* **2005**, *127*, 17377–17384.

45. Ezzili, C.; Mileni, M.; McGlinchey, N.; Long, J. Z.; Kinsey, S. G.; Hochstatter, D. G.; Stevens, R. C.; Lichtman, A. H.; Cravatt, B. F.; Bilsky, E. J. *J. Med. Chem.* **2011**, *54*, 2805–2822.

46. Kathuria, S.; Gaetani, S.; Fegley, D.; Valino, F.; Duranti, A.; Tontini, A.; Mor, M.; Tarzia, G.; La Rana, G.; Calignano, A.; Giustino, A.; Tattoli, M.; Palmery, M.; Cuomo, V.; Piomelli, D. *Nat. Med.* **2003**, *9*, 76–81.

47. Minkkila, A.; Myllymäki, M. J.; Saario, S. M.; Castillo-Melendez, J. A.; Koskinen, A. M. P.; Fowler, C. J.; Leppanen, J.; Nevalainen, T. *Eur. J. Med. Chem.* **2009**, *44*, 2994–3008.

48. Berger, A. B.; Vitorino, P. M.; Bogyo, M. *Am. J. Pharmacogenomics* **2004**, *4*, 371–381.

49. Cravatt, B. F.; Wright, A. T.; Kozarich, J. W. *Annu. Rev. Biochem.* **2008**, *77*, 383–414.

50. Jessani, N.; Liu, Y.; Humphrey, M.; Cravatt, B. F. *Proc. Natl. Acad. Sci. U.S.A.* **2002**, *99*, 10335–10340.

51. Boger, D. L.; Miyauchi, H.; Du, W.; Hardouin, C.; Fecik, R. A.; Cheng, H.; Hwang, I.; Hedrick, M. P.; Leung, D.; Acevedo, O.; Guimarães, C. R. W.; Jorgensen, W. L.; Cravatt, B. F. *J. Med. Chem.* **2005**, *48*, 1849–1856.

52. Speers, A. E.; Adam, G. C.; Cravatt, B. F. *J. Am. Chem. Soc.* **2003**, *125*, 4686–4687.

53. Powers, J. C.; Asgian, J. L.; Ekici, O. D.; James, K. E. *Chem. Rev.* **2002**, *102*, 4639–4750.

54. Hlasta, D. J.; Subramanyam, C.; Bell, M. R. *J. Med. Chem.* **1995**, *38*, 739–744.

55. Combrink, K. D.; Gülgeze, H. B.; Meanwell, N. A.; Pearce, B. C.; Zulan, P.; Bisacchi, G. S.; Roberts, D. G.; Stanley, P.; Seiler, S. M. *J. Med. Chem.* **1998**, *41*, 4854–4860.

56. Keith, J. M.; Jones, W. M.; Tichenor, M.; Liu, J.; Seierstad, M.; Palmer, J. A.; Webb, M.; Karbarz, M.; Scott, B. P.; Wilson, S. J.; Luo, L.; Wennerholm, M. L.; Chang, L.; Rizzolio, M.; Rynberg, R.; Chaplan, S. R.; Breitenbucher, J. G. *ACS Med. Chem. Lett.* **2015**, *6*, 1204–1208.

57. Chobanian, H. R.; Guo, Y.; Liu, P.; Chioda, M. D.; Fung, S.; Lanza, T. J.; Chang, L.; Bakshi, R. K.; Dellureficio, J. P.; Hong, Q.; McLaughlin, M.; Belyk, K. M.; Krska, S. W.; Makarewicz, A. K.; Martel, E. J.; Leone, J. F.; Frey, L.; Karanam, B.; Madeira, M.; Alvaro, R.; Shuman, J.; Salituro, G.; Terebetski, J. L.; Jochnowitz, N.; Mistry, S.; McGowan, E.; Hajdu, R.;

Rosenbach, M.; Abbadie, C.; Alexander, J. P.; Shiao, L.-L.; Sullivan, K. M.; Nargund, R. P.; Wyvratt, M. J.; Lin, L. S.; DeVita, R. J. *ACS Med. Chem. Lett.* **2014**, *5*, 717–721.

58. Zimmerman, M.; Morman, H.; Mulvey, D.; Jones, H.; Frankshun, R.; Ashe, B. M. *J. Biol. Chem.* **1980**, *255*, 9848–9851.

59. Lungarella, G.; Gardi, C.; Fonzi, L.; Comparini, L.; Share, N. N.; Zimmerman, M.; Martorana, P. A. *Exp. Lung Res.* **1986**, *11*, 35–47.

60. Martorana, P. A.; Share, N. N.; Zimmerman, M. *Eur. J. Respir. Dis.* **1985**, *66*, 297–301.

61. Groutas, W. C.; Houser-Archield, N.; Chong, L. S.; Venkataraman, R.; Epp, J. B.; Huang, H.; McClenahan, J. J. *J. Med. Chem.* **1993**, *36*, 3178–3181.

62. Hlasta, D. J.; Bell, M. R.; Boaz, N. W.; Court, J.; Desai, R. C.; Franke, C. A.; Mura, A. J.; Subramanyam, C.; Dunlap, R. P. *Bioorg. Med. Chem. Lett.* **1994**, *4*, 1801–1806.

63. Girard, Y.; Atkinson, J. G.; Rokach, J. *J. Chem. Soc., Perkin Trans. 1* **1979**, 1043–1047.

64. Boverie, S.; Antoine, M.-H.; Somers, F.; Becker, B.; Sebille, S.; Ouedraogo, R.; Counerotte, S.; Pirotte, B.; Lebrun, P.; de Tullio, P. *J. Med. Chem.* **2005**, *48*, 3492–3503.

65. Majumdar, K. C.; Ganai, S. *Beilstein J. Org. Chem.* **2013**, *9*, 503–509.

66. Hayao, S.; Stryker, W.; Phillips, B.; Fujimori, H.; Vidrio, H. *J. Med. Chem.* **1968**, *11*, 1246–1248.

67. Buckheit, R. W., Jr.; Fliakas-Boltz, V.; Decker, W. D.; Roberson, J. L.; Pyle, C. A.; White, E. L.; Bowdon, B. J.; McMahon, J. B.; Boyd, M. R.; Bader, J. P.; Nickell, D. G.; Barth, H.; Antonucci, T. K. *Antiviral Res.* **1994**, *25*, 43–56.

68. Arranz, M. E.; Díaz, J. A.; Ingate, S. T.; Witvrouw, M.; Pannecouque, C.; Balzarini, J.; De Clercq, E.; Vega, S. *Bioorg. Med. Chem.* **1999**, *7*, 2811–2822.

69. Combrink, K. D.; Gulgeze, H. B.; Thuring, J. W.; Yu, K.-L.; Civiello, R. L.; Zhang, Y.; Pearce, B. C.; Yin, Z.; Langley, D. R.; Kadow, K. F.; Cianci, C. W.; Li, Z.; Clarke, J.; Genovesi, E. V.; Medina, I.; Lamb, L.; Yang, Z.; Zadjura, L.; Krystal, M.; Meanwell, N. A. *Bioorg. Med. Chem. Lett.* **2007**, *17*, 4784–4790.

70. Schareina, T.; Zapf, A.; Mägerlein, W.; Müller, N.; Beller, M. *Chem. Eur. J.* **2007**, *13*, 6249–6254.

71. Backus, K. M.; Correia, B. E.; Lum, K. M.; Forli, S.; Horning, B. D.; González-Páez, G. E.; Chatterjee, S.; Lanning, B. R.; Teijaro, J. R.; Olson, A. J.; Wolan, D. W.; Cravatt, B. F. *Nature* **2016**, *534*, 570–574.

72. (a) Lohaus, G. *Chem. Ber.* **1972**, *105*, 2791–2799; (b) J. Kamei, Y. Igarashi, T. Hibino, and K. Aoki. **1973**. Patent WO 2004/026292 A1 (c) R. J. Cremlyn and T. Cronje, *Phosphorus, Sulfur Silicon, Relat. Elem.*, **1979**, *6*, 413–419.

73. Long, J. Z.; Li, W.; Booker, L.; Burston, J. J.; Kinsey, S. G.; Schlosburg, J. E.; Pavón, F. J.; Serrano, A. M.; Selley, D. E.; Parsons, L. H.; Lichtman, A. H.; Cravatt, B. F. *Nat. Chem. Biol.* **2009**, *5*, 37–44.

74. Cognetta, A. B.; Niphakis, M. J.; Lee, H.-C.; Martini, M. L.; Hulce, J. J.; Cravatt, B. F. *Chem. Biol.* **2015**, *22*, 928–937.

75. Kohda, M.; Tokuzawa, Y.; Kishita, Y.; Nyuzuki, H.; Moriyama, Y.; Mizuno, Y.; Hirata, T.; Yatsuka, Y.; Yamashita-Sugahara, Y.; Nakachi, Y.; Kato, H.; Okuda, A.; Tamaru, S.; Borna, N. N.; Banshoya, K.; Aigaki, T.; Sato-Miyata, Y.; Ohnuma, K.; Suzuki, T.; Nagao, A.; Maehata, H.; Matsuda, F.; Higasa, K.; Nagasaki, M.; Yasuda, J.; Yamamoto, M.; Fushimi, T.; Shimura, M.; Kaiho-Ichimoto, K.; Harashima, H.; Yamazaki, T.; Mori, M.; Murayama, K.; Ohtake, A.; Okazaki, Y. *PLOS Genet.* **2016**, *12*, e1005679.

76. Gao, J. G.; Simon, M. *J. Invest. Dermatol.* **2006**, *126*, 2087–2095.

77. Ivanova, E. M.; Borovika, D. A.; Vozny, I. V.; Trapencieris, P.; Žalubovskis, R. *Chem. Heterocycl. Compd.* **2012**, 1–3.

78. Tang, W.; Patel, N. D.; Xu, G.; Xu, X.; Savoie, J.; Ma, S.; Hao, M.-H.; Keshipeddy, S.; Capacci, A. G.; Wei, X.; Zhang, Y.; Gao, J. J.; Li, W.; Rodriguez, S.; Lu, B. Z.; Yee, N. K.; Senanayake, C. H. *Org. Lett.* **2012**, *14*, 2258–2261.

79. Jacob, P.; Anderson, G.; Meshul, C. K.; Shulgin, A. T.; Castagnoli, N. *J. Med. Chem.* **1977**, *20*, 1235–1239.

80. Patricelli, M. P.; Cravatt, B. F. *J. of Biol. Chem.* **2000**, *275*, 19177–19184.

Appendix 1

HPLC traces & NMR spectra for asymmetric Suzuki–Miyaura reaction

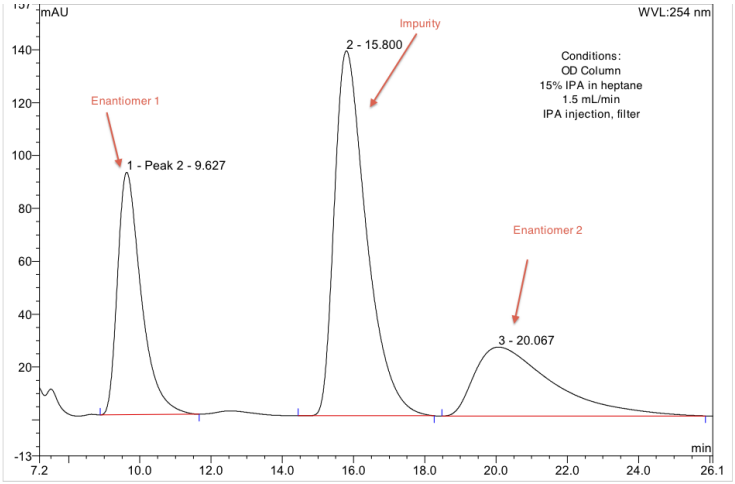

No.	Ret.Time min	Peak Name	Height mAU	Area mAU*min	Rel.Area %	Amount	Type
1	9.63	Peak 2	91.726	70.760	25.17	n.a.	BMB
2	15.80	n.a.	137.923	143.919	51.20	n.a.	BMB*
3	20.07	n.a.	26.107	66.418	23.63	n.a.	BMB*
Total:			255.756	281.097	100.00	0.000	

Figure A1-1 HPLC trace of **2.47** with impurity
Conditions: Chiral HPLC (Chiralpak OD, 15 % IPA in heptane, 1.5 mL/min, λ = 254 nm) t_R = 9.6 min, 15.8 and 20.1 min.

Impurity	Retention time (min)
Stille product (**2.42**)	6.9
Boronate ester (**2.46**)	2.9
PPh_3	2.6
PPh_3O	4.5
(*R*)-BINAP	2.7
De-boronated D ring (**2.54**)	6.8
D-ring dimer (**2.80**)	5.1
De-brominated Stille product (**2.55**)	16.2

Table A1-1 Potential Impurities and retention times on HPLC
Conditions: Chiral HPLC (Chiralpak OD, 15 % IPA in heptane, 1.5 mL/min, λ = 254 nm)

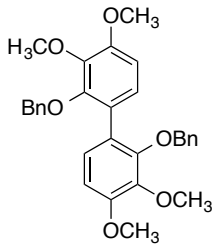

Compound 2.80, 2,2'-Bis(benzyloxy)-3,3',4,4'-tetramethoxy-1,1'-biphenyl

Aryl boronate ester **2.46** (0.017 g, 0.05 mmol) was added to a solution of **2.45** (0.010 g, 0.03 mmol), tetrakis(triphenylphosphine)palladium (0.004 g, 0.003 mmol) and potassium phosphate tribasic (0.020 mmol, 0.09 mmol) in dioxane:water (3:1 by volume, 0.31 mL total). The reaction mixture was degassed and refilled with argon five times, then heated to 101 °C in a sealed tube for 16 h. The mixture was allowed

to cool to rt, diluted with EtOAc (1 mL) and washed with brine (1 mL). The organic phase was dried over Na_2SO_4, filtered and concentrated *in vacuo*. The crude product was purified by column chromatography (9:1 Pet:EtOAc, R_f 0.34) to afford 2,2'-Bis(benzyloxy)-3,3',4,4'-tetramethoxy-1,1'-biphenyl as a light brown solid (0.015 g, 0.03 mmol, 99%). δ_H ($CDCl_3$, 400 MHz): 7.21-7.20 (6H, m, Ph-H); 7.08-7.06 (4H, m, Ph-H); 6.95 (2H, d, J = = 8.5, Ar-H); 6.72 (2H, d, J = 8.7, Ar-H); 4.82 (4H, s, OCH_2Ph); 3.93 (6H, s, OCH_3); 3.87 (6H, s, OCH_3); δ_C ($CDCl_3$, 101 MHz): 153.1, 150.9, 142.5, 137.9, 128.0, 127.5, 126.0, 125.7, 107.1 (2 x C), 74.8, 61.0, 56.1; ν_{max} (film) cm^{-1}: 2936 (w), 2361 (m),1594 (w), 1484 (s), 1452 (m), 1423 (w), 1370 (w), 1285 (m), 1219 (w), 1166 (w), 1093 (s), 1008 (m), 798 (w), 750 (w); HRMS calculated for $C_{30}H_{30}O_6$ $[M+Na]^+$: 509.1935; Found: 509.1928.

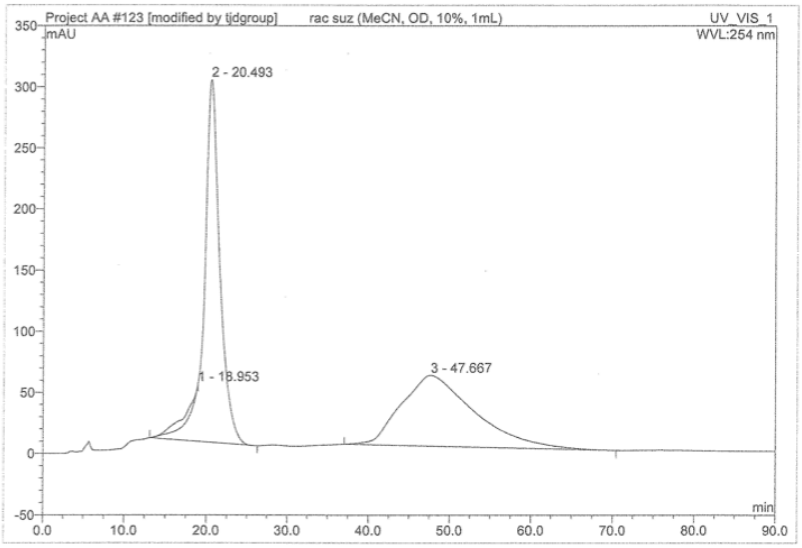

No.	Ret.Time min	Peak Name	Height mAU	Area mAU*min	Rel.Area %	Amount	Type
1	18.95	n.a.	0.000	21.081	1.62	n.a.	Ru*
2	20.49	n.a.	296.599	669.180	51.57	n.a.	BMB*
3	47.67	n.a.	58.106	607.301	46.80	n.a.	BMB*
Total:			354.705	1297.562	100.00	0.000	

Figure A1-2. HPLC trace of racemic sample of **2.47**
Conditions: Chiral HPLC (Chiralpak OD, 10 % IPA in heptane, 1.0 mL/min, λ = 254 nm) t_R = 20.5 min and 47.7 min. Note: ('skim') shoulder correction fitted to first peak.

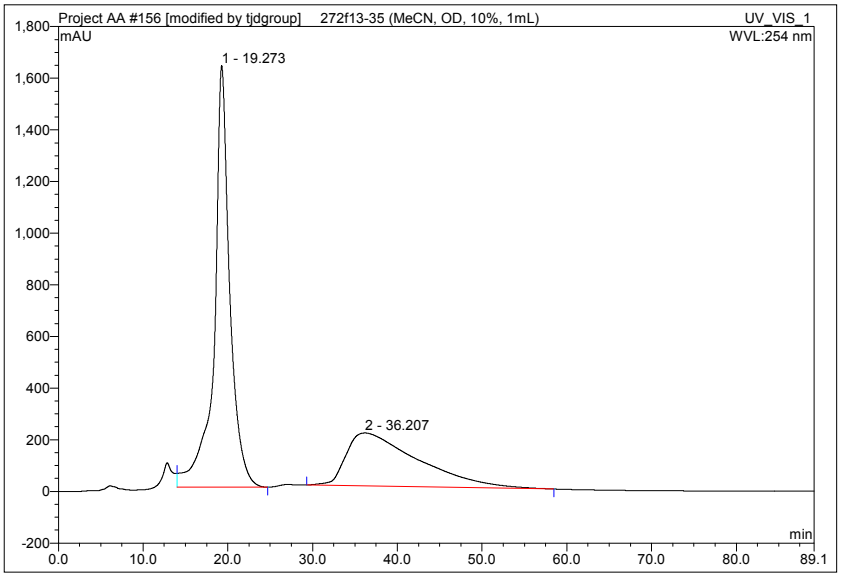

No.	Ret.Time min	Peak Name	Height mAU	Area mAU*min	Rel.Area %	Amount	Type
1	19.27	n.a.	1632.242	3482.232	63.36	n.a.	MB*
2	36.21	n.a.	205.200	2013.889	36.64	n.a.	BMB*
Total:			1837.442	5496.121	100.00	0.000	

Figure A1-3 HPLC trace of enantiomerically enriched **2.47** (using (*R*)-BINAP)
Conditions: Chiral HPLC (Chiralpak OD, 10 % IPA in heptane, 1.0 mL/min, λ = 254 nm); t_R (major) = 19.3 min, t_R = 36.2 min.

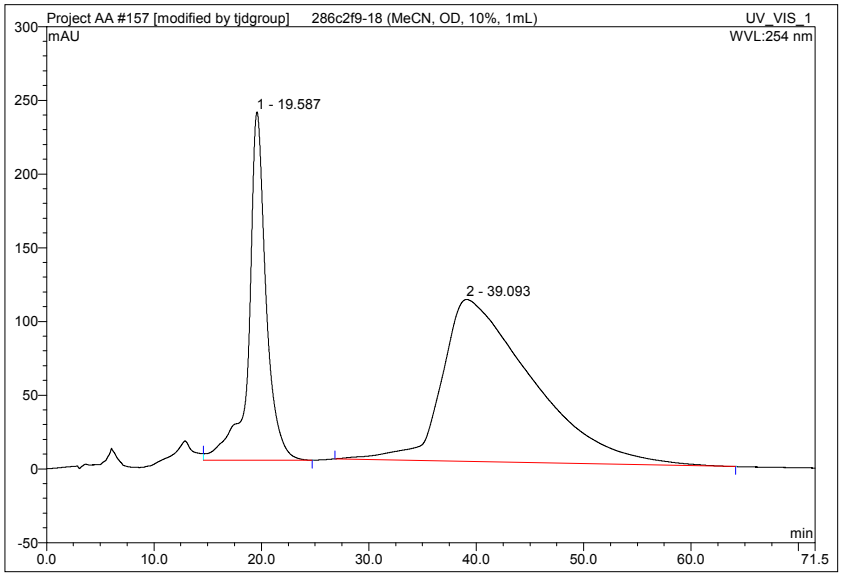

No.	Ret.Time min	Peak Name	Height mAU	Area mAU*min	Rel.Area %	Amount	Type
1	19.59	n.a.	236.202	442.127	29.22	n.a.	MB*
2	39.09	n.a.	109.858	1070.985	70.78	n.a.	BMB*
Total:			346.060	1513.112	100.00	0.000	

Figure A1-4. HPLC trace of enantiomerically enriched **2.47** (from phosphino hydrazone **2.63**) Chiral HPLC (Chiralpak OD, 10 % IPA in heptane, 1.0 mL/min, λ = 254 nm) t_R (major) = 39.1 min, t_R (minor) = 19.6 min.

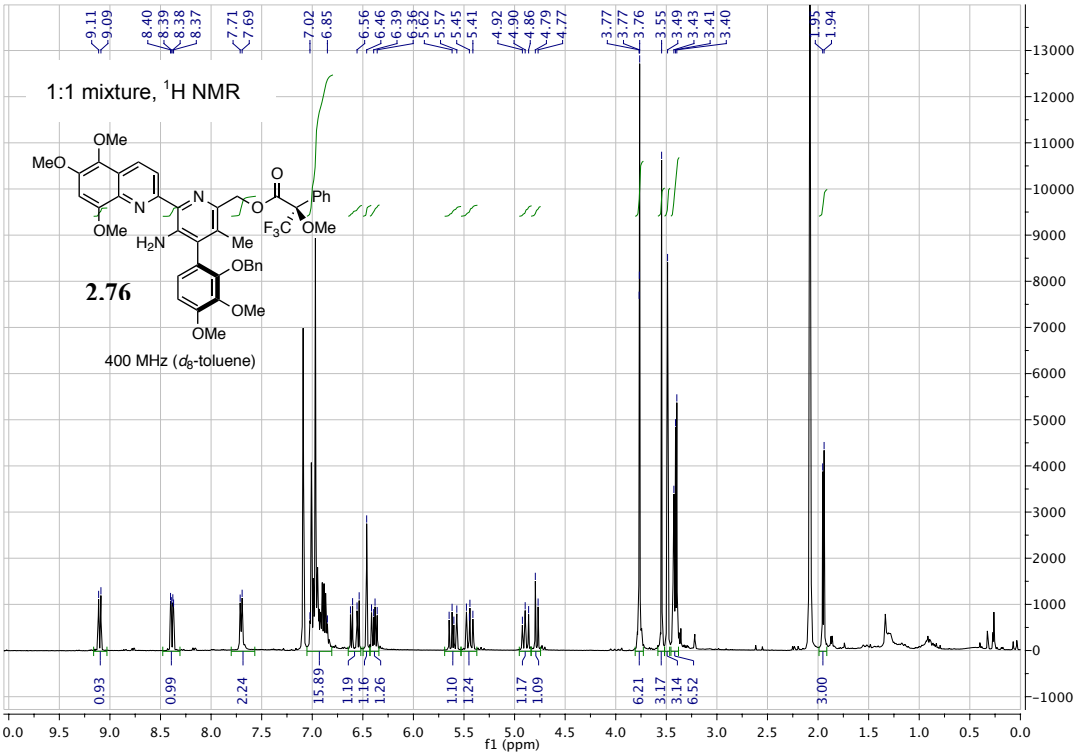
1:1 mixture, ^{1}H NMR
2.76
400 MHz (d_8-toluene)
f1 (ppm)

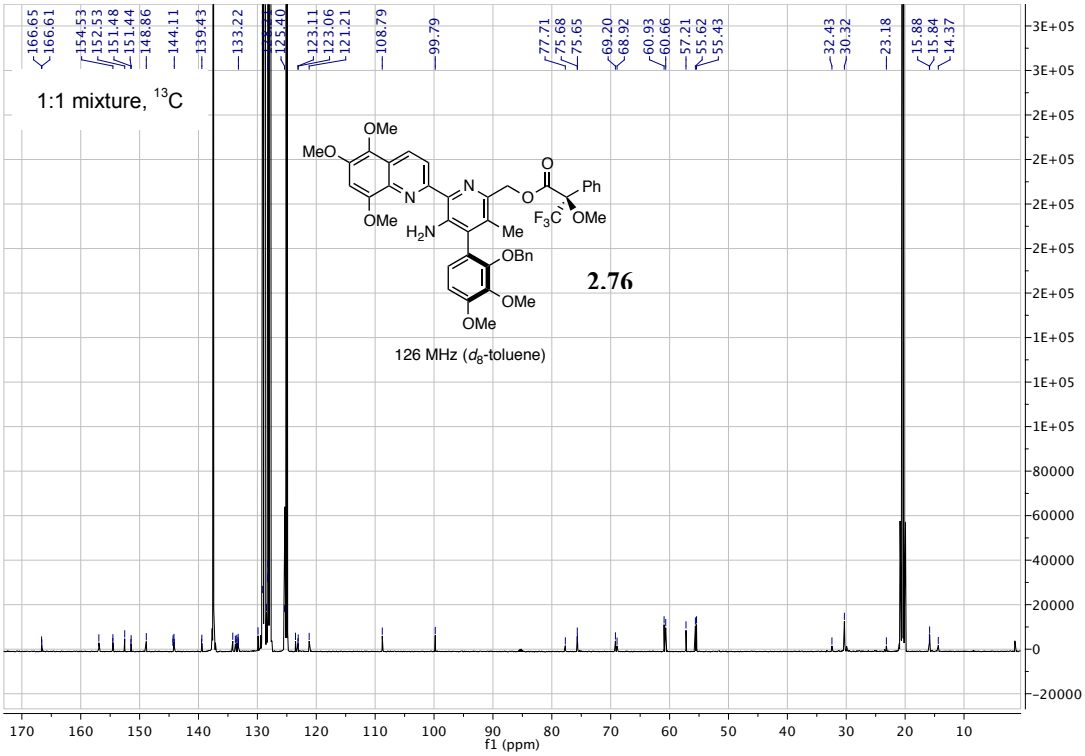
1:1 mixture, ^{13}C
2.76
126 MHz (d_8-toluene)
f1 (ppm)

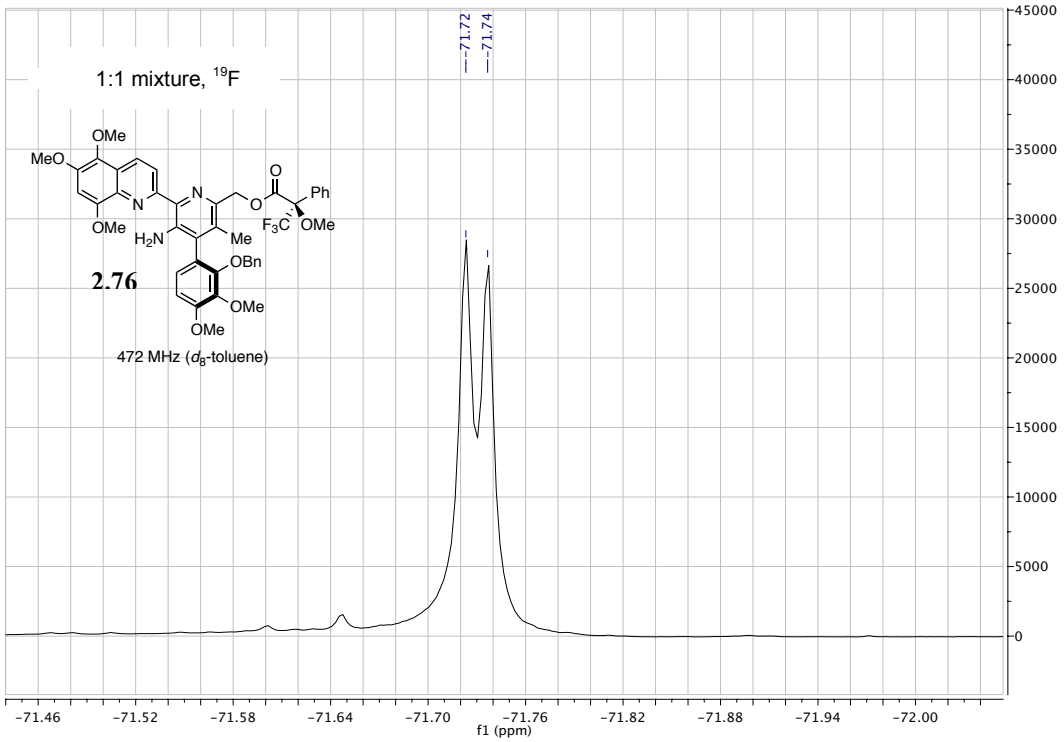
1:1 mixture, ^{19}F
OMe
MeO
OMe
N
N
O
O
Ph
F_3C
OMe
H_2N
Me
OBn
OMe
OMe
2.76
472 MHz (d_8-toluene)
-71.72
-71.74
45000
40000
35000
30000
25000
20000
15000
10000
5000
0
-71.46
-71.52
-71.58
-71.64
-71.70
-71.76
-71.82
-71.88
-71.94
-72.00
f1 (ppm)

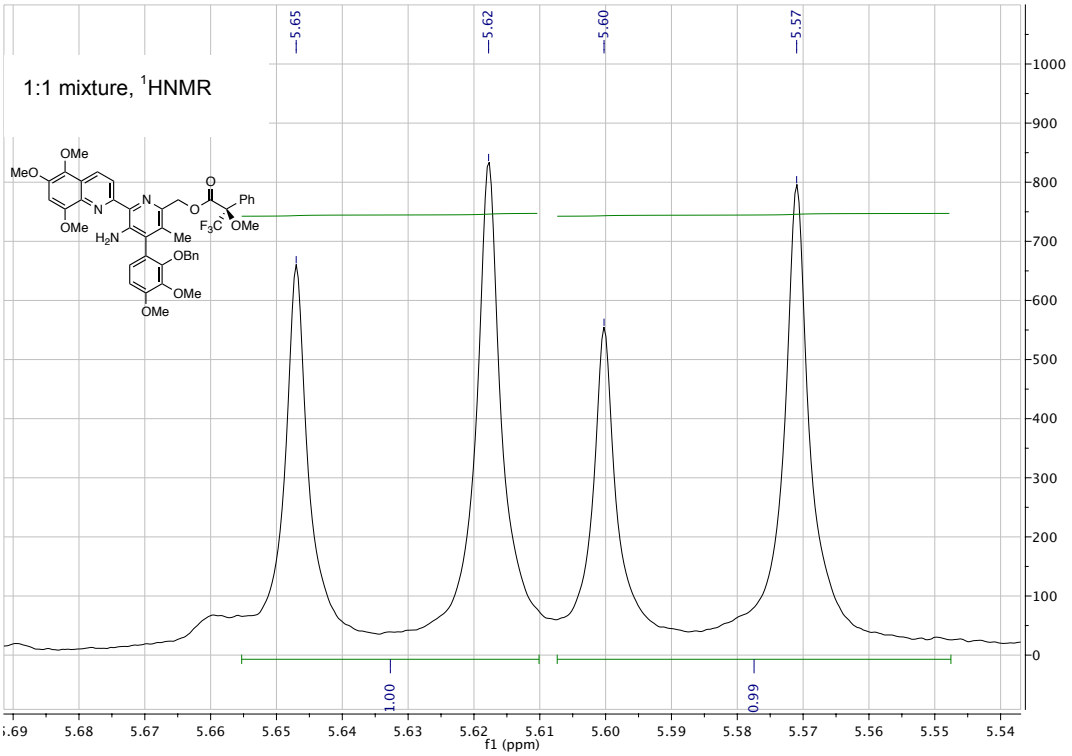
1:1 mixture, ^{1}HNMR
5.65
5.62
5.60
5.57
1.00
0.99
f1 (ppm)

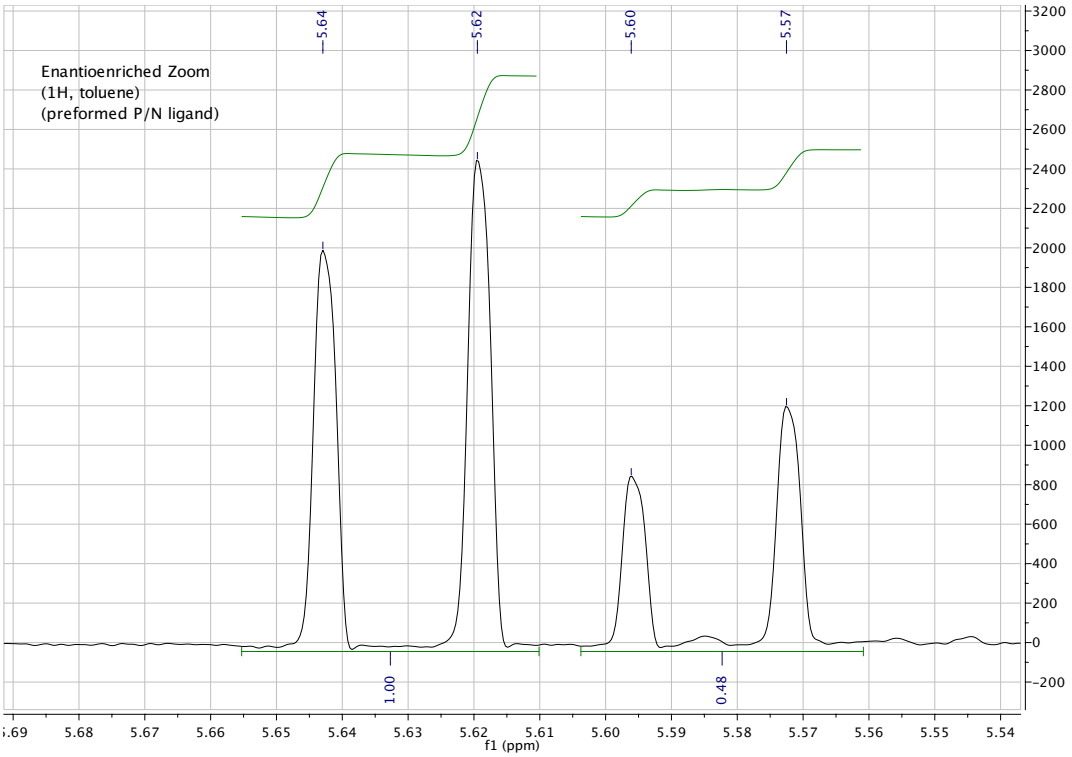
Enantioenriched Zoom
(1H, toluene)
(preformed P/N ligand)
5.64
5.62
5.60
5.57
1.00
0.48
f1 (ppm)

Appendix 2
Additional gel-based ABPP assays

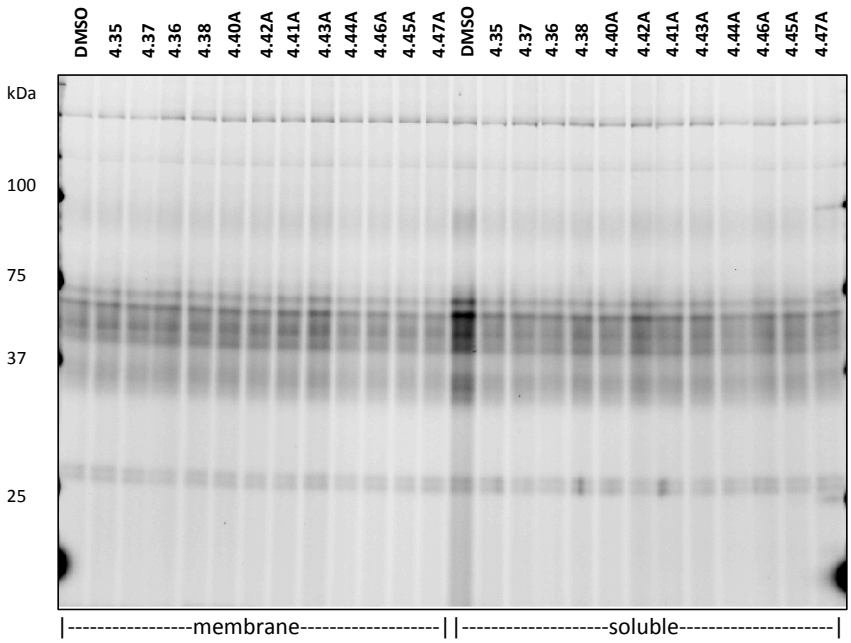

Figure A2-1. Competitive gel-based ABPP of benzothiadiazin-3-one 1,1-dioxides. Mouse brain membrane (left) and soluble (right) proteomes treated with compounds (all at 50 μM, 30 min incubation) then ATP-biotin (with KiNativ™ kit). Fluorescent images shown in gray;

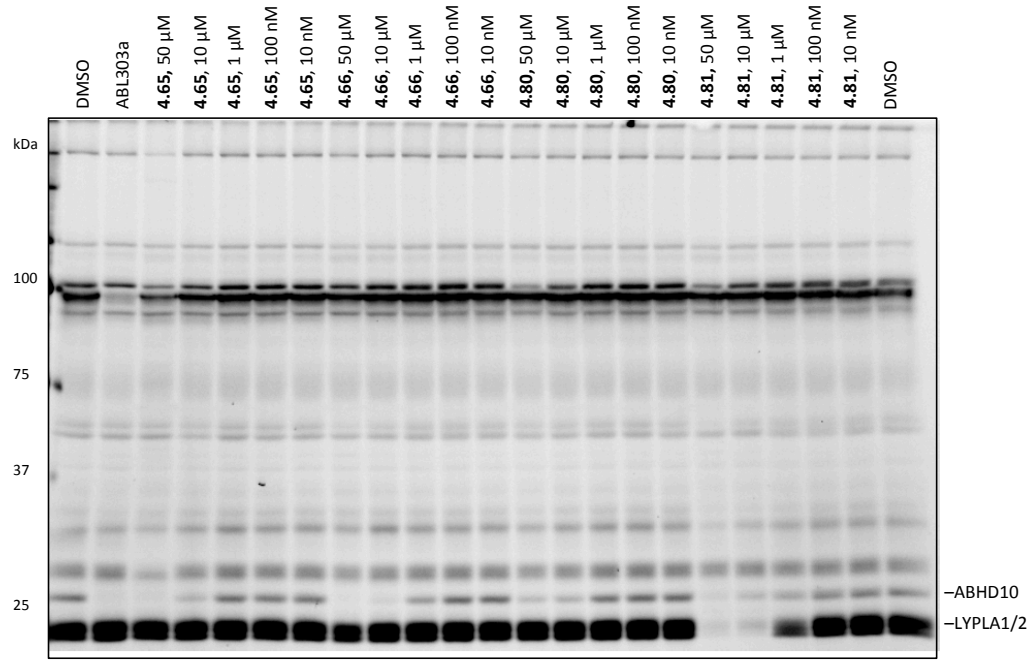

Figure A2-2. Competitive gel-based ABPP of benzoxathiazin-3-one 1,1-dioxides. Mouse brain soluble proteome fractions treated with compounds (with R^1 = H or CN, at 0.01–50 μM, 30 min incubation) then FP-rhodamine (1 μM, 30 min). Fluorescent images shown in gray;

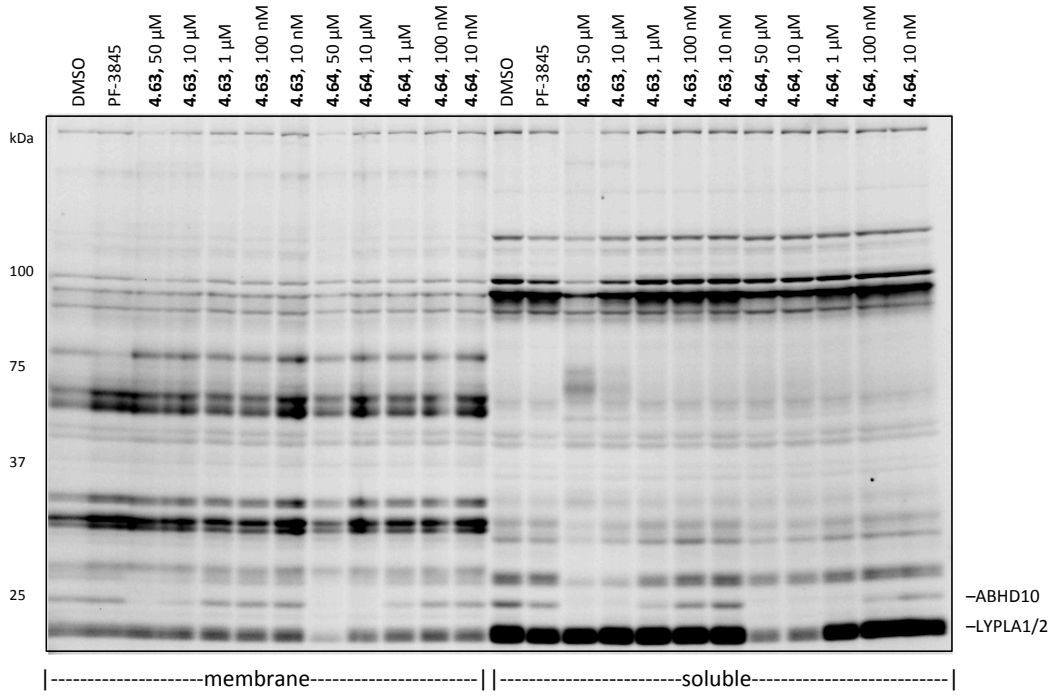

Figure A11-3. Competitive gel-based ABPP of benzoxathiazin-3-one 1,1-dioxides. Mouse brain membrane and soluble proteome fractions treated with compounds (with R^1 = Br, at 0.01–50 µM, 30 min incubation) then FP-rhodamine (1 µM, 30 min). Fluorescent images shown in gray;

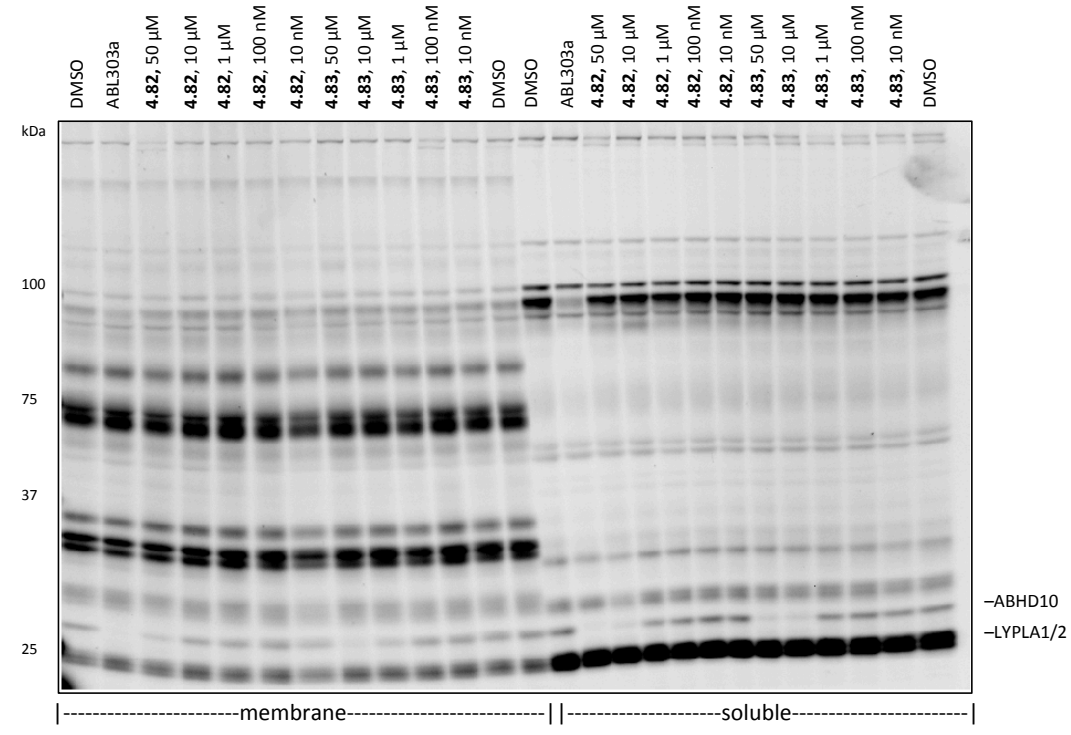

Figure A2-4. Competitive gel-based ABPP of benzoxathiazin-3-one 1,1-dioxides. Mouse brain membrane and soluble proteome fractions treated with compounds (with R^1 = OCH_3, at 0.01–50 µM, 30 min incubation) then FP-rhodamine (1 µM, 30 min). Fluorescent images shown in gray;

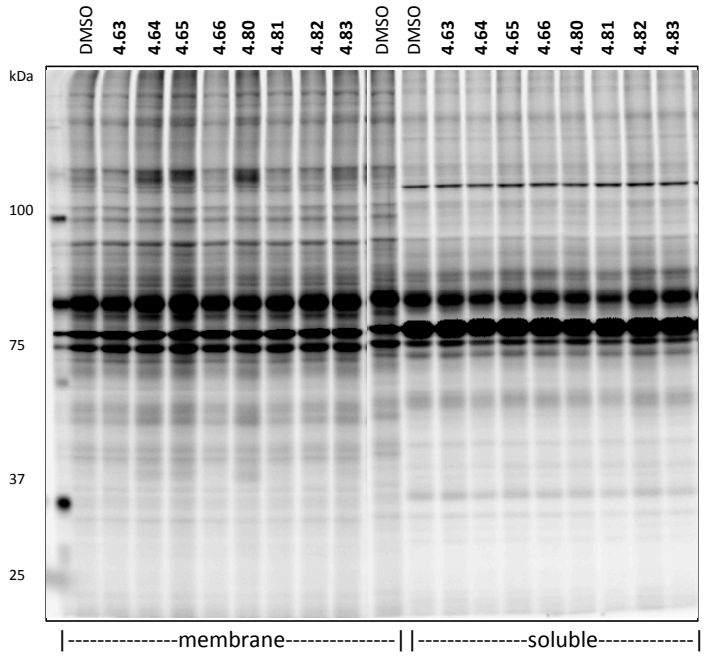

Figure A12-5. Competitive gel-based ABPP of benzoxathiazin-3-one 1,1-dioxides. Mouse brain membrane and soluble proteome fractions treated with compounds (all at 20 μM, 30 min incubation) then IA-rhodamine (1 μM, 30 min). Fluorescent images shown in gray;

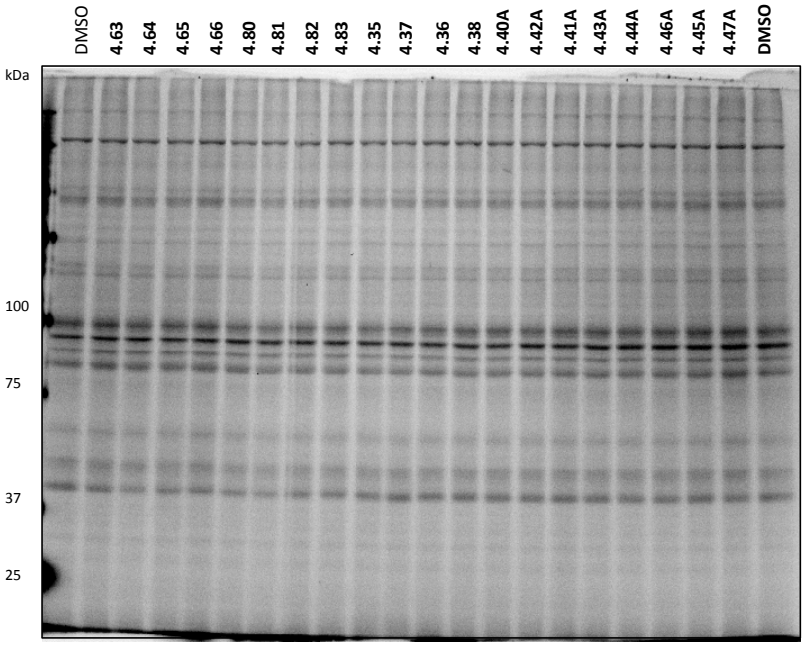

Figure A2-6. Competitive gel-based ABPP of benzothiadiazin-3-one 1,1-dioxides and benzoxathiazin-3-one 1,1-dioxides. Mouse brain membrane proteome fractions treated with compounds (all at 20 μM, 30 min incubation) then AlexaFluor (10 μM, 30 min). Fluorescent images shown in gray;

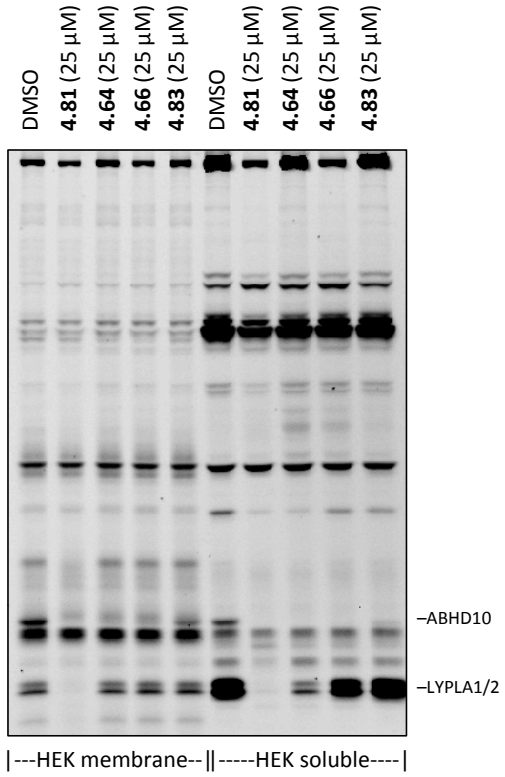

Figure A2-7. In vitro analysis of lead compounds (**4.83**, **4.66**, **4.81**) as well as **4.64** ($Br/(CH_2)_5Ph$ compound) with membrane and soluble proteome from HEK cell lysates; Proteome samples were treated with compounds (25 µM for 30 min) then FP-rhodamine (1 µM, 30 min).

Appendix 3
X-ray crystallography data

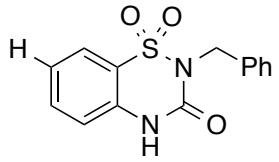

Compound 4.40A
CCDC 1501165
Data obtained by Arnold L. Rheingold, *UCSD Crystallography Lab*

Crystal data

Identification code	boger08	
Empirical formula	$C_{14}H_{12}N_2O_3S$	
Formula weight	288.32	
Temperature	100(2) K	
Wavelength	0.71073 Å	
Crystal system	Monoclinic	
Space group	P c	
Unit cell dimensions	a = 12.916(3) Å	α = 90°.
	b = 7.5579(17) Å	β = 99.551(9)°.
	c = 25.872(5) Å	γ = 90°.
Volume	2490.5(9) $Å^3$	
Z	8	
Density (calculated)	1.538 Mg/m^3	
Absorption coefficient	0.269 mm^{-1}	
F(000)	1200	
Crystal size	0.280 x 0.080 x 0.030 mm^3	
Theta range for data collection	1.596 to 25.735°.	
Index ranges	-15<=h<=15, -9<=k<=7, -31<=l<=24	
Reflections collected	11508	
Independent reflections	6994 [R(int) = 0.0644]	
Completeness to theta = 25.000°	99.9 %	
Absorption correction	Multi-scan	
Refinement method	Full-matrix least-squares on F^2	
Data / restraints / parameters	6994 / 2 / 679	
Goodness-of-fit on F^2	1.116	
Final R indices [I>2sigma(I)]	R1 = 0.0849, wR2 = 0.2013	
R indices (all data)	R1 = 0.1230, wR2 = 0.2263	
Absolute structure parameter	0.51(16)	
Extinction coefficient	n/a	
Largest diff. peak and hole	1.945 and -0.549 e. $Å^{-3}$	

Table 2. Atomic coordinates (x 10^4) and equivalent isotropic displacement parameters ($Å^2$ x 10^3) for boger08. U(eq) is defined as one third of the trace of the orthogonalized U^{ij} tensor.

	x	y	z	U(eq)
S(1A)	1511(2)	4458(4)	4874(1)	25(1)
S(1B)	5676(2)	9323(4)	3364(1)	25(1)
S(1C)	8479(2)	2903(4)	5145(1)	23(1)
S(1D)	4349(2)	8097(4)	6667(1)	27(1)
O(1A)	674(6)	5710(11)	4807(3)	28(2)
O(1B)	5815(7)	10578(13)	2973(3)	35(2)
O(1D)	4786(7)	9806(11)	6793(3)	29(2)
O(1C)	9308(7)	1621(12)	5213(3)	30(2)
O(2A)	1319(6)	2772(11)	4626(3)	24(2)
O(2B)	5218(7)	7671(11)	3205(3)	29(2)
O(2D)	4265(7)	6873(12)	7077(3)	30(2)
O(2C)	8663(7)	4576(11)	5389(4)	27(2)
O(3D)	5730(8)	7324(12)	5510(4)	23(2)
O(3C)	5771(7)	2343(12)	5496(4)	24(2)
O(3A)	4198(7)	4977(12)	4525(4)	20(2)
O(3B)	4220(7)	9960(12)	4512(4)	20(2)
N(1A)	3733(8)	3717(14)	5251(4)	26(3)
N(1B)	5777(8)	8599(14)	4486(4)	26(2)
N(1C)	6264(8)	3680(15)	4776(4)	27(2)
N(1D)	4198(9)	8743(14)	5539(4)	29(3)
N(2C)	7454(8)	1959(14)	5353(4)	24(2)
N(2D)	5050(8)	7085(14)	6264(4)	24(2)
N(2B)	4967(8)	10292(14)	3768(4)	25(2)
N(2A)	2543(8)	5430(14)	4672(4)	23(2)
C(1A)	2055(10)	4182(15)	5536(5)	17(3)
C(1D)	3197(11)	8368(17)	6240(6)	24(3)
C(1C)	8001(12)	3242(18)	4513(6)	30(3)
C(1B)	6837(10)	8977(18)	3799(6)	30(3)
C(2B)	7786(10)	8976(17)	3604(6)	22(3)
C(2C)	8627(10)	3207(17)	4093(5)	18(3)
C(2A)	1439(13)	4120(20)	5921(8)	43(5)
C(2D)	2190(16)	8400(20)	6413(7)	48(5)
C(3B)	8706(10)	8365(18)	4001(6)	23(3)
C(3C)	8094(14)	3770(20)	3576(5)	34(4)
C(3A)	1816(11)	3688(17)	6398(6)	25(3)
C(3D)	1345(12)	8891(18)	6111(6)	31(4)
C(4C)	7122(12)	4282(17)	3501(6)	30(3)
C(4B)	8587(11)	7917(17)	4482(6)	29(3)
C(4A)	2886(11)	3127(17)	6535(5)	25(3)
C(4D)	1389(12)	9398(17)	5587(6)	32(3)
C(5D)	2316(10)	9362(16)	5422(6)	25(2)
C(5A)	3498(10)	3159(16)	6148(6)	25(2)
C(5B)	7641(10)	7984(17)	4660(5)	20(3)
C(5C)	6485(12)	4287(19)	3875(5)	28(3)

C(6C)	6867(11)	3722(17)	4366(6)	22(3)
C(6B)	6734(10)	8556(17)	4303(5)	19(2)
C(6D)	3196(12)	8822(18)	5715(6)	25(3)
C(6A)	3074(10)	3706(17)	5635(5)	19(2)
C(7D)	5054(11)	7754(17)	5758(5)	29(3)
C(7C)	6463(10)	2688(16)	5221(5)	26(3)
C(7A)	3534(11)	4709(16)	4798(5)	26(3)
C(7B)	4951(10)	9640(17)	4264(5)	24(3)
C(8C)	7653(10)	657(17)	5799(5)	25(3)
C(8A)	2318(9)	6714(16)	4225(5)	26(3)
C(8D)	5863(10)	5776(17)	6473(5)	26(3)
C(8B)	4148(10)	11610(17)	3544(5)	27(3)
C(9C)	7848(10)	1419(17)	6321(5)	21(3)
C(9D)	6930(10)	6558(18)	6641(5)	20(2)
C(9B)	3017(12)	10849(19)	3354(5)	24(3)
C(9A)	2069(10)	5902(17)	3689(5)	20(2)
C(10A)	1070(11)	5356(19)	3510(5)	25(3)
C(10B)	2824(10)	10029(18)	2889(6)	21(3)
C(10D)	7233(15)	7390(19)	7135(6)	34(4)
C(10C)	8851(12)	2039(17)	6540(6)	24(3)
C(11A)	839(13)	4661(19)	3012(6)	25(2)
C(11D)	8238(12)	8004(19)	7264(5)	25(2)
C(11B)	1787(11)	9500(18)	2661(5)	23(3)
C(11C)	9089(13)	2813(18)	7037(6)	26(3)
C(12B)	1028(12)	9705(19)	3002(6)	29(3)
C(12C)	8305(13)	2920(20)	7304(6)	30(2)
C(12A)	1615(13)	4440(19)	2670(6)	30(2)
C(12D)	9005(14)	7790(20)	6988(7)	34(4)
C(13B)	1250(13)	10435(19)	3493(6)	27(3)
C(13A)	2655(12)	5018(19)	2897(6)	27(2)
C(13D)	8729(11)	6906(18)	6506(6)	27(2)
C(13C)	7316(13)	2324(19)	7151(6)	29(3)
C(14D)	7709(10)	6273(17)	6330(5)	21(3)
C(14A)	2829(10)	5768(18)	3371(5)	23(3)
C(14C)	7026(12)	1620(20)	6630(6)	27(3)
C(14B)	2243(12)	10992(19)	3658(6)	27(3)

Table 3. Bond lengths [Å] and angles [°] for boger08.

S(1A)-O(1A)	1.425(8)	S(1C)-O(1C)	1.433(9)
S(1A)-O(2A)	1.430(9)	S(1C)-C(1C)	1.667(15)
S(1A)-N(2A)	1.681(10)	S(1C)-N(2C)	1.671(10)
S(1A)-C(1A)	1.752(12)	S(1D)-O(1D)	1.426(9)
S(1B)-O(2B)	1.413(9)	S(1D)-O(2D)	1.426(9)
S(1B)-O(1B)	1.421(9)	S(1D)-N(2D)	1.674(10)
S(1B)-N(2B)	1.668(10)	S(1D)-C(1D)	1.711(14)
S(1B)-C(1B)	1.738(14)	O(3D)-C(7D)	1.210(16)
S(1C)-O(2C)	1.416(9)	O(3C)-C(7C)	1.260(16)

O(3A)-C(7A)	1.215(15)	C(9B)-C(10B)	1.34(2)
O(3B)-C(7B)	1.248(15)	C(9B)-C(14B)	1.38(2)
N(1A)-C(7A)	1.380(16)	C(9A)-C(10A)	1.360(19)
N(1A)-C(6A)	1.410(16)	C(9A)-C(14A)	1.384(18)
N(1B)-C(7B)	1.373(16)	C(10A)-C(11A)	1.38(2)
N(1B)-C(6B)	1.395(17)	C(10B)-C(11B)	1.427(19)
N(1C)-C(7C)	1.361(17)	C(10D)-C(11D)	1.37(2)
N(1C)-C(6C)	1.416(17)	C(10C)-C(11C)	1.40(2)
N(1D)-C(7D)	1.377(18)	C(11A)-C(12A)	1.45(2)
N(1D)-C(6D)	1.443(18)	C(11D)-C(12D)	1.32(2)
N(2C)-C(7C)	1.382(16)	C(11B)-C(12B)	1.43(2)
N(2C)-C(8C)	1.505(16)	C(11C)-C(12C)	1.32(2)
N(2D)-C(7D)	1.405(16)	C(12B)-C(13B)	1.37(2)
N(2D)-C(8D)	1.477(16)	C(12C)-C(13C)	1.35(2)
N(2B)-C(7B)	1.379(16)	C(12A)-C(13A)	1.44(2)
N(2B)-C(8B)	1.497(15)	C(12D)-C(13D)	1.41(2)
N(2A)-C(7A)	1.379(16)	C(13B)-C(14B)	1.35(2)
N(2A)-C(8A)	1.500(15)	C(13A)-C(14A)	1.34(2)
C(1A)-C(6A)	1.347(18)	C(13D)-C(14D)	1.405(19)
C(1A)-C(2A)	1.37(2)	C(13C)-C(14C)	1.44(2)
C(1D)-C(6D)	1.40(2)	O(1A)-S(1A)-O(2A)	117.8(5)
C(1D)-C(2D)	1.44(2)	O(1A)-S(1A)-N(2A)	107.3(5)
C(1C)-C(2C)	1.458(18)	O(2A)-S(1A)-N(2A)	109.7(5)
C(1C)-C(6C)	1.50(2)	O(1A)-S(1A)-C(1A)	111.8(6)
C(1B)-C(6B)	1.37(2)	O(2A)-S(1A)-C(1A)	110.1(5)
C(1B)-C(2B)	1.402(18)	N(2A)-S(1A)-C(1A)	98.4(5)
C(2B)-C(3B)	1.508(19)	O(2B)-S(1B)-O(1B)	118.6(6)
C(2C)-C(3C)	1.464(19)	O(2B)-S(1B)-N(2B)	108.9(6)
C(2A)-C(3A)	1.29(2)	O(1B)-S(1B)-N(2B)	107.5(5)
C(2D)-C(3D)	1.29(2)	O(2B)-S(1B)-C(1B)	109.3(6)
C(3B)-C(4B)	1.32(2)	O(1B)-S(1B)-C(1B)	111.4(6)
C(3C)-C(4C)	1.30(2)	N(2B)-S(1B)-C(1B)	99.5(6)
C(3A)-C(4A)	1.432(18)	O(2C)-S(1C)-O(1C)	118.8(6)
C(3D)-C(4D)	1.42(2)	O(2C)-S(1C)-C(1C)	107.9(6)
C(4C)-C(5C)	1.369(19)	O(1C)-S(1C)-C(1C)	111.8(6)
C(4B)-C(5B)	1.376(18)	O(2C)-S(1C)-N(2C)	108.7(5)
C(4A)-C(5A)	1.376(19)	O(1C)-S(1C)-N(2C)	106.7(5)
C(4D)-C(5D)	1.337(19)	C(1C)-S(1C)-N(2C)	101.4(7)
C(5D)-C(6D)	1.32(2)	O(1D)-S(1D)-O(2D)	119.6(6)
C(5A)-C(6A)	1.412(19)	O(1D)-S(1D)-N(2D)	108.7(5)
C(5B)-C(6B)	1.433(18)	O(2D)-S(1D)-N(2D)	106.4(5)
C(5C)-C(6C)	1.35(2)	O(1D)-S(1D)-C(1D)	108.0(6)
C(8C)-C(9C)	1.451(19)	O(2D)-S(1D)-C(1D)	113.1(6)
C(8A)-C(9A)	1.503(19)	N(2D)-S(1D)-C(1D)	99.0(6)
C(8D)-C(9D)	1.496(18)	C(7A)-N(1A)-C(6A)	123.5(11)
C(8B)-C(9B)	1.571(19)	C(7B)-N(1B)-C(6B)	122.9(11)
C(9C)-C(10C)	1.41(2)	C(7C)-N(1C)-C(6C)	126.5(11)
C(9C)-C(14C)	1.438(18)	C(7D)-N(1D)-C(6D)	126.4(12)
C(9D)-C(14D)	1.406(18)	C(7C)-N(2C)-C(8C)	119.0(10)
C(9D)-C(10D)	1.42(2)	C(7C)-N(2C)-S(1C)	120.0(9)

C(8C)-N(2C)-S(1C)	118.9(8)	C(5A)-C(6A)-N(1A)	118.6(11)
C(7D)-N(2D)-C(8D)	118.0(10)	O(3D)-C(7D)-N(1D)	121.9(12)
C(7D)-N(2D)-S(1D)	120.1(9)	O(3D)-C(7D)-N(2D)	120.8(12)
C(8D)-N(2D)-S(1D)	120.3(8)	N(1D)-C(7D)-N(2D)	116.9(12)
C(7B)-N(2B)-C(8B)	118.6(10)	O(3C)-C(7C)-N(1C)	122.7(12)
C(7B)-N(2B)-S(1B)	121.4(8)	O(3C)-C(7C)-N(2C)	119.4(12)
C(8B)-N(2B)-S(1B)	118.4(8)	N(1C)-C(7C)-N(2C)	117.8(11)
C(7A)-N(2A)-C(8A)	119.4(10)	O(3A)-C(7A)-N(1A)	122.3(12)
C(7A)-N(2A)-S(1A)	120.5(9)	O(3A)-C(7A)-N(2A)	120.9(11)
C(8A)-N(2A)-S(1A)	117.4(8)	N(1A)-C(7A)-N(2A)	116.8(11)
C(6A)-C(1A)-C(2A)	121.3(13)	O(3B)-C(7B)-N(1B)	120.0(11)
C(6A)-C(1A)-S(1A)	116.0(10)	O(3B)-C(7B)-N(2B)	122.5(11)
C(2A)-C(1A)-S(1A)	121.7(11)	N(1B)-C(7B)-N(2B)	117.5(10)
C(6D)-C(1D)-C(2D)	116.2(14)	C(9C)-C(8C)-N(2C)	115.7(11)
C(6D)-C(1D)-S(1D)	121.0(11)	N(2A)-C(8A)-C(9A)	115.6(10)
C(2D)-C(1D)-S(1D)	122.2(13)	N(2D)-C(8D)-C(9D)	113.9(11)
C(2C)-C(1C)-C(6C)	117.1(12)	N(2B)-C(8B)-C(9B)	116.0(10)
C(2C)-C(1C)-S(1C)	124.5(11)	C(10C)-C(9C)-C(14C)	117.1(13)
C(6C)-C(1C)-S(1C)	118.3(11)	C(10C)-C(9C)-C(8C)	120.9(12)
C(6B)-C(1B)-C(2B)	124.9(13)	C(14C)-C(9C)-C(8C)	121.9(12)
C(6B)-C(1B)-S(1B)	116.2(10)	C(14D)-C(9D)-C(10D)	117.8(13)
C(2B)-C(1B)-S(1B)	118.6(11)	C(14D)-C(9D)-C(8D)	119.0(12)
C(1B)-C(2B)-C(3B)	113.1(12)	C(10D)-C(9D)-C(8D)	122.7(13)
C(1C)-C(2C)-C(3C)	116.1(12)	C(10B)-C(9B)-C(14B)	120.3(14)
C(3A)-C(2A)-C(1A)	121.9(15)	C(10B)-C(9B)-C(8B)	118.4(13)
C(3D)-C(2D)-C(1D)	122.1(16)	C(14B)-C(9B)-C(8B)	121.3(12)
C(4B)-C(3B)-C(2B)	121.2(13)	C(10A)-C(9A)-C(14A)	120.1(13)
C(4C)-C(3C)-C(2C)	121.3(13)	C(10A)-C(9A)-C(8A)	119.0(12)
C(2A)-C(3A)-C(4A)	120.5(14)	C(14A)-C(9A)-C(8A)	120.9(12)
C(2D)-C(3D)-C(4D)	119.7(14)	C(9A)-C(10A)-C(11A)	118.7(14)
C(3C)-C(4C)-C(5C)	125.2(14)	C(9B)-C(10B)-C(11B)	121.6(13)
C(3B)-C(4B)-C(5B)	123.5(13)	C(11D)-C(10D)-C(9D)	118.5(14)
C(5A)-C(4A)-C(3A)	117.5(12)	C(11C)-C(10C)-C(9C)	123.9(14)
C(5D)-C(4D)-C(3D)	118.7(15)	C(10A)-C(11A)-C(12A)	123.3(14)
C(6D)-C(5D)-C(4D)	123.5(15)	C(12D)-C(11D)-C(10D)	126.3(14)
C(4A)-C(5A)-C(6A)	120.6(12)	C(12B)-C(11B)-C(10B)	113.9(11)
C(4B)-C(5B)-C(6B)	118.2(12)	C(12C)-C(11C)-C(10C)	115.8(15)
C(6C)-C(5C)-C(4C)	119.6(14)	C(13B)-C(12B)-C(11B)	123.7(14)
C(5C)-C(6C)-N(1C)	123.4(13)	C(11C)-C(12C)-C(13C)	126.7(14)
C(5C)-C(6C)-C(1C)	120.3(13)	C(13A)-C(12A)-C(11A)	114.1(12)
N(1C)-C(6C)-C(1C)	116.2(12)	C(11D)-C(12D)-C(13D)	115.8(15)
C(1B)-C(6B)-N(1B)	123.3(12)	C(14B)-C(13B)-C(12B)	117.4(15)
C(1B)-C(6B)-C(5B)	119.1(12)	C(14A)-C(13A)-C(12A)	120.4(13)
N(1B)-C(6B)-C(5B)	117.6(11)	C(12D)-C(13D)-C(14D)	122.3(14)
C(5D)-C(6D)-C(1D)	119.7(13)	C(12C)-C(13C)-C(14C)	118.9(14)
C(5D)-C(6D)-N(1D)	124.1(13)	C(13D)-C(14D)-C(9D)	119.0(13)
C(1D)-C(6D)-N(1D)	116.1(14)	C(13A)-C(14A)-C(9A)	123.2(14)
C(1A)-C(6A)-C(5A)	118.1(12)	C(9C)-C(14C)-C(13C)	117.3(14)
C(1A)-C(6A)-N(1A)	123.3(12)	C(13B)-C(14B)-C(9B)	122.5(14)

Table 4. Anisotropic displacement parameters ($Å^2$ x 10^3) for boger08. The anisotropic displacement factor exponent takes the form: $-2\pi^2[h^2 a^{*2} U^{11} + ... + 2 h k a^* b^* U^{12}]$

	U^{11}	U^{22}	U^{33}	U^{23}	U^{13}	U^{12}
S(1A)	23(2)	24(2)	29(2)	-1(1)	6(1)	2(1)
S(1B)	27(2)	24(2)	25(2)	2(1)	7(1)	1(1)
S(1C)	20(2)	21(2)	28(2)	0(1)	8(1)	2(1)
S(1D)	26(2)	26(2)	30(2)	2(1)	8(2)	3(1)
O(1A)	20(4)	26(5)	39(5)	-1(4)	4(4)	5(4)
O(1B)	39(5)	41(6)	27(5)	2(4)	15(4)	4(4)
O(1D)	30(5)	23(5)	33(5)	-4(4)	4(4)	-1(4)
O(1C)	26(5)	30(5)	35(5)	0(4)	9(4)	2(4)
O(2A)	26(5)	20(5)	25(4)	-1(4)	0(4)	-8(3)
O(2B)	26(5)	26(5)	32(5)	2(4)	0(4)	3(4)
O(2D)	39(5)	22(5)	32(5)	6(4)	13(4)	6(4)
O(2C)	21(4)	23(5)	37(5)	-4(4)	8(4)	-1(3)
O(3D)	29(6)	21(5)	19(5)	2(4)	3(5)	-13(4)
O(3C)	17(5)	21(5)	32(5)	3(4)	0(5)	-9(4)
O(3A)	18(4)	22(4)	23(4)	9(3)	11(4)	15(3)
O(3B)	18(4)	22(4)	23(4)	9(3)	11(4)	15(3)
N(1A)	28(6)	24(6)	28(6)	6(5)	10(5)	2(5)
N(1B)	20(6)	30(7)	30(6)	4(5)	10(5)	4(5)
N(1C)	26(6)	28(7)	28(6)	-2(5)	12(5)	-1(5)
N(1D)	32(6)	21(6)	37(7)	-3(5)	10(5)	2(5)
N(2C)	21(5)	19(6)	33(6)	1(5)	7(5)	-3(4)
N(2D)	25(5)	30(6)	18(5)	-3(5)	5(4)	0(5)
N(2B)	22(5)	26(6)	25(5)	2(5)	2(5)	8(5)
N(2A)	22(5)	22(6)	24(5)	3(5)	4(4)	3(4)
C(1A)	17(6)	16(6)	19(6)	-1(5)	5(5)	4(5)
C(1D)	33(8)	8(6)	29(7)	7(6)	-2(6)	-1(5)
C(1C)	35(8)	20(7)	36(8)	-10(6)	5(7)	-1(6)
C(1B)	23(7)	22(7)	44(9)	2(6)	7(7)	10(6)
C(2B)	13(6)	19(7)	32(7)	6(6)	-1(6)	6(5)
C(2C)	27(7)	18(7)	11(6)	-3(5)	12(5)	0(5)
C(2A)	32(9)	8(8)	91(14)	-9(8)	13(10)	2(6)
C(2D)	76(13)	27(9)	51(10)	-15(8)	41(11)	-23(9)
C(3B)	11(6)	20(7)	37(8)	-8(6)	3(6)	3(5)
C(3C)	67(11)	32(9)	4(6)	-4(6)	7(7)	-6(8)
C(3A)	26(7)	14(7)	38(8)	1(6)	12(7)	4(6)
C(3D)	37(8)	19(8)	42(9)	16(7)	14(7)	8(6)
C(4C)	39(9)	21(8)	29(8)	2(6)	4(7)	-1(6)
C(4B)	30(8)	19(7)	35(8)	11(6)	-3(7)	0(5)
C(4A)	30(7)	24(7)	22(7)	-1(6)	5(6)	-2(6)
C(4D)	31(8)	17(7)	49(9)	-8(7)	11(7)	3(6)
C(5D)	21(5)	9(4)	40(6)	-1(4)	-9(4)	0(3)
C(5A)	21(5)	9(4)	40(6)	-1(4)	-9(4)	0(3)
C(5B)	21(6)	26(7)	12(5)	-3(5)	3(5)	2(5)
C(5C)	35(8)	32(8)	17(6)	-1(6)	4(6)	-5(6)
C(6C)	30(7)	8(6)	30(7)	-5(5)	13(6)	-2(5)

C(6B)	19(4)	18(5)	21(4)	-3(3)	2(4)	0(3)
C(6D)	35(7)	10(6)	34(7)	-9(5)	20(6)	-4(5)
C(6A)	19(4)	18(5)	21(4)	-3(3)	2(4)	0(3)
C(7D)	37(8)	21(7)	27(7)	0(6)	6(7)	0(6)
C(7C)	20(6)	15(7)	44(8)	-9(6)	6(6)	3(5)
C(7A)	32(7)	16(7)	27(7)	5(5)	1(6)	6(5)
C(7B)	17(6)	28(7)	29(7)	4(6)	6(6)	0(5)
C(8C)	25(6)	21(7)	31(7)	-2(6)	11(6)	3(5)
C(8A)	18(6)	14(6)	45(8)	5(6)	1(6)	3(5)
C(8D)	34(7)	27(7)	17(6)	2(5)	9(6)	0(6)
C(8B)	32(7)	20(7)	31(7)	3(6)	9(6)	3(6)
C(9C)	25(7)	11(6)	28(7)	3(5)	7(6)	-3(5)
C(9D)	20(5)	15(5)	25(5)	4(4)	4(4)	5(4)
C(9B)	37(8)	20(7)	13(6)	5(6)	-2(6)	3(6)
C(9A)	20(5)	15(5)	25(5)	4(4)	4(4)	5(4)
C(10A)	31(8)	32(8)	12(6)	3(6)	5(6)	-6(6)
C(10B)	16(6)	18(7)	31(7)	6(6)	8(6)	1(5)
C(10D)	65(11)	18(8)	21(7)	-6(6)	16(7)	6(7)
C(10C)	29(8)	9(7)	36(8)	4(6)	10(7)	9(5)
C(11A)	39(6)	17(5)	19(5)	0(4)	0(5)	4(4)
C(11D)	39(6)	17(5)	19(5)	0(4)	0(5)	4(4)
C(11B)	34(7)	25(7)	12(6)	-8(5)	8(5)	-4(5)
C(11C)	28(7)	12(7)	39(8)	8(6)	4(7)	3(5)
C(12B)	27(8)	21(8)	36(8)	-9(6)	-3(7)	-11(6)
C(12C)	47(5)	19(4)	21(4)	-4(3)	2(4)	6(4)
C(12A)	47(5)	19(4)	21(4)	-4(3)	2(4)	6(4)
C(12D)	34(9)	24(8)	43(9)	16(7)	7(8)	7(6)
C(13B)	34(8)	23(8)	25(7)	2(6)	3(7)	-12(6)
C(13A)	21(5)	20(5)	43(6)	12(5)	16(5)	13(4)
C(13D)	21(5)	20(5)	43(6)	12(5)	16(5)	13(4)
C(13C)	46(9)	18(7)	27(7)	11(6)	12(7)	11(6)
C(14D)	18(6)	19(7)	26(7)	-2(5)	5(6)	-8(5)
C(14A)	23(7)	18(7)	28(7)	9(6)	6(6)	7(5)
C(14C)	33(8)	20(7)	29(7)	4(6)	12(7)	3(6)
C(14B)	43(9)	17(7)	21(7)	0(6)	3(7)	14(6)

Table 5. Hydrogen coordinates ($x10^4$) and isotropic displacement parameters ($Å^2 x 10^3$)

	x	y	z	U(eq)
H(3D)	5573	7694	5201	34
H(3C)	5201	2815	5362	36
H(3A)	4751	4436	4650	30
H(3B)	4345	9470	4807	30
H(2BB)	7844	9325	3257	26
H(2CB)	9340	2838	4152	22
H(2AB)	715	4411	5834	52
H(2DB)	2149	8036	6761	57

H(3BA)	9382	8300	3904	27
H(3CA)	8468	3770	3289	41
H(3AA)	1381	3741	6659	30
H(3DA)	697	8917	6238	38
H(4CA)	6828	4682	3161	36
H(4BA)	9188	7529	4718	35
H(4AA)	3162	2747	6881	30
H(4DA)	772	9755	5358	39
H(5DA)	2344	9746	5075	29
H(5AA)	4214	2809	6226	29
H(5BA)	7590	7659	5009	23
H(5CA)	5779	4684	3790	34
H(8CA)	7038	-139	5774	30
H(8CB)	8266	-79	5753	30
H(8AA)	2935	7497	4235	31
H(8AB)	1718	7465	4281	31
H(8DA)	5906	4874	6199	31
H(8DB)	5645	5168	6776	31
H(8BA)	4386	12204	3244	33
H(8BB)	4102	12525	3813	33
H(10A)	543	5453	3724	30
H(10B)	3389	9794	2707	26
H(10C)	6748	7517	7372	40
H(10D)	9400	1924	6340	29
H(11A)	137	4309	2886	30
H(11B)	8402	8650	7582	30
H(11C)	1617	9052	2314	28
H(11D)	9772	3239	7173	32
H(12A)	331	9313	2881	35
H(12B)	8453	3462	7639	36
H(12C)	1452	3956	2328	36
H(12E)	9699	8197	7108	40
H(13A)	726	10544	3709	33
H(13B)	3220	4865	2708	32
H(13C)	9251	6733	6291	32
H(13D)	6819	2368	7384	35
H(14A)	7547	5661	6006	25
H(14B)	3507	6233	3497	27
H(14C)	6321	1308	6495	32
H(14D)	2412	11503	3997	33

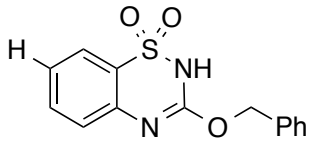

Compound 4.40B
CCDC 1501166
Data obtained by Arnold L. Rheingold, *UCSD Crystallography Lab*

Crystal Data

Identification code	boger07	
Empirical formula	$C_{14}H_{12}N_2O_3S$	
Formula weight	288.32	
Temperature	273(2) K	
Wavelength	0.71073 Å	
Crystal system	Monoclinic	
Space group	P 21/c	
Unit cell dimensions	a = 6.3237(14) Å	α = 90°.
	b = 13.019(3) Å	β = 91.713(14)°.
	c = 15.609(4) Å	γ = 90°.
Volume	1284.6(5) $Å^3$	
Z	4	
Density (calculated)	1.491 Mg/m^3	
Absorption coefficient	0.261 mm^{-1}	
F(000)	600	
Crystal size	0.450 x 0.080 x 0.030 mm^3	
Theta range for data collection	2.037 to 28.421°.	
Index ranges	-8<=h<=7, -14<=k<=17, -19<=l<=20	
Reflections collected	8811	
Independent reflections	3230 [R(int) = 0.0630]	
Completeness to theta = 25.000°	100.0 %	
Absorption correction	Multi-scan	
Refinement method	Full-matrix least-squares on F^2	
Data / restraints / parameters	3230 / 0 / 181	
Goodness-of-fit on F^2	0.986	
Final R indices [I>2sigma(I)]	R1 = 0.0503, wR2 = 0.1032	
R indices (all data)	R1 = 0.0990, wR2 = 0.1209	
Extinction coefficient	n/a	
Largest diff. peak and hole	0.389 and -0.433 $e.Å^{-3}$	

Table 2. Atomic coordinates ($x10^4$) and equivalent isotropic displacement parameters ($Å^3 \times 10^3$) for boger07. U(eq) is defined as one third of the trace of the orthogonalized U^{ij} tensor.

	x	y	z	U(eq)
S(1)	6150(1)	5196(1)	1921(1)	18(1)
O(1)	2553(2)	3006(1)	1281(1)	18(1)
O(2)	5153(3)	5825(1)	2559(1)	26(1)
O(3)	7303(3)	5741(1)	1285(1)	27(1)
N(1)	4371(3)	4510(1)	1450(1)	17(1)
N(2)	5393(3)	2957(1)	2135(1)	17(1)
C(1)	11122(4)	4009(2)	3203(2)	21(1)
C(2)	9782(4)	4686(2)	2793(2)	19(1)
C(3)	7851(4)	4339(2)	2444(1)	15(1)
C(4)	4150(3)	3540(2)	1625(2)	16(1)
C(5)	1107(4)	3549(2)	695(2)	18(1)
C(6)	-597(3)	2810(2)	423(2)	16(1)
C(7)	-2451(3)	3197(2)	39(2)	20(1)
C(8)	-4040(4)	2543(2)	-244(2)	24(1)
C(9)	-3817(4)	1496(2)	-153(2)	26(1)
C(10)	-1968(4)	1101(2)	222(2)	27(1)
C(11)	-374(4)	1750(2)	508(2)	22(1)
C(12)	7291(3)	3308(2)	2505(2)	15(1)
C(13)	8659(4)	2633(2)	2933(2)	17(1)
C(14)	10550(4)	2980(2)	3275(2)	19(1)

Table 3. Bond lengths [Å] and angles [°] for boger07.

S(1)-O(3)	1.4361(18)	C(12)-C(13)	1.391(3)
S(1)-O(2)	1.4478(19)	C(13)-C(14)	1.371(3)
S(1)-N(1)	1.5987(19)	O(3)-S(1)-O(2)	115.91(11)
S(1)-C(3)	1.737(2)	O(3)-S(1)-N(1)	108.87(11)
O(1)-C(4)	1.326(3)	O(2)-S(1)-N(1)	108.50(11)
O(1)-C(5)	1.456(3)	O(3)-S(1)-C(3)	108.80(11)
N(1)-C(4)	1.300(3)	O(2)-S(1)-C(3)	108.39(11)
N(2)-C(4)	1.338(3)	N(1)-S(1)-C(3)	105.91(11)
N(2)-C(12)	1.393(3)	C(4)-O(1)-C(5)	117.10(17)
C(1)-C(2)	1.369(3)	C(4)-N(1)-S(1)	121.69(17)
C(1)-C(14)	1.393(3)	C(4)-N(2)-C(12)	122.9(2)
C(2)-C(3)	1.397(3)	C(2)-C(1)-C(14)	119.9(2)
C(3)-C(12)	1.392(3)	C(1)-C(2)-C(3)	119.7(2)
C(5)-C(6)	1.497(3)	C(12)-C(3)-C(2)	120.5(2)
C(6)-C(11)	1.393(3)	C(12)-C(3)-S(1)	119.72(17)
C(6)-C(7)	1.395(3)	C(2)-C(3)-S(1)	119.82(18)
C(7)-C(8)	1.380(3)	N(1)-C(4)-O(1)	120.6(2)
C(8)-C(9)	1.377(4)	N(1)-C(4)-N(2)	127.6(2)
C(9)-C(10)	1.391(3)	O(1)-C(4)-N(2)	111.73(19)
C(10)-C(11)	1.379(3)	O(1)-C(5)-C(6)	107.39(18)

C(11)-C(6)-C(7)	118.7(2)	C(10)-C(11)-C(6)	120.4(2)
C(11)-C(6)-C(5)	122.7(2)	C(13)-C(12)-C(3)	119.1(2)
C(7)-C(6)-C(5)	118.5(2)	C(13)-C(12)-N(2)	120.5(2)
C(8)-C(7)-C(6)	120.6(2)	C(3)-C(12)-N(2)	120.4(2)
C(9)-C(8)-C(7)	120.4(2)	C(14)-C(13)-C(12)	120.1(2)
C(8)-C(9)-C(10)	119.5(2)	C(13)-C(14)-C(1)	120.7(2)
C(11)-C(10)-C(9)	120.4(2)		

Table 4. Anisotropic displacement parameters ($Å^2$ x 10^3) for boger07. The anisotropic displacement factor exponent takes the form: $-2\pi^2[h^2 a^{*2}U^{11} + ... + 2 h k a^* b^* U^{12}]$

	U^{11}	U^{22}	U^{33}	U^{23}	U^{13}	U^{12}
S(1)	23(1)	7(1)	24(1)	1(1)	-2(1)	0(1)
O(1)	19(1)	10(1)	23(1)	2(1)	-4(1)	-2(1)
O(2)	32(1)	11(1)	34(1)	-7(1)	-2(1)	6(1)
O(3)	29(1)	18(1)	33(1)	12(1)	-2(1)	-8(1)
N(1)	21(1)	10(1)	22(1)	0(1)	0(1)	0(1)
N(2)	19(1)	7(1)	24(1)	2(1)	-1(1)	-3(1)
C(1)	19(1)	25(1)	17(1)	-2(1)	-1(1)	-4(1)
C(2)	26(1)	13(1)	18(1)	-1(1)	1(1)	-2(1)
C(3)	20(1)	10(1)	15(1)	0(1)	1(1)	2(1)
C(4)	18(1)	12(1)	18(1)	1(1)	3(1)	2(1)
C(5)	24(1)	14(1)	17(1)	3(1)	-3(1)	3(1)
C(6)	18(1)	18(1)	13(1)	0(1)	2(1)	0(1)
C(7)	21(1)	19(1)	20(1)	-1(1)	1(1)	5(1)
C(8)	17(1)	34(2)	22(1)	3(1)	-1(1)	4(1)
C(9)	24(1)	28(2)	28(2)	3(1)	-4(1)	-8(1)
C(10)	32(2)	18(1)	31(2)	6(1)	-7(1)	-5(1)
C(11)	23(1)	16(1)	27(2)	5(1)	-5(1)	0(1)
C(12)	18(1)	10(1)	15(1)	-2(1)	3(1)	1(1)
C(13)	23(1)	9(1)	19(1)	1(1)	4(1)	2(1)
C(14)	21(1)	16(1)	21(1)	0(1)	0(1)	6(1)

Table 5. Hydrogen coordinates ($x10^4$) and isotropic displacement parameters ($Å^2 \times 10^3$) for boger07.

	x	y	z	U(eq)
H(9)	5002	2338	2240	20
H(1)	12414	4235	3433	25
H(12)	10154	5375	2747	23
H(8)	1854	3791	200	22
H(3)	500	4137	980	22
H(7)	-2617	3903	-27	24
H(6)	-5270	2811	-498	29
H(2)	-4894	1057	-340	32
H(4)	-1805	394	281	33
H(5)	856	1478	758	27
H(11)	8291	1945	2988	21
H(10)	11461	2523	3557	23

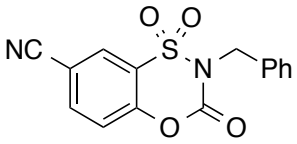

Compound 4.76
CCDC 1501167
Data obtained by Dr. Milan Gembicky, *UCSD Crystallography Lab*

Crystal Data

Identification code	Boger42	
Empirical formula	C15 H10 N2 O4 S	
Molecular formula	C15 H10 N2 O4 S	
Formula weight	314.31	
Temperature	100.15 K	
Wavelength	0.71073 Å	
Crystal system	Monoclinic	
Space group	P 1 21/n 1	
Unit cell dimensions	a = 7.3868(2) Å	α = 90°.
	b = 11.9333(4) Å	β = 98.1460(10)°.
	c = 15.7316(4) Å	γ = 90°.
Volume	1372.73(7) $Å^3$	
Z	4	
Density (calculated)	1.521 Mg/m^3	
Absorption coefficient	0.256 mm^{-1}	
F(000)	648	
Crystal size	0.38 x 0.28 x 0.25 mm^3	
Crystal color, habit	colorless block	
Theta range for data collection	2.150 to 26.032°.	
Index ranges	-9<=h<=9, -14<=k<=13, -19<=l<=19	
Reflections collected	19964	
Independent reflections	2713 [R(int) = 0.0291]	
Completeness to theta = 26.000°	100.0 %	
Absorption correction	Semi-empirical from equivalents	
Max. and min. transmission	0.4906 and 0.4467	
Refinement method	Full-matrix least-squares on F^2	
Data / restraints / parameters	2713 / 0 / 199	
Goodness-of-fit on F^2	1.059	
Final R indices [I>2sigma(I)]	R1 = 0.0291, wR2 = 0.0759	
R indices (all data)	R1 = 0.0323, wR2 = 0.0783	
Extinction coefficient	n/a	
Largest diff. peak and hole	0.366 and -0.419 $e.Å^{-3}$	

Table 2. Atomic coordinates ($x10^4$) and equivalent isotropic displacement parameters ($Å^2 \times 10^3$) for Boger42. U(eq) is defined as one third of the trace of the orthogonalized U^{ij} tensor.

	x	y	z	U(eq)
S(1)	5889(1)	7385(1)	5893(1)	13(1)
O(1)	8512(1)	8989(1)	6827(1)	16(1)
O(2)	10892(1)	7968(1)	6606(1)	20(1)
O(3)	5566(1)	6775(1)	6638(1)	19(1)
O(4)	5047(2)	7012(1)	5071(1)	21(1)
N(1)	123(2)	11136(1)	5633(1)	22(1)
N(2)	8139(2)	7464(1)	5867(1)	13(1)
C(1)	1577(2)	10790(1)	5804(1)	16(1)
C(2)	3395(2)	10338(1)	6025(1)	14(1)
C(3)	4762(2)	10970(1)	6516(1)	17(1)
C(4)	6483(2)	10521(1)	6763(1)	16(1)
C(5)	6809(2)	9426(1)	6533(1)	13(1)
C(6)	5455(2)	8801(1)	6046(1)	12(1)
C(7)	3741(2)	9249(1)	5775(1)	13(1)
C(8)	9279(2)	8110(1)	6439(1)	14(1)
C(9)	9012(2)	6556(1)	5406(1)	14(1)
C(10)	9539(2)	5527(1)	5943(1)	14(1)
C(11)	11321(2)	5404(1)	6362(1)	16(1)
C(12)	11835(2)	4439(1)	6830(1)	20(1)
C(13)	10577(2)	3588(1)	6878(1)	21(1)
C(14)	8798(2)	3699(1)	6453(1)	20(1)
C(15)	8283(2)	4666(1)	5992(1)	17(1)

Table 3. Bond lengths [Å] and angles [°] for Boger42_a.

S(1)-O(3)	1.4278(10)	C(5)-C(6)	1.3873(19)
S(1)-O(4)	1.4258(11)	C(6)-C(7)	1.3851(19)
S(1)-N(2)	1.6707(12)	C(7)-H(7)	0.9500
S(1)-C(6)	1.7423(14)	C(9)-H(9A)	0.9900
O(1)-C(5)	1.3799(16)	C(9)-H(9B)	0.9900
O(1)-C(8)	1.3744(17)	C(9)-C(10)	1.5099(19)
O(2)-C(8)	1.1955(18)	C(10)-C(11)	1.394(2)
N(1)-C(1)	1.146(2)	C(10)-C(15)	1.394(2)
N(2)-C(8)	1.3786(18)	C(11)-H(11)	0.9500
N(2)-C(9)	1.4997(17)	C(11)-C(12)	1.390(2)
C(1)-C(2)	1.443(2)	C(12)-H(12)	0.9500
C(2)-C(3)	1.401(2)	C(12)-C(13)	1.386(2)
C(2)-C(7)	1.392(2)	C(13)-H(13)	0.9500
C(3)-H(3)	0.9500	C(13)-C(14)	1.393(2)
C(3)-C(4)	1.383(2)	C(14)-H(14)	0.9500
C(4)-H(4)	0.9500	C(14)-C(15)	1.387(2)
C(4)-C(5)	1.387(2)	C(15)-H(15)	0.9500

O(3)-S(1)-N(2)	109.35(6)	C(6)-C(7)-H(7)	121.0
O(3)-S(1)-C(6)	109.04(6)	O(1)-C(8)-N(2)	117.70(12)
O(4)-S(1)-O(3)	118.89(7)	O(2)-C(8)-O(1)	118.14(12)
O(4)-S(1)-N(2)	107.60(6)	O(2)-C(8)-N(2)	124.15(13)
O(4)-S(1)-C(6)	111.28(6)	N(2)-C(9)-H(9A)	108.7
N(2)-S(1)-C(6)	98.77(6)	N(2)-C(9)-H(9B)	108.7
C(8)-O(1)-C(5)	123.56(11)	N(2)-C(9)-C(10)	114.26(11)
C(8)-N(2)-S(1)	122.18(10)	H(9A)-C(9)-H(9B)	107.6
C(8)-N(2)-C(9)	117.11(11)	C(10)-C(9)-H(9A)	108.7
C(9)-N(2)-S(1)	117.99(9)	C(10)-C(9)-H(9B)	108.7
N(1)-C(1)-C(2)	179.07(16)	C(11)-C(10)-C(9)	120.08(13)
C(3)-C(2)-C(1)	120.37(13)	C(15)-C(10)-C(9)	120.63(13)
C(7)-C(2)-C(1)	118.83(13)	C(15)-C(10)-C(11)	119.21(13)
C(7)-C(2)-C(3)	120.74(13)	C(10)-C(11)-H(11)	119.8
C(2)-C(3)-H(3)	119.7	C(12)-C(11)-C(10)	120.38(14)
C(4)-C(3)-C(2)	120.58(13)	C(12)-C(11)-H(11)	119.8
C(4)-C(3)-H(3)	119.7	C(11)-C(12)-H(12)	120.0
C(3)-C(4)-H(4)	120.7	C(13)-C(12)-C(11)	120.06(14)
C(3)-C(4)-C(5)	118.56(13)	C(13)-C(12)-H(12)	120.0
C(5)-C(4)-H(4)	120.7	C(12)-C(13)-H(13)	120.1
O(1)-C(5)-C(4)	116.90(12)	C(12)-C(13)-C(14)	119.87(14)
O(1)-C(5)-C(6)	122.25(13)	C(14)-C(13)-H(13)	120.1
C(4)-C(5)-C(6)	120.83(13)	C(13)-C(14)-H(14)	120.0
C(5)-C(6)-S(1)	117.69(11)	C(15)-C(14)-C(13)	120.05(14)
C(7)-C(6)-S(1)	120.65(11)	C(15)-C(14)-H(14)	120.0
C(7)-C(6)-C(5)	121.24(13)	C(10)-C(15)-H(15)	119.8
C(2)-C(7)-H(7)	121.0	C(14)-C(15)-C(10)	120.42(14)
C(6)-C(7)-C(2)	118.00(13)	C(14)-C(15)-H(15)	119.8

Table 4. Anisotropic displacement parameters ($Å^2$ x 10^3) for Boger42_a. The anisotropic displacement factor exponent takes the form: $-2\pi^2[h^2 a^{*2}U^{11} + ... + 2 h k a^* b^* U^{12}]$

	U^{11}	U^{22}	U^{33}	U^{23}	U^{13}	U^{12}
S(1)	11(1)	10(1)	16(1)	-1(1)	0(1)	-1(1)
O(1)	14(1)	16(1)	17(1)	-4(1)	-2(1)	1(1)
O(2)	12(1)	21(1)	27(1)	-5(1)	1(1)	-1(1)
O(3)	17(1)	14(1)	27(1)	5(1)	7(1)	1(1)
O(4)	19(1)	18(1)	24(1)	-7(1)	-6(1)	0(1)
N(1)	22(1)	17(1)	26(1)	-1(1)	0(1)	3(1)
N(2)	12(1)	14(1)	13(1)	-3(1)	2(1)	-1(1)
C(1)	22(1)	11(1)	15(1)	0(1)	2(1)	-1(1)
C(2)	16(1)	13(1)	13(1)	4(1)	3(1)	1(1)
C(3)	22(1)	12(1)	16(1)	0(1)	4(1)	0(1)
C(4)	18(1)	14(1)	15(1)	-2(1)	2(1)	-5(1)
C(5)	14(1)	15(1)	10(1)	2(1)	1(1)	-1(1)
C(6)	16(1)	11(1)	11(1)	1(1)	3(1)	-1(1)
C(7)	14(1)	14(1)	11(1)	2(1)	2(1)	-2(1)
C(8)	16(1)	14(1)	13(1)	0(1)	3(1)	-2(1)
C(9)	17(1)	15(1)	12(1)	-2(1)	4(1)	2(1)
C(10)	18(1)	14(1)	10(1)	-2(1)	4(1)	1(1)
C(11)	18(1)	18(1)	14(1)	-3(1)	3(1)	-1(1)
C(12)	23(1)	23(1)	13(1)	-2(1)	1(1)	6(1)
C(13)	33(1)	17(1)	14(1)	2(1)	7(1)	8(1)
C(14)	28(1)	15(1)	20(1)	-2(1)	12(1)	-3(1)
C(15)	17(1)	18(1)	16(1)	-4(1)	4(1)	0(1)

Table 5. Hydrogen coordinates (x10^4) and isotropic displacement parameters ($Å^2$ x 10^3) for Boger42_a.

	x	y	z	U(eq)
H(3)	4505	11712	6681	20
H(4)	7421	10954	7084	19
H(7)	2828	8826	5428	16
H(9A)	10122	6862	5204	17
H(9B)	8154	6331	4893	17
H(11)	12190	5984	6328	20
H(12)	13050	4363	7117	24
H(13)	10926	2930	7200	25
H(14)	7938	3113	6479	24
H(15)	7066	4741	5707	20

Anne F. Kornahrens

akorn@scripps.edu | https://www.linkedin.com/in/akornahrens | +1-858-230-2430

Curriculum Vitae

CURRENT ADDRESS:
The Scripps Research Institute
10550 N Torrey Pines Rd.
BCC-483
La Jolla, CA, USA 92121

SUMMARY

Organic chemist with experience in synthetic methodology, including cutting-edge method development, natural product synthesis and the creation of libraries for inhibitor discovery

EDUCATION

Skaggs-Oxford Program: Joint PhD/DPhil program in chemistry & biochemistry

University of Oxford, Oxford, UK **Sept 2011–April 2014**

The Scripps Research Institute (TSRI), La Jolla, CA, USA **May 2014–Oct 2016**

Boston College, Chestnut Hill, MA, USA **Sept 2007–May 2011**

College of Arts and Science, Bachelor of Science in Chemistry, Presidential Scholar, *Summa cum laude*, GPA: 3.894, Arts & Sciences Honors Program, Chemistry Honors

PUBLICATIONS

Shen, D.; Poole, D. L.; Shotton, C. C.; Kornahrens, A. F.; Healy, M. P.; Donohoe, T. J.; *Angew. Chem. Int. Ed.*, **2015**, *54*, 1642–1645.

Donohoe, T. J.; Jones, C. R.; Kornahrens, A. F.; Barbosa, L. C. A.; Walport, L. J.; Tatton, M. R.; O'Hagan, M.; Rathi, A. H.; Baker, D. B. *J. Org. Chem.* **2013**, *78*, 12338–12350.

Dabrowski, J.A.; Moebius, D.C.; Wommack, A.J.; Kornahrens, A.F.; Kingsbury, J.S. *Org. Lett.* **2010**, *12*, 3598-3601.

RESEARCH EXPERIENCE

Beckman Center for Chemical Sciences, TSRI **May 2014–Present**

Joint PhD/DPhil Student in the Boger Research Group

- Designed and synthesized small libraries of novel inhibitors for selective targeting of underexplored or undiscovered serine hydrolases
- Currently pursuing exciting preliminary results of selective LYPLA1/2 inhibition through activity-based proteomics to enable further exploration of the biochemistry of new targets
- Awarded and funded by a NSF Graduate Research Fellowship and the Skaggs–Oxford Fellowship

Chemistry Research Laboratory, Univ. of Oxford, Oxford, UK **Sept 2011–April 2014**

Joint PhD/DPhil Student in the Donohoe Research Group

- Developed a new method to provide a stereoselective synthesis of a biologically active natural product
- Optimized and conducted mechanistic studies of a cutting-edge metal-catalyzed transformation
- Mentored numerous junior students, built a new group website, and maintained analytical instruments

Boston College Chemistry Department, Chestnut Hill, MA, USA **Spring 2008–Spring 2011**
Undergraduate Lab Research Assistant in the Kingsbury Research Group

- Excelled in undergraduate research pursuing methodology utilizing reactive aryl-diazo compounds and TMS-diazomethane

TECHNIQUES AND SKILLS

Organic synthesis: methodology development; large-scale reactions and inert environments; analytical instrumentation use & maintenance (NMR, FTIR, HPLC);
Chemical biology: gel- and mass spectrometry-based activity-based protein profiling; computer image analysis (Image Lab, ImageJ);
Other: well-versed in Microsoft software; responsive webpage design; scientific & literature databases (i.e. SciFinder, Google Scholar, ChemBioDraw Ultra, Web of Science, Reaxys, Papers); advanced SCUBA diving certification;

COMMUNITY OUTREACH EXPERIENCE

Assoc. for Women in Science-San Diego Outreach Committee **March 2015–Present**
Committee Co-chair (since Sept 2015)

- Co-managing a dynamic and exciting group including supporting committee members by providing leadership growth and networking opportunities
- Planning and executing twelve events each year, reaching over 20,000 community members
- Targeting young women to enable their pursuit of STEM careers and also encouraging universal support of women in science
- Fostered a new partnership and new event opportunity which will allow the extension of our outreach activities to an underserved San Diego neighborhood and the extension of our partner network

Network for Women in Science, La Jolla, CA, USA **Jan 2015–Present**
Treasurer & Web Manager (Jan 2015–June 2016)

- Oversee and manage reimbursements and the budget to allow planning and execution of discussion groups, happy hours and female faculty lecture series
- Update and improve website to provide online resources such as event calendar, event summaries and networking opportunities

Science Saturdays Program, La Jolla, CA, USA **Jan 2016–Present**
Mentor

- Provide mentorship for a group of middle and high school students during a series of Saturday visits to learn about the scientists, research and facilities at TSRI

- Coordinated a group of three graduate students and 25 students to provide a series of demonstrations and tour of the lab space

Peer Coaching Program, La Jolla, CA, USA **July 2015–Present**
Peer Coach

- Helped to develop a pilot peer mentorship program at TSRI to provide support for first year graduate students
- Cultivated relationships with four first-year students and continue to monitor their progress over the course of the year through monthly email meetings and check in lunches

RSC Professional Development Policy Workshop, London, UK **8 November 2013**
Attendee

- Attended a one-day meeting to network and explore the Royal Society of Chemistry's policy work
- Engaged in a small group exercise to develop and present a strong policy statement (topic: banning the use of neonicotinoids in the EU) to a panel of science policy makers

CSCLeaders for Students, Rhodes House, Oxford, UK **3–6 December 2012**
Student Participant

- Actively participated in meetings, small groups and tours to learn about the migrant experience in Oxford
- Engaged in five-person working groups to research, develop and pitch a solution to the issue proposed: how to encourage bridge-building between host and origin countries for migrant communities

PRESENTATIONS

Graduate Student Symposium, Arrowhead, CA **Fall 2012, '13, '14, '15**
Poster presentations
Winter School in Catalysis, St. Catherine's College, Oxford, UK **17–18 December 2012**
Poster presentation
ACS National Conference, Washington D.C. and Boston, MA **August 2009 & 2010**
Poster presentation

AWARDS AND HONORS

AWIS Outstanding Volunteer Award (Innovation) 2016
AWIS Outstanding Volunteer Award (Outreach) 2015
Skaggs-Oxford Scholarship
NSF Graduate Research Fellowship
Scholar of the College Thesis
2010 Goldwater Scholar
Boston College Presidential Scholarship
Phi Beta Kappa Society

JOC The Journal of Organic Chemistry

Featured Article

pubs.acs.org/joc

Terms of Use CC-BY

Total Synthesis of the Antitumor Antibiotic (±)-Streptonigrin: First- and Second-Generation Routes for de Novo Pyridine Formation Using Ring-Closing Metathesis

Timothy J. Donohoe,*[,†] Christopher R. Jones,[†] Anne F. Kornahrens,[†] Luiz C. A. Barbosa,[†,‡] Louise J. Walport,[†] Matthew R. Tatton,[†] Michael O'Hagan,[†] Akshat H. Rathi,[†] and David B. Baker[†]

[†]Department of Chemistry, Chemistry Research Laboratory, University of Oxford, Mansfield Road, Oxford OX1 3TA, United Kingdom

[‡]Department of Chemistry, Federal University of Minas Gerais, A. Pres Antônio Carlos 6627, Campus Pampulha, CEP 31270-901, Belo Horizonte, MG, Brazil

Supporting Information

ABSTRACT: The total synthesis of (±)-streptonigrin, a potent tetracyclic aminoquinoline-5,8-dione antitumor antibiotic that reached phase II clinical trials in the 1970s, is described. Two routes to construct a key pentasubstituted pyridine fragment are depicted, both relying on ring-closing metathesis but differing in the substitution and complexity of the precursor to cyclization. Both routes are short and high yielding, with the second-generation approach ultimately furnishing (±)-streptonigrin in 14 linear steps and 11% overall yield from inexpensive ethyl glyoxalate. This synthesis will allow for the design and creation of druglike late-stage natural product analogues to address pharmacological limitations. Furthermore, assessment of a number of chiral ligands in a challenging asymmetric Suzuki−Miyaura cross-coupling reaction has enabled enantioenriched (up to 42% ee) synthetic streptonigrin intermediates to be prepared for the first time.

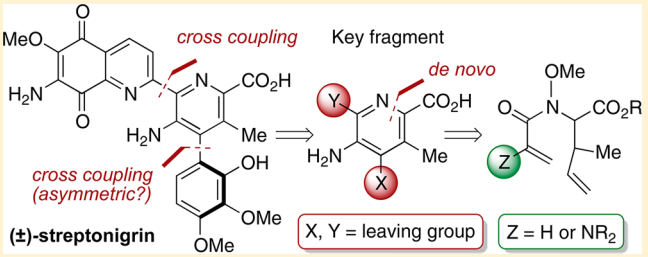

INTRODUCTION

Ever since its isolation from *Streptomyces flocculus* in 1959 by Rao and Cullen, the chemistry of streptonigrin (**1**) (Figure 1)

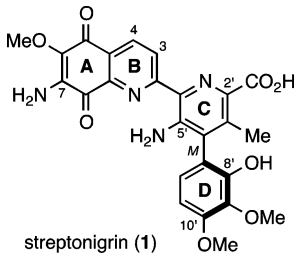

Figure 1. Streptonigrin.

has received considerable interest from both the synthetic organic and biochemical communities.[1,2] Rao, Biemann, and Woodward established the structure of the metabolite four years later through a series of elegant spectroscopic and chemical degradation studies, and the connectivity was then confirmed in 1975 by Chiu and Lipscomb via X-ray crystallographic analysis.[3,4]

The broad-spectrum anticancer activity displayed by streptonigrin has made it extremely attractive for medical application, reaching phase II clinical trials in the late 1970s.[5] However, allied to this activity was an unavoidably high degree of toxicity that caused the cessation of these trials. Subsequent structure−activity investigations involving **1** and a series of truncated analogs, as well as recent genome scanning studies, have led to a proposed biosynthesis and established the cytotoxic mode of action.[6−14] Mechanistically, it is believed that streptonigrin binds irreversibly to DNA in the presence of certain metal cations (e.g., Zn, Cu, Fe, Mn, Cd, Au) and is then activated via a one- or two-electron reductase, with NAD(P)H as a cofactor, to form a semiquinone or hydroquinone intermediate. Both of these species can react with in situ oxygen, through a Fenton-type reaction catalyzed by the metal, to regenerate streptonigrin and produce hydroxyl radicals that are ultimately responsible for DNA strand cleavage. The key structural elements responsible for this activity include the two pyridyl nitrogens in rings B and C, the C-ring carboxylic acid, and the 7-aminoquinoline-5,8-dione AB-ring system. Interestingly, streptonigrin has also been shown to be a potent and selective protein arginine deiminase (PAD 4) inhibitor.[15] Another important structural feature of streptonigrin is the configurationally stable C−D ring axis, which accounts for the observed optical activity of the natural product; circular dichroism studies determined the absolute stereochemistry as *M*.[16]

Received: October 25, 2013
Published: December 12, 2013

Prior to our recent communication,[17] Weinreb and coworkers had reported the only total synthesis of streptonigrin in 1980.[18,19] Two subsequent formal syntheses from the groups of Kende[20] in 1981 and Boger[21] in 1985 stopped five and seven steps short of the target, respectively. Strategically, Weinreb constructed the pyridine C-ring via an imino Diels–Alder reaction, Kende utilized a regioselective condensation of a β-ketoenamine with methyl acetoacetate, and Boger employed an inverse-electron-demand Diels–Alder reaction of a heterocyclic azadiene.

Despite the termination of clinical trials, interest has remained in generating analogues of streptonigrin as potential drug candidates.[2] However, these compounds have tended to be abridged versions of **1**, as the synthetic routes available to late-stage analogues can be lengthy.[18−21] Elsewhere, attempts to derivatize the metabolite itself have been limited to basic transformations,[16,22] as direct isolation from the fermentation of *Streptomyces* species yields only 13 mg per 1 L of culture filtrates.[23] The ability to generate late-stage streptonigrin analogues would enable a range of previously untried structural elements to be evaluated at key sites on **1**, therein revealing the potential to address the fundamental pharmacological limitations of streptonigrin. In order to facilitate this, it became evident that a more efficient and convergent pathway to **1** was required. To this end, we recently communicated a total synthesis of (±)-streptonigrin that should enable the preparation of such a set of compounds.[17] Herein, we report our full investigations into the synthesis of **1**, including a first-generation route to the core pentasubstituted pyridine fragment that is higher yielding overall, but two steps longer than the second generation approach. There is also a full discussion of Weinreb's end game, which proved capricious in our hands, and how we came to a revised route, plus recent studies evaluating chiral ligands for a demanding asymmetric Suzuki–Miyaura cross-coupling reaction.

Synthesis Plan. With a view toward future analogue preparation, our principal design objective was to assemble the core tetracyclic framework of streptonigrin at a late stage of the synthesis to allow for the greatest amount of derivatization on each ring prior to convergence. Inspired by reports on the coupling of biaryl fragments of streptonigrin,[24−28] we devised a retrosynthetic strategy that would see both the challenging 2,2′-bipyridyl AB-C linkage and the chiral C–D ring axis constructed via metal-catalyzed cross-coupling reactions, leaving the dual-activated pyridine C-ring **2** as the key fragment (Scheme 1). Here, we would also study the innate reactivity differences between the C-4 and C-6 leaving groups on the pyridine. It was envisaged that pentasubstituted pyridine **2** could be readily accessed through methodology recently developed in the group,[29−31] namely the generation of heteroaromatic compounds utilizing a ring closing metathesis (RCM) reaction as the cyclization step (Scheme 1 bottom). Subsequent elimination of the *N*-methoxy leaving group, functionalization, and aromatization would furnish pyridine **2**. The relatively sensitive quinoline-5,8-dione moiety **3** would be generated via a late-stage oxidation of a functionalized methoxy quinoline component, while the D-ring precursor **4** would come from commercial 2,3-dimethoxyphenol.

RESULTS AND DISCUSSION

Synthesis of Pentasubstituted Pyridine: First-Generation Route. According to the proposed RCM methodology, a suitable diene of type **6** was easily prepared in 92% yield over

Scheme 1. Retrosynthetic Analysis

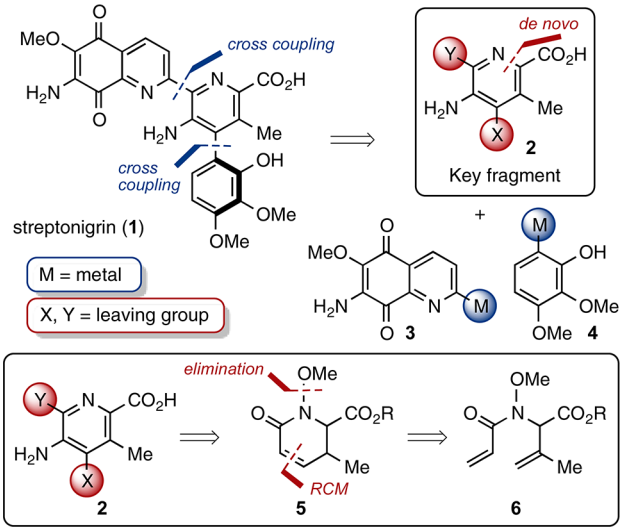

Scheme 2. Synthesis of Disubstituted Pyridone 12

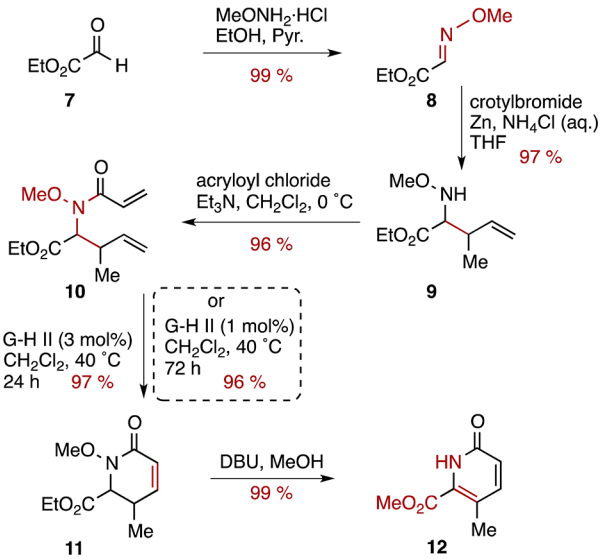

three steps from ethyl glyoxalate **7** (Scheme 2). Initial condensation of methoxyamine hydrochloride with ethyl glyoxalate, followed by a regioselective zinc-mediated crotylation of the resulting oxime ether **8**, furnished methoxyamine **9** in 96% yield over the two steps and as an inconsequential 3:2 mixture of diastereoisomers. Next, acylation with acryloyl chloride proceeded smoothly to generate the RCM precursor **10**. Pleasingly, the key RCM step was effected extremely efficiently using Hoveyda–Grubbs second-generation catalyst (3.0 mol % catalyst loading), which afforded dihydropyridone **11** in 97% yield. This reaction has been carried out on a 3.5 g (14.5 mmol) scale, and the catalyst loading can also be lowered to 1.0 mol % without a drop in yield, although reducing the amount of catalyst resulted in an increase in reaction time (from 24 to 72 h).

Next, elimination of the methoxy leaving group on nitrogen was effected using 1,8-diazabicyclo[5.4.0]undec-7-ene (DBU) as the base. Having observed a mixture of ethyl and methyl ester dihydropyridones when ethanol was used as the solvent, complete transesterification to a single methyl ester product **12** was achieved when the reaction was performed in methanol

dx.doi.org/10.1021/jo402388f | J. Org. Chem. 2013, 78, 12338−12350

(note: this ester interconversion enabled our route to converge to a late-stage formal intermediate from Weinreb's synthesis).[18]

With the core pyridone **12** in hand, we had to attach the appropriate functionality that adorns pyridine **2**. Central to our synthetic strategy is the ability to control the regioselectivity of the first of the late-stage cross-coupling reactions with dual-activated pyridine **2**, as there will be two sites capable of undergoing oxidative addition (C-4 and C-6). While pyridine is known to exert an innate preference for addition of Pd(0) into C−X bonds *ortho* to the pyridyl nitrogen,[32] aryl bromotriflates have been shown to undergo oxidative addition into either activated bond through the appropriate selection of reaction conditions.[33] It was therefore reasoned that installation of a bromine atom at the C-4 position of **2** and a trifluoromethanesulfonyl group at C-6 should offer both reagent and substrate control as potential sources of regioselectivity.

Owing to the inherent preference of pyridone **12** to undergo electrophilic substitution at C-5, it followed that nitration was the next step, and we were pleased to find that heating **12** in a 2:1 mixture of nitric and sulfuric acids in a sealed tube afforded the highly polar nitropyridone **13** in an excellent 88% yield (Scheme 3). This process proved capricious upon scale-up

Scheme 3. Synthesis of Pentasubstituted Pyridine 15

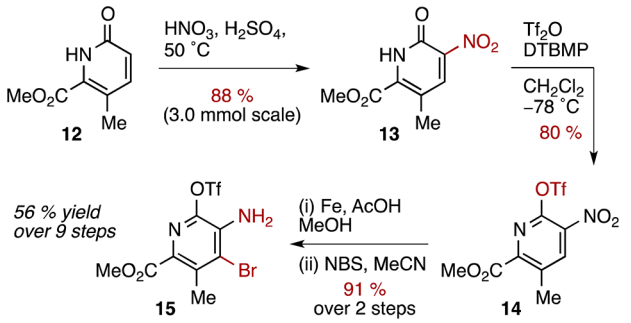

(>3.0 mmol) due to competing ester hydrolysis. Despite attempts to reliably reproduce the nitration on larger scales, the extent to which hydrolysis occurred proved to be highly batch-specific. While a good amount of nitropyridone was generated via this route and some of the acid byproduct could be restored to the methyl ester upon a separate addition of methanol, we would ultimately seek an alternative strategy for the synthesis of pyridine **2** to facilitate our objective of producing gram-quantities of late-stage streptonigrin compounds (vide infra).

Nevertheless, with nitropyridone **13** in hand, we treated this compound with triflic anhydride and 2,6-di-*tert*-butyl-4-methylpyridine (DTBMP) to furnish 6-triflylpyridine **14** in 80% yield. Reduction of the nitro group in the presence of iron powder and acetic acid afforded the free amine, and subsequent bromination with *N*-bromosuccinimide (NBS) gave the desired pyridine **15** in nine steps and 56% overall yield from ethyl glyoxalate. X-ray crystallographic analysis of **15** confirmed the correct substitution pattern around the pyridine core (see the Supporting Information).[34]

Synthesis of Pentasubstituted Pyridine 15: Second-Generation Route. During the course of our investigations into the synthesis of pyridine **15**, it became evident that the nitration of pyridone **12** was unreliable upon scale-up. As such we devised a shorter and more convergent RCM route to **15** that would not require this late-stage functionalization (Scheme 4). Introduction of the amine prior to RCM was a much more

Scheme 4. Second-Generation Route to Key Pentasubstituted Pyridine 15

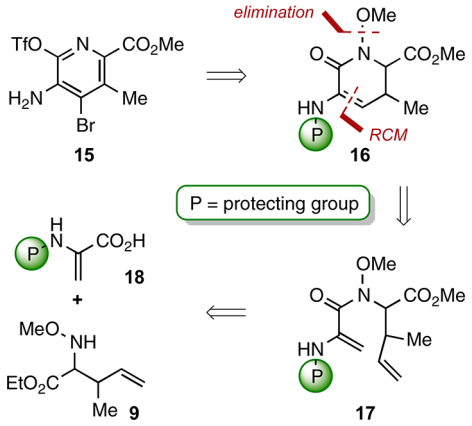

challenging proposition for the methodology, as it not only necessitated tolerating a bulky 1,1-disubstituted alkene **17**, but also an enamine moiety which had not previously been employed.

The choice of a suitable protecting group for α-amino acrylic acid **18** was crucial to the success of this new approach, as it had to be compatible with RCM as well as being easy to prepare and then remove following cyclization. Initial attempts to couple commercially available 2-acetamidoacrylic acid with methoxyamine **9** proved unsuccessful: the preparation of activated acids from peptide coupling reagents (HOBt, CDI, and DCC), a pentafluorophenyl ester, mixed anhydrides, and acid chloride all led to decomposition. Although no products could be isolated, it was postulated that the nucleophilic nature of the acetamide carbonyl oxygen was causing competing reactivity. With this in mind, we investigated the suitability of a phthalimide group, as the imide carbonyl was anticipated to be less nucleophilic than the amide and the requisite protected acid **20** can be readily prepared in one step from DL-serine and phthalic anhydride (Scheme 5).[35] Gratifyingly, when *N*-

Scheme 5. Attempted Synthesis of Amino-Substituted Dihydropyridone 22

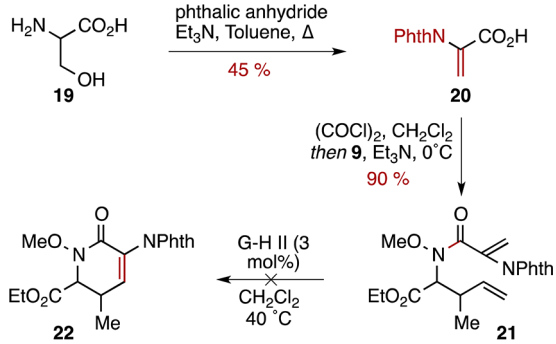

protected α-amino acrylic acid **20** was treated with oxalyl chloride it displayed no signs of decomposition and could be coupled in situ with methoxyamine **9** to furnish the RCM precursor **21** in 90% yield.

The challenging nature of the 1,1-disubstituted alkene substrate **21** was confirmed when application of the previous RCM reaction conditions (see Schemes 2 and 5) led to complete recovery of starting material. Increasing the catalyst loading to 10 mol % gave the same result (Table 1, entry 1).

dx.doi.org/10.1021/jo402388f | J. Org. Chem. 2013, 78, 12338−12350

Table 1. Initial Studies into Ring-Closing Metathesis of 1,1-Disubstituted Diene 21

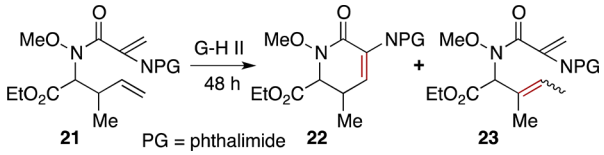

21 22 23

entry	catalyst loading (mol %)	solvent	temp (°C)	additive (20 mol %)	% 22[a]	% 23[a]
1	10	CH_2Cl_2	40	none	0	
2	10	CH_2Cl_2	70[b]	none	47	38
3	10	CH_2Cl_2	70[b]	BQ	48	
4	10 + 5[c]	CH_2Cl_2	70[b]	BQ	55	
5	10 + 5[c]	CH_2Cl_2	70[b]	TCBQ	39	
6	10 + 5[c]	toluene	110	BQ	58	
7	10	CH_2Cl_2	95[d]	BQ	47[e]	
8	10	toluene	160[b]	BQ	62[e]	
9	5 + 5[f]	toluene	160[b]	BQ	64[e]	
10	10	toluene	160[b]	BQ	70[g]	

[a]Isolated yield following chromatography. [b]Reaction performed in a sealed tube. [c]Second catalyst addition after 24 h. [d]Reaction performed in a microwave. [e]Reaction time 10 min. [f]Second catalyst addition after 5 min. [g]Reaction time 1 h. BQ = benzoquinone; TCBQ = tetrachlorobenzoquinone.

However, we were encouraged to find that upon raising the temperature to 70 °C (reaction carried out in a sealed tube) the desired dihydropyridone **22** could be isolated in 47% yield (entry 2).

With reaction at elevated temperatures, the recovered starting material **21** had actually undergone isomerization to the internal alkene **23**, present as an inseparable 2:1 mixture of *E*/*Z* isomers. Isomerizations of this kind are well documented, and commonly proposed mechanisms invoke the participation of ruthenium hydride species formed by decomposition of the metathesis catalyst.[36] Grubbs has reported that this process can be inhibited by the addition of species that quench any [Ru−H] formed in situ before isomerization can occur.[37] As a result, we performed the same reaction in the presence of benzoquinone (BQ) and tetrachlorobenzoquinone (TCBQ), with both additives preventing the formation of **23** (entries 3 and 5). Despite this improvement, significant amounts of starting material (unisomerized) were still recovered, prompting the addition of a second portion of metathesis catalyst part way through the reaction (entry 4). Switching the solvent to toluene enabled the reaction to be run at higher temperatures and again resulted in a small improvement in the yield (entry 6).

With the aim of increasing the reaction rate so that it might out-compete the rate of catalyst decomposition, the RCM was carried out in a microwave reactor under a variety of conditions (entries 7−10). We were pleased to discover that a catalyst loading of 10 mol % at 160 °C for 1 h produced dihydropyridone **22** in 70% yield. Unfortunately, upon attempted scale-up, these conditions were found to be reliable only on relatively small quantities of starting material (<0.25 g, 0.65 mmol). With the microwave presenting both chemical and logistical constraints with respect to scale-up, we decided to revert to thermal conditions in our pursuit of a reliably high-yielding process.

During the synthesis of the 10-membered macrolactone (−)-diplodialide C, Stoltz demonstrated that slow addition of a metathesis catalyst was crucial to the success of a challenging RCM.[38] In our case, gradual introduction of the catalyst appeared to offer a solution to the problems relating to decomposition. Thus, we attempted the RCM with slow addition of catalyst via syringe pump (Table 2).

Table 2. Ring-Closing Metathesis of 1,1-Disubstituted Diene 21 with Slow Catalyst Addition

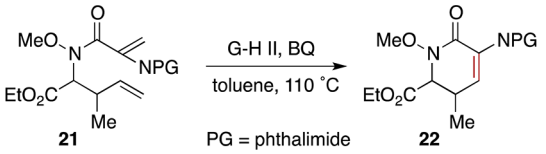

21 22

entry	catalyst loading (mol %)	catalyst addition time (h)	% 22[a]
1	10	5	63
2	10	10	78
3	10	20	61
4	5	10	76

[a]Isolated yield following chromatography, BQ = benzoquinone.

Pleasingly, this regimen worked extremely well, and we were able to efficiently generate RCM product **22** in 76% yield using just 5.0 mol % of Hoveyda−Grubbs second-generation catalyst added as a solution in toluene over 10 h to a mixture of precursor **21** and BQ in refluxing toluene (entry 4). Moreover, this reaction has been performed reliably on a 1.5 g (3.9 mmol) scale, which has facilitated the production of gram-quantities of late-stage synthetic material.

With an efficient and scaleable RCM protocol in place, attention turned to the manipulations required to convert *N*-phthalimide-protected dihydropyridone **22** to pentasubstituted pyridine **15**. To our surprise, treatment of **22** with DBU in methanol only led to decomposition, instead of the corresponding pyridone. As a result, we tested a range of bases with pK_a values similar to DBU and found that quinuclidine reliably effected elimination of the *N*-methoxy leaving group (Scheme 6). Because of partial phthalimide

Scheme 6. One-Pot, Trifunctional Procedure en Route to Pentasubstituted Pyridine 15

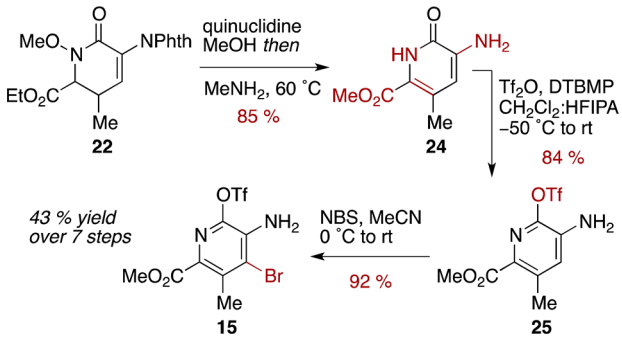

opening under these conditions, we identified an opportunity to extend the tandem elimination−transterification sequence (see Scheme 2). To this end, methylamine was added to the reaction mixture, once elimination was complete, to finish cleavage of the phthalimide group, affording aminopyridone **24** in an excellent 85% yield from dihydropyridone **22**. Thus, an efficient trifunctional one-pot procedure has been developed

dx.doi.org/10.1021/jo402388f | J. Org. Chem. 2013, 78, 12338−12350

that accomplishes elimination, transesterification, and deprotection.

In order to converge with pyridine **15** from the first route, it was necessary to introduce a trifluoromethanesulfonyl group selectively on the pyridone oxygen, as opposed to the arylamine. Due to its high polarity, **24** proved to be only sparingly soluble in all but the most polar solvents, and when treated with triflic anhydride in DMF, the sole product isolated was that from sulfonylation at the aryl amine; evidenced in the ^{1}H NMR spectrum by the appearance of a downfield 1H singlet corresponding to the electron deficient sulfonamide N–H. Pleasingly, when the triflation was conducted in a 25:1 mixture (by volume) of dichloromethane and hexafluoroisopropyl alcohol (HFIPA), a highly polar but only weakly nucleophilic solvent, **24** was converted to pyridine **25** in 84% yield (Scheme 6). Neither *N*-sulfonylation nor a deleterious reaction between the alcohol and triflic anhydride were observed. The spectroscopic data of **25** were an exact match to the data obtained via the first-generation route.

Having intercepted the previous route, we could see that the second-generation approach afforded key pyridine fragment **15** in 43% yield and seven steps from ethyl glyoxalate (counting the one-pot transformation of **22** into **24** as one step). This compares to 56% yield over nine steps from the first synthesis. Crucially though, the second-generation route proved to be more scaleable and has been used routinely to prepare multigram-quantities of material for the latter stages of the synthesis. Both of the approaches described have showcased the utility of the RCM methodology to efficiently prepare highly substituted pyridines in few synthetic transformations from commercial chemicals.

Synthesis of the D-Ring Fragment. Both Quéguiner[39] and Holzapfel[25] have shown that the C–D ring linkage in model streptonigrin systems can be constructed using a Suzuki–Miyaura cross-coupling reaction. Following a similar strategy here necessitated the preparation of a boronate ester derivative of the D-ring fragment **4**. Consequently, commercially available 2,3-dimethoxyphenol (**26**) was brominated[40] with NBS in THF at −78 °C to give bromophenol **27** as a single regioisomer (confirmed by X-ray crystallography; see the Supporting Information)[41] in near-quantitative yield (Scheme 7). Next, phenol **27** was *O*-benzyl protected; as Weinreb's synthesis had employed the same protecting group this would enable our route to converge to a late-stage intermediate from that synthesis. Finally, treatment of the benzylated compound with *t*-BuLi and 2-isopropoxy-4,4,5,5-tetramethyl-1,3,2-dioxaborolane furnished boronic acid pinacol ester **28**.

Scheme 7. Synthesis of D-Ring Boronate Ester 28

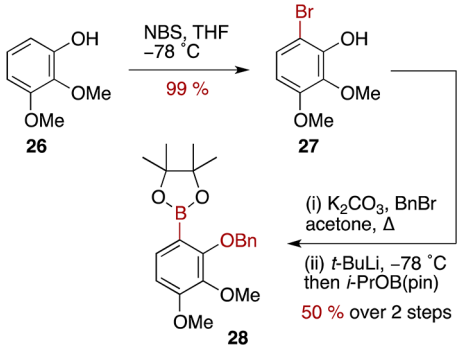

Synthesis of the AB-Ring Fragment. Establishing unsymmetrical 2,2′-bipyridyl motifs, as present around the AB–C ring linkage of **1**, via metal-catalyzed cross-coupling reactions can be challenging.[42,43] Most notably the preparation of an organometallic partner is potentially problematic due to the increased reactivity at the site *ortho* to the pyridyl nitrogen. However, this strategy has been successful in model streptonigrin systems, although functionality was often reduced on one or both of the components.[26,27] In order to provide as much tactical variation as possible, it was envisaged that 5,6,8-trimethoxyquinolines **34** and **35** (see Scheme 8), with appropriate leaving groups in the C-2 position, would provide access to a range of possible metal-substituted coupling partners.

Scheme 8. Synthesis of 2-Stannylquinoline 36

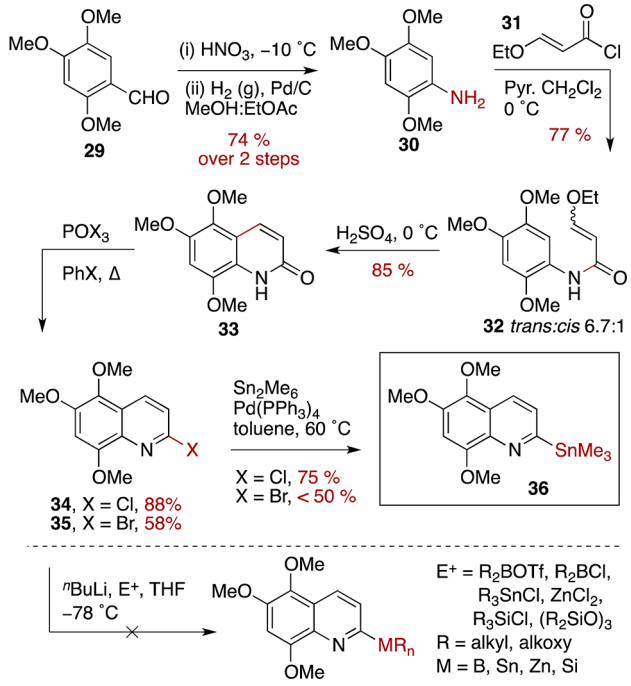

Synthesis of the quinolines began with the conversion of commercially available 2,4,5-trimethoxybenzaldehyde (**29**) to the corresponding nitro compound in 80% yield upon treatment with a cold aqueous solution of nitric acid (Scheme 8).[44] Reduction of this nitro group with Pd/C and hydrogen smoothly afforded aniline **30**, which was subsequently acylated with (*E*)-3-ethoxyacryloyl chloride[45] **31** to generate aryl amide **32** in 72% yield over the two steps and as an inconsequential 6.7:1 ratio of *trans*/*cis* stereoisomers. Cyclization to **33** proceeded efficiently in sulfuric acid to establish the AB-ring scaffold in 85% yield, while subsequent treatment with phosphorus oxychloride effected aromatization to chloroquinoline **34** in 88% yield. The corresponding 2-bromoquinoline **35** was synthesized using phosphorus oxybromide in 58% yield.

With quinolines **34** and **35** in hand, we attempted to construct the corresponding boron-, tin-, zinc-, and silicon-containing compounds (Scheme 8 bottom). However, standard lithium/halogen exchange conditions, followed by trapping of the resultant anion, failed to furnish any 2-metalated quinolines, instead yielding mixtures of protodehalogenated quinoline and dimerized 5,5′,6,6′,8,8′-hexamethoxy-2,2′-biquinoline.

dx.doi.org/10.1021/jo402388f | J. Org. Chem. 2013, 78, 12338–12350

At this stage, we were encouraged by Padwa's report into the synthesis of analogues of lavendamycin,[46] whereby 2-stannylquinolines were generated using hexamethylditin and Pd(0), a different mode of reactivity to the electrophilic trapping described above. Gratifyingly, when chloroquinoline **34** was treated with hexamethylditin and catalytic $Pd(PPh_3)_4$, the corresponding stannane **36** was obtained in 75% yield, albeit contaminated with triphenylphosphine oxide (4:1 stannane/$POPh_3$ by ^1H NMR spectroscopy). Stannane **36** was unstable to chromatography so was used without purification. Applying these conditions to the more reactive bromoquinoline **35** led to added complexity in the crude reaction mixture, with less than 50% conversion to stannane **36** by analysis of the ^1H NMR spectrum.

Unification of the Ring Fragments. We now had access to the three principal fragments **15**, **28**, and **36** required to construct the tetracyclic framework of streptonigrin (see Scheme 1). The next task was to test the hypothesis that the C-6 position of pyridine **15** would be more reactive than C-4 toward oxidative addition of Pd(0). With this prediction in mind, we began by investigating the Stille reaction between **15** and **36** that would potentially establish the AB−C ring linkage of **1** (Scheme 9). We were pleased to verify that coupling

Scheme 9. Synthesis of Tetracyclic Quinone 39

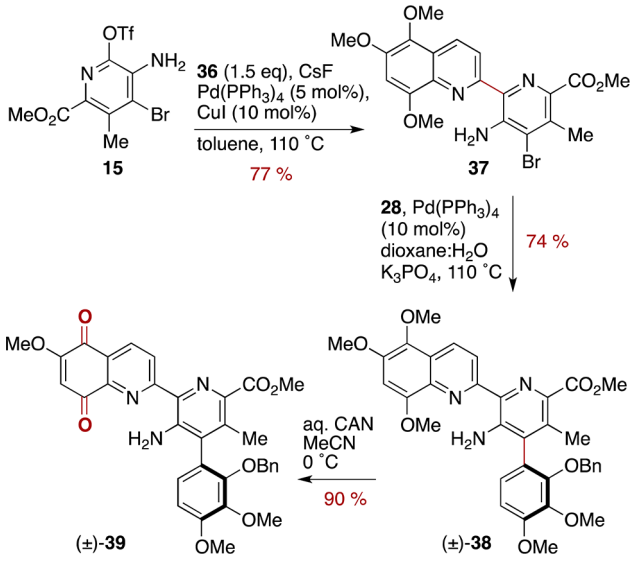

occurred exclusively at C-6 and that no products relating to either competing reaction at C-4 nor protodebromination were observed. Following optimization of reaction conditions it was found that the addition of CuI and CsF to $Pd(PPh_3)_4$ (5.0 mol %) in toluene at reflux with 1.5 equiv of stannane **36** afforded the greatest yield of the tricyclic ABC fragment **37** (77% yield compared to 62% in the absence of additives, and just 52% when equimolar amounts of **15** and **36** were used).[47]

Next, a Suzuki−Miyaura coupling of bromopyridine **37** and aryl borate ester **28** was studied. Initial investigations using $Pd(OAc)_2$ (25 mol %) and 2-dicyclohexylphosphino-2′,6′-dimethoxybiphenyl (S-Phos) (30 mol %) in the presence of an aqueous solution of Na_2CO_3 led to the formation of tetracyclic fragment **38** in an encouraging 71% yield. However, subsequent attempts to reduce the catalyst loading had a significant detrimental effect on the yield (10 mol % $Pd(OAc)_2$ led to 53% of **38**). Further investigations revealed that $Pd(PPh_3)_4$ was the most efficient catalyst; loadings of 10 mol % afforded **38** in 74% yield with aqueous K_3PO_4 as the optimal base.

With the tetracyclic framework of **1** established, a highly regioselective ceric ammonium nitrate (CAN)-mediated oxidation[48] of quinoline **38** to quinoline-5,8-dione **39** resulted in the interception of a late-stage intermediate in Weinreb's total synthesis. The preparation of an aged aqueous CAN solution proved to be key to this transformation, as solutions made immediately prior to the reaction led to significant decomposition and only produced **39** in 20−35% yields. It was postulated that by allowing the CAN solution to stand for a period of time it had tempered the acidity and/or oxidizing potential of the one electron oxidant and reduced the propensity for decomposition. Consequently, it was discovered that a solution prepared 24 h in advance would reliably produce the desired *p*-quinone in 90% yield, without any decomposition or trace of the regioisomeric *o*-quinone.

Having intercepted Weinreb's late-stage intermediate, we were able to verify that our spectroscopic data matched those previously reported. A summary of our streptonigrin formal synthesis illustrates the convergent modular strategy: quinoline-5,8-dione **39** has been prepared in ten linear steps in an overall yield of 22% from inexpensive ethyl glyoxalate.[18−21]

Asymmetric Suzuki−Miyaura Cross-Coupling Reactions. Cross-coupling reactions to form hindered biaryl units are challenging by their nature.[49] In terms of catalytic asymmetric variants, following pioneering studies from Buchwald[50] and Cammidge,[51] there have been a number of further reports, although the level of generality has typically been modest.[52,53] In line with our design criteria, we embarked on a program to investigate the feasibility of rendering asymmetric the Suzuki−Miyaura reaction between pyridyl bromide **37** and aryl boronate ester **28** that constructs the chiral C-D ring axis of streptonigrin. This would potentially enable the synthesis of enantiomerically enriched streptonigrin, as well as late-stage analogues, for the first time.

Preliminary investigations revealed that an enantiomeric excess (ee) of 22% can be obtained by using (*R*)-BINAP, instead of S-Phos, in the presence of $Pd(OAc)_2$ at 60 °C (Table 3, entry 1).[17] These initial studies also revealed that chiral monodentate phosphine ligands, such as (*R*)-(+)-2-(diphenylphosphino)-2′-methoxy-1,1′-binaphthyl ((*R*)-MOP),[54] do not impart any degree of stereocontrol, while the bidentate amino phosphine ligand, (R_p)-1-[(1*S*)-(1-aminoethyl)]-2-(diphenylphosphino)ferrocene,[51] showed very little catalytic activity. Given these results, we were encouraged to pursue this transformation further and focused our attention on bidentate phosphines.

To this end, lowering the reaction temperature to 40 °C with (*R*)-BINAP led to the desired increase in enantioselectivity but with a decrease in yield (entry 2). Employing a number of commercially available chiral bidentate bisphosphine ligands revealed that those based around a BINAP scaffold (entries 1−5) tended to afford higher levels of atroposelectivity compared to standard SEGPHOS ligands (entries 6−8); (*R*)-DM-BINAP generated the tetracyclic compound **38** in 36% ee (entry 5).

Lassaletta and co-workers have recently shown that phosphino hydrazone precatalysts such as **40** are effective at catalyzing Suzuki−Miyaura cross-coupling reactions of hindered biaryls with a good degree of stereocontrol.[53] When **40** was employed in our system, we were pleased to observe an increase in enantioselectivity (note: the product was the opposite enantiomer to that obtained with (*R*)-BINAP), albeit

dx.doi.org/10.1021/jo402388f | J. Org. Chem. 2013, 78, 12338−12350

Table 3. Investigating Chiral Bidentate Phosphine Ligands

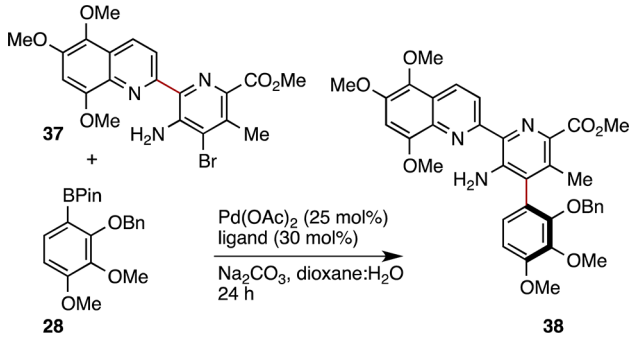

entry	ligand	temp (°C)	yield (%)[a]	ee (%)[b]
1	(*R*)-BINAP	60	65	(−) 22
2	(*R*)-BINAP	40	37	(−) 27 [20][c]
3	(*R*)-tol-BINAP	40	20	(−) 35
4	(*R*)-H_8−BINAP	40	43	(−) 27
5	(*R*)-DM-BINAP	40	25	(−) 36
6	(*R*)-SEGPHOS	40	41	(−) 13
7	(*R*)-DM-SEGPHOS	40	38	(−) 15
8	(*R*)-DTBM-SEGPHOS	40	15	(−) 22
9[d]	precatatyst **40**	40	17	(+) 40 [35][c]
10[e]	phosphino hydrazone **41**	40	65	(+) 42
11[e]	phosphino hydrazone **41**	60	85	(+) 29 [22][c]
12[e]	phosphino hydrazone **41**	110	54	(+) 8

[a]Isolated yield following chromatography. [b]Determined by chiral HPLC analysis (the absolute stereochemistry of the major enantomer is unknown). [c]Figure in square brackets determined by analysis of the ^{1}H NMR spectrum of the Mosher's ester derivative of the corresponding primary alcohol **42**. [d]Palladium−phosphino hydrazone precatalyst **40** (25 mol %) used. [e]Phosphino hydrazone ligand **41** (25 mol %) and $Pd_2(dba)_3$ (12.5 mol %) used.

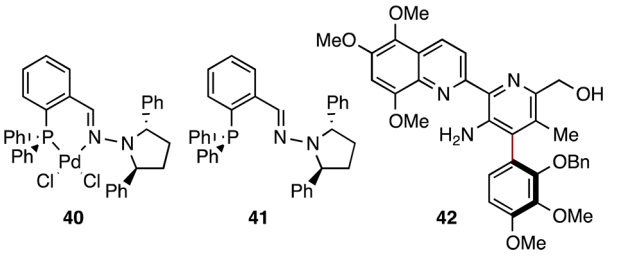

with a lower yield (entry 9). Gratifyingly, catalytic activity improved markedly when the free phosphino hydrazone ligand **41** was used in conjunction with $Pd_2(dba)_3$, affording cross-coupled product **38** in 65% yield and 42% ee (entry 10). Attempts to further improve conversion by increasing the temperature resulted in lower levels of stereocontrol (entries 11 and 12). The use of alternative bases such as CsF[55] and Ag_2O[56] resulted in no reaction, while the employment of CuI as an additive[57] to improve catalytic activity also returned starting material.

During the course of these studies, we became aware of a potential small inaccuracy in the data obtained from chiral HPLC analysis. This was attributed to a few causes, including the limited solubility of the product, broad peaks in the UV traces, as well as the presence of a small impurity with the same retention time as one of the enantiomers that could not be removed despite many attempts at purification. As a result, a representative sample of the products obtained in Table 3 were each reduced to primary alcohol **42** and then acylated with (*R*)-(−)-α-methoxy-α-(trifluoromethyl)phenylacetyl chloride to afford the corresponding Mosher's esters. Subsequent analysis of the ^{1}H and ^{19}F NMR spectra of these samples (see figures in square brackets in Table 3)[58] largely corroborated the previous data, although it did suggest that a slight overestimation of the atroposelectivity (approximately 5−7%) had resulted from chiral HPLC analysis.

At this stage, having studied a number of variables in an attempt to improve both the activity and selectivity of this demanding transformation, we decided to move on to investigating the end game for synthesizing the natural product. The preparation of a late-stage tetracyclic streptonigrin intermediate **38** has been achieved in 65% yield and with a moderate level of enantiocontrol (42% ee from chiral HPLC analysis), using a phosphino hydrazone ligand **41**. This is the first report of an enantioenriched intermediate or analog of **1** to be obtained via synthesis and work to augment the degree of atroposelectivity is ongoing in our laboratories.

End Game. Returning to the synthesis of (±)-streptonigrin, conversion of intermediate quinoline-5,8-dione **39** into the natural product required the introduction of the C-7 amino group, removal of the D-ring benzyl ether, and hydrolysis of the pyridine methyl ester. Weinreb had already achieved these transformations in 17% yield over five steps in his synthesis,[19,59] but the end game itself has received virtually no attention since the original publication; hence, we decided to look more closely at the sequence.

During their synthesis of ABC-ring analogues of streptonigrin, Harding demonstrated that an azide could be installed on quinoline-5,8-dione **43** and then efficiently reduced to primary amine **44** using Pd/C and hydrogen (Scheme 10).[27] Similarly, we found that exposing quinoline-5,8-dione intermediate **39** to the reducing conditions led smoothly to the deprotected phenol **45** (Scheme 11).

Scheme 10. Harding's Azide Reduction in Streptonigrin Analog Synthesis Using Pd/C and Hydrogen

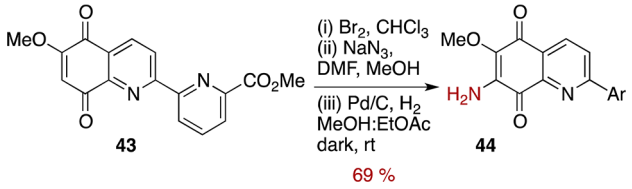

Given these observations, we believed that there was the opportunity to telescope the azide reduction and hydrogenolysis steps from Weinreb's end game (**47** → **48**, Scheme 12) and so we began investigating a modified approach that would shorten the sequence from five to four steps.

Scheme 11. Model Streptonigrin Benzyl Ether Hydrogenolysis Using Pd/C and Hydrogen

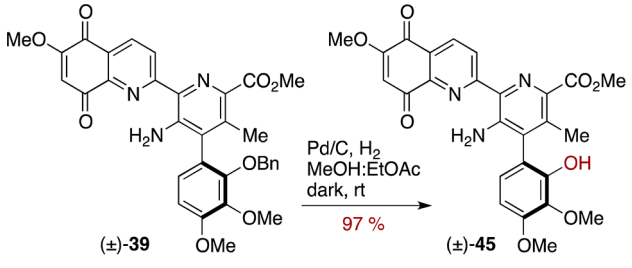

dx.doi.org/10.1021/jo402388f | J. Org. Chem. 2013, 78, 12338−12350

Scheme 12. Proposed Shortened Sequence for the End Game

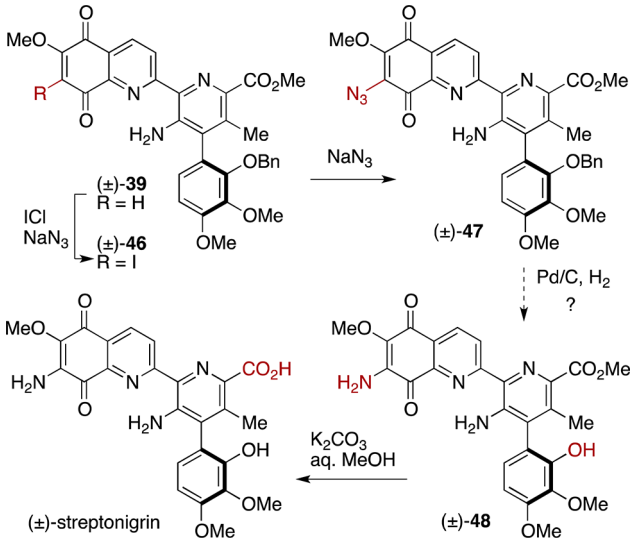

Taking the established tactics as a starting point, we sought to introduce iodine at the 7-position of **39** using IN_3 generated in situ from ICl and sodium azide. However, in our hands, we were unable to reliably reproduce this transformation, and despite exhaustively studying the preparation and handling of IN_3 we consistently obtained a complex mixture of products; only small amounts (<10%) of the desired iodo compound **46** were detected in the ^{1}H NMR spectra of crude material. We confirmed in situ generation of iodine azide[60] by successfully performing an iodoazidation of cinnamaldehyde dimethyl acetal;[61] while Ciufolini has used these tactics effectively at the end of his synthesis of streptinigrone,[48] it should be noted that the C-5′ amino pyridine is protected as a Cbz group and the authors do draw attention to the instability of their intermediates.

Having been unable to accomplish the initial iodination step of the end game, we briefly investigated alternative reagents for the direct installation of nitrogen on either quinoline-5,8-dione **39** or quinoline **38**. Disappointingly, electrophilic amination[62] of **39** using chloramine[63] returned starting material, whereas methods to nitrate quinoline **38** led predominantly to the quinoline-5,8-dione **39**, as a product of oxidation, without introducing the desired nitro group.[64]

As a result of these findings, we ceased investigations into direct amination and returned our attention to the functionalization of **39** via initial halogenation and subsequent nucleophilic azide displacement. In order to develop an understanding of the inherent reactivity of the quinoline-5,8-dione toward halogenation, **39** was exposed to a series of halogenating reagents (Table 4).

Treatment of **39** with various iodinating and chlorinating reagents resulted in no reaction and complete recovery of starting material (Table 4, entries 1 to 5). On the other hand, **39** proved to be reactive toward a range of brominating agents. Interestingly, it was found that initial bromination occurred preferentially on the D-ring to afford **49**, and when **39** was treated with 1.1 equiv of brominating reagent a mixture of **49**, dibrominated **50**, and starting material was observed (entries 6−8). Increasing the amount of bromine led to complete consumption of starting material, producing 80% of the dibrominated derivative **50** (entry 9), with a small amount of

Table 4. Halogenation of Quinoline-5,8-dione 39

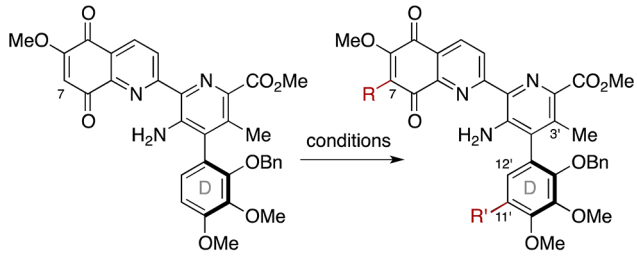

entry	conditions[a]	conversion[b] (%)
1	ICl, MeCN, 0 °C	no reaction
2	NIS, $CHCl_3$, rt	no reaction
3	I_2, $CHCl_3$, 0 °C to rt	no reaction
4	I_2, $AgNO_3$, $CHCl_3$, 0 °C to rt	no reaction
5	NCS, $CHCl_3$, 0 °C to rt	no reaction
6	NBS, $CHCl_3$, rt	**39**:**49**:**50**(1:1:1)
7	TBCO, $CHCl_3$, rt	**39**:**49**:**50**(1:1:1)
8	Br_2, $CHCl_3$, rt	**39**:**49**:**50** (2:1:2)
9[c]	Br_2, $CHCl_3$, rt	**50**, 80%
10[c]	Br_2, pyr, $CHCl_3$, rt	**50**, 99%

[a]1.1 equiv of halogenating reagent used. [b]Conversions measured by ^{1}H NMR spectroscopy. [c]4.0 equiv of bromine used. NIS = *N*-iodosuccinimide, NCS = *N*-chlorosuccinimide, NBS = *N*-bromosuccinimide, TBCO = 2,4,4,6-tetrabromo-2,5-cyclohexadienone.

decomposition visible in the ^{1}H NMR spectrum of the crude material. It was postulated that this decomposition resulted from the generation of HBr during the reaction, so an excess of pyridine was added to buffer the reaction mixture. Pleasingly, this led to the complete conversion of **39** to the dibrominated compound **50** (entry 10). Based on a steric rationale, the site of D-ring bromination was presumed to be C-11′, and this was confirmed by an observed NOE correlation between the C-3′ methyl group and the remaining proton on the D-ring, indicating that the proton is at C-12′.[17] This innate preference for D-ring bromination is advantageous, as it represents an attractive handle for possible manipulation in future streptonigrin analog syntheses, yet it should be readily removed under the proposed hydrogenation conditions later in the end game; overall, **50** appeared to be a viable alternative to the iodo compound **46** from Weinreb's route.

Dibrominated compound **50** was found to be unstable to chromatography, so it was immediately treated with sodium azide in DMF at 0 °C to furnish azido derivative **51** (Scheme 13). This compound also proved to be unstable, so **51** was subjected directly to the hydrogenation conditions used previously (see Schemes 11 and 12). To our satisfaction, catalytic Pd/C and hydrogen in a mixture of methanol and ethyl acetate did indeed effect the three planned transformations: azide reduction, benzyl ether hydrogenolysis, and reduction of the D-ring aryl bromide. Pleasingly, this trifunctional hydrogenative procedure proved to be robust and reliable. Including bromination and the nucleophilic displacement with azide, streptonigrin methyl ester **48** was generated in 57% overall yield from the formal quinoline-5,8-dione intermediate **39**.

Finally, according to Weinreb's synthesis,[19] treatment of **48** with potassium carbonate in aqueous methanol revealed the free C-ring carboxylic acid, affording (±)-streptonigrin **1** in

dx.doi.org/10.1021/jo402388f | J. Org. Chem. 2013, 78, 12338−12350

Scheme 13. Revised Streptonigrin End Game

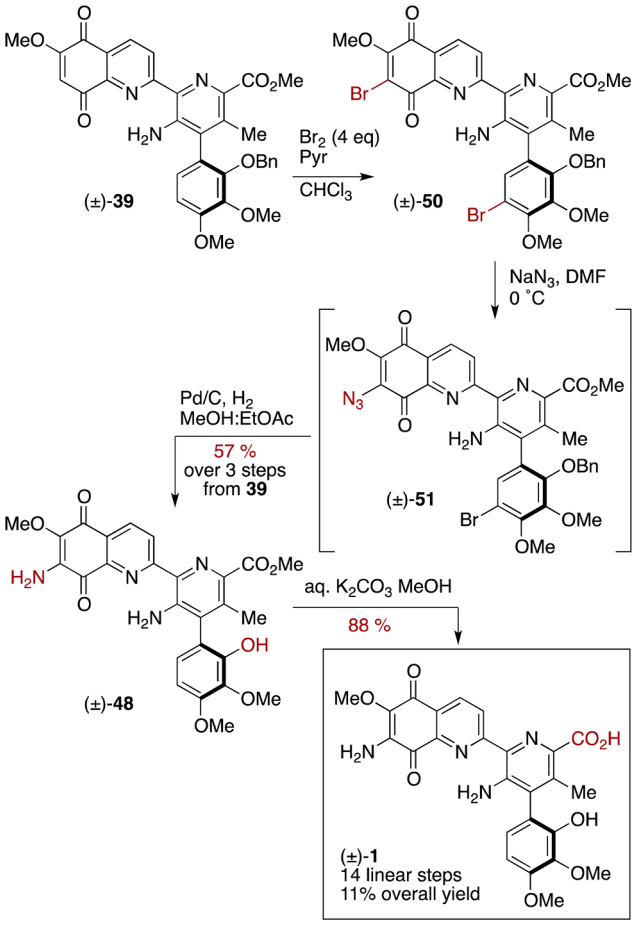

88% yield, the spectroscopic data of which matched those reported in the literature and that of an authentic sample of the natural product.[65] Attempts to reduce the relatively long reaction time for hydrolysis (48 h) by increasing the concentration led to lower yields of the acid.

Overall, the synthetic sequence for converting late-stage formal intermediate **39** into the natural product has been revised and now stands at 50% yield over four steps. Key to the success of this approach was the development of a trifunctional hydrogenative protocol, which has enabled the revised route to be both reliable and robust and will facilitate the future synthesis of a library of late-stage streptonigrin analogs for biological evaluation.

CONCLUSION

We have completed a concise and efficient total synthesis of the antitumor agent (±)-streptonigrin (**1**) in 14 linear steps from inexpensive ethyl glyoxalate with an overall yield of 11% (counting the one-pot transformation of **22** into **24** as one step). The synthesis showcases recent methodology in the rapid generation of a complex substituted pyridine, which has been accessed via two different pathways, and also revises the long-standing end game for streptonigrin, providing a more streamlined and robust set of tactics. The first-generation route to pyridine **15** afforded streptonigrin in a slightly longer sequence (16 linear steps) but an increased 14% overall yield. However, this approach is limited to small-scale synthesis and hence the second-generation route offers a more practical alternative to prepare the natural product and late-stage analogues whose biological activity could be quickly evaluated. Finally, investigations into the use of chiral ligands to effect a challenging asymmetric Suzuki–Miyaura cross-coupling reaction, and so enable the synthesis of enantioenriched streptonigrin, revealed moderate levels of enantioselectivity in the presence of bidentate phosphino hydrazone and bisphosphine ligands.

EXPERIMENTAL SECTION

General experimental considerations are provided in the Supporting Information. Experimental procedures and spectroscopic analysis for new compounds are listed below; for the experimental procedures and characterization data of the remaining compounds, see ref 17.

Ethyl 2-(*N*-Methoxyacrylamido)-3-methylpent-4-enoate (10). Acryloyl chloride (2.9 mL, 35 mmol) was added dropwise to a stirred solution of methoxylamine **9** (4.40 g, 23.5 mmol) and triethylamine (6.9 mL, 50 mmol) in dichloromethane (47 mL) at 0 °C. The mixture was allowed to warm to rt and was stirred for 16 h. The mixture was diluted with dichloromethane (50 mL) and quenched with water (50 mL). The aqueous phase was re-extracted with dichloromethane (3 × 20 mL), and the combined organic extracts were washed with brine (50 mL), dried over Na_2SO_4, filtered, and concentrated in vacuo. The crude product was purified by column chromatography (gradient 8:1 to 4:1 PE/EtOAc, R_f 0.31 in 8:1) to afford **10** as a light yellow oil (5.44 g, 96%) as a 2:1 mixture of diastereoisomers which were not separated. The ^{1}H and ^{13}C NMR data provided are for the major diastereomer. ^{1}H (400 MHz, $CDCl_3$) δ: 6.71 (1H, dd, J = 10.4, 17.6 Hz, COC=CH_2), 6.46 (1H, dd, J = 1.6, 17.0 Hz, COCH=CH_2), 5.83–5.67 (2H, m, COCH=CH_2 and CH(CH_3)CH=CH_2), 5.13 (1H, d, J = 17.3 Hz, CH(CH_3)CH=CH_2), 5.03 (1H, d, J = 10.1 Hz, CH(CH_3)CH=CH_2), 4.82 (1H, d, J = 9.8 Hz, C$H$$CO_2$Et), 4.20–4.12 (2H, m, $CO_2CH_2CH_3$), 3.81 (3H, s, OCH_3), 3.04–2.98 (1H, m, C$H$$CH_3$), 1.24 (3H, t, J = 6.9 Hz, $CO_2CH_2CH_3$), 1.03 (3H, d, J = 6.7 Hz, CHCH_3). ^{13}C (101 MHz, $CDCl_3$) δ: 169.9, 168.1, 139.5, 130.7, 126.1, 116.4, 64.9, 64.7, 61.4, 37.8, 17.5, 14.4. IR (thin film) ν_{max}: 3082 (w), 2981 (m), 2940 (w), 1744 (s), 1669 (s), 1621 (m), 1409 (s), 1270 (m), 1194 (m), 1029 (m), 787 (m) cm^{-1}. HRMS (ESI-TOF) m/z: [M + Na]$^+$ calcd for $C_{12}H_{19}NO_4Na$ 264.1206, found 264.1205.

Ethyl 1-Methoxy-3-methyl-6-oxo-1,2,3,6-tetrahydropyridine-2-carboxylate (11). To a solution of Hoveyda–Grubbs second-generation catalyst (170 mg, 0.271 mmol) in dichloromethane (280 mL) was added a solution of **10** (2.18 g, 9.04 mmol) in dichloromethane (20 mL). The solution was heated at reflux for 24 h. The reaction mixture was cooled to rt and concentrated in vacuo. The crude product was purified by column chromatography (1:1 PE/EtOAc, R_f 0.29) to afford **11** as a light brown oil (1.87 g, 97%) as a 2:1 mixture of diastereoisomers which were not separated. The ^{1}H and ^{13}C NMR data provided are for the major diastereomer. ^{1}H (400 MHz, $CDCl_3$) δ: 6.16 (1H, dd, J = 10.0, 1.4 Hz, COCH=CH), 5.84 (1H, dd, J = 9.9, 2.8 Hz, COCH=CH), 4.33 (1H, d, J = 7.3 Hz, C$H$$CO_2$Et), 4.16 (2H, q, J = 7.19 Hz, OCH_2CH_3), 3.77 (3H, s, OCH_3), 3.29–3.21 (1H, m, C$H$$CH_3$), 1.26 (3H, t, J = 7.3 Hz, $CO_2CH_2CH_3$), 1.20 (3H, d, J = 7.5 Hz, CHCH_3). ^{13}C (101 MHz, $CDCl_3$) δ: 168.9, 166.3, 143.2, 123.9, 66.7, 63.2, 61.9, 34.5, 16.2, 14.5. IR (thin film) ν_{max}: 2979 (s), 2940 (s), 2904 (s), 2818 (w), 1669 (s), 1625 (s), 1460 (s), 1385 (s), 1199 (s), 1022 (s), 818 (s), 706 (s) cm^{-1}. HRMS (ESI-TOF) m/z: [M + Na]$^+$ calcd for $C_{10}H_{15}NO_4Na$ 236.0893, found 236.0895.

Methyl 3-Methyl-6-oxo-1,6-dihydropyridine-2-carboxylate (12). DBU (1.67 mL, 11.2 mmol) was added to a solution of **11** (1.69 g, 7.93 mmol) in methanol (23 mL), and the resulting mixture was stirred for 15 h at rt. The reaction mixture was concentrated in vacuo to yield the crude product which was purified by column chromatography (gradient EtOAc to 9:1 EtOAc/MeOH, R_f 0.12 in EtOAc) to afford **12** as a white solid (1.31 g, 99%). ^{1}H (400 MHz, $CDCl_3$) δ: 9.84 (1H, br s, NH), 7.29 (1H, d, J = 9.5 Hz, COCH=CH), 6.71 (1H, d, J = 9.2 Hz, COCH=CH), 3.95 (3H, s, OCH_3), 2.40 (3H, s, CCH_3). ^{13}C (101 MHz, $CDCl_3$) δ: 162.2, 161.7, 145.8,

dx.doi.org/10.1021/jo402388f | J. Org. Chem. 2013, 78, 12338–12350

129.7, 126.9, 121.8, 53.4, 18.6. Mp: 120−121 °C (recrystallized from CH_2Cl_2) (lit.[31] mp 120−123 °C). These data were in accordance with the literature values.[31]

Methyl 3-Methyl-5-nitro-6-oxo-1,6-dihydropyridine-2-carboxylate (13). Concentrated sulfuric acid (1.2 mL) was added dropwise to a screw-top tube containing a solution of pyridone **12** (0.500 g, 2.99 mmol) in concd nitric acid (2.0 mL) at 0 °C, and the reaction vessel was then sealed. After 5 min, the reaction mixture was allowed to warm to rt and then heated at 50 °C. After 7 h, the reaction mixture was allowed to cool to rt and then poured into ice−water. The aqueous layer was extracted six times with ethyl acetate (until the yellow color had faded), and the combined organic layers were dried over Na_2SO_4, filtered, and concentrated in vacuo. The product was then purified by column chromatography (19:1 EtOAc/MeOH, R_f 0.50) to afford **13** as a yellow solid (0.558 g, 88%). ^{1}H (400 MHz, DMSO-d_6) δ: 12.82 (1H, br s, N−H), 8.41 (1H, s, C^4-*H*), 3.88 (3H, s, OCH_3), 2.31 (3H, s, CH_3). ^{13}C (126 MHz, DMSO-d_6) δ: 162.1, 153.3, 141.0, 139.1, 118.8, 53.0, 16.6 (note: one peak not observed in ^{13}C NMR spectrum). IR (thin film) ν_{max}: 3054 (br), 2956 (w), 2851 (m), 1670 (s), 1271 (s), 1208 (s) cm^{-1}. HRMS (ESI-TOF) *m*/*z*: [M + Na]$^+$ calcd for $C_8H_8N_2O_5Na$ 235.0331, found 235.0326.

Methyl 3-Methyl-5-nitro-6-(((trifluoromethyl)sulfonyl)oxy)-picolinate (14). Trifluoromethanesulfonic anhydride (0.71 mL, 4.25 mmol) was added dropwise to a solution of nitropyridone **13** (0.500 g, 2.36 mmol) and 2,6-di-*tert*-butyl-4-methylpyridine (0.723 g, 3.54 mmol) in dichloromethane (25 mL) at −78 °C. The solution was allowed to warm to 0 °C and was stirred at 0 °C for 4 h. The reaction mixture was washed with satd aq $NaHCO_3$, dried over Na_2SO_4, filtered, and concentrated in vacuo. The product was then purified by column chromatography (4:1 PE/EtOAc, R_f 0.60) to afford **14** as a pale yellow oil (0.649 g, 80%). ^{1}H (400 MHz, $CDCl_3$) δ: 8.47 (1H, s, Ar*H*), 4.01 (3H, s, OCH_3), 2.72 (3H, s, CH_3). ^{13}C (101 MHz, $CDCl_3$) δ: 163.4, 149.0, 143.8, 139.9, 137.8, 136.8, 118.4 (q, J = 319 Hz, CF_3), 53.3, 19.0. IR (thin film) ν_{max}: 3001 (w), 2941 (w), 1736 (s), 1582 (s), 1540 (s), 1427 (s), 1321 (s), 1212 (s), 1126 (s), 1037 (s), 881 (s), 829 (s) cm^{-1}. HRMS (ESI-TOF) *m*/*z*: [M + Na]$^+$ calcd for $C_9H_7F_3N_2O_7Na$ 366.9818, found 366.9809.

Methyl 5-Amino-3-methyl-6-(((trifluoromethyl)sulfonyl)-oxy)picolinate (25). Iron powder (325 mesh, 0.975 g, 17.4 mmol) was added to a solution of nitropyridine **14** (0.400 g, 1.16 mmol) in methanol (7.0 mL) and acetic acid (7.0 mL). The reaction mixture was heated at reflux for 2 h and then allowed to cool to rt and neutralized through the addition of solid Na_2CO_3. Water (10 mL) was added, and the aqueous layer was extracted with dichloromethane (3 × 10 mL), dried over Na_2SO_4, filtered, and concentrated in vacuo. The crude product was purified by column chromatography (4:1 PE/EtOAc, R_f 0.48) to afford **25** as a colorless crystalline solid (0.361 g, 99%). ^{1}H (400 MHz, $CDCl_3$) δ: 7.01 (1H, s, Ar-H), 4.31 (2H, br s, NH_2), 3.89 (3H, s, OCH_3), 2.58 (3H, s, CH_3); ^{13}C (126 MHz, $CDCl_3$) δ: 164.9, 139.8, 139.6, 136.2, 132.4, 127.1, 118.5 (q, J = 319 Hz, CF_3), 52.2, 19.9. Mp: 108−110 °C (recrystallized from CH_2Cl_2). These data were in accordance with the literature values.[17]

Methyl 5-Amino-4-bromo-3-methyl-6-(trifluoromethylsulfonyloxy)picolinate (15). *N*-Bromosuccinimide (0.260 g, 1.46 mmol) was added to a solution of **25** (0.418 g, 1.33 mmol) in acetonitrile (13 mL) at 0 °C, and the reaction mixture was allowed to warm to rt and was stirred for 4 h. Solvent was removed in vacuo, and the residue was redissolved in dichloromethane (30 mL) and was washed with 1 M HCl (30 mL), satd aq $NaHCO_3$ (30 mL), and brine (30 mL). The organic phase was dried over Na_2SO_4, filtered, and concentrated in vacuo. The crude product was purified by column chromatography (7:1 PE/EtOAc, R_f 0.22) to afford **15** as a colorless crystalline solid (0.480 g, 92%). ^{1}H (500 MHz, $CDCl_3$) δ: 4.81 (2H, br s, NH_2), 3.92 (3H, s, OCH_3), 2.71 (3H, s, CH_3). ^{13}C (126 MHz, $CDCl_3$) δ: 164.8, 138.8, 138.1, 135.0, 132.8, 123.0, 118.5 (q, J = 319 Hz, CF_3), 52.6, 19.5. Mp: 117−118 °C (recrystallized from CH_2Cl_2). These data were in accordance with the literature values.[17]

Ring-Closing Metathesis Procedures Using Diene 21. *Procedure A: Thermal without Benzoquinone Additive.* Hoveyda−Grubbs second-generation catalyst (0.016 g, 0.026 mmol) was added to a reaction tube charged with diene **21** (0.100 g, 0.259 mmol) in dichloromethane (2.6 mL). The solution was degassed by bubbling argon through for 5 min; the tube was then sealed and the reaction heated to 70 °C for 48 h. The reaction mixture was cooled to rt and concentrated in vacuo to yield a mixture that was purified by flash column chromatography to afford the desired product **22** (0.044 g, 47%, 3:2 PE/EtOAc R_f 0.20) and the isomerized starting material **23** (0.038 g, 38%, 1:1 PE:EtOAc, R_f 0.36), both as olive-colored oils. Each was obtained as an inseparable 2:1 mixture of diastereoisomers.

Procedure B: Microwave. Hoveyda−Grubbs second-generation catalyst (0.041 g, 0.065 mmol) was added to a reaction tube charged with diene **21** (0.250 g, 0.648 mmol) and benzoquinone (0.014 g, 0.130 mmol) in toluene (6.5 mL). The solution was degassed by bubbling argon through for 5 min; the tube was then sealed and the reaction subjected to microwave irradiation at 160 °C for 1 h. The reaction mixture was cooled to room temperature and concentrated in vacuo to yield the crude product which was purified by flash chromatography (3:2 PE/EtOAc, R_f 0.20) to afford **22** as an olive-colored oil (0.162 g, 70%) and as an inseparable 2:1 mixture of diastereoisomers.

Procedure C: Optimized. A solution of Hoveyda-Grubbs' second generation catalyst (0.126 g, 0.201 mmol) in toluene (10 mL) was added dropwise over 10 h *via* a syringe pump to a refluxing solution of **21** (1.55 g, 4.01 mmol) and benzoquinone (0.065 g, 0.602 mmol) in toluene (40 mL). Once addition was complete, the mixture was heated at reflux for a further 6 h. The reaction mixture was allowed to cool to rt; dimethyl sulfoxide (1.07 mL, 15.0 mmol) was added, and the resulting solution was stirred at rt for 1 h. The crude mixture was preadsorbed onto silica gel (3.0 g) and the solvent removed in vacuo. The product was then purified by column chromatography (3:2 PE/EtOAc, R_f 0.20) to afford **22** as a colorless oil (1.09 g, 76%) and as an inseparable 2:1 mixture of diastereoisomers.

Ethyl 5-(1,3-Dioxoisoindolin-2-yl)-1-methoxy-3-methyl-6-oxo-1,2,3,6-tetrahydropyridine-2-carboxylate (22). The ^{1}H and ^{13}C NMR spectroscopic data provided for **22** are for the major diastereoisomer. ^{1}H (500 MHz, $CDCl_3$) δ: 7.90−7.87 (2H, m, 2 × Ar-H), 7.76−7.74 (2H, m, 2 × Ar-H), 6.39 (1H, d, J = 2.6 Hz, C^4−H), 4.46 (1H, dd, J = 7.3 Hz, C*H*CO$_2$Et), 4.36−4.26 (2H, m, CO$_2$CH_2CH$_3$), 3.83 (3H, s, OCH_3), 3.52 (1H, dqn, J = 7.3, 2.5 Hz, C*H*CH$_3$), 1.33−1.31 (6H, m, CO$_2$CH$_2$CH_3 and CHCH_3). ^{13}C (126 MHz, $CDCl_3$) δ: 167.9, 166.9, 162.0, 143.0, 134.3, 131.9, 124.3, 123.7, 66.3, 62.5, 62.0, 32.5, 15.7, 14.1. These data were in accordance with the literature values.[17]

Ethyl 2-(2-(1,3-Dioxoisoindolin-2-yl)-*N*-methoxyacrylamido)-3-methylpent-3-enoate (23). The ^{1}H and ^{13}C NMR spectroscopic data provided for **23** are for the major diastereoisomer. ^{1}H (500 MHz, $CDCl_3$) δ: 7.88 (2H, dd, J = 3.2, 5.4 Hz, 2 × Ar*H*), 7.75 (2H, dd, J = 3.2, 5.4 Hz, 2 × Ar*H*), 6.23 (1H, s, NC=CH_2), 5.97 (1H, d, J = 1.0 Hz, NC=CH_2), 5.59 (1H, qt, J = 1.3, 6.6 Hz, CH$_3$C*H*=C), 5.30 (1H, s, NC*H*CO$_2$Et), 4.21 (2H, q, J = 7.3 Hz, OCH_2CH$_3$), 3.76 (3H, s, OCH_3), 1.74 (3H, s, C(CH_3)=C), 1.67 (3H, d, J = 7.6 Hz, CH_3CH=C), 1.27 (3H, t, J = 7.0 Hz, OCH_2CH_3). ^{13}C (126 MHz, $CDCl_3$) δ: 168.9, 166.2, 164.2, 134.5, 131.7, 130.1, 128.2, 127.5, 123.8, 121.3, 67.6, 64.8, 61.6, 15.2, 14.1, 13.7. IR (thin film) ν_{max} 2962 (w), 2941 (w), 1789 (w), 1726 (s), 1660 (m), 1630 (m), 1369 (m), 1210 (m), 1101 (m), 1027 (m), 919 (m), 731 (m), 716 (m) cm^{-1}. HRMS (ESI-TOF) *m*/*z*: [M + Na]$^+$ calcd for $C_{20}H_{22}N_2O_6Na$ 409.1370, found 409.1369.

2-Bromo-5,6,8-trimethoxyquinoline (35). Phosphorus oxybromide (0.129 mL, 1.27 mmol) was added to a solution of **33** (0.050 g, 0.212 mmol), pyridine (0.103 mL, 1.27 mmol), and DMF (0.005 mL) in bromobenzene (1.0 mL) at rt, and the resulting mixture was heated at reflux for 1.5 h. The reaction mixture was allowed to cool to rt and quenched upon slow addition of satd aq $NaHCO_3$ (20 mL). The mixture was extracted with EtOAc (3 × 50 mL), and the combined organic layers were washed with brine (50 mL), dried over $MgSO_4$, filtered, and concentrated in vacuo. The crude product was purified by column chromatography (2:1 PE/EtOAc, R_f 0.40) to afford **35** as a colorless crystalline solid (0.037 g, 58%). ^{1}H (400 MHz,

dx.doi.org/10.1021/jo402388f | J. Org. Chem. 2013, 78, 12338−12350

$CDCl_3$) δ: 8.21 (1H, d, J = 8.8 Hz, 2 × Ar*H*), 7.50 (1H, d, J = 8.8 Hz, 2 × Ar*H*), 6.86 (1H, s, Ar*H*), 4.05 (3H, s, OCH_3), 4.02 (3H, s, OCH_3), 3.91 (3H, s, OCH_3). ^{13}C (100 MHz, $CDCl_3$) δ: 151.7, 149.0, 138.8, 135.5, 135.3, 132.5, 126.8, 123.4, 99.2, 61.5, 57.0, 56.2. IR (thin film) ν_{max} 3002 (w), 2931 (w), 2847 (w), 1610 (m), 1567 (s), 1384 (s), 1238 (s), 1098 (s), 913 (s), 826 (s), 777 (s) cm^{-1}. HRMS (ESI-TOF) m/z: [M + H]$^+$ calcd for $C_{12}H_{13}BrNO_3$ 298.0073 and 300.0053, found 298.0070 and 300.0047. Mp: 149−150 °C (recrystallized from CH_2Cl_2).

General Procedure for the Asymmetric Suzuki−Miyaura Reaction. A solution of the palladium source (0.008 mmol) and ligand (0.010 mmol) in dioxane (0.1 mL) was stirred at rt for 30 min. A solution of aryl boronate ester **28** (0.049 mmol) and pyridine **37** (0.032 mmol) in dioxane (0.22 mL) was subsequently added. The reaction mixture was degassed and refilled with argon five times, and then a solution of sodium carbonate (1.0 M, 0.10 mL) was added. The mixture was degassed and refilled with argon five times again and then heated at the designated temperature for 24 h. The mixture was allowed to cool to rt, diluted with EtOAc (1.0 mL), and washed with brine (1.0 mL). The organic phase was dried over Na_2SO_4, filtered, and concentrated in vacuo. The crude product was purified by column chromatography (2:1 PE:EtOAc, R_f 0.32) to afford **38** as a yellow solid. A sample obtained using phosphino hydrazone ligand **41** that afforded product with 30% ee (by chiral HPLC analysis) gave $[\alpha]_D^{25}$ + 51.5 (c = 0.29, $CHCl_3$).

Methyl 5-Amino-4-(2-(benzyloxy)-3,4-dimethoxyphenyl)-3-methyl-6-(5,6,8-trimethoxyquinolin-2-yl)picolinate (38). ^{1}H (200 MHz, $CDCl_3$) δ: 8.88 (1H, d, J = 9.1 Hz, Ar-H), 8.49 (1H, d, J = 9.1 Hz, Ar-H), 7.12−7.10 (3H, m, Ar-H), 7.05−7.01 (2H, m, Ar-H), 6.88 (2H, s, Ar-H), 6.83 (1H, s, Ar-H), 4.93 (1H, d, J = 11.0 Hz, OCH_2Ph), 4.86 (1H, d, J = 11.0 Hz, OCH_2Ph), 4.04 (3H, s, OCH_3), 4.01 (6H, s, 2 × OCH_3), 3.97 (6H, s, 2 × OCH_3), 3.95 (3H, s, OCH_3), 2.29 (3H, s, CH_3). ^{13}C (62.5 MHz, $CDCl_3$) δ: 167.2, 155.7, 154.1, 152.1, 150.7, 148.7, 145.2, 143.4, 137.1, 136.6, 135.8, 134.4, 133.1, 133.0, 132.7, 130.0, 128.1 (2 × C), 128.0 (2 × C), 127.7, 125.1, 123.0, 122.1, 120.9, 108.4, 98.3, 75.2, 61.6, 61.1, 57.2, 56.1 (2 × C), 52.1, 17.5. Mp 209−210 °C (recrystallized from CH_2Cl_2). These data were in accordance with the literature values.[17]

(*S*)-(5-Amino-4-(2-(benzyloxy)-3,4-dimethoxyphenyl)-3-methyl-6-(5,6,8-trimethoxyquinolin-2-yl)pyridin-2-yl)methyl 3,3,3-Trifluoro-2-methoxy-2-phenylpropanoate (52). A solution of $LiAlH_4$ (1.0 M, 0.062 mL) was added to a solution of racemic **38** (0.013 g, 0.021 mmol) in THF (0.20 mL) at −30 °C. The mixture was warmed to rt and stirred for 4 h. A saturated aqueous solution of Na_2SO_4 was added until excess $LiAlH_4$ was quenched, and solid Na_2SO_4 had precipitated. The solution was then filtered and concentrated in vacuo. The crude product **42** was used without further purification. DMAP (0.011 g, 0.086 mmol) and (*R*)-(−)-α-methoxy-α-(trifluoromethyl)phenylacetyl chloride (0.013 mL, 0.069 mmol) were added to a solution of **42** (0.0079 g, 0.013 mmol) in dichloromethane (0.13 mL). The reaction was stirred at rt for 16 h or until TLC indicated consumption of the starting material. The reaction was filtered through a small silica plug and then purified by column chromatography (gradient PE to 2:1 PE/EtOAc, R_f 0.30 in 2:1) to afford **52** as a red solid (0.0087 mg, 48%). ^{1}H (400 MHz, $CDCl_3$) δ: 8.80 (1H, d, J = 9.2 Hz, Ar-H), 8.42 (1H, d, J = 9.2 Hz, Ar-H), 7.58−7.54 (2H, m, Ph), 7.33−7.29 (3H, m, Ph), 7.08−6.93 (5H, m, Mosher Ph), 6.87 (2H, s, Ar-H), 6.83 (1H, s, Ar-H), 5.65−5.57 (1H, m, $CH_2OC(O)$), 5.48−5.41 (1H, m, $CH_2OC(O)$), 4.93−4.86 (1H, m, CH_2Ph), 4.80−4.77 (1H, m, CH_2Ph), 4.04 (3H, s, OCH_3), 4.00 (3H, s, OCH_3), 3.96 (6H, s, OCH_3), 3.94 (3H, s, OCH_3), 3.52 (3H, s, Mosher OCH_3), 1.92 (3H, s, CH_3). ^{13}C (126 MHz, toluene-d_8) δ: 166.6 (2 × C), 156.9, 154.5 (2 × C), 152.5, 151.5, 151.4, 148.9, 144.3 (q, CF_3), 139.5, 139.4, 134.2, 133.7, 133.6, 133.5, 133.3 (2 × C), 133.2, 129.9, 123.5, 123.1 (2 × C), 121.2, 108.8, 99.8, 69.2, 68.9, 60.9, 60.7, 57.2, 55.6, 55.4, 14.4. δ_F (472 MHz, toluene-d_8): 71.73, 71.76. IR (thin film) ν_{max}: 3460 (w), 3321 (w), 2930 (m), 2850 (m), 1746 (m), 1625 (m), 1600 (m), 1581 (m), 1490 (m), 1465 (m), 1422 (w), 1358 (m), 1228.21 (br m), 1169 (w), 1098 (s), 1069 (w), 1001 (w), 921 (w), 719 (w) cm^{-1}. HRMS (ESI-TOF) m/z: [M + Na]$^+$ calcd for $C_{44}H_{42}F_3N_3O_9Na$ 836.2771, found 836.2736. Mp: 190−195 °C (recrystallized from CH_2Cl_2).

(±)-Methyl 5-Amino-4-(2-hydroxy-3,4-dimethoxyphenyl)-6-(6-methoxy-5,8-dioxo-5,8-dihydroquinolin-2-yl)-3-methylpicolinate (45). Palladium (10 wt.% on carbon, 0.007 g) was added to a solution of quinoline-5,8-dione **39** (0.020 g, 0.034 mmol) in methanol/EtOAc (3:1 by volume, 13.5 mL total). The reaction mixture was degassed in vacuo, placed under an atmosphere of H_2 (g), and stirred in the dark at rt for 12 h. The mixture was filtered through a pad of Celite eluting with EtOAc (10 mL), and the combined organic layers were concentrated in vacuo. The crude product was purified by column chromatography (1:1 PE/EtOAc, R_f 0.28) to afford debenzylated **45** as a dark red/brown solid (0.017 g, 97%). ^{1}H (200 MHz, $CDCl_3$) δ: 9.04 (1H, d, J = 8.4 Hz, Ar-H), 8.50 (1H, d, J = 8.4 Hz, Ar-H), 6.82 (1H, d, J = 8.7 Hz, Ar-H), 6.67 (1H, d, J = 8.6 Hz, Ar-H), 6.29 (1H, s, Ar-H), 5.89 (1H, br s, OH), 3.99 (6H, s, OCH_3), 3.96 (3H, s, OCH_3), 3.95 (3H, s, OCH_3), 2.34 (3H, s, CH_3). ^{13}C (126 MHz, $CDCl_3$) δ: 182.8, 179.4, 167.0, 163.1, 160.5, 152.7, 147.0, 146.2, 145.6, 138.0, 136.3, 135.7, 134.4, 132.9, 130.7, 125.7, 125.4, 125.1, 113.7, 109.9, 105.1, 61.2, 56.6, 56.0, 55.2, 17.4. IR (thin film) ν_{max}: 3467 (br), 3249 (br), 2953 (w), 1707 (s), 1687 (s), 1656 (m), 1610 (s), 1586 (s), 1460 (m), 1296 (s), 1243 (s), 1088 (s) cm^{-1}. HRMS (ESI-TOF) m/z: [M + Na]$^+$ Ccalcd for $C_{26}H_{23}N_3O_8Na$ 528.1377, found 528.1355. Mp: 113−114 °C (recrystallized from CH_2Cl_2).

(±)-Methyl 5-Amino-4-(2-(benzyloxy)-3,4-dimethoxyphenyl)-6-(6-methoxy-5,8-dioxo-5,8-dihydroquinolin-2-yl)-3-methylpicolinate (39). Example of an attempted nitration of quinoline **38**: Silver(II) oxide (0.016 g, 0.128 mmol) and nitric acid (35% aq, 0.04 mL) were added to a solution of quinoline (0.020 g, 0.032 mmol) in acetonitrile/water (4:1 by volume, 0.20 mL in total). The reaction mixture was allowed to stir at rt for 16 h, water was then added, and the mixture was extracted with ethyl acetate (3 × 5.0 mL). The combined organic layers were washed with satd aq $NaHCO_3$ and , brine, dried over Na_2SO_4, filtered, and concentrated in vacuo. The crude product was purified by column chromatography (1:1 PE/EtOAc, R_f 0.52) to afford *p*-quinoline-5,8-dione **39** as a dark red crystalline solid (0.013 g, 68%). ^{1}H (200 MHz, $CDCl_3$) δ: 9.02 (1H, d, J = 8.5 Hz, Ar-H), 8.49 (1H, d, J = 8.5 Hz, Ar-H), 7.13−7.07 (3H, m, Ar-H), 7.02−6.98 (2H, m, Ar-H), 6.87 (1H, d, J = 8.7 Hz, Ar-H), 6.82 (1H, d, J = 8.7 Hz, Ar-H), 6.28 (1H, s, Ar-H), 4.96 (1H, d, J = 11.2 Hz, OCH_2Ph), 4.89 (1H, d, J = 11.2 Hz, OCH_2Ph), 3.99 (3H, s, OCH_3), 3.96 (3H, s, OCH_3), 3.94 (6H, s, OCH_3), 2.24 (3H, s, CH_3). ^{13}C (62.5 MHz, $CDCl_3$) δ: 182.7, 179.3, 166.9, 163.0, 160.4, 154.3, 150.5, 146.2, 145.5, 143.4, 137.8, 137.1, 135.5, 134.3, 133.9, 130.4, 128.1 (2 × C), 127.9 (2 × C), 127.8, 125.4, 125.3, 124.8, 121.3, 109.8, 108.6, 75.1, 61.1, 56.6, 56.1, 52.2, 17.6. Mp: 242−246 °C (recrystallized from CH_2Cl_2) (lit.[19] mp 242−243 °C). These data were in accordance with the literature values.[17]

(±)-Methyl 5-Amino-4-(2-(benzyloxy)-5-bromo-3,4-dimethoxyphenyl)-6-(7-bromo-6-methoxy-5,8-dioxo-5,8-dihydroquinolin-2-yl)-3-methylpicolinate (50) and (±)-Methyl 5-Amino-4-(2-(benzyloxy)-5-bromo-3,4-dimethoxyphenyl)-6-(6-methoxy-5,8-dioxo-5,8-dihydroquinolin-2-yl)-3-methylpicolinate (49). Example bromination with 1.1 equiv of brominating reagent: Bromine (19 μL, 0.037 mmol) was added to a solution of quinoline-5,8-dione **39** (0.020 g, 0.034 mmol) in chloroform (1.1 mL) in the dark at rt The resulting reaction mixture was stirred for 8 h. Water (5.0 mL) was added, and the aqueous layer was extracted with dichloromethane (3 × 5.0 mL). The combined organic layers were dried over Na_2SO_4, filtered, and concentrated in vacuo to afford a mixture of starting material **39**, monobrominated quinone **49**, and dibromo-quinone **50** in a 2:1:2 ratio (by analysis of the ^{1}H NMR spectrum of the crude material, quantitative recovery). The brominated compounds were unstable to silica, but small quantities of purified dibromo **50** (2:1 PE/EtOAc, R_f 0.70) and monobromo **49** (2:1 PE/EtOAc, R_f 0.50) could be obtained following silica gel chromatography, the data for which follows:

Dibromo **50**. ^{1}H (500 MHz, $CDCl_3$) δ: 9.05 (1H, d, J = 8.5 Hz, Ar-H), 8.46 (1H, d, J = 8.5 Hz, Ar-H), 7.14−7.11 (3H, m, Ar-H), 7.10 (1H, s, Ar-H), 7.01−6.99 (2H, m, Ar-H), 4.95 (1H, d, J = 11.3 Hz, OCH_2Ph), 4.88 (1H, d, J = 11.3 Hz, OCH_2Ph), 4.37 (3H, s, OCH_3),

4.04 (3H, s, OCH_3), 4.00 (3H, s, OCH_3), 3.99 (3H, s, OCH_3), 2.25 (3H, s, CH_3). ^{13}C (125 MHz, $CDCl_3$) δ: 178.5, 176.7, 166.7, 162.8, 158.6, 151.9, 150.2, 148.8, 145.7, 144.5, 137.7, 136.6, 135.6, 134.4, 132.5, 130.4, 128.2, 128.1, 127.9 (2 × C), 125.9, 125.6, 125.2, 121.8, 112.9, 75.2, 62.1, 61.3, 61.2, 52.2, 17.6. Mp: 115−116 °C (recrystallized from CH_2Cl_2). These data were in accordance with the literature values.[17]

Monobromo **49**. ^1H (500 MHz, $CDCl_3$) δ: 9.04 (1H, d, J = 8.6 Hz, Ar-H), 8.52 (1H, d, J = 8.5 Hz, Ar-H), 7.14−7.10 (4H, m, Ar-H), 7.02−7.00 (2H, m, Ar-H), 6.31 (1H, s, Ar-H), 4.94 (1H, d, J = 11.2 Hz, OCH_2Ph), 4.88 (1H, d, J = 11.2 Hz, OCH_2Ph), 4.03 (3H, s, OCH_3), 4.00 (3H, s, OCH_3), 3.99 (3H, s, OCH_3), 3.96 (3H, s, OCH_3), 2.26 (3H, s, CH_3). ^{13}C (126 MHz, $CDCl_3$) δ: 182.7, 179.3, 166.7, 162.8, 160.5, 151.9, 150.2, 148.8, 145.7, 145.5, 137.6, 136.6, 135.6, 134.4, 132.4, 130.8, 128.3, 128.1, 128.0, 127.9, 125.7, 125.5 (2 × C), 112.9, 110.0, 75.3, 61.4, 61.2, 56.7, 52.2, 17.6. IR (thin film) ν_{max}: 3431 (br), 3235 (br), 2946 (w), 1711 (s), 1685 (s), 1661 (m), 1609 (m), 1586 (s), 1453 (m), 1242 (s), 1212 (s) cm^{-1}. HRMS (ESI-TOF) m/z: $[M + Na]^+$ calcd for $C_{33}H_{28}BrN_3O_8Na$ 696.0963 and 798.0934, found 696.0963 and 698.0966; mp 252−254 °C (recrystallized from CH_2Cl_2).

(±)-Streptonigrin (1). Potassium carbonate (0.167 g, 1.21 mmol) was added to a solution of streptonigrin methyl ester **48** (0.007 g, 0.013 mmol) in methanol/water (2:1 by volume, 10.8 mL total), and the resulting solution was stirred at rt for 48 h. The methanol was removed *in vacuo* and the resulting mixture neutralized with 3 M HCl. The mixture was extracted with dichloromethane (3 × 5.0 mL), and the combined organic layers were dried over Na_2SO_4, filtered, and concentrated in vacuo. The crude product was purified by column chromatography using pH 6.8 buffered silica gel[66] (49:1 CH_2Cl_2/CH_3OH, R_f 0.20) to afford streptonigrin (**1**) as a dark brown/black crystalline solid (0.006 g, 88%). ^1H (500 MHz, DMSO-d_6) δ: 12.32 (1H, br s, CO_2H), 9.01 (1H, d, J = 8.4 Hz, Ar-H), 8.92 (1H, s, Ar−OH), 8.36 (1H, d, J = 8.5 Hz, Ar-H), 6.92 (2H, br s, Ar-NH_2), 6.73 (1H, d, J = 8.5 Hz, Ar-H), 6.70 (1H, d, J = 8.6 Hz, Ar-H), 3.85 (3H, s, OCH_3), 3.81 (3H, s, OCH_3), 3.76 (3H, s, OCH_3), 2.18 (3H, s, CH_3). ^{13}C (126 MHz, DMSO-d_6) δ: 180.3, 175.9, 167.0, 159.8, 153.1, 148.1, 145.7, 144.1, 141.6, 136.9, 136.2, 135.7, 134.5, 134.0, 133.4, 129.5, 126.7, 125.9, 124.6, 114.9, 104.4, 60.3, 59.7, 55.7, 17.0. Mp: 289−290 °C (recrystallized from CH_2Cl_2). These data were in accordance with the literature values.[17,65]

■ ASSOCIATED CONTENT

Ⓢ Supporting Information

Copies of the ^1H and ^{13}C NMR spectra of all new compounds in addition to HPLC traces and Mosher's ester analysis of enantioenriched **38** and details of the attempted amination of quinoline-5,8-dione **39** and nitration of quinoline **38**. Details of the X-ray crystal structures of compounds **15** and **27** and the relevant crystallographic data are also included. This material is available free of charge via the Internet: http://pubs.acs.org.

■ AUTHOR INFORMATION

Corresponding Author

*E-mail: timothy.donohoe@chem.ox.ac.uk.

Notes

The authors declare no competing financial interest.

■ ACKNOWLEDGMENTS

We thank St. John's College, Oxford (C.R.J.), Skaggs-Oxford Scholarship Program and NSF GRFP (A.F.K.), the Brazilian Research Council (CNPq) for a Fellowship (L.C.A.B.), the University of Oxford (L.J.W., M.O.H.), EPSRC and AstraZeneca (M.R.T.), Exeter College & the Narotam Sekhsaria Foundation (A.H.R.), and Lilly UK (D.B.B.) for supporting this project.

■ REFERENCES

(1) Rao, K. V.; Cullen, W. P. *Antibiot. Annu.* **1959−1960**, 950.
(2) For a review of synthetic approaches to streptonigrin and related analogues, see: Bringmann, G.; Reichert, Y.; Kane, V. V. *Tetrahedron* **2004**, *60*, 3539.
(3) Rao, K. V.; Biemann, K.; Woodward, R. B. *J. Am. Chem. Soc.* **1963**, *85*, 2532.
(4) Chiu, Y.-Y. K.; Lipscomb, W. N. *J. Am. Chem. Soc.* **1975**, *97*, 2525.
(5) Von Hoff, D. D.; Rozencwieg, M.; Soper, W. T.; Hellman, J. J.; Penta, J. S.; Davis, H. L.; Muggia, F. M. *Cancer Treat. Rep* **1977**, *61*, 759.
(6) Bolzán, A. D.; Bianchi, M. S. *Mutat. Res.* **2001**, *488*, 25.
(7) Hadju, J. *Met. Ions Biol. Syst.* **1985**, *19*, 53.
(8) Gould, S. J.; Weinreb, S. M. *Fortschr. Chem. Org. Natur.* **1982**, *41*, 77.
(9) Harding, M. M.; Long, G. V. *Curr. Med. Chem.* **1997**, *4*, 405.
(10) White, J. R. *Biochem. Biophys. Res. Commun.* **1977**, *77*, 387.
(11) Cone, R.; Hasan, S. K.; Lown, J. W.; Morgan, A. R. *Can. J. Biochem.* **1976**, *54*, 219.
(12) (a) Hassett, D. J.; Britigan, B. E.; Svendsen, T.; Rosen, G. M.; Cohen, M. S. *J. Biol. Chem.* **1987**, *262*, 13404. (b) Gutteridge, J. M. *Biochem. Pharmacol.* **1984**, *33*, 3059.
(13) Fryatt, T.; Pettersson, H. I.; Gardipee, W. T.; Bray, K. C.; Green, S. J.; Slawin, A. M. Z.; Beall, H. D.; Moody, C. J. *Bioorg. Med. Chem.* **2004**, *12*, 1667.
(14) (a) Boger, D. L.; Yasuda, M.; Mitscher, L. A.; Drake, S. D.; Kitos, P. A.; Collins Thompson, S. *J. Med. Chem.* **1987**, *30*, 1918. (b) Xu, F.; Kong, D.; He, X.; Zhang, Z.; Han, M.; Xie, X.; Wang, P.; Cheng, H.; Tao, M.; Zhang, L.; Deng, Z.; Lin, S. *J. Am. Chem. Soc.* **2013**, *135*, 1739.
(15) Knuckley, B.; Jones, J. E.; Bachovchin, D. A.; Slack, J.; Causey, C. P.; Brown, S. J.; Rosen, H.; Cravatt, B. F.; Thompson, P. R. *Chem. Commun.* **2010**, *46*, 7175.
(16) Tennant, S.; Rickards, R. W. *Tetrahedron* **1997**, *53*, 15101.
(17) Donohoe, T. J.; Jones, C. R.; Barbosa, L. C. A. B. *J. Am. Chem. Soc.* **2011**, *133*, 16418.
(18) Basha, F. Z.; Hibino, S.; Kim, D.; Pye, W. E.; Wu, T.-T.; Weinreb, S. M. *J. Am. Chem. Soc.* **1980**, *102*, 3962.
(19) Weinreb, S. M.; Basha, F. Z.; Hibino, S.; Khatri, N. A.; Kim, D.; Pye, W. E.; Wu, T.-T. *J. Am. Chem. Soc.* **1982**, *104*, 536.
(20) Kende, A. S.; Lorah, D. P.; Boatman, R. J. *J. Am. Chem. Soc.* **1981**, *103*, 1271.
(21) Boger, D. L.; Panek, J. S. *J. Am. Chem. Soc.* **1985**, *107*, 5745.
(22) Take, Y.; Kubo, A.; Takemori, E.; Inoyue, Y.; Nakamura, S.; Nishimura, T.; Suzuki, H.; Yamaguchi, H. *J. Antibiot.* **1989**, *42*, 968.
(23) Herlt, A. J.; Rickards, R. W.; Wu, J.-P. *J. Antibiot.* **1985**, *38*, 516.
(24) Godard, A.; Marsais, F.; Plé, N.; Trécourt, F.; Turck, A.; Quéguiner, G. *Heterocycles* **1995**, *40*, 1055.
(25) Crous, R.; Dwyer, C.; Holzapfel, C. W. *Heterocycles* **1999**, *51*, 721.
(26) McElroy, W. T.; Deshong, P. *Org. Lett.* **2003**, *5*, 4779.
(27) Kimber, M.; Anderberg, P. I.; Harding, M. M. *Tetrahedron* **2000**, *56*, 3575.
(28) Fryatt, T.; Goroski, D. T.; Nilson, Z. D.; Moody, C. J.; Beall, H. D. *Bioorg. Med. Chem. Lett.* **1999**, *9*, 2195.
(29) Donohoe, T. J.; Bower, J. F.; Basutto, J. A.; Fishlock, L. P.; Procopiou, P. A.; Callens, C. K. A. *Tetrahedron* **2009**, *65*, 8969.
(30) Donohoe, T. J.; Fishlock, L. P.; Basutto, J. A.; Bower, J. F.; Procopiou, P. A.; Thompson, A. L. *Chem. Commun.* **2009**, *65*, 3008.
(31) Donohoe, T. J.; Fishlock, L. P.; Procopiou, P. A. *Org. Lett.* **2008**, *10*, 285.
(32) Reimann, S.; Erfle, S.; Villinger, A.; Langer, P. *Synlett* **2010**, 1528.
(33) Espino, G.; Kurbangalieva, A.; Brown, J. M. *Chem Commun.* **2007**, 1742.
(34) CCDC 867147 contains the supplementary crystallographic data for compound **15**; see ref 17 for further details.
(35) Yim, A.-M.; Vidal, Y.; Viallefont, P.; Martinez, J. *Tetrahedron: Asymmetry* **2002**, *13*, 503.

(36) Schmidt, B. *Eur. J. Org. Chem.* **2004**, 1865.
(37) Hong, S. H.; Sanders, D. P.; Lee, C. W.; Grubbs, R. H. *J. Am. Chem. Soc.* **2005**, *127*, 17160.
(38) Tadross, P. M.; Virgil, S. C.; Stoltz, B. M. *Org. Lett.* **2010**, *12*, 1612.
(39) Marsais, F.; Rovera, J. C.; Turck, A.; Godard, A.; Quéguiner, G. *J. Chem. Soc., Perkin Trans. 1* **1990**, 2611.
(40) Pla, D.; Albericio, F.; Álvarez, M. *Eur. J. Org. Chem.* **2007**, 1921.
(41) CCDC 867146 contains the supplementary crystallographic data for compound **27**; see ref 17 for further details.
(42) Newkome, G. R.; Patri, A. K.; Holder, E.; Schubert, U. S. *Eur. J. Org. Chem.* **2004**, 235.
(43) Hapke, M.; Brandt, L.; Lützen, A. *Chem. Soc. Rev.* **2008**, *37*, 2782.
(44) Downer, N. K.; Jackson, Y. A. *Org. Biomol. Chem.* **2004**, *2*, 3039.
(45) Fernández, F.; García-Mera, X.; Morales, M.; Rodríguez-Borges, J. E. *Synthesis* **2001**, 239.
(46) Verniest, G.; Wang, X.; De Kimpe, N.; Padwa, A. *J. Org. Chem.* **2010**, *75*, 424.
(47) Mee, S. P. H.; Lee, V.; Baldwin, J. E. *Angew. Chem., Int. Ed.* **2004**, *43*, 1132.
(48) Chan, B. K.; Ciufolini, M. A. *J. Org. Chem.* **2007**, *72*, 8489.
(49) Yin, J.; Rainka, M. P.; Zhang, X.-X.; Buchwald, S. L. *J. Am. Chem. Soc.* **2002**, *124*, 1162.
(50) Yin, J.; Buchwald, S. L. *J. Am. Chem. Soc.* **2000**, *122*, 12051.
(51) Cammidge, A. N.; Crépy, K. V. L *Chem. Commun.* **2000**, 1723.
(52) Review of asymmetric Suzuki reactions: Baudoin, O. *Eur. J. Org. Chem.* **2005**, 4223.
(53) Ros, A.; Estepa, B.; Bermejo, A.; Álvarez, E.; Fernández, R.; Lassaletta, J. M. *J. Org. Chem.* **2012**, *77*, 4740 and references cited therein.
(54) Willis, M. C.; Powell, L. H. W.; Claverie, C. K.; Watson, S. J. *Angew. Chem., Int. Ed.* **2004**, *43*, 1249.
(55) Uenishi, J.; Beau, J.-M.; Armstrong, R. W.; Kishi, Y. *J. Am. Chem. Soc.* **1987**, *109*, 4756.
(56) Korenaga, T.; Kosaki, T.; Fukumura, R.; Ema, T.; Sakai, T. *Org. Lett.* **2005**, *7*, 4915.
(57) Sindkhedkar, M. D.; Mulla, H. R.; Wurth, M. A.; Cammers-Goodwin, A. *Tetrahedron* **2001**, 2991.
(58) See the Supporting Information for full details of the Mosher's ester analyses.
(59) This end game had also been developed independently: Kende, A. S.; Naegely, P. C. *Tetrahedron Lett.* **1978**, *48*, 4775.
(60) For information on IN_3, see: Hassner, A. In *Encyclopedia of Reagents for Organic Synthesis*; Paquette, L. A., Ed.; John Wiley and Sons: New York, 1995; Vol. *4*, p 2802.
(61) Padwa, A.; Blacklock, T.; Tremper, A.*Organic Synthesis*; Wiley: New York, 1988; Collect. Vol. *VI*, p 893.
(62) For a review of electrophilic amination, see: Dembach, P.; Seconi, G.; Ricci, A. *Chem.—Eur. J.* **2000**, *6*, 1281.
(63) Hynes, J., Jr.; Doubleday, W. W.; Dyckman, A. J.; Godfrey, J. D., Jr.; Grosso, J. A.; Kiau, S.; Leftheris, K. *J. Org. Chem.* **2004**, *69*, 1368.
(64) See the Supporting Information for further details of amination and nitration experiments.
(65) Streptonigrin NMR spectroscopic data: Wang, H.; Yeo, S. L.; Xu, J.; Xu, X.; He, H.; Ronca, F.; Ting, A. E.; Wang, Y.; Yu, V. C.; Sim, M. M. *J. Nat. Prod.* **2002**, *65*, 721 and references cited therein.
(66) Silica gel stirred for 1 min in a pH 6.8 phosphate buffer and then dried in an oven at 110 °C, see ref 11.

Angewandte Communications

Di Shen, Darren L. Poole, Camilla C. Shotton, Anne F. Kornahrens, Dr. Mark P. Healy, Prof. Timothy J. Donohoe: Hydrogen-Borrowing and Interrupted-Hydrogen-Borrowing Reactions of Ketones and Methanol Catalyzed by Iridium: Angew. Chem. Int. Ed. 2015. 54. 1642–1645.

DOI: 10.1002/anie.201410391

Synthetic Methods

Hydrogen-Borrowing and Interrupted-Hydrogen-Borrowing Reactions of Ketones and Methanol Catalyzed by Iridium**

*Di Shen, Darren L. Poole, Camilla C. Shotton, Anne F. Kornahrens, Mark P. Healy, and Timothy J. Donohoe**

Abstract: *Reported herein is the use of catalytic [{Ir(cod)Cl}$_2$] to facilitate hydrogen-borrowing reactions of ketone enolates with methanol at 65 °C. An oxygen atmosphere accelerates the process, and when combined with the use of a bulky monodentate phosphine ligand, interrupts the catalytic cycle by preventing enone reduction. Subsequent addition of pronucleophiles to the reaction mixture allowed a one-pot methylenation/conjugate addition protocol to be developed, which greatly expands the range of products that can be made by this methodology.*

The use of transition metals to perform the alkylation of ketone enolates using hydrogen-borrowing reactions is an interesting and powerful alternative to enolate formation/alkylation reactions under more traditional reaction conditions (e.g. lithium amide bases coupled with alkyl halide electrophiles).[1] Recently we disclosed that rhodium was an effective metal for catalyzing the hydrogen-borrowing reactions of methanol and we developed a reaction for the methylation of ketones under relatively mild reaction conditions (carbonate base and 65 °C reaction temperature; Scheme 1).[2] Performing the reaction under an atmosphere of oxygen was an important modification resulting in higher yields and shorter reaction times (Scheme 1).

Methanol is an important feedstock chemical that has been utilized in a variety of chemical transformations which involve dehydrogenation to formaldehyde.[3] It is also important to note that the use of methanol in hydrogen borrowing is exceptional in that it confers the ability (by the formation of reactive formaldehyde) to form branched products from enolates and allows the production of more complex carbonyl compounds than previous cases.[2] However, our preliminary studies revealed two areas in need of improvement. Firstly, the ketone methylation reaction required between 5 and 10 mol% of rhodium metal, thus making the sequence potentially costly. Secondly, we predicted that it was difficult for other more hindered alcohols to form branched products from ketones because of adverse steric interactions in the aldol intermediates formed en route to the alkylated products.

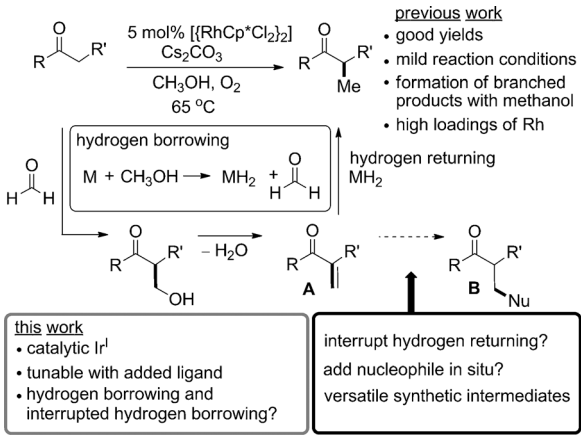

Scheme 1. Hydrogen borrowing with methanol and the concept of interrupted hydrogen borrowing. The reduced form of the catalyst may be MH or MH$_2$. Cp* = C$_5$Me$_5$.

Our idea for producing diverse branched products was to interrupt the hydrogen-borrowing process by preventing enone reduction, thus enabling the introduction of a nucleophile in situ. Subsequent conjugate addition could follow to form a wide range of complex products. This concept is shown in Scheme 1 (**A**→**B**). In this scenario we should be able to incorporate functionality beyond a methyl group, yet harness the enhanced reactivity which comes with methanol-based hydrogen borrowing. There is a small amount of precedent for interrupting hydrogen-borrowing alkylations using either oxygen gas or a reactive alkene to intercept metal hydrides in situ, but these methods go no further than the production of unsaturated derivatives.[4]

We sought to address both issues raised above by examining a relatively inexpensive iridium(I) catalyst system which is precedented to participate in hydrogen borrowing but works best with an added ligand.[5] This requirement meant that we could adjust the balance of

[*] D. Shen, D. L. Poole, C. C. Shotton, A. F. Kornahrens, Prof. T. J. Donohoe
Department of Chemistry, University of Oxford
Chemistry Research Laboratory
Mansfield Road, Oxford, OX1 3TA (UK)
E-mail: timothy.donohoe@chem.ox.ac.uk
Dr. M. P. Healy
Novartis Institute for BioMedical Research
250 Massachusetts Avenue, Cambridge, MA 02139 (USA)

[**] We thank the EPSRC/Pharma Organic Synthetic Chemistry Studentships programme, EPSRC, Pfizer, Novartis, and the Oxford Skaggs DPhil programme for financial support. We thank Dr. Louis K. M. Chan for preliminary experiments.

Supporting information for this article is available on the WWW under http://dx.doi.org/10.1002/anie.201410391.

Table 1: Effect of phosphine ligand and atmosphere on product distribution.

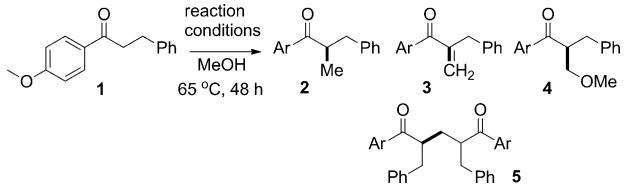

Entry	Conditions	Product distribution [%]				
		1	**2**	**3**	**4**	**5**
1	1 mol% [{Ir(cod)Cl}$_2$], 4 mol% PPh_3, 2 equiv KOH, O_2	–	*94*	–	–	–
2	1 mol% [{Ir(cod)Cl}$_2$], 4 mol% PPh_3, 2 equiv KOH, Ar	4	75	–	trace	trace
3	2 mol% [{Ir(cod)Cl}$_2$], 8 mol% PCy_3, 3 equiv KOH, O_2	12	23	9	50	–
4	2 mol% [{Ir(cod)Cl}$_2$], 8 mol% cataCXium A, 3 equiv KOH, O_2	2	4	*6*	*75*	–
5	2 mol% [{Ir(cod)Cl}$_2$], 8 mol% cataCXium A, 3 equiv KOH, Ar	50	29	1	13	–
6	1 mol% [{Ir(cod)Cl}$_2$], 5 equiv Cs_2CO_3, O_2 (24 h)	–	–	–	14	*83*

[a] Determined by ^{1}H NMR spectroscopy of the material after chromatography. CataCXium A = (adamantyl)$_2$PBu, cod = 1,5-cyclooctadiene.

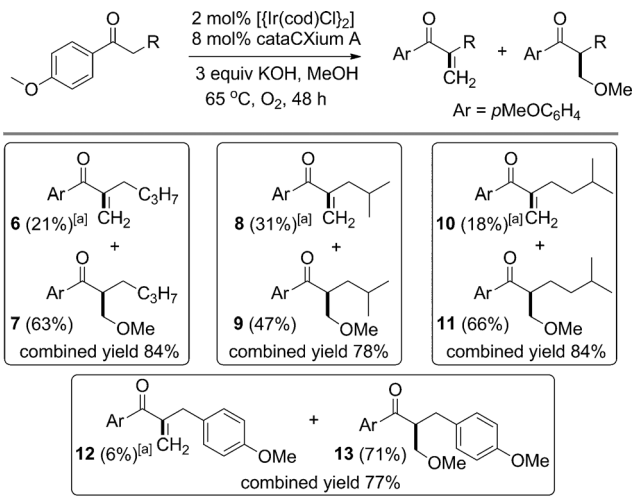

Scheme 2. Methylenation of ketones. Yield is that of isolated products. [a] Enone contaminated with a few percent of inseparable starting material and/or methylated material. Yields adjusted accordingly.

reactivity between the hydrogen borrowing and hydrogen returning events. Preliminary experiments with [{Ir(cod)Cl}$_2$], together with a variety of phosphine ligands proved promising. Reactions of the ketone **1** with low loadings of catalyst (1–2 mol%) and different ligands are shown in Table 1. These experiments revealed that the ligand plays a crucial role in determining the products which are formed. Compare entry 1 (PPh_3 ligand, which forms the methylated compound **2**) with entries 3 and 4 (bulky PCy_3 or cataCXium A[6] ligands which form two interrupted intermediates, the enone **3** and methoxy addition product **4** in 59–81% combined yield). Interestingly, the beneficial role of oxygen in enhancing the efficiency of both the methylation and methylenation reactions is also clear (entries 2 and 5).[7] Note that the combination of a hindered phosphine and an oxygen atmosphere is particularly effective in stopping enone reduction during the hydrogen-borrowing cycle (entry 4).[8] We do not yet know the precise mechanism by which the metal hydride (or dihydride) is returned to the catalytic cycle after methanol oxidation, but speculate that the recycling process involves such a metal hydride being oxidized by molecular oxygen.[9] Although the details are not yet clear, the reactivity of any iridium hydrides formed in situ is clearly influenced by the added ligand. Taken together, this set of results proves that low loadings of iridium(I) can be used with methanol in both hydrogen-borrowing and interrupted-hydrogen-borrowing chemistry depending upon the ligand added.

For the following investigation, we decided to concentrate on the reactions of *p*-methoxyphenyl ketones. This substrate class is an interesting ketone because there are many possibilities for the formation of functionalized esters, after hydrogen-borrowing sequences, through a regioselective Baeyer–Villiger reaction. Therefore, we examined the efficiency of the optimized interrupted hydrogen-borrowing methylenation conditions (Table 1, entry 4) with several aryl ketones and found that this was a general process which formed both the enone and methoxy addition product in good combined yield (Scheme 2). Note that control experiments have shown that the enone and methoxy adduct products are in equilibrium, and so the ratio formed in a particular reaction varies according to the precise substrate employed. Because of this reversibility, we predicted that both products would be equally useful in subsequent reactions.

The success of this iridium-catalyzed interrupted process allowed us to develop a one-pot methylenation/conjugate addition sequence (Scheme 3). The enone and methoxy adduct were not isolated but reacted in situ with an external nucleophile and extra base. In most cases we found it beneficial to treat the crude reaction mixture with a metal scavenging resin (SiliaMetS DMT)[10] while stirring the solution, open to the atmosphere, for 1 hour, before the addition of base and the external nucleophile. We suggest that the resin removes most of the metal catalyst from solution and prevents complications caused by methanol oxidation during the second phase of the reaction. Moreover, stirring the reaction vessel when it is open to the atmosphere concentrates the reaction and may remove unwanted formaldehyde. We found that each set of nucleophiles required a minor variation in the conditions to optimize the yields. The supplementary nucleophiles which can be added to the methylenation reaction are diverse, including nitro compounds (**14**,**15**), ketones (**16**,**17**) and even *tert*-butyl hydroperoxide to form epoxides (**18**,**19**) in good to excellent yields, and all in one pot from methylene ketones. In addition, we were also able to perform a tandem rhodium-catalyzed conjugate addition of a boroxine or boronic acid to form the doubly benzylated compound **20**, and analogue **21**, again in good overall yields for a sequence which involves multiple reaction steps.[11] For this latter type of addition, the scavenger resin was not added because it slowed down the metal-

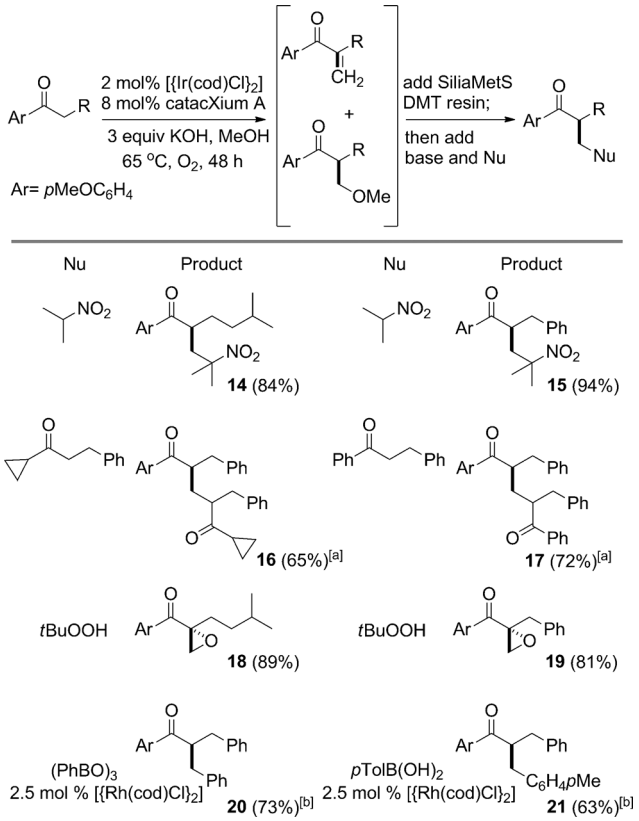

Scheme 3. One-pot methylenation/conjugate addition of aryl ketones. Yield is that of isolated products. [a] Reaction run under an atmosphere of oxygen. [b] SiliaMetS DMT scavenger resin not added to the reaction mixture before addition of nucleophile. Reaction run under argon.

catalyzed conjugate addition. The wide variety of nucleophiles which are compatible with this protocol greatly enhance the types of products which can be accessed directly from ketones through a hydrogen-borrowing-based methodology.

Given the propensity of iridium to participate in methanol hydrogen-borrowing processes,[12] we also examined the alternative catalytic system shown in entry 1 of Table 1 (Ph_3P, O_2 atmosphere), to improve our recently reported enolate methylation reaction, (Scheme 4, methylation). The outcome was a broadly applicable methylation reaction of alkyl ketones using lower loadings of iridium (2 mol% metal) compared to rhodium (10 mol% metal).

This procedure was then extended to a one-pot double alkylation of *p*-methoxyacetophenone with a primary alcohol at 100 °C (conditions developed by Ishii to form a monoalkylated ketone exclusively).[5] The subsequent methylation was accomplished by cooling to the reaction mixture to 65 °C and adding methanol, Ph_3P, KOH, and a balloon of oxygen (**22**–**30**; Scheme 4). A variety of different alcohols were subjected to this regimen, thus demonstrating a useful double-alkylation reaction using 2 mol% of iridium to perform both carbon–carbon bond-forming steps in good overall yields.

Finally, our goal was to showcase the synthetic utility of the intermediates provided by this methodology. In this

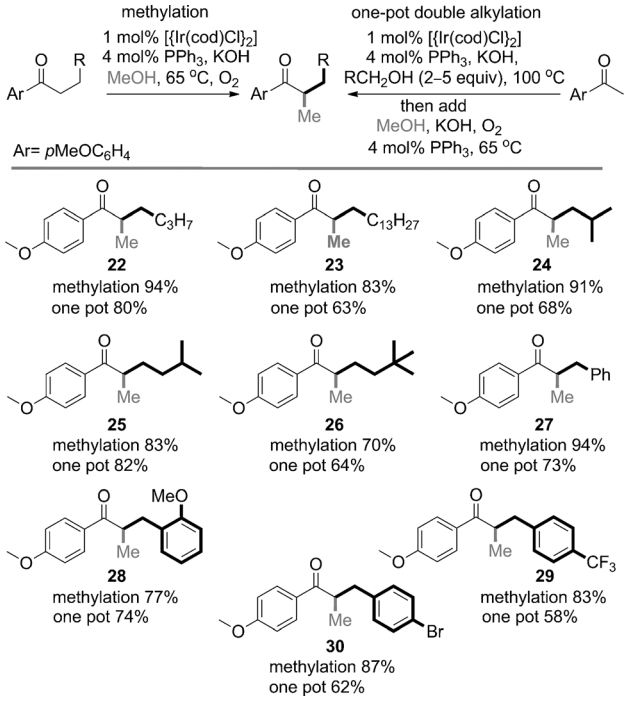

Scheme 4. Iridium-catalyzed methylation and double alkylation of *p*-methoxyphenyl-substituted aryl ketones. The KOH loading was dependent on the substrate (see the Supporting Information for details). Yield is that of isolated products.

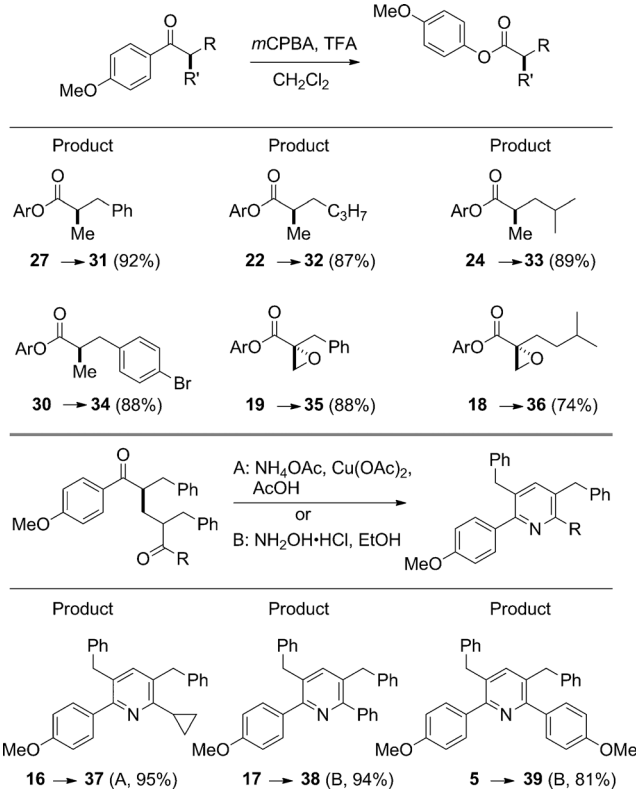

Scheme 5. Regioselective Baeyer–Villiger and aromatizaton reactions of the aryl ketone products. Yield is that of isolated products. Baeyer–Villiger products formed with ≥20:1 regioselectivity in each case. *m*CPBA = *m*-chloroperbenzoic acid, TFA = trifluoroacetic acid.

regard, the pMeOC_6H_4 group is an ideal candidate for regioselective migration during a Baeyer–Villiger oxidation.[13] Scheme 5 shows that a variety of different esters (**31**–**36**) can be made by reaction with *m*CPBA, including those armed with a reactive epoxide functionality. This reaction expands the range of the products which can be formed, solves the problem of esters being unstable to the basic methanol conditions, and introduces the potential for many additional reactions of the more oxidized carbonyl group in the product. Curiously, the ketone **15**, bearing a nitro group, proved to be extremely resistant to such oxidation under a variety of reaction conditions.

In addition, we examined the oxidative (and aromatizing) transformation of the three 1,5-diketone derivatives made in this work (Scheme 5).[14] Reaction of the compounds **5**, **16**, and **17** with either ammonium acetate and Cu^{II} or hydroxylamine hydrochloride formed the corresponding tetrasubstituted pyridines in excellent yields.

To conclude, we have shown that $[\{Ir(cod)Cl\}_2]$ is an excellent catalyst for enolate methylenation and methylation reactions using methanol and low loadings of metal at relatively low temperatures. The combination of a sterically hindered phosphine ligand and O_2 interrupts the hydrogen-borrowing reaction sequence and prevents enone reduction, therefore enabling the addition of a nucleophile to the unsaturated intermediates formed in situ. The synthetic utility of the products can be enhanced further by performing a regioselective Baeyer–Villiger reaction which gives access to products at the carboxylic acid oxidation state.

Received: October 23, 2014
Published online: December 9, 2014

Keywords: hydrogen borrowing · iridium · Michael addition · oxidation · synthetic methods

[1] For reviews of the different strategies involved, see: a) C. Gunanathan, D. Milstein, *Science* **2013**, *341*, 1229712; b) P. J. Black, G. Cami-Kobeci, M. G. Edwards, P. A. Slatford, M. K. Whittlesey, J. M. J. Williams, *Org. Biomol. Chem.* **2006**, *4*, 116–125.

[2] L. K. M. Chan, D. L. Poole, D. Shen, M. P. Healy, T. J. Donohoe, *Angew. Chem. Int. Ed.* **2014**, *53*, 761–765; *Angew. Chem.* **2014**, *126*, 780–784.

[3] For hydrogen production from methanol, see: a) M. Nielsen, E. Alberico, W. Baumann, H.-J. Drexler, H. Junge, S. Gladiali, M. Beller, *Nature* **2013**, *495*, 85–89; b) R. E. Rodríguez-Lugo, M. Trincado, M. Vogt, F. Tewes, G. Santiso-Quinones, H. Grützmacher, *Nat. Chem.* **2013**, *5*, 342–347; c) P. Hu, Y. Diskin-Posner, Y. Ben-David, D. Milstein, *ACS Catal.* **2014**, *4*, 2649–2652; for C–N bond formation, see: d) F. Li, J. Xie, H. Shan, C. Sun, L. Chen, *RSC Adv.* **2012**, *2*, 8645–8652; e) N. Ortega, C. Richter, F. Glorius, *Org. Lett.* **2013**, *15*, 1776–1779; for C–C bond formation via nitriles, see: f) R. Grigg, T. R. B. Mitchell, S. Sutthivaiyakit, N. Tongpenyai, *Tetrahedron Lett.* **1981**, *22*, 4107–4110; g) K. Motokura, N. Fujita, K. Mori, T. Mizugaki, K. Ebitani, K. Jitsukawa, K. Kaneda, *Chem. Eur. J.* **2006**, *12*, 8228–8239; for C–H functionalisation of MeOH: h) J. Moran, A. Preetz, R. A. Mesch, M. J. Krische, *Nat. Chem.* **2011**, *3*, 287–290; for indole functionalization, see: i) C. Sun, X. Zou, F. Li, *Chem. Eur. J.* **2013**, *19*, 14030–14033; for alcohol functionalization, see: j) Y. Li, H. Li, H. Junge, M. Beller, *Chem. Commun.* **2014**, *50*, 14991.

[4] a) M. S. Kwon, N. Kim, S. H. Seo, I. S. Park, R. K. Cheedrala, J. Park, *Angew. Chem. Int. Ed.* **2005**, *44*, 6913–6915; *Angew. Chem.* **2005**, *117*, 7073–7075; b) M. I. Hall, S. J. Pridmore, J. M. J. Williams, *Adv. Synth. Catal.* **2008**, *350*, 1975–1978; see also c) N. A. Owston, A. J. Parker, J. M. J. Williams, *Chem. Commun.* **2008**, 624–625; d) E. Y. Lee, Y. Kim, J. S. Lee, J. Park, *Eur. J. Org. Chem.* **2009**, 2943–2946; see Ref. [3i].

[5] K. Taguchi, H. Nakagawa, T. Hirabayashi, S. Sakaguchi, Y. Ishii, *J. Am. Chem. Soc.* **2004**, *126*, 72–73.

[6] A. Zapf, A. Ehrentraut, M. Beller, *Angew. Chem. Int. Ed.* **2000**, *39*, 4153–4155; *Angew. Chem.* **2000**, *112*, 4315–4317.

[7] a) C. Liu, S. Liao, Q. Li, S. Feng, Q. Sun, X. Yu, Q, Xu, *J. Org. Chem.* **2011**, *76*, 5759–5773; b) S. Liao, K. Yu, Q. Li, H. Tian, Z. Zhang, X. Yu, Q. Xu, *Org. Biomol. Chem.* **2012**, *10*, 2973–2978.

[8] Experiments performed under identical reaction conditions to those shown in entries 1 and 4, but without any iridium catalyst returned starting material in high yield.

[9] See: a) B. Jiang, Y. Feng, E. A. Ison, *J. Am. Chem. Soc.* **2008**, *130*, 14462–14464; b) A. Gabrielsson, P. van Leeuwen, W. Kaim, *Chem. Commun.* **2006**, 4926–4927.

[10] SiliaMetS DMT is claimed by the manufacturer (SiliCycle Inc.) to show scavenging ability for a range of transition metals including Ir and Rh. SiliCycle Inc. "SiliaMetS Metal Scavenger Selection Table" can be found under http://www.silicycle.com/eu/products/metal-scavengers/siliabond-metal-scavengers-selection-guide, **2013**. For an example see: K. B. Woody, A. Palkar, J. E. Bullock, (Phillips 66 Company), US 2014/0221590 A1, **2014**.

[11] For example, see: a) M. Sakai, T. Hayashi, N. Miyaura, *Organometallics* **1997**, *16*, 4229–4231; b) T. Senda, M. Ogasawara, T. Hasahi, *J. Org. Chem.* **2001**, *66*, 6852–6856; for reviews, see: c) G. Berthon, T. Hayashi in *Catalytic Asymmetric Conjugate Reactions* (Ed.: A. Córdova), Wiley-VCH, Weinheim, **2010**, pp. 1–70; d) T. Hayashi, *Synlett* **2001**, 0879–0887.

[12] Subsequent to our initial report using rhodium, Obora reported the iridium(III)-catalyzed methylation of ketones with methanol using 10 mol% metal, under an Ar atmosphere at 120–140°C. S. Ogawa, Y. Obora, *Chem. Commun.* **2014**, *50*, 2491–2493.

[13] M. Renz, B. Meunier, *Eur. J. Org. Chem.* **1999**, 737–750.

[14] a) N. S. Gill, K. B. James, F. Lions, K. T. Potts, *J. Am. Chem. Soc.* **1952**, *74*, 4923–4928; b) D. Sielemann, R. Keuper, N. Risch, *Adv. Synth. Catal.* **1999**, *341*, 487–491; for related chemistry see, A. J. Watson, A. C. Maxwell, J. M. J. Williams, *Org. Biomol. Chem.* **2012**, *10*, 240–243.

